Luteal Regression in the Marmoset Monkey

By

Fiona Margaret Young B.Sc (HONS).

A Thesis submitted to the University of Edinburgh
in fulfilment of the requirements for the degree of
Doctor of Philosophy.

Centre for Reproductive Biology
The University of Edinburgh
December 1999.

For

Alex

Table of Contents

TITLE PAGE **1**

TABLE OF CONTENTS **3**

LIST OF FIGURES **7**

SUMMARY **9**

DECLARATION **11**

ACKNOWLEDGEMENTS **12**

PUBLICATIONS ARISING FROM INVESTIGATIONS REPORTED IN THIS THESIS. **14**

CHAPTER 1: INTRODUCTION **15**

1.0 INTRODUCTION 16
1.1.1 Aims of Project *16*
1.1.2 Hypotheses *17*
1.1.3 Choice of Animal Model *17*
1.2 BACKGROUND INFORMATION ABOUT MARMOSETS 20
1.2.1 Female Marmoset Reproductive Cycle *22*
1.3 DEVELOPMENT AND STRUCTURE OF THE FOLLICLE 22
1.3.1 Development of the Oocyte *22*
1.3.2 Folliculogenesis *23*
1.3.3 Endocrinology of folliculogenesis. *25*
1.3.4 Ovulation *26*
1.3.5 Formation of the Corpus Luteum *28*
1.3.6 Accessory corpora lutea *30*
1.4 THE FUNCTIONING CORPUS LUTEUM 30
1.41 Luteal Phase Steroid Hormone Production *30*
1.42 The Regulation of Luteal Cells *32*
1.5.0 REGRESSION OF THE CORPUS LUTEUM 33
1.5.1 LH in Luteal Regression. *33*
1.5.2 PGF2α in Luteal Regression *36*
1.5.3 Luteal Blood Flow and PGF2α *38*
1.5.4 Oxygen Free Radicals and PGF2α *39*
1.5.5 LH Receptor: Structure, Secondary Messenger Pathways and Interaction with PGF2α *41*
1.5.6 PGF2α and Luteal Cells in vitro. *45*
1.5.7 Summary of the Luteolytic Actions of PGF2α *45*
1.5.8 Leukocytes, Cytokines and Growth Factors During Functional Luteal Regression *46*
1.5.9 Oestrogen in Luteal Regression *48*
1.5.10 Oxytocin in Luteal Regression *49*
1.5.11 Apoptosis and Luteolysis *49*
1.5.12 Luteal vasculature and luteolysis. *58*
1.6 CONCLUSIONS 61

CHAPTER 2: MATERIALS AND METHODS **62**

2.0 MARMOSET HOUSING AND MAINTENANCE 63
2.0.1 Housing *63*
2.0.2 Diet *63*
2.0.3 Environmental Cues. *63*

2.1 PROGESTERONE CONCENTRATIONS AND REPRODUCTIVE CYCLICITY 63
2.1.1 Progesterone Radioimmunoassay. *63*
2.1.2 Analysis of Reproductive Cyclicity. *65*
2.1.3 Progesterone Values at Time of Ovary Collection *70*
2.2 COLLECTION OF MARMOSET OVARIES 76
2.2.1 Spontaneous Luteal Regression *76*
2.2.2 Induced Luteal Regression *76*
2.2.3 Tissue Collection and Preparation *77*
2.2.4 Overview of Ovaries Used. *80*
2.3 LUTEAL MORPHOLOGY 81
2.3.1 Morphometric Analysis of H&E Stained Sections. *81*
2.3.2 The Effect of Location on Morphology Within Corpora Lutea. *89*
2.3.3 Comparison of Morphology between Corpora Lutea from the Same Animal. *89*
2.4 IMMUNOCYTOCHEMISTRY AND HISTOLOGY 90
2.4.1 Bromoxydeuridine (BrdU) Protocol I *93*
2.4.2 BrdU Protocol II *93*
2.4.3 Haematoxylin and Eosin (H&E) Staining *94*
2.4.4 Light Green Counterstaining *95*
2.4.5 Oil Red O Staining *95*
2.5 QUANTIFICATION AND STATISTICAL ANALYSIS OF IMMUNOCYTOCHEMICAL PROCEDURES ..95
2.5.1 Quantification of von Willebrand Factor VIII and Proliferating Cell Nuclear Antigen (PCNA) *95*
2.5.2 Statistical Analysis of von Willebrand Factor VIII *97*
2.5.3 Identification of PCNA-Positive Cells. *97*
2.5.4 Statistical Analysis of Proliferating Cell Nuclear Antigen *106*
2.5.7 Statistical Analysis of Ki67 ..... *107*
2.5.8 Quantification of Bromoxydeuridine *108*
2.5.9 *Statistical Analysis of Bromoxydeuridine* *110*
2.5.10 Quantification of von Willebrand Factor VIII and BrdU Colocalisation *110*
2.5.11 Statistical Analysis of von Willebrand Factor VIII and BrdU Colocalisation *110*
2.6 OLIGONUCLEOSOME FORMATION IN CORPORA LUTEA. 111
2.6.1 Positive Controls for Oligonucleosome Formation *111*
2.6.2 Negative Controls for Oligonucleosome Formation *112*
2.6.3 DNA Extraction and Oligonucleosome Detection. *112*
2.6.4 In situ 3' End Labelling of Marmoset Corpora Lutea. *114*

CHAPTER 3: CELL MORPHOLOGY AND CELL DEATH IN THE CORPUS LUTEUM OF THE MARMOSET MONKEY. 117

3.0 INTRODUCTION 118
3.0.1 The Cellular Composition of Corpora Lutea. *118*
3.0.2 Mechanisms of Cell Death *120*
3.0.3 Aims of Study. *124*
3.1 RESULTS 124
3.1.1 Identification of Steroidogenic Cells by Immunocytochemistry for 3β Hydroxysteroid Dehydrogenase Isomerase (3β HSD). *124*
3.1.2 Morphological Analysis Of Haematoxylin and Eosin Stained Sections of Marmoset Corpora Lutea. *128*
3.1.3 Localisation of Lipids in Marmoset Corpora Lutea. *147*
3.1.4 Oligonucleosome Formation in Marmoset Corpora Lutea. *150*
3.1.5 In situ 3' End Labeling of Marmoset Corpora Lutea *155*
3.1.6 Ubiquitin Expression During Luteal Regression *165*
3.2 DISCUSSION 168
3.2.1 Identification of Steroidogenic Cells *168*
3.2.2 Steroidogenic Cell Morphology During Luteal Regression. *169*
3.2.3 Non-steroidogenic Cell Numbers During Luteal Regression. *170*
3.2.4 Identification and Quantification of Apoptosis *171*
3.2.5 Temporal Expression of Apoptosis During the Luteal Phase *172*

3.2.6 Initiation of Apoptosis in Corpora Lutea *173*
3.2.8 Limitations of the Systems Used to Detect Apoptosis *175*
3.2.9 Ubiquitin Expression During Luteal Regression. *177*
3.2.11 Summary. *178*
3.2.12 Conclusions. *179*

CHAPTER 4: THE VASCULATURE OF THE CORPUS LUTEUM. **181**

4.0 INTRODUCTION 182
4.0.1 Blood Flow in the Corpus Luteum. *182*
4.0.2 Effects of Luteolytic Agents on Luteal Blood Flow. *183*
4.0.3 The Morphology of Luteal Vasculature. *184*
4.0.4 Vascular Endothelial Growth Factor. *185*
4.0.5 Aims *186*
4.1 RESULTS 186
4.1.1 Identification of Endothelial Cells using Von Willebrand Factor VIII Antigen (vW). *186*
4.1.2 Quantification of vW Immunoreactivity After Spontaneous Luteal Regression. *190*
4.1.3 Quantification of vW Immunoreactivity After Induced Luteal Regression. *190*
4.1.4 Vascular Morphology During the Luteal Phase and Spontaneous Luteal Regression. *195*
4.1.5 Further Techniques for Identification of Endothelial Cells *198*
4.1.6 Immunolocalisation of Vascular Endothelial Growth Factor (VEGF). *199*
4.2 DISCUSSION 207
4.2.1 Comparison of Nonsteroidogenic and Endothelial Cell Numbers in Corpora Lutea. *207*
4.2.2 Effects of Administration of Luteolytic Agents on Luteal Vasculature. *208*
4.2.3 Morphology of Marmoset Luteal Vasculature. *209*
4.2.4 Vascular Endothelial Growth Factor in the Corpus Luteum. *212*
4.2.5 Summary *213*
4.2.6 Conclusions. *214*

CHAPTER 5: PROLIFERATION IN THE CORPUS LUTEUM OF THE MARMOSET MONKEY. **215**

5.0 INTRODUCTION 216
5.0.1 Evaluation of Proliferation *216*
5.0.2 Methods for Assessing Cell Proliferation *218*
5.0.3 Comparison of Ki67, Tritiated Thymidine, Bromodeoxyuridine and PCNA. *219*
5.0.4 Proliferation in Corpora Lutea *220*
5.0.5 Aims *221*
5.1 RESULTS 221
5.1.1 PCNA Immunocytochemistry *221*
5.1.2 Ki67 Immunocytochemistry *228*
5.1.3 BrdU Immunocytochemistry *240*
5.1.4 Identification of BrdU Positive Cells *247*
5.1.5 Comparison of Ki67 and BrdU ICC *257*
5.2 DISCUSSION 260
5.2.1 The Automated Quantification System. *260*
5.2.2 Suitability of Experimental Design. *261*
5.2.3 Interpretation of Data from PCNA Study. *262*
5.2.4 Steroidogenic Cell Proliferation in Marmoset Corpora Lutea. *262*
5.2.5 Nonsteroidogenic Cell Proliferation in Marmoset Corpora Lutea. *264*
5.2.6 Summary *267*
5.2.7 Conclusions *267*

CHAPTER 6: DISCUSSION **268**

6.0 DISCUSSION 269
6.1 Cell Death and Luteal Regression *269*

6.2 Vascular Changes and Luteal Regression 272
6.3 The Role of PGF2α in Luteal Regression 274
6.4 The Relationship Between Functional and Structural Luteal Regression. 278
6.5 Future Directions 280
6.6 Summary 280
6.7 Conclusion 281

BIBLIOGRAPHY 283

APPENDIX 1: MARMOSET DETAILS AND OVARY USAGE 308

APPENDIX 2: IMMUNOCYTOCHEMISTRY PROCEDURES 311

List of Figures

FIGURE 1.0: THE GENETIC CONTROL OF APOPTOSIS....55
FIGURE 2.1: FREQUENCY OF DIFFERENT LUTEAL PHASE LENGTHS IN MARMOSETS....69
FIGURE 2.2: SERUM PROGESTERONE CONCENTRATIONS IN THE MARMOSET....73
FIGURE 2.3: PROGESTERONE CONCENTRATIONS IN THE MARMOSET AFTER INDUCED LUTEAL REGRESSION....75
FIGURE 2.4: ACCUMULATIVE MEANS OF LUTEAL CELL TYPES. 88
FIGURE 2.5: NUCLEAR MORPHOMETRY OF STEROIDOGENIC AND NONSTEROIDOGENIC CELLS IN MARMOSET CORPORA LUTEA. 100
FIGURE 2.6: THE RELATIONSHIP BETWEEN OPTICAL DENSITY AND RATIO OF ELLIPTICAL AXES IN PCNA IMMUNOSTAINED LUTEAL CELL NUCLEI. 102
FIGURE 2.7: COMPARISON OF LUTEAL CELL NUCLEI IDENTIFICATION BY MANUAL AND AUTOMATIC SCORING METHODS....105
FIGURE 2.8: RANGE OF RESULTS IN 3 SEPARATE BRDU PROCEDURES IN ONE MARMOSET CORPUS LUTEUM COLLECTED DURING THE EARLY LUTEAL PHASE. 109
FIGURE 3.1: 3β HYDROXYSTEROID DEHYDROGENASE (3βHSD) IMMUNOCYTOCHEMISTRY IN MARMOSET CORPORA LUTEA AFTER INDUCED LUTEAL REGRESSION. 127
FIGURE 3.2: HAEMATOXYLIN AND EOSIN STAINED MARMOSET CORPORA LUTEA DURING SPONTANEOUS LUTEAL REGRESSION. 130
FIGURE 3.3: HAEMATOXYLIN AND EOSIN STAINED MARMOSET CORPORA LUTEA AFTER INDUCED LUTEAL REGRESSION. 132
FIGURE 3.4: HAEMATOXYLIN AND EOSIN STAINED SECTIONS OF MARMOSET CORPORA LUTEA. 134
FIGURE 3.5: MEAN NUMBER OF CELLS PER UNIT AREA IN MARMOSET CORPORA LUTEA....137
FIGURE 3.6: NUMBER OF NONSTEROIDOGENIC CELLS IN MARMOSET CORPORA LUTEA. 139
FIGURE 3.7: PERCENTAGE OF NONSTEROIDOGENIC CELLS IN MARMOSET CORPORA LUTEA. 141
FIGURE 3.8: AMOUNT OF APOPTOSIS IN H&E STAINED SECTIONS OF MARMOSET CORPORA LUTEA. 144
FIGURE 3.9: PERCENT APOPTOSIS IN MARMOSET CORPORA LUTEA. 146
FIGURE 3.10: OIL-RED-O STAINED LIPID IN MARMOSET CORPORA LUTEA AFTER INDUCED REGRESSION....149
FIGURE 3.11: OLIGONUCLEOSOME FORMATION IN BOVINE, HUMAN AND MARMOSET CORPORA LUTEA. 152
FIGURE 3.12: OLIGONUCLEOSOME FORMATION IN MARMOSET CORPORA LUTEA....154
FIGURE 3.13: *IN SITU* 3' END LABELLING IN MID LUTEAL PHASE MARMOSET CORPUS LUTEUM. 158
FIGURE 3.14: *IN SITU* 3' END LABELLING IN REGRESSING MARMOSET CORPUS LUTEUM....160
FIGURE 3.15: *IN SITU* 3' END LABELLING MARMOSET CORPUS LUTEUM AFTER INDUCTION OF LUTEOLYSIS WITH PGF2α....162
FIGURE 3.16: *IN SITU* 3' END LABELLING MARMOSET CORPUS LUTEUM AFTER INDUCTION OF LUTEOLYSIS WITH GNRH ANTAGONIST. 164
FIGURE 3.17: IMMUNOHISTOLOGICAL DETECTION OF UBIQUITIN IN MARMOSET CORPORA LUTEA. 167
FIGURE 4.1: VON WILLEBRAND FACTOR VIII ANTIGEN (VW) IMMUNOCYTOCHEMISTRY IN MARMOSET CORPORA LUTEA. 189
FIGURE 4.2: AREA OF ENDOTHELIAL CELL SPECIFIC STAINING IN MARMOSET CORPORA LUTEA. 192
FIGURE 4.3: AREA OF ENDOTHELIAL CELL SPECIFIC STAINING IN MARMOSET CORPORA LUTEA AFTER INDUCED LUTEAL REGRESSION....194
FIGURE 4.4: THE RELATIONSHIP BETWEEN LUTEAL AGE AND THE NUMBER OF BLOOD VESSELS IN MARMOSET CORPORA LUTEA. 197
FIGURE 4.5: VASCULAR ENDOTHELIAL GROWTH FACTOR (VEGF) IMMUNOLOCALISATION IN MID LUTEAL PHASE MARMOSET CORPUS LUTEUM. 202
FIGURE 4.6: VASCULAR ENDOTHELIAL GROWTH FACTOR (VEGF) IMMUNOLOCALISATION THROUGHOUT THE LUTEAL PHASE OF THE MARMOSET. 204
FIGURE 4.7: VASCULAR ENDOTHELIAL GROWTH FACTOR (VEGF) IMMUNOLOCALISATION DURING INDUCED LUTEAL REGRESSION....206

FIGURE 5.1: THE CELL CYCLE 217
FIGURE 5.2: PROLIFERATING CELL NUCLEAR ANTIGEN (PCNA) IMMUNOCYTOCHEMISTRY IN A MID-LUTEAL PHASE MARMOSET OVARY 223
FIGURE 5.3: NUMBERS OF PROLIFERATING CELL NUCLEAR ANTIGEN (PCNA) IMMUNOPOSITIVE CELLS IN SPONTANEOUSLY REGRESSING CORPORA LUTEA. 225
FIGURE 5.4: NUMBERS OF PROLIFERATING CELL NUCLEAR ANTIGEN (PCNA) IMMUNOPOSITIVE CELLS IN CORPORA LUTEA AFTER INDUCED LUTEAL REGRESSION. 227
FIGURE 5.5: KI67 IMMUNOCYTOCHEMISTRY IN MID LUTEAL PHASE DAY 10 CORPUS LUTEUM. 230
FIGURE 5.6: KI67 IMMUNOCYTOCHEMISTRY IN MARMOSET CORPUS LUTEUM AFTER INDUCED LUTEAL REGRESSION. 232
FIGURE 5.7: KI67 IMMUNOCYTOCHEMISTRY IN SPONTANEOUSLY REGRESSING MARMOSET CORPORA LUTEA. 234
FIGURE 5.8: NUMBERS OF KI67 IMMUNOPOSITIVE CELLS IN SPONTANEOUSLY REGRESSING MARMOSET CORPORA LUTEA. 237
FIGURE 5.9: NUMBERS OF KI67 IMMUNOPOSITIVE CELLS IN MARMOSET CORPORA LUTEA AFTER INDUCED LUTEAL REGRESSION. 239
FIGURE 5.10: BROMODEOXYURIDINE (BRDU) IMMUNOCYTOCHEMISTRY IN FUNCTIONALLY REGRESSING CORPUS LUTEUM. 242
FIGURE 5.11: BROMODEOXYURIDINE (BRDU) IMMUNOCYTOCHEMISTRY IN SPONTANEOUSLY REGRESSING CORPORA LUTEA. 244
FIGURE 5.12: NUMBERS OF BROMODEOXYURIDINE (BRDU) IMMUNOPOSITIVE CELLS IN SPONTANEOUSLY REGRESSING MARMOSET CORPORA LUTEA. 246
FIGURE 5.13: IMMUNOCYTOCHEMISTRY FOR BROMODEOXYURIDINE (BRDU) COLOCALISED WITH 3β HYDROXYSTEROID DEHYDROGENASE (3βHSD) IN SPONTANEOUSLY REGRESSING MARMOSET CORPORA LUTEA. 249
FIGURE 5.14: IMMUNOCYTOCHEMISTRY FOR BROMODEOXYURIDINE (BRDU) COLOCALISED WITH VON WILLEBRAND FACTOR VIII ANTIGEN (VW) IN SPONTANEOUSLY REGRESSING MARMOSET CORPORA LUTEA. 251
FIGURE 5.15: NUMBERS OF BROMODEOXYURIDINE (BRDU) IMMUNOPOSITIVE CELLS IN SPONTANEOUSLY REGRESSING MARMOSET CORPORA LUTEA AFTER TWO SEPARATE IMMUNOCYTOCHEMICAL PROCEDURES. 254
FIGURE 5.16: NUMBERS OF PROLIFERATING CELLS AFTER COLOCALISATION IMMUNOCYTOCHEMISTRY WITH BROMODEOXYURIDINE (BRDU) AND VON WILLEBRAND FACTOR VIII ANTIGEN (VW). 256
FIGURE 5.17: PERCENTAGES OF KI67 AND BRDU IMMUNOPOSITIVE CELLS IN SPONTANEOUSLY REGRESSING MARMOSET CORPORA LUTEA. 259
FIGURE 5.18: INTERANIMAL VARIATION IN KI67 IMMUNOCYTOCHEMISTRY QUANTIFICATION. 266
FIGURE 6.1: MECHANISMS OF FUNCTIONAL LUTEAL REGRESSION. 278

Summary

In the ovary, follicular development and oocyte maturation are followed by ovulation. Cells comprising the follicle then luteinise and form the corpus luteum. Progesterone production by the corpus luteum peaks during the mid luteal phase. In primates, in the absence of pregnancy, progesterone production declines 2-3 weeks after ovulation, and the corpus luteum regresses. This thesis examines cellular and biochemical changes which occur in the corpus luteum during luteal regression in the primate, using the marmoset monkey, Callithrix jacchus as a model. The hypotheses that PGF2α, apoptosis and changes in the vasculature are involved in luteolysis are explored.

Ovaries were studied on luteal days 10, 18 and 22 (corresponding to the mid luteal phase, functional luteal regression and structural luteal regression respectively), and also 12 and 24 hours after administration of either PGF2α or GnRH antagonist. Decreased progesterone concentrations indicative of functional luteal regression were apparent 12 hours later.

Analysis of haematoxylin and eosin stained sections of corpora lutea indicated that the administration of PGF2α or GnRH antagonist resulted in apoptosis, and also in the formation of cytoplasmic vacuoles in steroidogenic cells. Apoptosis in corpora lutea was further investigated by 3' end labelling DNA extracted from corpora lutea, and by *in situ* 3' end labelling of sections of ovarian tissue. Apoptosis was found to occur after induced luteolysis and in naturally regressing corpora lutea but only after progesterone had decreased to follicular phase values. Therefore the decline in progesterone characteristic of functional luteal regression was not caused by the apoptotic cell death of steroidogenic cells. However, apoptosis played a role in structural luteal regression.

Ubiquitin is expressed only by live cells undergoing a process of non-apoptotic cell death. Ubiquitin expression was only found in PGF2α, but not in GnRH antagonist

treated luteal tissue, suggesting three possible explanations: that the cells in GnRH antagonist treated animals were dead prior to the collection point of 12 hours, or that the cells were not in a cell death pathway, or that cell death was occurring via different mechanisms in PGF2α and GnRH antagonist treated animals.

The importance of the vasculature in luteal regression was investigated by labelling endothelial cells with an antibody against von Willebrand Factor VIII Antigen. Endothelial cell numbers remained constant after administration of luteolytic agents, indicating that induced luteal regression was not effected by vascular changes. Similarly, the vascualture did not change during funçtional regression in untreated animals. Vascular remodelling, however, occurred during structural luteal regression, when the vasculature changed from an extensive network of small capillaries to a system comprised of a lower number of larger blood vessels.

Three different techniques were used to assess cell proliferation during luteal regression; immunocytochemistry with antibodies directed against the cell cycle markers Proliferating Cell Nuclear Antigen and Ki67, and also by measurement of *in vivo* incorporation of bromoxydeuridine. Luteal cell proliferation decreased during functional luteal regression, but rose again during structural luteal regression.

Although the instigating mechanism for functional luteal regression in the primate remains unknown, it is possible that the endogenous production of PGF2α causes functional luteal regression in primates. These studies have demonstrated that structural luteal regression is effected by decreased luteal cell proliferation concomitant with increased apoptosis. The extensive vascular network conducive for steroidogenesis in the functioning corpus luteum is replaced by a less extensive vascular network of larger vessels during structural luteal regression. This probably facilitates the transportation of the cellular debris of regression away from the ovary, and allows the process of structural luteal regression to proceed.

Declaration.

The experimental work described in this thesis was conducted in the Centre for Reproductive Biology, Medical Research Council, 37 Chalmers Street, Edinburgh, during 1993-1998. The data presented are from original studies by the author and any input from colleagues is duly acknowledged.

Dr. Hamish Fraser and Dr. Peter Illingworth suggested the initial area of research, and some subsequent areas for investigation. Dr Fraser facilitated the use of marmosets and laboratory resources, and Dr Illingworth advised on statistical analysis. Kieth Morris and staff maintained the marmoset colony, provided marmoset blood samples and administered luteolytic treatments. Initially progesterone assays were carried out by Gwen Cowan, and later by Ian Swanston and staff.

This dissertation has not previously been submitted, wholly or in part, to any other University for any degree or diploma. I consent to this thesis being made available for photocopying and loan if accepted for the award of the degree.

Fiona Margaret Young.

Acknowledgements.

I would like to acknowledge and thank the following individuals for the help and assistance they have given during these studies. I wish to express grateful appreciation for the extreme patience and persistence of my supervisors, Dr. Hamish Fraser and Dr. Peter Illingworth, who continued to advise and support me regardless of changing circumstances. Professor Alan McNeilly and the staff and students of the Centre of Reproductive Biology provided a supportive and intellectually stimulating environment in which to conduct research. In particular I would like to thank members of 'Team CL'; Stephen Lunn, Faye Rodger, Colin Duncan, Gwen Cowen and Pawlina Largue, for their invaluable help, comments and lively conversation! Phillipa Saunders, Pam Brown and Mike Miller gave valuable technical advice, and John Aitken, Karen Eidne and Henry Jabbour kindly allowed me to use their equipment and reagents. Judy McNeilly, Sheila McPherson and others gave warm support and wise advice about combining the roles of mother and research. Tom and Ted contributed considerable expertise regarding the presentation of data and images, while denizens of the academic concourse helped me to maintain a social perspective throughout these studies.

I would like to thank Keith Morris and the staff of the Primate facility for care of the marmosets used in these studies, and Ian Swanston and the staff in the assay laboratory for measuring progesterone concentrations. Dr. Evelyn Telfer and staff kindly taught me techniques for extracting apoptotic DNA. Dr. David Harrison and Dr. Evelyn Grey taught me how to identify apoptosis, gave me many hours usage on their HOME image analysis system, and also made excellent coffee! Denise Lawler and Elaine Watson gave bovine and equine luteal tissue for use in the apoptosis studies, and Nora Spears and Stuart Baker gave excellent advice about visualising apoptotic DNA. Sue Widdicombe and Rehema White gave broad support and specific advice about statistical analysis.

In Australia, the Endocrine Department of Flinders Medical Centre, Adelaide, was crucial to the success of this PhD, which would not have been written up without the support of its staff. Professors Stephen Judd and John Willouby very kindly allowed

me to use facilities in their laboratories to complete this thesis. In particular, Ray Rodgers, John Oliver, Tina Lavranos, Jenny Hiscock and Margaret Menadue helped me enormously with their experience, advice and freindship.

I have had unwavering support from my parents and other members of my family. Their belief in me has been a wonderful source of motivation, and the many forms of practical support they have given have been invaluable in the completion of these studies. Lastly, loving thanks go to Alex, who constantly reminds me about the important things in life.

Publications Arising From Investigations Reported in this Thesis.

Young FM, Lunn SF, Illingworth PJ, Harrison D and Fraser HM (1997) Cell death during luteal regression in the marmoset monkey (Callithrix jacchus), *Journal of Reproduction and Fertility*. **111**, 109-119.

Young FM, Illingworth PJ and Fraser HM (1998) Ubiquitin and apoptosis in the corpus luteum of the marmoset monkey (Callithrix jacchus). *Journal of Reproduction and Fertility*, **114** 163-168.

Young FM., Rodger FE, Illingworth PJ and Fraser HM (2000) Cell proliferation and vascular morphology in the marmoset corpus luteum. *Human Reproduction*, **15** 557-566.

Rodger FE, Young FM, Fraser HM and Illingworth PJ (1997) Endothelial cell proliferation follows the mid-cycle luteinizing hormone surge, but not human chorionic gonadotrophin rescue in the human corpus luteum. *Human Reproduction*, **12** 1723-1729.

Duncan WC, Illingworth PJ, Young FM and Fraser HM (1998) Induced luteolysis in the primate: rapid loss of luteinising hormone (LH) receptors. *Human Reproduction* **13** 2532-2540.

Chapter 1: Introduction

1.0 Introduction

In primates, two ovoid ovaries lie on either side of the uterus. The mean (± S.D) size of preovulatory marmoset ovaries is 5.3 (±0.7) x 4.3(±0.6) x 3.6 (±0.9)mm (Cui and Mathews, 1994). Each ovary consists of an outer cortex, an inner medulla and the hilus which is the anterior margin where the ovary is attached to a double fold of the peritoneum (Clement , 1987). Primordial follicles, consisting of an oocyte surrounded by a layer of granolosa cells, are located in the cortex of the ovary (Guedes and Miraglia, 1977). In mature female primates, primordial follicles increase in size until gonadotrophins bring about the process of ovulation (Macklon and Fauser 1998; Kholkute and Nandedkar 1983), whereby the oocyte is released from the follicle into the oviduct. Cells comprising the follicle differentiate into the cells of the corpus luteum and commence progesterone production (Wehrenberg *et al.*, 1997; Einspanier *et al.*, 1997). Progesterone produced by the corpus luteum prevents the ovulation of additional follicles (Soules *et al.*, 1984, Baird *et al.*, 1975). If the ovulated oocyte is not fertilised it is crucial that progesterone production by the corpus luteum cease in order to allow the ovulation of another, potentially fertilisable oocyte, and hence ensure survival of the species (Behrman *et al.*, 1993). It is also necessary to remove luteal tissue to make room for subsequent follicular development. The mid-luteal phase human corpus luteum occupies 50% of the total ovarian volume and weighs approximately 3g (Clement 1987). The reproductive lifespan of a woman is in the order of 500 ovulations, which would result in a 1.5kg gain in luteal weight if there were not some mechanism to remove luteal tissue. Luteal regression is the cessation of steroid hormone production by the corpus luteum, and the removal of luteal tissue.

1.1.1 Aims of Project

The mechanisms which confer a species-specific life-span upon primate corpora (Fairchild Benyo *et al.*, 1993) or which initiate primate luteal regression (Michael *et al.*, 1994) or which control the time taken to complete luteal regression (Behrman *et al.*, 1993) are not known. The ability to understand and modify these mechanisms

would benefit the treatment of early pregnancy losses caused by luteal phase defects (Fairchild Benyo *et al.*, 1993).

The aim of this project is to examine luteal regression for the first time in a commonly used primate model, the marmoset monkey (*Callithrix jacchus*). Endocrinological and cellular changes that occur during luteal regression will be described, and candidate mechanisms for the initiation and regulation of luteal regression will be examined.

1.1.2 Hypotheses

Marmoset luteal regression is initiated *in vivo* by one of the following:

a) PGF2α.
b) Apoptotic cell death.
c) Changes in the vasculature.

1.1.3 Choice of Animal Model

The following strategies were adopted in order to investigate these hypotheses:

- To induce luteal regression by *in vivo* administration of a PGF2α analogue. PGF2α-treated corpora lutea to be compared with corpora lutea collected from (a) animals treated *in vivo* with a GnRH antagonist to block LH-stimulated steroidogenesis and (b) untreated, spontaneously regressing corpora lutea. This strategy assumes that pharmacological induction of luteolysis with a mechanism that mimics the natural, *in vivo* luteolytic signal will result in corpora lutea with morphological and functional characteristics similar to those seen in spontaneously regressing corpora lutea.
- To collect ovarian tissue from different stages of the luteal phase and after induced luteal regression, and to quantify apoptotic cell death in these corpora lutea.
- To identify and quantify vascular endothelial cells in corpora lutea from different stages of the luteal phase and after induced luteal regression.

The use of human corpora lutea for these studies was considered, but it was not ethically permissible to administer luteolytic agents to women, and also the numbers of willing donors were insufficient for these studies. In addition, tracking human reproductive cycles and collecting tissue was time-consuming and costly in terms of expertise and administration. Of the non-human primates, the marmoset, *Callithrix jacchus*, was selected for these studies because:

- Protocols for inducing luteal regression with GnRH antagonist and PGF2α were well characterised and permitted for use in marmosets. In addition, PGF2α does not reliably induce luteal regression when administered intravenously to other primates, therefore the proposed hypothesis would be more difficult to investigate in macaques or humans.
- Procedures for tracking the reproductive cycle were well established, inexpensive, and relatively stress-free for the animals and handlers.
- Sufficient numbers of animals from a successful, captive-bred colony were available for use.
- Marmosets were less expensive and easier to house than other non-human primates.

1.1.3.1 Marmosets as a Primate Model.

Species differences exist between primates, therefore no one primate can be said to be completely representative of all primates. A brief comparison of corpora lutea of humans, Old World macaque monkeys and New World marmoset monkeys is as follows:

Species	Length of Luteal Phase	Luteal Morphology	Steroid Production by CL
Homo sapiens	14 days	Theca-lutein surround granulosa-lutein, occasionally penetrating along vascular septa (1)	Oestradiol and progesterone (2)
Macaca arctoides	17 days	Theca-lutein surround granulosa-lutein, occasionally penetrating along vascular septa (3)	Oestradiol and progesterone (4)
Callithrix jacchus	18 days	One population of evenly distributed steroidogenic cells (5)	Oestradiol and progesterone (6)

1. Clement, 1987
2. Retamales *et al.*, 1994
3. Fraser *et al.*, 1997
4. Zelinski-Wooten *et al.*, 1991
5. Webley GE *et al* 1990
6. Torii R *et al* 1996

The major difference between primate and non-primate luteal regression is that PGF2α derived from the uterus does not cause luteolysis in humans (Beling *et al.*, 1970) or rhesus macaques (Neill *et al.*, 1969), whereas it does in non-primates (Poyser, 1981; Knickerbocker *et al.*, 1988). Although uterine-derived PGF2α does not induce regression in primates, endogenous luteal production of PGF2α may play a role. In humans, systemically administered PGF2α resulted in a transient decrease in circulating progesterone concentrations (Karim and Hillier, 1979). PGF2α injected into the corpus luteum of rhesus macaques caused luteolysis (Auletta *et al.*, 1984) and systemically administered PGF2α caused luteolysis in marmosets when applied after day 8 of the luteal phase (Summers *et al.*, 1985).
Although marmoset and human luteal morphology is dissimilar (Webley *et al.*, 1990), corpora lutea are functionally similar with regards to types, although not levels, of steroid hormone production (Ohara A *et al.*, 1987; Steinetz *et al.*, 1995). Human and marmoset corpora lutea have similar patterns of inhibin (Smith *et al.*,

1990; Groome *et al.*, 1996) and oxytocin production (Einspanier *et al.*, 1994; Khan-Dawood 1987) while melatonin stimulates luteal cell progesterone production in both human (Webley *et al.*, 1988) and marmoset corpora lutea (Webley and Hearn 1987). Human chorionic gonadotrophin prevents luteal regression in both humans (Zeleznik) and marmosets (Hearn and Webley 1987), and there is a high degree of conservation between marmoset and human chorionic gonadotrophins (Simula *et al.*, 1995).

The factors, or order of events, which initiate and regulate luteolysis in marmosets and humans are likely to be similar, if not identical. However, it is also likely that species differences would manifest as variations in the concentration, threshold of effectiveness and time of action of these factors. Despite species differences, the examination of luteolytic mechanisms in marmosets is more likely to provide data relevant to human luteolysis, than would an equivalent investigation using a non-primate model.

In the UK, marmosets comprise 37% of the primates used by contract research laboratories and pharmaceutical companies (Owen *et al.*, 1997). Marmosets have been used as model primates in other studies (Puri *et al.*, 1989). It is therefore important to identify the differences and similarities between marmosets and humans accurately, in order to determine the extent to which data derived from studies conducted in marmosets may be extrapolated to humans. This project will therefore add to current information regarding marmoset reproductive endocrinology, thus promoting the usefulness of the marmoset as a primate model.

1.2 Background Information about Marmosets

Marmoset are platyrrhine primates with approximately 15 taxa (Tagliaro *et al.*, 1997) and phylogeny as follows (Orr, 1976):

Class	Mammalia
Infraclass	Eutheria
Order	Primates
Suborder	Anthropoidea
Infraorder	Platyrrhini
Family	Callithricidae
Genus	jacchus

Marmosets are common in the eastern and coastal rain forests of Brazil (In *Biology, Rearing and Care of Young Primates, 1977*), where they are arboreal and diurnal. They are omnivorous, eating fruit, tree sap, seeds, insects, rodents and occasionally small birds (Hearn 1987). They occur in groups of up to 30 animals consisting primarily of a mating pair and their mature, subadult, juvenile and infant offspring, and also some unrelated individuals (Hearn 1983). Mates are monogamous and pair for life, and there appears to be no breeding season in the wild with births occurring at all times of the year (Hearn 1983; Harter and Erkert 1993). Female reproductive cycles are independent of male presence, since isolated female marmosets had a cycle length of 28.8±4.9 days, which was similar to the cycle-length of female adults housed with vasectomized or castrated males (Harter and Erkert 1993: Harding *et al.*, 1982).

Intrasex dominance hierarchies are established in family groups (Abbot *et al.*, 1988) and marmoset populations appear to be regulated by the suppression of subordinate female reproductive cyclicity by the dominant female. Most subordinate females do not secrete LH, and are therefore anovulatory (Abbot *et al.*, 1988). Secretion of LH after administration of an exogenous GnRH challenge is proportional to social status. The LH response in subordinate females is significantly lower than in females who are higher in the dominance hierarchy. Isolation of subordinate females restores serum LH concentrations and ovulation. GnRH secretion is similar in dominant and subordinate females, therefore inhibition of LH production seems to occur at the level of the pituitary (Abbot *et al.*, 1997). Suppression of ovulation is not absolute; breeding females are more effective at suppressing subordinate ovulation than non-breeding dominant females, however even subordinates that ovulate do not become pregnant (Saltzman *et al.*, 1997). The dominant female can also cause a decrease in circulating testosterone concentrations in subordinate males (Hearn, 1983), so effectively ensuring that there is only one breeding pair in each family group.

In captivity, singletons, twins or triplets are born at 5-6 month intervals (Hearn, 1987) after a gestation of 144 ± 2 days (Hearn, 1983). Ovulation can occur 10.5±0.7 days after parturition (Hearn, 1983); lactation therefore does not inhibit folliculogenesis in the marmoset.

Marmosets display little sexual dimorphism, and there is no difference in growth rate or adult weight (350-450g) between males and females (Abbot and Hearn 1978). Adult size is reached by one year of age, and puberty occurs at about 15 months of age (Hearn, 1983). Females may continue breeding up to 16 years of age, and may live as long as twenty years.

1.2.1 Female Marmoset Reproductive Cycle

The female marmoset does not menstruate (Abbot and Hearn 1978) but the concentration of peripheral plasma progesterone increases after ovulation, therefore elevated progesterone levels are indicative of the luteal phase (Hillier *et al.*, 1988). Harding *et al* (1982) found that the total cycle length in female marmosets was 30.1 ± 3.8 days (mean ± SD, n=30, range 24-41 days, median 29.5 days) and during this time progesterone levels were below 10ng/ml for 8.8 ± 3.7 days, but higher than 10 ng/ml, therefore assumed to be post-ovulatory and indicative of the luteal phase, for 21.5 ± 2.2 days (mean ± SD, n=30, range 14-29 days, median 21.5) (Harding *et al.*, 1982). Marmosets in another colony were found to have a cycle length of 28.6 ± 1 days (mean ± s.e.m) with a luteal phase of 19.2 ± 0.6 days (Summers *et al.*, 1985, Harlow *et al.*, 1984) which is slightly lower than that found in Hardings' study. Combining these studies suggests that in the captive marmoset the preovulatory or follicular phase lasts approximately 9 days, during which peripheral concentrations of estrogen are elevated (0.1-3 ng/ml, Abbot, 1992) and progesterone concentrations are less than 10ng/ml. The luteal phase lasts approximately 19 days and is characterised by peripheral progesterone concentrations higher than 10ng/ml.

1.3 Development and Structure of the Follicle

1.3.1 Development of the Oocyte.

Mammalian somatic cells contain two copies of each chromosome, and are therefore diploid (2n). Sexual reproduction requires the fusion of two haploid (1n) gametes, the spermatazoa and the oocyte, each of which contains only one copy of each chromosome. The production of haploid gametes occurs by meiosis, which consists of two sequential cell division processes (Cell cycle and replication 1993 In:

Wheater's Functional Histology 3rd Edition Editors: PR Wheater, HG Burkitt, VG Daniels pp 31-40). In females, the first cell division results in the formation of two genetically distinct diploid daughter cells, one of which progresses to the second meiotic division, the other degenerates and forms a polar body. The second division produces one haploid daughter cell, and another polar body (In: *Wheater's Functional Histology 1993*; Eppig, 1991). Cell divisions consists of prophase, metaphase, anaphase and teleophase, which are analogous to the stages found in somatic cell mitotic division.

During embryonic development, primordial germ cells migrate to the genital ridge and form a primitive ovary (Eppig, 1991). The primordial germ cells initially undergo mitosis to produce large numbers of diploid oogonia. In humans, oogonia begin meiosis in the fifth month of fetal life, but this process is arrested in the prophase of the first meiotic division. Meiotic arrest occurs before birth, but after the formation of primordial follicles; structures 15 – 20μm in diameter consisting of an oocyte surrounded by a layer of flattened granulosa cells (In: *Wheater's Functional Histology 1993*; Eppig, 1991). Meiosis is reinitiated by a preovulatory surge of LH, a situation that only occurs post-puberty. The gonadotrophin surge stimulates completion of the first meiotic division and production of the first polar body. Ovulated oocytes are therefore diploid, and are arrested in metaphase II. Spermatazoan penetration stimulates completion of metaphase II and the second meiotic division, resulting in the production of a haploid oocyte and a second polar body. Fertilisation could be said to occur when the male and female gamete nuclei coalesce to produce a new diploid genetic combination (Eppig, 1991).

1.3.2 Folliculogenesis

Reports regarding the number of primordial follicles present in human ovaries at birth vary from 400 000 (Clement, 1987) to two million (Macklon and Fauser 1998). Follicular development to the early antral stage occurs throughout childhood, but further follicular development does not occur in the absence of ovulatory concentrations of gonadotrophins, and these follicles become atretic. Consequently, approximately 500 000 primordial follicles are present when menstruation begins

(Macklon and Fauser 1998). A small study of only three prepubertal marmosets found that oocytes in the outer ovarian cortex were not surrounded by granulosa cells, but that 2 or more rows of follicular cells surrounded oocytes of the inner cortex. This study also concluded that granulosa cells originated in the stroma of the ovarian medulla, and migrated along 'cords' to surround the oocytes in the outer cortex in order to form primordial follicles (Guedes and Miraglia 1977). The process of maturation from primordial follicle to ovulation is known as folliculogenesis. This takes approximately six months in women (Gougeon, 1982), with the last 14 days of folliculogenesis occurring during the first half of the menstrual cycle.

Follicular development begins when granulosa cells in a primordial follicle begin to proliferate. It is not known what initiates granulosa cell proliferation (Robker and Richards, 1998) but the relatively slow increase in cell numbers results in the formation of a primary follicle. Vascularisation of the surrounding stroma occurs, and when the follicle diameter is about 0.15mm in humans (Gougeon, 1998) the surrounding stroma differentiates into the theca interna and theca externa layers to form a multi-layered secondary follicle (Macklon and Fauser 1998). Baboon primordial follicles developed into secondary follicles *in vitro* in defined gonadotrophin-free media (Wandjii *et al.*, 1997), indicating that gonadotrophins are not required for primordial to secondary follicle development in primates. Secondary follicle theca interna cells acquire LH receptors, followed by granulosa cell acquisition of FSH receptors in the late secondary/early antral stage of development (Macklon and Fauser 1998). Theca interna cells of secondary follicles secrete androstenedione and testosterone in response to LH, (Gougeon, 1998). Granulosa cells convert androstenedione and testosterone into estrone and estradiol in response to FSH (Macklon and Fauser 1998). In marmosets, granulosa cells of late secondary/early antral follicles expressed nuclear androgen receptors (Hillier *et al.*, 1997) and androgen stimulated the growth of pre- and early antral follicles in rhesus macaques (Vendola *et al.*, 1998). Late secondary to early antral primate follicle development, during which human follicles only grow from approximately 0.18 to 0.2 mm in diameter, may therefore proceed according to the following sequence of events:

- Theca cell LH expression
- Theca cell production of androgens
- Granulosa cell expression of nuclear androgen receptors
- Granulosa cell expression of FSH receptors
- Granulosa cell conversion of androgens into estrogens.

Subsequent follicular development results in granulosa cell expression of LH receptors. Acquisition of gonadotrophin receptors is concurrent with increased proliferation and the rapid formation of large preovulatory follicles (Robker and Richards 1998). As already mentioned, human preantral follicular diameter is approximately 0.18mm and the early antral follicle 0.2mm (Gougeon 1998). The smallest antral follicles measured in marmoset ovaries were 0.6mm in diameter (Gilchrist *et al.*, 1999). In cycling marmoset ovaries 90% of antral follicles were 0.5-1.0mm in diameter, and the remaining 10% of antral follicles were 1-1.9mm in diameter (Hillier *et al.*, 1987). The one to three follicles destined to ovulate were 2±0.2mm 4 days before ovulation, and ovulating follicles had diameters 2.3±0.2mm 2 days before ovulation (Oerke *et al.*, 1996; Nubbemeyer *et al.*, 1997). Marmoset follicles grow to a maximum of 4mm in diameter before ovulating (Oerke *et al.*, 1996; Hillier *et al.*, 1987) whereas human ovulatory follicles increase from 2mm to over 20mm in diameter during the 14 day follicular phase (Hillier 1991).

1.3.3 Endocrinology of folliculogenesis.

In humans, it takes approximately 90 days for a follicle to develop from the early antral to the preovulatory size. Estradiol production is proportional to size in follicles which have a diameter larger than 8mm (Macklon and Fauser 1998). Estradiol, however, inhibits hypothalamic production of FSH. The length of time that a follicle is capable of responding to elevated FSH levels prior to the initiation of negative feedback mechanisms is thought to result in the selection of a dominant follicle (Macklon and Fauser 1998). The majority of antral follicles respond to falling FSH levels by undergoing atresia, but the dominant follicle is apparently more sensitive to FSH than follicles destined for atresia, and can therefore continue to function despite

falling FSH levels. Increased FSH sensitivity is not via increased FSH receptor expression (Gougeon 1998), but may be attributable to synergistic enhancement of receptor action by growth factors; as well as dominant follicle suppression of subordinate follicles by production of inhibin B. FSH upregulates steroidogenic enzyme activity in marmoset granulosa cells *in vitro* and also stimulates granulosa cell LH receptor expression (Hillier *et al.*, 1988). Optimal exposure to FSH may result in sufficient LH receptors to allow gonadotrophin stimulated steroidogenesis to occur in the face of falling FSH levels.

Marmosets ovulate 1-4 oocytes, and follicle selection appears to occur around day 8 of the follicular phase, when follicles with a diameter >2mm will eventually ovulate, but smaller follicles undergo atresia (Tardif *et al.*, 1993). In 64% of cycles examined, all the follicles which later ovulated were of the same size and had similar rates of growth. Ovulatory follicles were found on both ovaries in the same cycle, and analysis of the distribution of ovulation points suggested the existence of interovarian mechanisms to control the number of ovulatory follicles (Tardif *et al.*, 1993).

1.3.4 Ovulation

Follicular oestradiol stimulates LH production by causing the gonadotrophs of the anterior pituitary to become progressively more sensitive to GnRH. As the follicular phase proceeds, the gonadotrophs therefore produce increasing amounts of LH in response to the same amount of GnRH (Yen, 1972). In normal cycles in women the amplitude and frequency of GnRH pulses increases throughout the follicular phase, and these result in corresponding amplitude and frequency increases in LH pulsitility, culminating in a huge surge of LH immediately before ovulation (March *et al.*, 1979).

In marmosets, follicles destined to ovulate protruded from the surface of the ovary one or two days prior to ovulation. They were highly vascularised around the base and the prospective ovulation point (Torii *et al.*, 1996). Increased blood flow and increased vascular permeability in the thecal layers are part of the ovulatory process (Brannstrom and Janson 1991). Careful observation of granulosa cells collected from women who had received an IVF regime of follicle stimulation and ovulation

induction, revealed the presence of 'multiple, balloon-like structures tethered to the cells surface' (Antczak *et al.*, 1997). Immunohistochemical techniques identified the 'balloons' contents' as being VEGF, leptin and transforming growth factor β (TGFβ). 'Balloon' formation seemed to be related to plasma levels of gonadotrophins, suggesting that the ovulatory LH surge might stimulate granulosa cell secretion of VEGF, which might be a mechanism through which vascular permeability is increased in the theca layer. TGFβ receptor expression has been demonstrated in luteinising theca and granulosa cells in marmosets (Wehrenberg *et al.*, 1998) and the nuclear receptor, steroidogenic factor-1, is also expressed by luteinising theca cells in the marmoset (Wehrenberg *et al.*, 1997). The LH surge causes granulosa cells to cease cycling and begin differentiating into luteal cells (Robker and Richards 1998) by inhibiting cell cycle activators, cyclin D2 and cyclin E, and inducing cell cycle inhibitors such as $p27^{kip1}$ (Robker and Richards 1998). The granulosa cells of $p27^{kip1}$ null mice do not luteinise, and the mice are unable to maintain pregnancy (Robker and Richards 1998). Granulosa cell luteinisation is also associated with loss of the cyclic AMP response element binding protein (Somers *et al.*, 1995), the upregulation of progesterone receptors (Chandrasekher *et al.*, 1991) in marmoset preovulatory follicles (Einspanier *et al.*, 1997), and the upregulation of oxytocin and its receptor in preovulatory follicles (Einspanier *et al.*, 1997) The periovulatory rise in progesterone that has been described in women (March *et al.*, 1979), pigs (Einspanier *et al.*, 1991) and rhesus monkeys (Stouffer *et al.*, 1993) probably occurs in response to increasing LH-stimulation of luteinised theca and granulosa cells (McNatty *et al.*, 1979).

Increasing levels of LH cause desensitisation of LH receptors on theca cells with a subsequent decrease in production of androgens and consequent decrease in oestradiol production (Brannstrom and Janson 1991). The LH surge also stimulates hyaluronic acid accumulation between granulosa cells, resulting in the disruption of gap junctions and granulosa cell dissociation. Granulosa cells become detached from the basement membrane in the apical regions, but in other parts of the follicle appear to migrate towards the thecal layer (Brannstrom and Janson 1991). Extrusion of the cumulus-oocyte complex onto the surface of the ovary is not caused by increased

follicular pressure, but by weakening of the follicle wall at the point of ovulation. The combination of follicle wall, collogen layers and overlying ovarian epithelium comprises the morpho-functional unit of ovulation (Brannstrom and Janson 1991). The surface epithelial cells contain lysosomes which probably contribute to the breakdown of the follicular wall during ovulation (Brannstrom and Janson 1991). The surface epithelium is separated from the follicle by collogen-rich tissue. During ovulation collogen fibres at the ovulatory point become dissociated and fragmented, smooth muscle cells in the theca externa become elongated, and rupture of thecal vasculature occurs (Brannstrom and Janson 1991). Dissociation of collogen fibres and the breakdown of the follicle wall may be mediated by progesterone, which inhibits collagen formation in human follicle cultures *in vitro* (Brannstrom and Janson 1991). Progesterone stimulates the production of prostaglandins and the activation of collagenases (Brannstrom and Janson 1991). LH may also stimulate prostaglandin production directly, with multiple consequences. Prostaglandins act on the vasculature, and may interact with VEGF to increase blood flow and vascular permeability. Prostaglandins also have chemotactic effects on leukocytes, which secrete proteases, and stimulate the production of plasminogen activator, thus enhancing proteolysis and tissue remodelling (Brannstrom and Norman 1993). Increased blood flow and vascular permeability are thought to maintain intrafollicular pressure during the process of oocyte-cumulus extrusion through the ruptured follicle wall (Brannstrom and Janson 1991).

In marmosets, serum levels of progesterone during the follicular phase are less than 20nmol/L, but rise to a mean value of 50nmol/L within 48 hours of the LH surge (Harlow *et al.*, 1984). Marmosets commonly ovulate 1-4 oocytes, but ovulation is not synchronous, and time lags of 12-20 hours were found between ovulations in the same animal (Torii *et al.*, 1996; Oerke *et al.*, 1996).

1.3.5 Formation of the Corpus Luteum

During ovulation the basement membrane separating the theca from the granulosa cell layer is disrupted and blood vessels invade the luteinising granulosa layer (Niswender *et al.*, 1994). Luteinising theca cells also migrate into the granulosa-

lutein, resulting in a wheel-like organisation in which the blood vessels and associated thecal cells are the spokes of the wheel, the theca-lutein the rim, and luteinised granulosa cells fill the spaces between the spokes (Baird 1991; Corner 1956). The granulosa layer folds inwards, so reducing the size of the antrum (Van Blerkom and Motta 1978), and both theca-lutein and granulosa lutein undergo hypertrophy (Niswender *et al.*, 1994). In five human corpora lutea collected on the day of ovulation, or day 1 of the luteal phase, Corner (1956) noted that numerous erythrocytes were caught in a fine fibrin network filling the central cavity, as well as being lodged between granulosa cells. The vasculature was also dilated and engorged. Theca cells were vacuolated, and were beginning to luteinise. By luteal day 2 the thecal layer was completely luteinised and many theca cells were vacuolated. Granulosa cells in the vicinity were also luteinised, but did not contain vacuoles. Capillaries were beginning to invade the granulosa layer, which also had the appearence of streaming towards the central, fibrin-filled cavity. By luteal day 4 angiogenesis was completed and capillaries vascularised the entire granulosa layer and protruded into the central cavity. Granulosa cell luteinisation continued on luteal day 5, and this gave the histological appearence of reducing the space between granulosa-lutein cells as their cytoplasmic volume increased. Fibroblasts started to appear in the central cavity, and theca and granulosa lutein could be distinguished by different nuclei:cytoplasm volumes, in theca-lutein the ratio was greater than 1:3, but in granulosa-lutein the ratio was lower. On luteal day 6 granulosa cell luteinisation was nearly completed, the granulosa lutein cells were densely packed together and their cytoplasm contained lipid droplets. In theca-lutein cells, however, the nucleus occupied most of the cell and the small amount of cytoplasm was vacuolated. Corner (1956) notes that the corpus luteum was probably fully functional by luteal day 7, and that luteinisation of the granulosa layer was completed. Generally the two steroidogenic cell types are easily distinguished and are confined to clearly defined areas (Sawyer *et al.*, 1991). In new world monkeys, however, the steroidogenic luteal cells are of uniform morphological appearance, and it is not clear whether they derive from both theca and granulosa cells, or from just one of these cell types (Webley *et al.*, 1990). The steroidogenic cells in marmoset corpora lutea have diameters larger than 10μm and show a size distribution consistent with one

population of cells. There is a significant increase in mean cell diameter from luteal day 6 to luteal day 14, but no increase thereafter (Webley *et al.*, 1990).

1.3.6 Accessory corpora lutea

Accessory corpora lutea are thought to be formed when non-ovulated follicles become luteinised (Behrman *et al.*, 1993). In marmosets, corpora lutea accessoria (Cla) formation occurs in the periovulatory phase, when large antral follicles with the morphological features of atresia: wide intercellular spaces between granulosa cells, disrupted granulosa layer architecture and cell death around the periphery of the antrum, undergo luteinisation in the outer theca cell layer and in the granulosa cell layer closest to the basement membrane. The outer, luteinising cells of otherwise atretic follicles express nuclear SF-1/Ad4BP. Mature Cla consist of layers of luteinised cells which express SF-1/Ad4BP, whereas true CL do not express SF-1/Ad4BP (Wehrenberg *et al.*, 1997). It is possible that steroidogenic cells in Cla may also be larger in diameter than the steroidogenic cells of true corpora lutea (Wulff *et al.*, 1996)

1.4 The Functioning Corpus Luteum

1.4.1 Luteal Phase Steroid Hormone Production.

Steroid hormones are derived from cholesterol, and the major source of cholesterol in human corpora lutea is plasma low density lipoprotein (LDL) which is taken up by steroidogenic luteal cells via specific LDL receptors (Brannian *et al.*, 1991; Fairchild-Benyo *et al.*, 1993: Strauss and Miller 1991). Cholesterol can either be stored, or transferred across mitochondrial membranes where it is converted to pregnenolone by cholesterol side-chain cleavage cytochrome P450 enzyme (P450scc, Niswender *et al.*, 1994). Pregnenelone is in turn converted to progesterone by the enzyme 3 beta hydroxysteroid dehydrogenase isomerase (3β HSD, Savard, 1973), or is converted into androgens by 17α hydroxylase cytochrome P450 ($P450_{17\alpha}$). Androgens can be converted into oestrogens by aromatase cytochrome P450 (P450arom). The enzyme 17 beta hydroxysteroid dehydrogenase (17β HSD)

converts androstenedione or oestrone to testosterone or oestradiol respectively (Savard, 1973; Strauss and Miller 1991). In human corpora lutea, the pattern of steroidogenesis is similar to that found in the follicle (Ohara *et al.*, 1987). Theca-lutein cells, or small luteal cells, contain the enzymes $P450_{17\alpha}$ and P450scc and produce both progesterone and androgen in response to stimulation by LH, Granulosa-lutein, or large luteal cells, contain the enzymes P450arom and P450scc and produce oestrogen and high basal levels of progesterone (Behrman *et al.,* 1993; Sasano *et al.,* 1989).

The human corpus luteum produces the steroid hormones progesterone, 17-hydroxy-progesterone, 4-androstenedione, estrone, 17β-estradiol, pregnenolone and 20α-hydroxy-4-pregnen-3-one and possesses all the biosynthetic enzymes of the steroidogenic pathway (Savard, 1973; Sasano *et al.,* 1989).

The primate luteal phase can be separated into three periods based on the amount of progesterone produced. In marmosets, the first period is characterised by increasing progesterone concentrations, which rise from 40ng/ml to 87.4ng/ml by the mid luteal phase (Harding *et al.*, 1982). Progesterone concentrations remain at this level during the second period, then decrease during the third period to <10ng/ml over the course of three to five days (Harding *et al.*, 1982). The same pattern occurs in women. During the follicular phase in normally menstruating women between 24 and 34 years old, progesterone concentrations are 0.3±0.03 ng/ml (n=5) (Soules *et al.,* 1984). After ovulation progesterone levels increase during the early luteal phase, then are maximal at 7.5±1.7 ng/ml (n=5) (Soules *et al.,* 1984) from day 8-12 of the mid luteal phase, then decrease gradually in the late luteal phase until menstruation occurs (Zeleznik 1991). Similar patterns of secretion and progesterone concentrations have also been observed in baboons (Stevens *et al.*, 1970) and rhesus macaques (Monroe *et al.,* 1970).

1.4.2 The Regulation of Luteal Cells

In ruminents, theca-lutein, or small luteal cells, responded to LH with a 20-fold increase in progesterone production, but granulosa-lutein, or large luteal cell progesterone production was not stimulated by LH (Niswender *et al.*, 1994). Both cell types expressed LH receptors (Harrison *et al.*, 1987), but LH-binding only stimulated formation of the secondary messenger cAMP in small luteal cells, and the effect of LH-binding on large luteal cells was unclear. Large luteal cells also had receptors for the prostaglandins E and F2α, whereas these were not apparent on small luteal cells (Knickerbocker *et al.*, 1988; Sawyer *et al.*, 1991). Human theca lutein cells responded to hCG with an increase in progesterone and androgen production, whereas granulosa lutein did not respond to hCG (Ohara *et al.*, 1987; Behrman *et al.*, 1993). Small and large luteal cells isolated from macaque corpora lutea responded to hCG or the secondary messenger analogue dbcAMP with increased progesterone production (Hild-Petito *et al.*, 1989), so apparently both cell types have the ability to respond to LH in at least one non-human primate. Marmosets have only one population of steroidogenic cells (Webley *et al.*, 1990) which may be derived from both granulosa and theca cells, or from only one of these populations. Marmoset steroidogenic cells from any stage of the luteal phase responded to hCG with a two-fold increase in progesterone production (Michael and Webley, 1993). The *in vivo* plasma progesterone concentrations were the same on luteal day 3 and luteal day 14 (Michael and Webley, 1993), but the *in vitro* gonadotrophin-free basal production of progesterone by pieces of luteal tissue decreased with increasing age of the source corpus luteum. Corpora lutea obtained on luteal days 3, 6 and 14 secreted 700, 21 and 8.2 pmol/mg tissue respectively (Michael and Webley, 1993). Cloprostenol did not reduce plasma progesterone concentrations *in vivo* on luteal day 3, but did inhibit hCG-stimulated cAMP accumulation in 3 out of 5 day 3 corpora lutea *in vitro.* These results suggest that PGF2α receptors were present and functional on luteal day 3, but that basal progesterone production was more important than gonadotrophin-stimulated progesterone production in the early luteal phase, and that the gonadotrophin-

stimulated component of progesterone production became increasingly prevalent as the corpus luteum aged.

1.5.0 Regression of the Corpus Luteum

1.5.1 LH in Luteal Regression.

Withdrawal of LH causes a rapid decrease in luteal steroidogenesis. LH withdrawal and inhibition of steroidogenesis were effected by hypophysectomy in rats (Smith, 1930) or by immunoneutralisation of LH in sheep (Fuller and Hansel, 1970) or by administration of a GnRH antagonist in women (Mais *et al.*, 1986) and macaques (Fraser *et al.*, 1986; Hutchinson *et al.*, 1986). Reduction in levels of circulating gonadotrophins by administration of GnRH antagonists also caused decreased progesterone production in marmosets (Hodges *et al.,* 1988) suggesting that decreased plasma LH concentrations, and/or pulsitility, might precede the luteal decrease in steroidogenesis *in vivo*. However gonadotrophin secretion did not decrease *in vivo* at the time of luteolysis in macaques or women (Salamonsen *et al* 1973; Hutchison *et al.,* 1986; Sotrel *et al.*, 1981) and in marmosets a PGF2α analogue caused luteolysis without a corresponding decrease in plasma LH concentrations (Webley *et al.,* 1991) suggesting that decreased serum gonadotrophin levels were either unnecessary for luteolysis in marmosets, or that the administered PGF2α superseded the effects of LH.

The frequency of LH pulsitility *in vivo* decreased from one pulse per hour in the mid-luteal phase to one pulse every eight hours in the late luteal phase in macaques (Zeleznik, 1991) but maintenance of LH pulsitility at one pulse per hour did not delay luteolysis nor extend the luteal phase (Zeleznik 1991; Hutchinson *et al.,* 1986). Therefore, although LH is luteotrophic and steroidogenesis can not proceed in the absence of LH, *in vivo* luteal regression is not caused by decreased LH pulsitility nor decreased serum concentrations. However, it is possible that the endogenous production of PGF2α might disconnect the LH receptor from its secondary

messenger pathway, so reducing the ability of luteal cells to respond to LH (see subsequent section).

Administration of GnRH antagonist results in decreased steroidogenesis, but induction of luteal regression depends upon the duration of administration, and is also affected by the stage of the luteal phase. This was shown in macaques in which the hypothalamus was surgically disconnected from the pituitary. This prevented GnRH stimulation of the pituitary and resulted in decreased endogenous gonadotrophin production. Pulsatile infusion of exogenous GnRH to induce a normal menstrual cycle provided a model in which GnRH could be withdrawn at any stage of the cycle and its effects examined. Complete withdrawal of LH in the early or mid luteal phase resulted in a cessation of steroidogenesis, but when GnRH infusion was resumed three days later steroidogenesis also resumed, and luteolysis occured 14-16 days after ovulation as though there had been no interruption in progesterone production. Withdrawing LH from days 8 to 11 of the luteal phase also resulted in decreased steroidogenesis, and menses began on day 11. If GnRH infusion was resumed on day 11, however, progesterone production was similar to that seen in control untreated cycles and onset of menses occurred at the same time in both groups. LH withdrawal during luteal regression on day 14 did not, however, result in restoration of progesterone production when GnRH infusion was resumed 3 days later (Hutchison and Zeleznik, 1985). Therefore it was argued that although LH is obligatory for maintenance of luteal progesterone secretion, it appears that there is a separate mechanism for regulating luteal lifespan. LH can also be withdrawn by using GnRH antagonists instead of surgery (Mais *et al.,* 1986) but administration of GnRH antagonist in women from days 7-9 of the luteal phase caused early onset of menses and normal progesterone production was resumed in only one of the four subjects. The latter may be attributed to only partial suppression of LH production to 48% of normal. It was therefore assumed that steroidogenesis still continued during the period of antagonist treatment, and in addition, the luteal phase of women is slightly shorter than that of macaques, so administration of the GnRH antagonist may have occurred at the beginning of luteal regression. Administration of a single dose of GnRH antagonist to stumptailed macaques at different stages of the luteal phase also resulted in a suppression of serum progesterone at all stages followed by a

subsequent resumption of steroidogenesis and luteal phases of the normal length (Fraser *et al.,* 1986). Administration of GnRH antagonist to macaques for three consecutive days at different stages of the luteal phase, however, suppressed LH secretion for 4 days, prevented subsequent resumption of steroidogenesis and caused early onset of menses (Fraser *et al.*, 1987). Therefore it appears that the duration of LH inhibition determines whether luteolysis occurs early or not. If inhibition of LH is 1-3 days, length of the primate luteal phase remains unchanged, and under these circumstances it appears that there are separate mechanisms for regulating steroidogenesis and luteal lifespan.

In marmosets, peak progesterone production occurs during the mid-luteal phase, which can conservatively be designated as being from luteal day 8 to luteal day 12. A single dose of GnRH antagonist on luteal day 10 should therefore inhibit steroidogenesis, but not cause luteal regression. The studies described above suggest that LH secretion and steroidogenesis in marmosets should resume after clearance of administered GnRH antagonist. It is not known, however, whether LH-withdrawal during the mid-luteal phase causes any morphological changes to primate corpora lutea, and this will be examined in the marmoset corpora lutea collected in the course of these studies. Secondly, administration of PGF2α to marmosets also resulted in decreased steroidogenesis (Summers *et al.,* 1985). If the sole action of PGF2α was to decrease steroidogenesis by inhibiting LH receptor secondary messenger pathways (see subsequent section), it is reasonable to expect PGF2α-treated corpora lutea to be similar to GnRH antagonist treated corpora lutea. Alternatively, and more probably, PGF2α inhibited steroidogenesis by alternative mechanisms (see subsequent section). And affected other aspects of luteal function. If PGF2α does have multiple effects upon corpora lutea, it can be hypothesised that PGF2α-treated corpora lutea will be functionally and morphologically different from GnRH antagonist treated corpora lutea.

1.5.2 PGF2α in Luteal Regression

Goding (1974) showed that in the ewe PGF2α produced by the uterus was transported to the ovary by the uterine vein and a countercurrent system allowed PGF2α to pass from the vein into the ovarian artery and hence into the ovary to instigate functional luteolysis. Removal of the uterus prevented production of a luteolytic dose of PGF2α and delayed the onset of luteolysis (Horton and Poyser, 1976). Interestingly, in rats, although luteolysis was delayed after hysterectomy, it still occurred after an extended luteal phase (Wang *et al.*, 1993), indicating that although uterine PGF2α is the usual luteolytic mechanism in rats, there may also be additional intraovarian luteolytic mechanisms. Hysterectomy did not delay luteolysis in humans (Beling *et al.*, 1970) or macaques (Neill *et al.*, 1969), therefore primate luteolysis is not a consequence of uterine prostaglandin production. Intramuscular administration of PGF2α to baboons *in vivo* did not cause luteolysis (Eley *et al.*, 1987) but this was probably due to rapid clearance of PGF2α before it was able act on the ovary. Intraluteal administration of PGF2α caused decreased steroidogenesis in marmosets (Summers *et al.,* 1985; Hearn and Webley 1987) macaques (Auletta *et al.,* 1984; Zelenski-Wooten and Stouffer, 1990) and humans (Bennegard *et al.,* 1991) which suggests that a luteolytic pathway utilising PGF2α may also occur in primates although the source of PGF2α may differ from other eutherian mammals. The *in vivo* administration of PGF2α caused an immediate decrease in progesterone production without a corresponding decrease in plasma LH concentration in marmosets (Webley *et al.,* 1991) and humans (Bennegard *et al.*, 1991) indicating that PGF2α did not exert a luteolytic effect by inhibiting LH production, but probably acted locally within the corpus luteum.

Human corpora lutea produce PGF2α, PGE_2, PGI_2 (prostacyclin), PGD_2 and thromboxanes (Challis *et al.,* 1976; Swanston *et al.*, 1977; Valenzuela *et al.*, 1983). The intraluteal concentrations of PGE_2 and PGF2α in women were highest during the early luteal phase and decreased as the corpus luteum aged (Challis *et al.*, 1976; Swanston et al., 1977; Patwardhan and Lanthier 1985). PGF2α concentrations

decreased proportionally more than PGE_2, therefore the ratio of PGE_2:PGF2α increased with increasing luteal age (Challis et al., 1976, Table 1). During the mid luteal phase there was approximately 4 times more PGE_2 than PGF2α, and this increased to a ratio of 8:1 PGE_2 to PGF2α in the late luteal phase (Challis *et al,* 1976). Later work confirmed this increase in the ratio of PGE_2:PGF2α (Vijayakumar and Walters, 1983). Conversely, in another study utilising 16 human corpora lutea, PGE_2 decreased more markedly than did PGF2α (Patwardhan and Lanthier 1985). In rhesus macaques, PGE_2 concentrations were highest during the early luteal phase and decreased with increasing luteal age (Houmard and Ottobre 1989) whereas PGF2α concentrations were high during the early luteal phase, decreased to a nadir during the mid luteal phase, and increased again during the late luteal phase.

Table 1: Endogenous Prostaglandin and Steroid Concentrations in Human Corpora Lutea.

	PGE ng/g	**PGF2α ng/g**	**Prog. ng/g**	**Oestradiol 17β ng/g**	**Author**
Early-Mid Luteal Phase	34	10	7500	750	Challis *et al* 1976 n=21
	-	3	2000	200	Swanston *et al* 1977 n=40
Late Luteal Phase	22	3	6000	200	Challis *et al* 1976 n=21
		3.5	500	100	Swanston *et al* 1977 n=40
	-	13-46			Shutt *et al.*, 1975 n=4

PGE_2, PGI_2 and PGD_2 stimulate progesterone production *in vitro* in human corpora lutea (Bennegard *et al.,* 1990). PGE_2 and PGF2α are also luteotrophic during the mid luteal phase, and stimulate *in vitro* progesterone production by macaque (Stouffer et al., 1979) and marmoset () luteal cells. However, prostaglandin-stimulated steroidogenesis is lower than that caused by hCG stimulation (Stouffer *et al.*, 1979).

The trophic effect of prostaglandins during the mid luteal phase was confirmed by the *in vitro* treatment of macaque mid luteal phase cells with prostaglandin synthase inhibitors. Basal progesterone production was halved, and hCG-stimulated progesterone production completely abolished (Zelinski-Wooten *et al.*, 1990). Progesterone production was also decreased after the *in vivo* administration of prostaglandin synthesis inhibitor to women (Fulghesu *et al.*, 1993).

The *in vivo* administration of PGF2α from the mid to late luteal phase inhibits progesterone production in marmosets (Summers *et al.*, 1985, Michael and Webley, 1993) and macaques (Auletta and Kelm, 1994). Administration of a prostaglandin synthesis inhibitor to women during functional luteal regression (Gibson and Auletta 1986) slowed the endogenous decline in progesterone production. This suggests that intraluteal prostaglandins inhibit steroidogenesis *in vivo*, and reducing prostaglandin synthesis by the *in vivo* administration of ibuprofen decreased this inhibition and functional luteolysis was therefore slower than in controls. The *in vivo* administration of PGF2α did not abolish hCG-stimulated steroidogenesis in macaques (Auletta and Kelm, 1994) or marmosets (Hearn and Webley 1987), in marked contrast to its effects *in vitro.* PGF2α inhibited hCG-stimulated steroidogenesis in human (Dennefors *et al.*, 1982; Bennegard *et al.*, 1984) macaque (Sotrel *et al.*, 1981; Zelinski- Wooten *et al.*, 1990) and marmoset luteal cells *in vitro* (Michael and Webley 1993).

1.5.3 Luteal Blood Flow and PGF2α

PGF2α receptors are found on steroidogenic luteal cells (Rao *et al.,* 1977; Powell *et al.,* 1974), but are not found in the vasculature either in the corpus luteum nor in the rest of the ovary (Orlicky *et al.*, 1992), so although PGF2α is a potent vasoconstrictor its immediate luteolytic effects upon the corpus luteum are unlikely to be mediated by vasoconstriction and decreased blood flow. Intraluteal injection of PGF2α in humans did not cause any changes in blood flow or oxygen saturation (Bennegard *et al.*, 1991) and in rabbits, luteal blood flow was decreased by only 29% eight hours after adminstration of PGF2α (Bruce and Hillier, 1974) Additional

animal studies support the premise that functional luteolysis precedes decreased luteal blood flow (Wiltbank *et al.,* 1989; Wiltbank *et al.*, 1990)

1.5.4 Oxygen Free Radicals and PGF2α

Oxygen free radicals are atoms or molecules which contain unpaired electrons, and their reactivity is related to their ability to oxidise (remove electrons from) other molecules (Halliwell and Gutteridge, 1989). The superoxide anion radical (O_2^-) is mildly reactive and is usually degraded to the even less reactive hydrogen peroxide radical (H_2O_2) by superoxide dismutase. H_2O_2 in turn is degraded to water and oxygen by catalase or by glutathione peroxidase (Halliwell and Gutteridge, 1989). However O_2^- can react with H_2O_2 in the presence of transition metals such as iron to form the highly reactive hydroxyl radical OH^- by the Haber-Weiss reaction (Fridovich, 1986). The hydroxyl radical is capable of extracting a hydrogen atom from unsaturated fatty acids and so can initiate lipid peroxidation of cell membranes, a process which can result in the formation of cytotoxic aldehydes which have longer half-lives than oxygen radicals and can attack enzymes, receptors and other membrane proteins (Riley and Berhman, 1991). Lipid peroxidation causes a reduction in membrane fluidity, aggregation and rearrangement of membrane phospholipids, increased permeablility, loss of compartmentalisation and eventually complete loss of membrane architecture (Riley and Berhman, 1991). One defense mechanism against lipid peroxidation is the removal of peroxidized fatty acids by phospholipase A_2, and lipid peroxides stimulate phospholipase A_2 pathways.

Corpora lutea have high concentrations of antioxidants: oestradiol (Murdoch 1998), α-tocopheral, ascorbic acid and β-carotene, as well as superoxide dismutase, glutathione peroxidase and catalase (Behrman *et al.*, 1993). P450 enzymes, which contain a cytochrome iron group, generate free radicals during steroidogenesis, and it is likely that high concentrations of luteal antioxidants are required to scavenge these free radicals (Young *et al.,* 1994). There are a number of interactions between the antioxidants. Vitamin E plays a major role in terminating lipid peroxidation chain reactions and in protecting cell membranes from oxygen free radical attack (Behrman

et al., 1993). Cytoplasmic water-soluble ascorbic acid recycles oxidised inactive lipid-soluble α-tocophoral back to the active, reduced state, hence ascorbic acid depletion can be an indicator for the presence of oxygen free radicals (Behrman *et al.*, 1993). Ascorbic acid concentrations are depleted during luteal regression, but α-tocopherol levels increase (Aten *et al.,* 1992).

Nitric oxide is a highly reactive free radical gas which is produced by vascular endothelial cells and macrophages (Bredt and Snyder, 1994) and which can inhibit the conversion of cholesterol to pregnenolone in a hCG-stimulated murine Leydig cell line. Nitric oxide also inhibits LH-stimulated testosterone production in rat Leydig cells (Punta *et al.,* 1996) and inhibits steroidogenesis in human granulosa lutein cells (Van Vooris *et al.,* 1994). Inhibition of nitric oxide synthesis caused an increase in estradiol production but did not affect progesterone production by rat luteal cells *in vitro* (Olson *et al.*, 1996). Nitric oxide can be generated by the enzyme nitric oxide synthase (NOS) and there are two different isoforms of NOS, the constituitively expressed endothelial NOS (eNOS) and the inducible isoform of NOS (iNOS). Immunocytochemistry has demonstrated positive eNOS immunoreactivity around the blood vessels of the corpora lutea in rats (Zackrisson *et al.,* 1996), but iNOS immunoreactivity is highest in non-steroidogenic cells during luteal regression (Jablonka-Shariff and Olson, 1997).

Ovaries collected from rats at various times after PGF2α administration have been used as a source of plasma membrane preparations. Plasma progesterone concentrations in rats are significantly reduced 20 minutes after administration of PGF2α, and continue to decline thereafter. Sawada *et al.*(1991) noted a significant 3-fold increase in membrane superoxide radical levels in ovaries removed 10 minutes after PGF2α injection, but O_2^- levels were reduced to pre-treatment values in ovaries removed 40 minutes after PGF2α injection, and did not increase again in the subsequent 2 hours. Phospholipase A_2 activity was significantly elevated 20 minutes after PGF2α treatment and lipid peroxidation was significantly higher than controls 2 hours post PGF2α although activities of superoxide dismutase, catalase and

glutathione peroxidase remained unchanged (Sawada and Carlson, 1991). Major sources of superoxide include the enzymes NADPH oxidase and xanthine oxidase which has luteolytic effects in rat luteal cells (Gatzuli *et al.,* 1991). In endothelial cells, xanthine oxidase is activated after ischemic insult, but it has also been shown that neutrophils stimulate conversion of xanthine dehydrogenase to xanthine oxidase in endothelial cells in a dose dependent fashion. This is not caused by neutrophil generated oxygen free radicals, but by cell-cell contact (Phan *et al.*, 1989). Hydrogen peroxide is also produced during luteolysis (Riley and Behrman 1991b) and it inhibits LH-stimulated cAMP-dependent transport of cholesterol into mitochondria in rat luteal cells *in vitro* with a consequent decrease in steroidogenesis (Behrman and Aten, 1991). It has also been suggested that hydrogen peroxide inhibits cAMP production by uncoupling the G-protein (Behrman and Preston, 1989), thus disconnecting the LH-receptor from its secondary messenger pathway.

In summary, hydrogen peroxide and the superoxide radical (Sawada *et al.*1991) are generated during PGF2α-induced luteolysis. Hydrogen peroxide (H_2O_2) directly inhibits steroidogenesis (Behrman and Aten, 1991; Behrman and Preston, 1989). Hydrogen peroxide and superoxide can generate a third radical, hydroxyl (OH^-), which causes lipid peroxidation. Subsequent membrane perturbation may cause generalised disruption of luteal cell support by gonadotrophins and other factors. Nitric oxide inhibits luteal steroidogenesis (Van Vooris *et al.,* 1994) and nitric oxide synthesis increases during luteolysis (Jablonka-Shariff and Olson, 1997).

1.5.5 LH Receptor: Structure, Secondary Messenger Pathways and Interaction with PGF2α

PGF2α does not affect basal progesterone production in isolated corpora lutea and in human granulosa-lutein cells *in vitro*, but it does inhibit LH and hCG-stimulated progesterone production (Michael *et al.*, 1994). PGF2α does not inhibit LH production in marmosets (Webley *et al.,* 1991) or macaques (Sotrel *et al.*, 1981) therefore its inhibitory effects on LH and hCG-stimulated progesterone production

may occur by (i) decreasing ligand binding or by (ii) decreasing functional LH receptor levels or by (iii) inhibiting intracellular LH receptor secondary messenger signalling.

LH and hCG both bind to the same glycoprotein cell surface receptor, found on steroidogenic cells in corpora lutea (Fitz *et al.,* 1982; Harrison *et al.,* 1987) The LH/hCG receptor has an extracellular hormone-binding domain (Rodriguez and Segaloff, 1990), seven transmembrane domains and a small intracellular domain which binds to G-proteins.
Ligand-binding activates the GTP-binding G(s) protein and activates adenylate cyclase, which can trigger off three different intracellular secondary messenger pathways. The cyclic adenosine-3',5'-monophosphate (cAMP)-protein kinase A (PKA) signal transduction pathway has been shown to mediate gonadotrophin-stimulated steroidogenesis (Marsh, 1970; Behrman *et al.,* 1993). Adenylate cyclase is also known to activate phospholipase C (PLC) which can hydrolise phosphotidylinositol to form diacylglycerol (DAG) which can remain as a membrane-bound second messenger that regulates the activation of protein kinase C (PKC) while the inositol triphosphate (IP3) fragment can move into the cytoplasm and regulate calmodulin-dependent kinase activity by releasing cytosolic stores of Ca^{2+}. The third intracellular pathway regulated by activated adenylate cyclase is protein kinase mediated phosphorylation of glycoprotein porous channels to permit an influx of Ca^{2+} which depolarizes the membrane.

1.5.5.1 Effects of PGF2α on binding affinity of the LH/hCG receptor.

Luteal membrane preparations were obtained from rats treated with luteolytic doses of PGF2α and the amount of iodinated hCG bound by these fractions was determined. There was no decrease in receptor affinity or binding two hours after administration of PGF2α, although there was a 70% decrease in progesterone concentration at this time (Grinwich *et al.*, 1976). Similarly, levels of iodinated LH-binding to sections of human corpora lutea were not decreased 14 days after ovulation when progesterone levels were falling (Duncan *et al.,* 1996) and luteal LH

receptor binding affinity is also maintained while progesterone production decreases in macaques (Cameron and Stouffer, 1982; Sotrel *et al.,* 1981). Therefore PGF2α does not exert its inhibitory effects on LH and hCG-stimulated progesterone production by decreasing LH binding or LH affinity for its receptor.

1.5.5.2 Effects of PGF2α on functional LH/hCG receptor levels.

In humans, LH receptor numbers correlate to progesterone levels and are low during the early luteal phase, high during the mid luteal phase and decrease after functional luteal regression (Lee *et al.*, 1973; McNeilly *et al.,* 1980). PGF2α causes decreased expression of functional LH receptors in rats (Grinwich et al., 1976), and macaques (Cameron and Stouffer, 1982) but only after progesterone levels have decreased, indicating that the loss of LH receptor is not the cause of functional regression. LH/hCG receptor mRNA expression increases in the early luteal phase but then remains constant throughout the rest of the luteal phase in cynomologus monkeys (Ravindranath *et al.,* 1992) and in humans (Duncan *et al.,* 1996) but decreases in the late luteal phase when functional luteal regression is well advanced (Nishimori *et al.*, 1995).

Messenger RNA splice variants which encode a truncated LH-R without a transmembrane domain but with regions of the hCG and LH-binding extracellular domain have been found in rat, human, pig and sheep corpora lutea (Bacich *et al.*, 1994). The A-form is the full length functional mRNA for the receptor, but there is 3.5 times more B-form than A-form splice variant in mid luteal phase sheep corpora lutea. The B-form lacks a protein kinase-C phosphorylation consensus site, so although its protein product would be indistiguishable from the A-form protein product in binding studies and mRNA assays, its functional effect upon steroidogenesis may differ significantly. It is not known what proportion of mRNA splice variants are translated, if any, neither is it known how proportions of differing splice variants change with increasing luteal age, nor whether PGF2α upregulates functionally inactive LH receptor.

1.5.5.3 Effects of PGF2α on LH receptor secondary messenger pathways.

Like the LH receptor, the PGF2α receptor is also coupled to signal transduction enzymes and ion channels by GTP-binding proteins, but unlike the LH receptor PGF2α stimulates cyclic guanosine phosphate (cGMP) accumulation (Sotrel *et al.*, 1981). PGF2α also stimulates the calcium-dependent protein kinase C (PKC), which has been shown to mediate the antigonadotrophic actions of PGF2α in ovine luteal cells (Wiltbank *et al.*, 1990) and human granulosa-lutein cells (Abaysekara *et al.*, 1993). Classically PKC activation is by phospholipase C catalysed hydrolysis of membrane phosphoinositides with consequent generation of diacylglycerol (DAG) and inositol triphosphate (IP3), but phosphoinositides are not generated during luteolysis in the rat (Lahav *et al.*, 1988) or marmoset (Michael and Webley 1993) therefore PGF2α may cause activation of phospholipase A_2 (Sawada and Carlson, 1991; Riley and Carlson 1987) which is capable of generating arachidonic acid which in turn can activate PKC (Lopez-Ruiz *et al.*, 1992). PGF2α also activates cyclic nucleotide phosphodiesterases which inactivate cAMP, and it has been shown that cAMP phosphodiesterase activity is mediated by PKC-dependent mechanisms (Michael and Webley, 1991). Formation of LH-dependent cAMP was inhibited 15 minutes after administration of PGF2α in rats (Thomas *et al.*, 1978, Dorflinger *et al.*, 1983) and this is due to uncoupling of the G(s) protein from adenyl cyclase (Abayasekara *et al.*, 1993). PGF2α inhibited cAMP accumulation in LH-stimulated marmoset slices from mid luteal phase corpora lutea *in vitro*, but did not affect basal progesterone production or basal cAMP accumulation (Michael and Webley, 1993). In rat corpora lutea PGF2α increased membrane phospholipase A_2 activity and lipid peroxidation (Sawada and Carlson, 1991) with a subsequent decrease in membrane fluidity and inhibition of LH receptor and G-protein diffusion. This is a potential mechanism for uncoupling G-proteins from the catalytic subunit of adenyl cyclase (Michael *et al.*, 1994).

In summary, PGF2α does not decrease LH binding, nor LH affinity for its receptor, but it does cause disconnection of the LH receptor from its intracellular signaling pathway.

1.5.6 PGF2α and Luteal Cells *in vitro*.

Administration of PGF2α to dispersed rat (Thomas *et al.*, 1978) or marmoset (Webley *et al.*, 1989) mid luteal phase cells *in vitro* stimulates progesterone production. Since *in vivo* administration of PGF2α inhibits progesterone production, it seems that the vasculature may be involved in mediating the luteolytic effects of PGF2α *in vivo*. However, this is a somewhat paradoxical conclusion because PGF2α receptors have not been identified in luteal vasculature (Orlicky *et al.*, 1992). It is possible that cell dispersion techniques modify PGF2α receptors on the steroidogenic cells in a way that prevents inhibition and permits stimulation of steroidogenesis. It is also possible that PGF2α binds to its receptors on luteal steroidogenic cells which respond by producing factors which stimulate oxygen free radical production by endothelial cells of the vasculature, or by vascular leukocytes. Another possiblity is that PGF2α acts directly on endothelial cells by a mechanism that does not require a classical PGF2α-receptor.

1.5.7 Summary of the Luteolytic Actions of PGF2α

The first luteolytic action of PGF2α is to stimulate the production of the superoxide and hydrogen peroxide radicals. PGF2α-stimulated radical production may be mediated by vascular leukocytes or endothelial cells. Hydrogen peroxide inhibits LH-stimulated cholesterol transport into mitochondria, so immediately inhibits steroidogenesis.

Superoxide and hydrogen peroxide can generate hydroxyl radicals, which can cause lipid peroxidation. Lipid peroxides stimulate phospholipase A2 pathways, which stimulate protein kinase C, which mediates cyclic nucleotide phosphodiesterase inactivation of cAMP. Lipid peroxidation may also cause dissociation of G-proteins from the catalytic subunit of adenyl cyclase (Michael *et al.*, 1994). The second luteolytic action of PGF2α is therefore to disconnect the LH receptor from its intracellular signaling pathway. The third luteolytic action of PGF2α, inhibition of LH receptor expression, occurs after progesterone production has decreased. The

main luteolytic action of PGF2α is therefore to prevent LH-stimulated progesterone production.

1.5.8 Leukocytes, Cytokines and Growth Factors During Functional Luteal Regression.

Immunosuppressive glucocorticoid prevents natural, but not PGF2α-induced luteolysis in the rat, which suggests a role for the immune system in luteolysis (Wang *et al.*, 1993). Changing LH pulsitility does not directly affect the duration of the functional luteal phase, but it may regulate steroidogenic cell production of factors which attract leukocytes into the corpus luteum. Luteal steroidogenic cells secrete granulocyte macrophage colony stimulating factor (Jasper *et al.,* 1996) which is a chemoattractant for lymphocytes, neutrophils and macrophages, and macrophage numbers increase as the luteal phase proceeds in rabbits (Bagavandoss *et al.*, 1988), sheep and humans (Lei *et al* 1991, Gillim *et al.,* 1969) and pigs (Zhao *et al.*, 1998). Monocyte chemoattractant protein-1 (MCP-1) increases during luteolysis in bovine corpora lutea (Penny *et al.*, 1998). Hehnke *et al* (1994) found that macrophage numbers were significantly increased 6 hours after intraluteal administration of PGF2α to pigs in the mid luteal phase, whereas progesterone levels were only significantly decreased 12 hours after administration. Implants containing vehicle resulted in an increase in macrophage numbers but no change in progesterone concentration, indicating that the presence of macrophages alone did not induce luteolysis, but that the combination of macrophages and PGF2α was necessary for induction of functional luteolysis (Hehnke *et al.,* 1994).

Macrophages secrete interleukin 1, which stimulates oxygen free radical production by both neutrophils and monocytes (Behrman *et al.,* 1991). Interleukin 1 also stimulates steroidogenic cell PGF2α production (Benyo-Fairchild and Pate 1992), although IL-1β mRNA did not change prior to or during luteolysis in bovine corpora lutea (Petroff *et al.*, 1999). Additionally, macrophages secrete tumour necrosis factor α (TNFα). Intraluteal administration of TNFα induced luteolysis in pigs (Wuttke *et*

al., 1992) probably by inhibiting gene expression of P450scc, 3βHSD and P450aromatase (Wuttke *et al* 1995). TNFα also inhibited LH-stimulated progesterone production and stimulated PGF2α production in bovine luteal cells *in vitro* (Benyo and Pate 1992) but did not inhibit progesterone production by human luteal cells *in vitro*, although it did significantly potentiate IFNγ-induced progesterone inhibition (Wang *et al.*, 1992).

TNFα immunoreactivity was found in the endothelial cells of porcine corpora lutea, but this immunoreactivity diminished during functional luteal regression (Hehnke-Vagnoni *et al.,* 1995). However, another study using porcine corpora lutea found that TNFα immunostaining was associated primarily with macrophages in the vasculature, but not the microvasculature, and appeared to increase as the luteal phase progressed (Zhao *et al.*, 1998). These contradictory results may be attributable to the greater specificity of antibodies used in the latter study. TNFα immunostaining was also found in granulosa lutein and theca lutein cells of human corpora lutea. Immunostaining intensity peaked during the mid luteal phase, decreased in the late luteal phase and diminished further as regression proceeded (Kondo *et al.*, 1995). Regressed corpora lutea, however, were bordered by macrophage-like cells which exhibit intense immunostaining for TNFα (Kondo *et al.*, 1995). TNFα mRNA was not found within luteal tissue after PGF2α-induced luteolysis in sheep (Ji *et al.*, 1991), although it increased during the late luteal phase and after PGF2α induced luteolysis in bovine corpora lutea (Petroff *et al.*, 1999). It is possible that TNFα inhibits the expression of Steroidogenic Acute Regulatory Protein (StAR) and therefore inhibits progesterone production (Chen *et al.*, 1999). TNFα therefore appears to have luteolytic potential, but the mechanism of action in luteolysis *in vivo* is presently unknown.

Neutrophilic granulocytes and lymphocytes are also present in regressing human corpora lutea, but these cell numbers do not increase with increasing luteal age (Wang *et al.*, 1992). Lymphocytes secrete interleukin-2 (IL-2) and interferon γ (IFN-γ), and these cytokines inhibit hCG-stimulated progesterone production by granulosa-lutein cells *in vitro* (Wang *et al.,* 1991; Wang *et al.*, 1992). However, mRNA for IL-2 nor its receptor were detected in bovine corpora lutea, and IFN-γ

mRNA decreased prior to luteolysis (Petroff *et al.*, 1999). Neutrophils have been shown to adhere to endothelial cells and induce nitric oxide production (Phan *et al.*, 1989).

Immunoreactive TGFβ1 and β2 have been detected in the steroidogenic cells of human corpora lutea and in corpora albicantes (Chegnini and Flanders 1992).

In summary, immune system cells and cytokines occur in primate corpora lutea, and they have the ability to inhibit LH-stimulated progesterone production, and to stimulate the production of oxygen free radicals. Leukocyte and cytokine interactions with PGF2α or the luteal vasculature have not been examined in primate corpora lutea, and research in these areas is likely to yield data that would increase understanding of luteolysis in primates.

1.5.9 Oestrogen in Luteal Regression

Administration of oestrogen caused luteal regression in macaques (Auletta *et al.*, 1976) and women (Gore *et al.*, 1973). Sotrel *et al* (1980) demonstrated that progesterone production was significantly decreased 3.5 hours after intraluteal administration of oestradiol, but that intraluteal administration of PGF2α caused a significant decrease in progesterone levels after only 40 minutes. There was no concomitant decrease in LH levels, but the luteolytic action of oestradiol was blocked by a prostaglandin synthesis inhibitor, which suggest that the luteolytic effects of oestradiol were mediated by prostaglandin. In contrast to these findings Hutchison *et al* (1987) found that oestrogen was only luteolytic in macaques in the presence of a progesterone-mediated decrease in LH pulse frequency (Hutchison *et al.*, 1987). It appears that oestrogen may have two luteolytic sites of action, one in the hypothalamus and another locally in the corpus luteum, and that its actions are mediated by progesterone and PGF2α respectively. However, a physiological role for oestradiol in luteolysis has yet to be established.

1.5.10 Oxytocin in Luteal Regression

Ruminant luteal cells secrete oxytocin which binds to oxytocin receptors in the uterus. Oxytocin receptors are expressed in the uterus in increasing numbers as the luteal phase proceeds, and ligand binding initiates production of uterine prostaglandin which in turn causes luteolysis (Roberts and McCracken 1976). Oxytocin and oxytocin receptors are found in primate corpora lutea (Einspanier *et al.*, 1994; Dawood and Khan-Dawood 1986), and oxytocin infusion shortened the luteal phase in rhesus macaques (Auletta *et al.*, 1984). Oxytocin has been found to both stimulate and inhibit progesterone production by luteal cells *in vitro*, and these differential effects appear to be related to stage of the luteal phase (Wuttke *et al*, 1995). Low numbers of oxytocin receptors were found in baboon corpora lutea collected during the early luteal phase, receptor numbers peaked during the mid luteal phase, but were not detectable during the late luteal phase (Khan-Dawood *et al.,* 1993). It is likely that estrogen, progesterone and oxytocin interact to regulate oxytocin receptor expression, so although it appears that oxytocin does play a role in paracrine regulation within the corpus luteum, the lack of oxytocin receptors during the late luteal phase suggests that oxytocin does not play a role in primate luteal regression.

1.5.11 Apoptosis and Luteolysis

Primate luteal regression does not seem to occur in response to a clearly defined extra-ovarian signal, therefore it has been suggested that an intra-ovarian mechanism may play a role in controlling luteal regression in primates (Zeleznik, 1991). What instigates the gradual decrease in serum progesterone levels during the late luteal phase? An alternative hypothesis to endogenous PGF2α-induced regression is that steroidogenic cell numbers decrease, thus reducing the steroidogenic capacity of the corpus luteum (Zeleznik, 1991). This hypothesis requires a mechanism that would selectively delete luteal cells without affecting other ovarian compartments such as follicles or stroma. It also requires regulation of the time of cell death since inappropriate early or late steroidogenic cell death would disrupt the normal reproductive cycle.

Apoptosis is one form of cell death in which specific cells die in response to intracellular genetic stimuli (Kerr 1971; Bellamy *et al.*, 1995; Cohen 1991; Majno and Joris, 1995). Apoptosis has been demonstrated in the regressing corpora lutea of rabbits (Dharmarajan *et al.*,1994), rats (Orlicky *et al.*, 1992), sheep (O'Shea *et al.*, 1977, Sawyer *et al* 1990, Kenny *et al.*, 1994) and cows (Juengel *et al.*, 1993, Zheng *et al.*,1994; Rueda *et al.*, 1995), but these studies have not determined the temporal relationship between luteal regression and apoptosis. Additionally, apoptosis had not been examined in the corpora lutea of a primate species when these studies commenced in 1993.

In order that apoptotic cell death can be differentiated from other types of cell death, an examination of the different forms of cell death follows. The specific features of apoptosis will then be described within this context.

1.5.11.1 Types of Cell Death

There are numerous causes of cell death, for example, increases or reductions in physiological supplies: oxygen, substrates or trophic support. The disruption of cellular regulatory processes; osmotic control, ion transport or protein production, can also cause cell death (Haecker and Vaux 1994). Physical damage is yet another cause of cell death. Cell death can be the consequence of multiple circumstances: ischemia, viral infection, wounding or toxic shock, to name but a few (Vaux and Haecker, 1995). Cell death caused by processes originating from within the body is sometimes classified as being physiological, whereas cell death resulting from an external source such as wounding or exposure to a toxic substance is sometimes classified as being non-physiological (Vaux and Haecker, 1995). In practice, the source of the death-inducing agent is irrelevant to the cell, it is the mechanism of action of that agent combined with the internal status of the cell, which determines the cellular response (Hockenberry, 1995). It seems that initial cell responses to fatal stimulants may be as varied as the death-agents themselves, but later responses are common to all cells regardless of the initial mechanism by which death was induced (Majno and Joris 1995). To take one example, cell death caused by ischemia is characterised by the impaired action of ion pumps and decreased intracellular calcium and sodium regulation. Consequent increases in intracellular calcium levels,

acidosis and osmotic shock follow (Bowen 1984). This is associated with nuclear swelling and flocculation of the chromatin (Ueda and Shah 1994). The process continues with lysosome swelling, dilation and vesiculation of the endoplasmic reticulum and loss of compartmentalisation and cell oedema (Bowen 1984; Trump *et al.*, 1981; Cohen 1991). Rupture of the cells' contents frequently invokes an inflammatory response (Ueda and Shah, 1994). If swelling does not result in cell rupture, cells can then enter the pathway common to all cells regardless of the initial mode of death. This pathway has been termed 'necrosis' (Majno and Joris, 1995) and is characterised by irreversible changes in the nucleus (random DNA fragmentation and disappearance) and in the cytoplasm: condensation, eosinophilia and cell shrinkage.

Some forms of cell death do not appear to be initiated by changes in the extracellular environment, but are apparently under intracellular genetic control, and perhaps represent a form of 'terminal differentiation' (Majno and Joris, 1995). Intracellular, genetically-derived death signals have been termed 'programmed cell death', and can result in a variety of cell death pathways, only one of which is apoptosis (Majno and Joris, 1995). Programmed cell death occurs at specific times and locations during embryonic development; the formation of digits is due to the death of web-space cells and formation of the central nervous system also utilises this mechanism (Saunders, 1966; Hamburger and Levi-Montalcini, 1949). Programmed cell death also occurs after withdrawal of a growth factor or hormone (Kyprianou *et al.,* 1988). Apoptosis is a particular type of programmed cell death defined by a specific series of morphological and biochemical characteristics (Kerr *et al.,* 1972). The first visible morphological features of apoptosis are cytoplasmic and nuclear condensation accompanied by the loss of microvilli and cell-cell junctions, and the formation of cell surface convolutions (Schwartzman and Cidlowski, 1993). There is little or no swelling of mitochondria or other cytoplasmic organelles. This is followed by chromatin margination, the condensation of chromatin into crescent-shaped aggregates lining the nuclear membrane convolutions (Schwartzman and Cidlowski, 1993). The nucleus fragments into membrane-bound 'beads' of very dense chromatin; a process termed nuclear fragmentation or karyorhexis. This is followed by fragmentation of the entire cell into membrane bound apoptotic bodies some of

which contain chromatin. Alternatively the cell may shrink into a dense, rounded mass and so form one apoptotic body (Hsueh *et al.*, 1994). Apoptotic bodies are removed from intercellular spaces through phagocytosis by neighboring or immune system cells, or by being shed into the lumen of the gut or capillaries of the vasculature (Kerr *et al.*, 1972; Wyllie and Morris, 1982; Morris *et al.*, 1984). Apoptosis is a relatively fast process, in one case taking only 34 minutes from initial blebbing to the formation of apoptotic bodies (Majno and Joris 1995; Bursch *et al.*, 1990), therefore a small amount of apoptosis detected in tissue sections can indicate quite a substantial rate of cell loss and tissue degeneration. However, subsequent phagocytosis or removal of apoptotic bodies can take hours (Bursch *et al.*, 1990). A biochemical feature specific to apoptosis is a characteristic DNA fragmentation pattern caused by specific endonucleases which cleave the DNA at 185bp intervals (Wyllie, 1980, Arends *et al.*, 1990). This can be examined by labelling the 3' ends of the DNA fragments with a radioisotope prior to gel electrophoresis and visualising the resulting 185bp ladder pattern by autoradiography (Tilly and Hsueh 1993) or the DNA fragments can be visualised *in situ* by labelling 3' ends of the DNA fragments with digoxigenin-11-UTP (Gavrieli *et al.,* 1992). However, there are some instances in which cells display morphological characteristics of apoptotic cell death but do not display this characteristic DNA ladder (Walker *et al.*, 1993) and other instances in which specific DNA fragmentation occurred in the absence of morphological markers of apoptosis (Enright *et al.*, 1994).

1.5.11.2 Ubiquitin: A Protein Associated With Cell Death

Ubiquitin is a highly conserved 76-amino acid polypeptide which covelantly conjugates to cytoplasmic proteins and marks them for subsequent proteolytic degradation through an ATP-dependent process . Ubiquitin ligation has also been found to modify protein function; ubiquitin-histone conjugation results in a decreased histone turnover rate and may regulate chromatin structure during transcription. Ubiquinylated histones may also have a role in mitosis since they disappear during metaphase and reappear shortly afterwards (reviewed by Hershko, 1988). Others have also demonstrated that ubiquitin-protein ligation is important for cell cycle progression and viability and that ubiquitin can be immunochemically

detected in both cytoplasm and nucleus (Haas and Bright 1985). Ubiquitin upregulation has been associated with apoptosis. In the tobacco hawkmoth *Manduca sexta* the developmentally programmed cell death of intersegmental muscles is associated with a 10-fold increase in total ubiquitin polypeptide (Haas *et al.*, 1996; Myer and Schwartz, 1996). The colonial sea squirt *Botryullus schlosseri* also undergoes a cyclical death process which is characterised by cell shrinkage, chromatin condensation and margination followed by nuclear and cytoplasmic fragmentation into membrane bound parcels of ultrastructurally intact organelles which are either shed into the lumen of the stomach or phagocytosed by macrophages: these are all classical features of apoptosis (Wyllie and Morris, 1982; Cohen, 1991). In the sea squirt a second form of cell death was also observed in conjunction with apoptotic cell death; it was characterised by flocculation of the nuclear chromatin, mitochondrial swelling and cellular lysis. A marked increase in cytoplasmic ubiquitin immunoreactivity was noted in all dying cells, including apoptotic cells phagocytosed by macrophages (Lauzon *et al.*, 1993). Murine myoblasts committed to apoptosis show an increased expression of ubiquitin (Sandri *et al.*, 1997) and ubiquitin mRNA is upregulated and nuclear proteins are ubiquinated in human lymphocytes induced to undergo apoptosis (Delic *et al.*, 1993). In contrast, embryonic neurones can be induced to undergo apoptosis *in vitro* by withdrawing nerve growth factor from the culture medium, but under these conditions ubiquitin mRNA is not upregulated (D'Mello and Galli, 1993) which indicates that the role and sub-cellular localisation of ubiquitin during apoptosis is not entirely clear.

1.5.11.3 The Genetic Control of Apoptosis

Apoptosis probably evolved as a means of regulating and repairing DNA damage (Basu and Haldar 1998) and counteracting viral infection (Haeker and Vaux, 1994). The specific morphological and biochemical events that occur during apoptosis are controlled by genes that become activated in specific sequences (Majno and Joris 1995). There are also numerous signals that activate suicidal apoptotic programmes: receptor mediated specific inducers of apoptosis typified by hormones or growth factors, cytotoxic immune system cells, anticancer drugs, toxins and injury (Schwarzman and Cidlowski, 1993).

Professor Wyllie (Pathology, School of Medicine, Edinburgh University) presented a seminar (Western General Hospital, November 1994) in which he related cell cycle to the expression of genes associated with apoptosis. His hypothesis was the basis for Figure 1.0, to which additional genes were added as they were discovered. Tissue maintenance occurs through proliferative cell cycles and the removal of damaged cells by cell death, and these process are mediated by the activation of genes in specific sequences (Basu and Halder 1998). Cells that are arrested in the Go stage of the cell cycle do not express growth factors or c-myc. Environmental changes that result in the entrance of cells to the G1 stage of the cell cycle are often mediated by the proto-oncogene transcription factors c-fos, c-jun or c-myc (Cole 1986, Evan *et al.*, 1992). Further progression around the cell cycle requires the expression of additional genes such as the inner mitochondrial membrane protein Bcl-2 (Schwarzman and Cidlowski, 1993). Wyllie hypothesised that cells could only enter an apoptotic cycle from the G1 phase of the cell cycle, and that the genes that regulated movement between different stages of the cell cycle might also play a role in the regulation of apoptosis. One example of this is the gene Bcl-2, which suppresses apoptosis (Hockenbery *et al.*, 1991) whereas p53 promotes it (Clarke *et al.*, 1993). Bcl-2 stimulates cell proliferation, whereas a Bcl-2 homologous protein, Bax competes with Bcl-2. Bax-Bax homodimers therefore induce apoptosis, but Bax-Bcl-2 heterodimers suppress apoptosis (Basu and Haldar 1998). Bcl-2 and Bax are transcriptional targets for p53, which induces cell cycle arrest and initiates apoptosis in response to DNA damage (Basu and Haldar 1998).

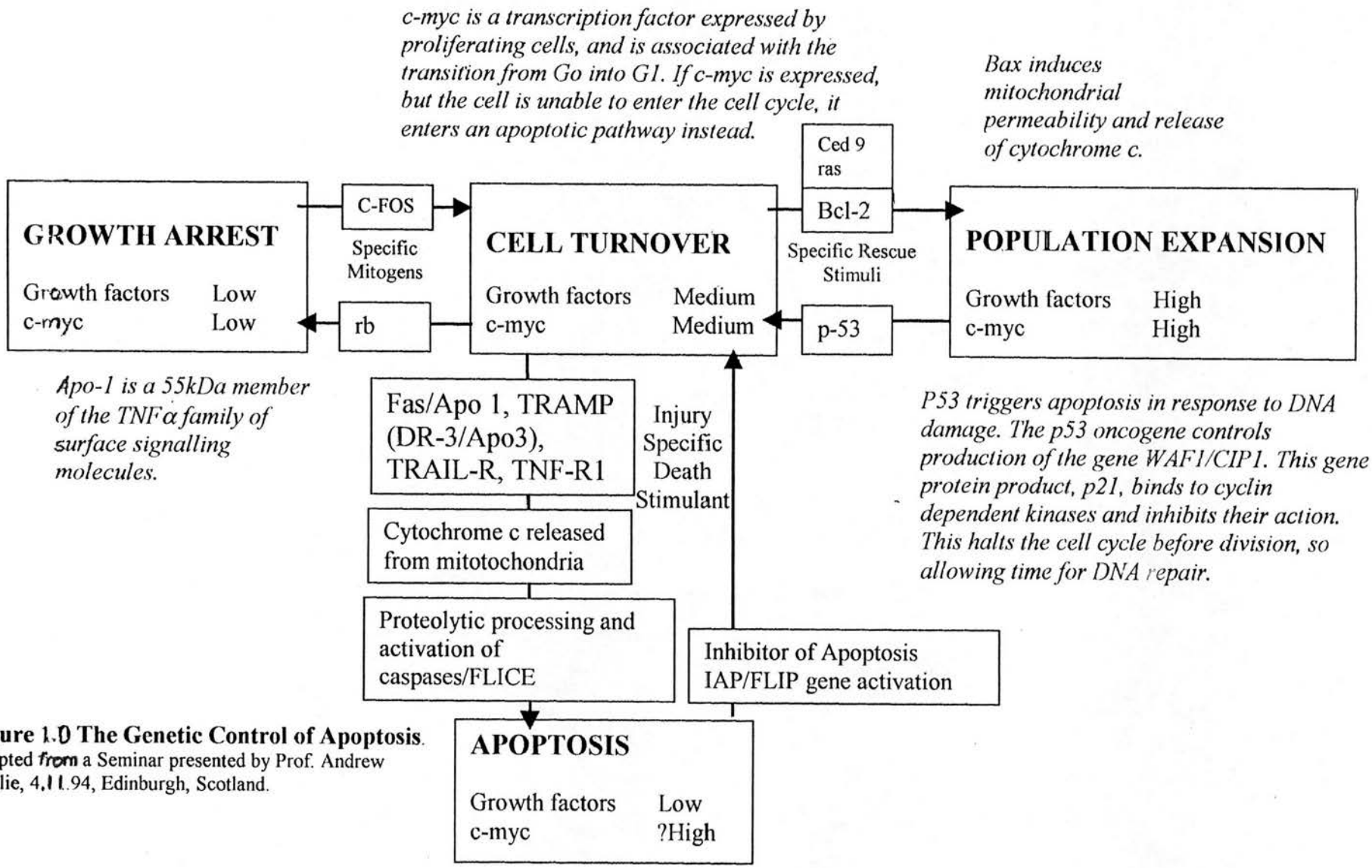

Figure 1.0 The Genetic Control of Apoptosis.
Adapted from a Seminar presented by Prof. Andrew Wyllie, 4.11.94, Edinburgh, Scotland.

Apoptotic gene pathways may be initiated only from the cell turnover, G1 phase of the cell cycle (Figure 1). Ligand binding to four different receptors, Fas, TRAMP, TRAIL and the TNF receptor 1, individually or in combination trigger intracellular apoptotic pathways (Irmler *et al.*, 1997). Bax also stimulates apoptosis by causing the release of cytochrome c from mitochondria into the cytoplasm where it stimulates the processing of caspases 3 and 6 (Deveraux *et al.*, 1997). Fas receptor binding recruits or activates caspase 8, (also known as FLICE or Mach or Mch5) which in turn associates with Fas and TNF-R1 receptor complexes and initiates a cascade that results in caspase 3 activation and subsequent apoptosis (Deveraux *et al.*, 1997). The X chromosome linked Inhibitor of Apoptosis (IAP) gene, also known as FLIP (for FLICE-inhibitory protein, Irmler *et al.*, 1998) inhibits caspases 3 and 7, and therefore prevents apoptosis stimulated by the death receptors (Deveraux *et al.*, 1997). Intracellular calcium levels increase after apoptotic stimuli, and may be a prerequirement for the activation of endonucleases (Schwarzman and Cidlowski, 1993) which cause the internucleosomal fragmentation characteristic of apoptosis.

The proto-oncogene c-myc has been associated with apoptosis, and has been identified in the corpus luteum of the marmoset (Fraser *et al.*, 1995) and human (Illingworth *et al.*, 1994). Bcl-2 also occurs in human corpus luteum (Rodger *et al.*, 1995), but its expression did not decrease prior to luteolysis. Human granulosa cells luteinised *in vitro* expressed Fas, and binding of Fas ligand caused apoptosis. This was enhanced by culturing with interferon gamma and hCG (Quirk *et al.*, 1995). Genes associated with apoptosis were expressed in rat corpora lutea: sulfated glycoprotein 2, Y81, Gas-1 and Integrin-Associated Protein (Guo *et al.*, 1998) and expression was upregulated in the early stages of functional luteolysis.

1.5.11.4 Control of Apoptosis in the Ovary

The majority of follicles in the ovary undergo atresia (Tilly *et al.*, 1991, Giebel *et al.*, 1997) during which granulosa cells undergo apoptosis. A number of factors have been found to affect follicular apoptosis (Tilly *et al.*, 1992; Witty *et al.*, 1996). Estrogen prevents and testosterone stimulates apoptosis in atretic rat follicles (Billig *et al.*, 1993), however it has been found that steroid hormone regulation of apoptosis

is tissue specific, with the same hormone having differing effects in different tissues (Hseuh *et al.*, 1994). The gonadotrophins LH and FSH prevented spontaneous apoptosis in rat follicles *in vitro* (Chun *et al.*, 1994). The withdrawal of trophic support from *in vitro* cultured rabbit corpora lutea also resulted in increased levels of apoptotic DNA fragmentation, whereas the addition of the gonadotrophin hCG dose-dependently suppressed luteal apoptosis (Dharmarajan *et al.*, 1994). Granulosa cell apoptosis is also associated with decreased levels of FSH and LH receptor mRNA (Tilly *et al.*, 1992). Changed LH pulsitility or LH serum levels do not induce luteal regression *in vivo* (Zeleznik 1991) therefore apoptosis in primate corpora lutea is unlikely to be caused by decreasing LH or LH pulsitility.
Gonadotrophin levels are controlled by gonadotrophin releasing hormone (GnRH), and GnRH receptors are present in granulosa and theca cells of the rat (Hsueh and Jones, 1981). Treatment of estrogen-replaced hypophysectomised rats with a GnRH agonist stimulated granulosa cell apoptosis. Simultaneous administration of a GnRH antagonist prevented agonist-induced apoptosis, but apoptosis in animals treated with GnRH antagonist alone was not different from untreated controls (Billig *et al.*, 1994). Macrophage numbers increase as the luteal phase proceeds (Lei *et al* 1991, Gillim *et al.,* 1969), and macrophages secrete TNFα, which has been found to upregulate intracellular ceramide and induce apoptosis in granulosa cells (Witty *et al.*, 1996). Intraluteal administration of TNFα induced luteolysis in pigs (Wuttke *et al.,* 1992) and was found during the mid luteal phase in human corpora lutea (Kondo *et al.*, 1995). TNFα may therefore play a role in the early induction of apoptotic pathways *in vivo*.

In summary, one form of programmed cell death, apoptosis, occurred during luteal regression in a number of non-primate species (Dharmarajan *et al.*, 1994; Orlicky *et al.*, 1992; O'Shea *et al.,* 1977, Sawyer *et al* 1990, Kenny *et al.*, 1994; Juengel *et al.*, 1993, Zheng *et al.*, 1994; Rueda *et al.*, 1995). It was therefore hypothesised that functional luteal regression in primates might occur by the apoptotic cell death of steroidogenic luteal cells.

1.5.12 Luteal vasculature and luteolysis.

Approximately 50% of the cells in primate corpora lutea are endothelial cells (Lei *et al.*, 1991; Christenson and Stouffer, 1996), and an extensive capillary network penetrates the corpus luteum, so much so that every steroidogenic cell is in contact with at least one capillary (Redmer and Reynolds 1996). The primary function of the corpus luteum is the production of steroid hormones, and steroidogenesis is entirely dependent upon the delivery of cholesterol substrates and regulatory gonadotrophins through the vasculature. Peak progesterone production does not occur until the luteal vasculature is fully developed. Early luteal phase corpora lutea cultured *in vitro* and stimulated with gonadotrophins secrete more progesterone than mid and late luteal phase corpora lutea (Hild-Petito *et al.*, 1989), but maximal secretory activity does not occur *in vivo* until the mid luteal phase, and it is thought that this is due to inadequate development of the luteal vasculature in the early luteal phase (McClellan *et al.*, 1975). It is believed that the vasculature is absolutely vital to normal functioning of the corpus luteum, but it is not clear what role it plays in luteal regression. It is not known whether changes in the vasculature, or changes in blood flow, precede functional luteal regression in the primate, and neither is it clear when or how the vasculature changes during the process of structural regression.

1.5.12.1 Blood Flow in the Corpus Luteum.

Blood flows through the corpus luteum at the rate of approximately 10 - 15 ml per minute per gram of tissue (Abdul-Karim and Bruce 1973; Bruce and Moor 1976) and this rate of flow is higher than that to any other organ of the body; flows of 0.61, 1.86, and 1.78 ml per minute per gram of heart, brain and kidney respectively have been observed (Bruce and Moor, 1976). Within the ovary rates of blood flow are 2.66 and 6.68 ml per minute per gram of stroma or follicles respectively, showing that blood flow to the follicles is of the same order as that seen to corpora lutea (Bruce and Moor, 1976). It is not known why blood flow through the corpus luteum is so much higher than through other tissues. Blood flow to the ovary bearing the corpus luteum, and also through the corpus luteum, decreases as the luteal phase advances (Niswender *et al.*, 1976; Bruce and Moor, 1976) and studies utilising

radioactive microspheres indicate that approximately 90% of the blood flowing to the ovary goes through the corpus luteum during the mid luteal phase (Niswender *et al.,* 1976; Abdul-Karim and Bruce, 1973), but that this decreases to 28% in the late luteal phase (Bruce and Moor, 1976). It has been suggested that a mechanism for reducing luteal blood flow exists, and an arteriole-venule shunting system which results in reduced blood flow to individual steroidogenic cells has been proposed (Niswender *et al.,* 1976).

1.5.12.2 Effects of Luteolytic Agents on Luteal Blood Flow.

LH may have effects on luteal blood flow. Administration of anti-LH antibodies to sheep causes a decrease in serum progesterone levels and a concomitant decrease in blood flow to the ovary, and infusion of additional LH causes an increase in serum progesterone levels and an increase in blood flow (Niswender *et al.,* 1976) but the temporal relationships between changes in steroid hormone production and changes in luteal blood flow are unclear. Administration of PGF2α *in vivo* to rabbits does not, however, cause a decreased blood flow to the corpora lutea until 6 hours after a significant decrease in plasma progesterone concentration has occurred (Bruce and Hillier, 1974), so the luteolytic action of PGF2α is unlikely to be mediated by reduced blood flow. It does, however, appear to be mediated by endothelial cells because steroidogenesis was not inhibited by PGF2α in pure cultures of bovine luteal steroidogenic cells, but steroidogenesis was inhibited in mixed cultures of endothelial and steroidogenic cells (Girsh *et al.,*1995). Disruption of the vasculature also prevents the luteolytic effect of PGF2α on dispersed rat or dispersed marmoset luteal cells *in vitro* (Thomas et al., 1978; Webley *et al.*, 1989). In addition, PGF2α has longer term effects on luteal vasculature; 24 hours after *in vivo* administration of PGF2α to sheep 28% of endothelial cells were morphologically abnormal and capillary lumina were occluded with cellular debris (Sawyer *et al.*, 1990; Stacey *et al.,* 1976). It has also been suggested that vascular occlusion during luteal regression could result in hypoxic conditions, and that ischemia could therefore be a component of structural luteal regression.

A number of studies have quantified different cell types of the corpus luteum. In one study, the cellular composition of sheep corpora lutea was determined by a 'hit' technique whereby luteal components were classified as large or small luteal cells, capillaries or connective tissue. The number of 'hits' in endothelial cells or capillary lumina decreased by approximately 50% from the mid to late luteal phase, but the number of 'hits' in leukocytes and in intracapillary debris increased during the same time period, while connective tissue quantification remained constant (Niswender *et al.*, 1976). The decrease in the number of endothelial cell 'hits' occurred before serum progesterone levels decreased, suggesting that changes in luteal vasculature may instigate functional regression. The majority of workers, however, have found that in ruminants structural changes are first seen in the vasculature concomitant with falling serum progesterone values, and that during luteal regression there appears to be a change in the vasculature bought about by the loss of small capillaries and an increase in larger microvessels (Zheng *et al.*, 1993; Redmer and Reynolds 1996). The mid-phase bovine corpus luteum has a dense capillary network made up of fully differentiated endothelial cells with a flattened elongated morphotype and numerous tight junctions (Modlich *et al.,* 1996). Early luteal regression is characterised by the dissociation of endothelial tight junctions, widening capillary basal lamina and disruption of osmotic regulation. Endothelial cell nuclei condense and may fragment in a process which closely resembles the initial stages of apoptosis, and the cells then slough off into the lumen of the blood vessel, so forming localised blockages (O'Shea *et al.*, 1977; Modlich *et al.,* 1996). This loss of endothelial cells further perturbs the integrity of capillary basal lamina and probably accelerates the loss of osmotic equilibrium. Occlusion of the capillaries may also cause ischemia (O'Shea *et al.*, 1977). Parenchymal steroidogenic cells then undergo degenerative changes (Deane *et al.*, 1966), either by the formation of vacuoles, or by apoptosis (Modlich *et al.,* 1996). The loss of steroidogenic cells appears to be accompanied by the loss of small capillaries and their replacement with larger microvessels (Modlich *et al.,* 1996).

In summary, luteal regression in non-primates is associated with decreased blood flow through the corpus luteum, and with decreased numbers of endothelial cells. Luteal vasculature has not been examined during the late luteal phase in primates, and the importance of vascular morphology to the process of luteolysis is unknown.

1.6 Conclusions

It is possible that luteal regression in primates is mediated by a combination of prostaglandin production, immune system cells and products, luteal vasculature and oxygen free radicals. Apoptotic deletion of steroidogenic cells might result in decreased plasma progesterone concentrations, and decreased steroidogenesis might stimulate the endogenous production of PGF2α, with subsequent oxygen free radical production and a further decrease in steroidogenesis. This thesis examines factors which have the potential to initiate and regulate luteal regression in the marmoset monkey.

Chapter 2: Materials and Methods

2.0 Marmoset Housing and Maintenance

Marmosets were 18 months old when first recruited into the study. Femoral vein blood samples were taken three times a week and assayed for progesterone.

2.0.1 Housing

Cages were 1 x 1 x 0.65 m in size, with wooden perches and wood shavings on the floor to allow foraging behaviour. Nesting boxes were positioned at the highest point of the cage. There were 6 cages in each room, and each cage contained one vasectomised male and one adult female.

2.0.2 Diet

Animals were fed once a day on a selection of the following:

- Peanuts, raisins, dates, sunflower seeds, brown bread,
- Fruit – apple, orange, pear, tomato, banana, grapes
- Porridge Mix: Casilan, Farex baby rice, multi vitamin drops, complan and vitamin D3.

2.0.3 Environmental Cues.

High level glass windows meant the animals experienced a normal diurnal light-dark cycle. Animal house staff however, noted no seasonality in the breeding animals.

2.1 Progesterone Concentrations and Reproductive Cyclicity

2.1.1 Progesterone Radioimmunoassay.

Marmoset blood samples (300µl) were collected every two or three days by femoral venipuncture into 1ml heparinized syringes. The syringes were sealed with a cap and centrifuged at 1000g for 20 minutes at 4°C. The separated plasma was transferred to an eppendorf tube and stored at ˉ18°C until progesterone concentrations were measured by radioimmunoassay. Marmoset samples were thawed, vortexed and 2.5µl of serum diluted into 147.5µl of progesterone assay buffer (1M phosphate citrate and 1% gelatin, pH 6). Each standard or sample was assayed in duplicate.

The progesterone assay standard curve comprised 100 µl of progesterone standard diluted to the following concentrations; 2.5, 5, 10, 25, 50, 100, 250, 500 and 1000 ng/ml. In addition non-specific binding was calculated by omitting primary antibody and using 200µl assay buffer instead of progesterone standard, and Bo zero counts were calculated by using 100µl of assay buffer instead of progesterone standard. 2.5µl of human post-menopausal serum (PMS) diluted in 47.5µl of assay buffer was added to each of the above items in order that the volume and components of the standard curve remain consistent with the samples, with the exception that PMS does not contain progesterone. Three quality control (QC's) samples of progesterone concentrations equivalent to the highest, mid and lowest ranges of the assay were incorporated into the assay. The QC's were dispensed in the same manner as unknown samples of serum. The primary antibody, sheep anti-progesterone, was diluted 1:1000 in assay buffer and 100µl added to all samples and standards except for those measuring non-specific binding. The radioactive tracer was iodinated thymidine progesterone (^{125}I PGT, Amersham, Bucks., England) which was stored in ethanol at 4°C until required. An aliquot of tracer was diluted in 1:5000 in tracer buffer (1M phosphate citrate pH6) and the number of radioactive counts per minute (cpm) in an aliquot of 100µl was determined. The tracer concentration was adjusted to generate 15000cpm/100µl. ANSA (8-anilino-1-naptha-lenesulfonic-acid) was then added at 0.1% w/v., and 100µl of tracer added to each tube in the assay. In addition two tubes containing only 100µl of tracer each were added to the assay, in order to determine the total number of counts possible. Assay tubes were vortexed briefly then incubated at room temperature for 3 hours.

The secondary antibody was donkey anti goat serum diluted 1:64 in assay buffer, and 100µl was added to each tube except those measuring total radioactive counts. Normal sheep serum was diluted 1:32000 in assay buffer and 100 µl/tube added. Assay tubes were vortexed then incubated at 4°C overnight. 1 ml of 0.9% saline/tritonX/polyethylene glycol was added to each tube, they were centrifuged at 3000rpm at 4°C for 30 minutes and the supernatant removed from the resulting pellet. Pellets were left to dry before counting the amount of radioactivity incorporated into each pellet on a gamma counter.

The sensitivity of the assay was 0.07 pmol per tube (0.022 ng/ml) and the inter- and intra-assay coefficients of variation were 15% and 4% respectively.

2.1.2 Analysis of Reproductive Cyclicity.

The following study was conducted in order to determine the length of the reproductive cycle in the animals of the MRC Primate Centre.

Progesterone assay results for all animals sampled during the three years of these studies, and for the two years prior to these studies, were collected and analysed. Mr Keith Morris and staff of the MRC primate colony collected blood samples, and Mrs Gwen Cowen processed blood samples and performed the progesterone assays which generated the data analysed here. Data were only included in the analysis if a minimum of 2.5 consecutive reproductive cycles were available, and if sampling frequency during those cycles were ≤4 days. Approximately one third of the animals included in this study had blood samples taken every two days with three day intervals occurring over weekends, whereas the remaining animals had progesterone values every third or fourth day. The follicular phase was defined as that period during which progesterone concentrations were 31.9 nmol/L or less, and animals were assumed to have entered the luteal phase when progesterone concentrations rose above 32 nmol/L and remained elevated.

Because there were up to three days between progesterone values, a further set of criteria were used to determine which part of the cycle the animal was in. At the end of the follicular phase, if progesterone was >16 nmol/L, the luteal phase was assumed to begin the following day and progesterone values were assumed to be higher than 32 nmol/L 24 hour later. If progesterone was <16 nmol/L, the luteal phase was assumed to begin 48 hours later. At the end of the luteal phase, if progesterone values were <200 nmol/L the follicular phase was assumed to begin 24 hours later, and if values were greater than 200nmol/L, it was assumed that the follicular phase began 48 hours later. In total, 87 complete cycles were studied in 24 different animals. Many animals were not included in this analysis because one or

two samples were taken less frequently than 4 days, which excluded that cycle from the analysis, and therefore reduced the number of consecutive cycles available. Since the estimated lengths of cycles and estimated lengths of luteal phases were ± one day, analysis was conducted on range intervals, and each cycle or luteal phase was put in its appropriate range. Hence the frequency with which a particular length of cycle or luteal phase occurred could be calculated. Data was then pooled by redistributing the animals in every second range interval evenly to the group either side, so halving the total number of range groups, but maintaining the frequency distribution of luteal phase lengths. This was expressed as the total number of animals per frequency interval, and is presented as a histogram with no standard error bars.

Marmosets in the MRC Primate Centre had a reproductive cycle of 30.17 ± 11.30 days (mean ± S.D., n=87, range 13 - 70 days, median 27 days, Figure 2.1) and a luteal phase of 20.26 ± 10.34 days (mean ± S.D, n=87, range 6 - 63 days). Median length of luteal phase, however, was 18 days (Figure 2.1). No animal had a luteal phase which was shorter than 5 days, but 31% of the cycles had extended luteal phases of 23 to 60 days. Extended luteal phases often included periods of time in which progesterone levels were decreased to approximately 60nmol/L but failed to fall below the 32nmol/L threshold which defined a follicular phase.

Others have found captive marmosets to have a 28-30 day long reproductive cycle with an 8 - 9 day follicular phase and a 16 - 22 day luteal phase (Harding *et al.,* 1982; Harlow *et al.*, 1984; Summers *et al.*, 1985). The mean length of 87 complete cycles in 24 different animals was 30.17 ± 11.3 days, which is in remarkably good agreement with Harding *et al* (1982) who found that the total cycle length in female marmosets was 30.1 ± 3.8 days over a decade earlier in the same colony of animals. Reports of shorter cycle lengths were from a different colony (Harlow *et al.*, 1984; Summers *et al.*, 1985) and may reflect the influence that a limited number of animals has on establishing a colony; natural variation in cycle length in a wild population may not be represented by founding members of a colony and lead to the formation of 'clines' in isolated populations such as those seen in closed captive colonies. Alternatively the method of analysis may lead to discrepancies in estimated cycle

length. In this study one criteria for inclusion was that data for at least 2.5 consecutive cycles be available, however, progesterone values >32nmol/L for >40 days may have been excluded from other studies on the grounds that they were indicative of abnormal cycling. Excluding cycles with extended luteal phases would result in lower estimates of mean cycle length. In this study it is possible that luteal phases which appeared to last 50-60 days may have actually been two separate cycles in which progesterone concentrations did not decrease beneath the defined threshold during the follicular phase.

Mean luteal phase lengths were 20.26 ± 10.34 with a median of 18 days, and this shows good agreement with the 19.2 ± 0.6 day luteal phase reported by Harlow *et al* (1984) and is slightly shorter than the 21.5 ± 2.2 days (mean ± SD, median 21.5) reported by Harding *et al* (1982).

Figure 2.1: Frequency of Different Luteal Phase Lengths in Marmosets.

The lengths of 87 different luteal phases in 24 different animals in the MRC Reproductive Biology Unit Primate Centre are shown distributed in 2 day frequency intervals.

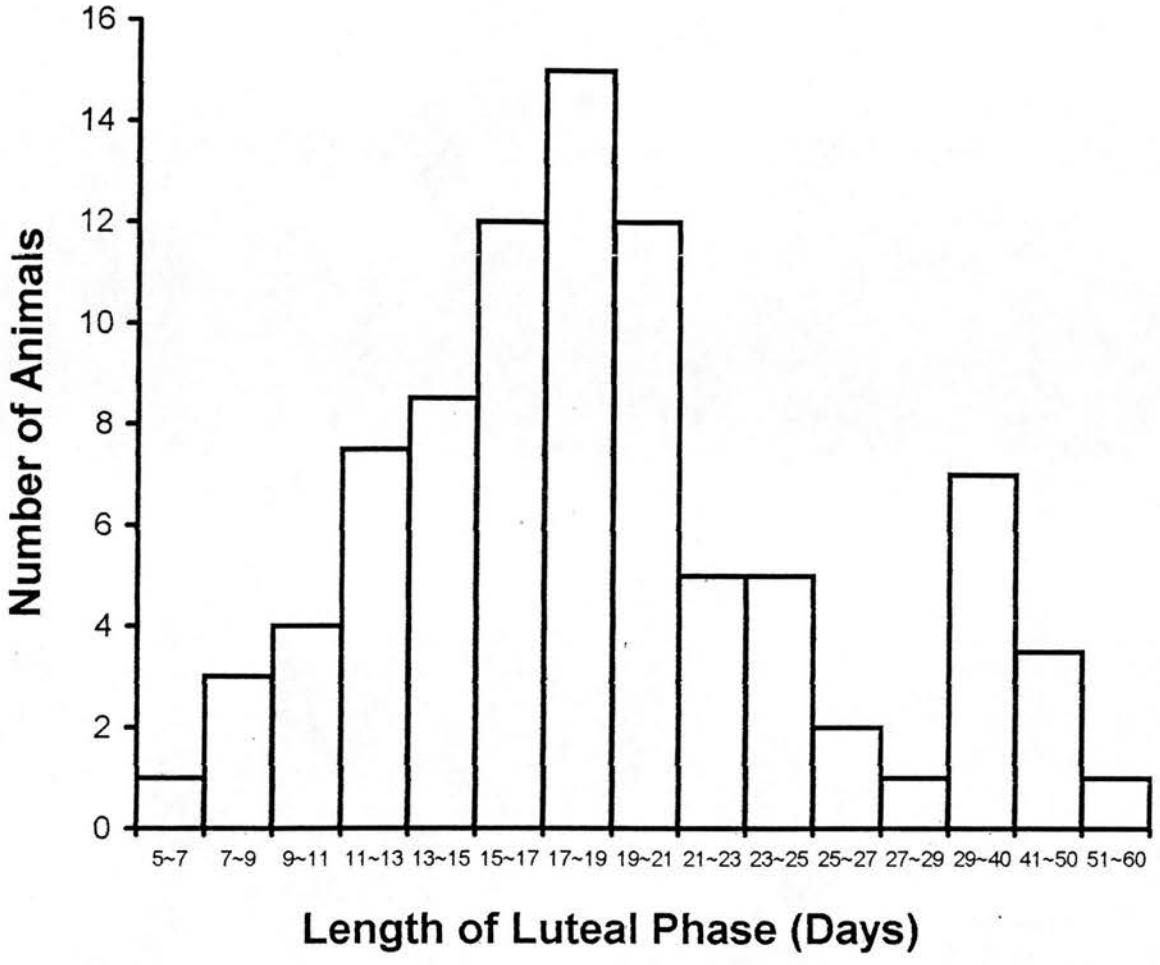

Figure 2.1: Frequency of Different Luteal Phase Lengths in Marmosets.

2.1.3 Progesterone Values at Time of Ovary Collection

In the cycle preceding luteolytic treatment and ovarian collection animals used in the *in situ* 3' end labelling study had progesterone concentrations in the follicular phase of 16±4 nmol/l (mean ± SD. n=18). Progesterone levels increased to 172±50 nmol/l by day 2 of the luteal phase, were 206±64 nmol/l from luteal days 3 to 12, and were decreased to 39±9 nmol/l by day 18 (Figures 2.2 and 2.3).

Progesterone concentrations for animals whose ovaries were collected on days 10 and 18 of the luteal phase were 206±104 nmol/l (n=4) and 226±51 nmol/l (n=3) respectively at time of collection (Figure 2.2). Animals whose ovaries were collected on day 22 of the luteal phase had progesterone concentrations of 12.7±0 6nmol/l (n=3) at time of collection (Figure 2.2). Animals treated with GnRH antagonist or PGF2α had plasma progesterone concentrations of 372±284 (n=4) and 289±213 (n=4) nmol/l respectively on luteal day 9. Luteolytic treatment resulted in a marked decrease to 32±23 nmol/l and 23±10 nmol/l for GnRH ant. and PGF2α treated animals respectively (Figure 2.3).

Different animals were used in the study examining ubiquitin expression after induced luteal regression. Follicular phase values were 16±2.6 nmol/l (mean±s.e.m. n=9),.85±27 nmol/l (mean±s.e.m. n=9), by day 2 of the luteal phase, and were 292±66 nmol/l (mean±s.e.m. n=9) from days 3 - 9 of the luteal phase. Mid luteal phase day 10 values were 311±48 nmol/l (mean±s.e.m. n=3), and this was significantly decreased 24 hours after administration of a luteolytic dose of GnRH antagonist (36.35±16, mean±sem, $p<0.01$) or PGF2α (18.33±3.7, mean±sem, $p<0.01$).

Ovaries were collected 12 hours after administration of luteolytic agents. Animals had progesterone concentrations of 513±153 nmol/l (mean±s.e.m, n=3) on luteal day 10 at time of administration of PGF2α, and had progesterone concentrations of 364±60 nmol/l (mean±s.e.m, n=3) at time of GnRH antagonist administration. Progesterone concentrations 12 hours later when ovaries were collected were 19±6 nmol/l (mean±s.e.m) and 13±0 nmol/l (mean±s.e.m) for PGF2α and GnRH antagonist treated animals respectively. These six animals were used in all studies with a 12 hour post-induced regression time-point.

Progesterone concentrations reported here are for a total of 33 animals from three separate studies, but are representative of values obtained from all the animals described in this thesis, and amply illustrate the wide variation in both cycle length and progesterone concentrations found in these animals. However, progesterone values for corresponding stages of the cycle were essentially similar in all studies. Previously reported progesterone concentrations for marmoset monkeys in the luteal phase were 30 - 250nmol/L (Abbott *et al.*, 1988), 20-140ng/ml (Abbott and Hearn, 1978) and 87.4 ± 3.7ng/ml (mean maximum ± SD, n=30) on day 10 of the luteal phase (Harding *et al.*, 1982) and these are simular to levels reported here; 206±64 nmol/l from luteal days 3 to 12 (mean ± SD., n=18).

Harding *et al* (1982) noted that intra-animal cycle variance was due to changes in both follicular and luteal phase length, and that it was difficult to predict phase length using data obtained from a previous cycle. This is illustrated in our studies which used naturally regressing corpora lutea. In one example progesterone concentrations were 226±51 nmol/l (mean±s.e.m, n=3) on luteal day 18 when the corpora lutea were collected, whereas the same animals had progesterone values of 39±9 nmol/l on luteal day 18 of the previous cycle. Although 226±51 nmol/l is still within the mid luteal range of progesterone concentration, it was assumed that in this instance the corpora lutea were regressing because progesterone levels had been decreasing for the previous 5 days in these particular animals.

Treatment with either the PGF2α analogue, cloprostenol, or the GnRH antagonist, antarelix, caused a decrease in circulating progesterone indicative of functional luteolysis as shown previously (Summers *et al.*, 1985; Michael and Webley, 1993; Hodges *et al.*, 1987). Progesterone values both12 hours and 24 hours after administration of luteolytic agents were less than 32nmol/L, suggesting collection at an earlier time point would be necessary in order to observe changes associated with functional luteal regression. Since these two methods for inducing luteal regression gave results in our hands similar to those described by other workers, we judged them suitable techniques to use in studies investigating the instigation and regulation of luteal regression.

Figure 2.2: Serum Progesterone Concentrations in the Marmoset.

Mean (± SEM) concentrations of plasma progesterone (nmol L^{-1}) in marmoset ovulatory cycles and in the subsequent cycle of ovarian collection. Ovaries were collected on luteal day 10 (n=4,—□—), luteal day 18 (n=3, ---O---) and luteal day 22 (n=3, ----▲ ----). Arrows indicate day of collection.

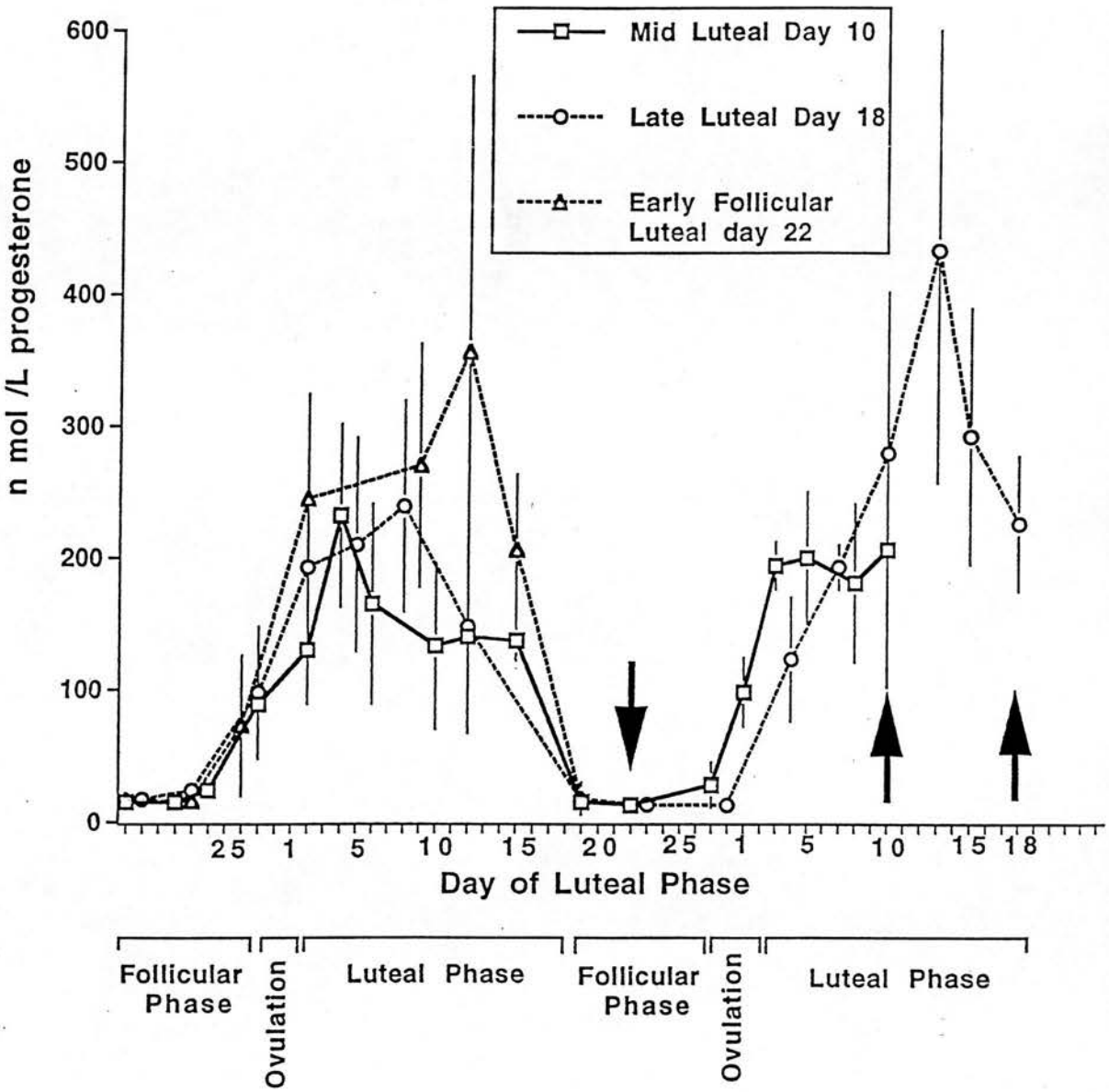
Mid Luteal Day 10
Late Luteal Day 18
Early Follicular
Luteal day 22
n mol /L progesterone
600
500
400
300
200
100
0
25 1 5 10 15 20 25 1 5 10 15 18
Day of Luteal Phase
Follicular Phase
Ovulation
Luteal Phase
Follicular Phase
Ovulation
Luteal Phase

Figure 2.3: Progesterone Concentrations in the Marmoset after Induced Luteal Regression.

Mean (±SEM) concentrations of serum progesterone (nmol L^{-1}) in marmoset ovulatory cycles and before and safter administration of a prostaglandin 2α analogue (n=4, cloprostenol 1μg i.m., ▲-) or a GnRH antagonist (n=4, antarelix 1mgKg^{-1} s.c., --▼--) on day 9 of the luteal phase. Ovaries were collected 24 hours later on day 10 of the luteal phase. Control marmosets (n=4,—□—) were given no treatment and ovaries were collected on day 10 of the luteal phase. Arrows indicate progesterone concentration at time of ovarian collection.

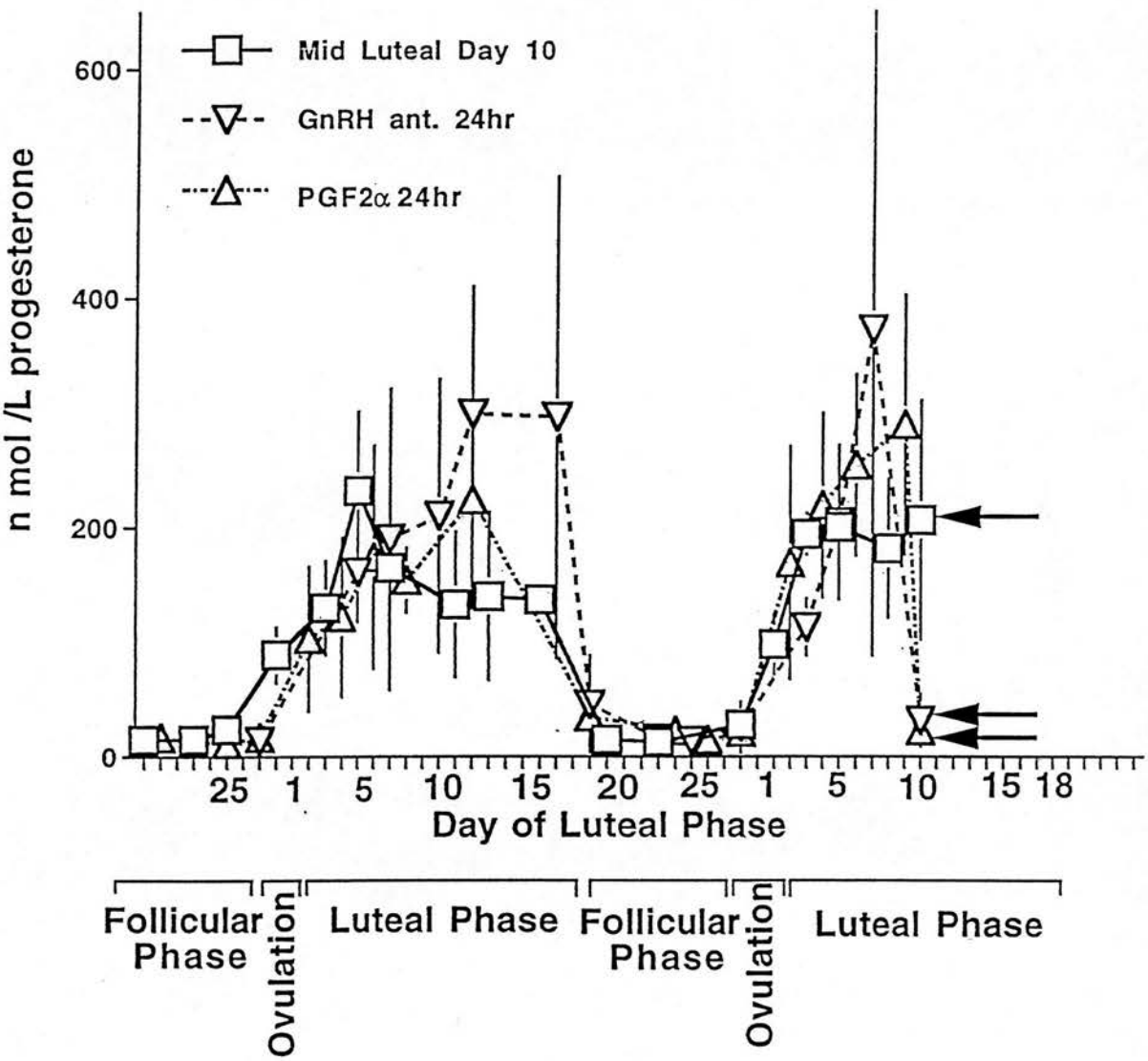
Mid Luteal Day 10
GnRH ant. 24hr
PGF2α 24hr
n mol /L progesterone
600
400
200
0
25 1 5 10 15 20 25 1 5 10 15 18
Day of Luteal Phase
Follicular Phase
Ovulation
Luteal Phase
Follicular Phase
Ovulation
Luteal Phase

2.2 Collection of Marmoset Ovaries.

The follicular phase was defined as that period during which progesterone concentrations were 31.9 nmol/L or less. Day 1 of the luteal phase was defined as the day when progesterone concentrations rose above 32 nmol/L.

2.2.1 Spontaneous Luteal Regression

Control ovaries were obtained during the mid luteal phase on day 10, ovaries containing functionally regressing corpora lutea were collected from animals in the late luteal phase on day 18, and ovaries containing structurally regressing corpora lutea were collected from animals in the early follicular phase (days 20 - 24 of the preceding luteal phase) and the late follicular phase (days 25 - 28 of the preceding luteal phase).

2.2.2 Induced Luteal Regression

GnRH antagonist, antarelix (Deghenghi *et al.*, 1993; Hodges *et al.*, 1988; Fraser *et al.*, 1995a; Fraser *et al.*, 1995b) 1mg/kg s.c., or a PGF2α analogue (Summers *et al.*, 1985; Michael and Webley, 1993; Hodges *et al.*, 1987) 1μg cloprostenol (Planate, Coopers Animal Health Ltd., Crewe, Cheshire, UK) i.m., were administered on day 9 of the luteal phase. Ovaries were collected 12 hours, or 24 hours later on day 10 of the luteal phase. In addition, some animals had either GnRH antagonist or PGF 2α administered for 48 hours on luteal days 8 and 9 prior to ovarian collection on luteal day 10. Corpora lutea induced to undergo luteal regression were compared with ovaries collected from untreated animals on day 10 of the luteal phase.

LH pulsitility decreases (Zeleznik, 1991) but serum LH concentrations are maintained during the luteal phase in macaques and humans (Salamonsen *et al* 1973; Hutchison *et al.,* 1986; Sotrel *et al.*, 1981) and this suggests that GnRH levels are also maintained. Therefore the use of GnRH antagonist to deplete LH concentrations during the mid luteal phase is a non-physiological induction of luteal regression.

PGF2α concentrations change during the luteal phase in humans (Challis *et al.,* 1976; Swanston *et al.*, 1977; Valenzuela *et al.*, 1983), and it is likely that intra-luteal PGF2α concentrations change during regression in marmosets, although no data has

been published in this regard. The endogenous production of PGF2α might disconnect the LH receptor from its secondary messenger pathway (Michael and Webley, 1993; Michael *et al.,* 1994), so reducing the ability of luteal cells to respond to LH. Administration of a PGF2α analogue may therefore mimic the natural, physiological process of luteal regression.

One way to test the hypothesis that the main luteolytic action of PGF2α causes a reduction in the ability of steroidogenic cells to respond to LH by inhibiting LH receptor secondary messenger pathways, was to deplete serum LH by the administration of a GnRH antagonist. If the hypothesis were correct, 'removal' of LH by GnRH antagonist should give similar results to the effective, functional 'removal' of LH by administration of PGF2α. In order that LH 'removal' should be equivalent and comparable, the doses selected for these experiments were intended to prevent LH-stimulated steroidogenesis in the case of PGF2α, and to remove circulating LH in the case of GnRH antagonist.

2.2.3 Tissue Collection and Preparation

Ovaries were collected after animals were sedated with 100μl ketamine hydrochloride (Parke-Davies Veterinary, Pontypool, Gwent, UK) i.m. and euthanased with 400μl Euthetal i.v. (sodium pentobarbitone, Rhône Mérieux, Essex, UK). A terminal blood sample was taken before removing ovaries and organs used in other studies. Animals and treatments are summarised in Appendix 1, and described in further detail below.

2.2.3.1 Tissue Collected for Analysis of Oligonucleosome Formation

The ovary with the largest, most obvious corpus luteum was taken first, weighed, and the largest corpus luteum was dissected out of the ovary. This was labeled as 'CL1', and snap frozen immediately in liquid nitrogen. Additional corpora lutea were collected in the same way, and labeled according to the sequence in which they were dissected out of the ovarian tissue. The time the animal died, and the times each CL was snap frozen were noted. The last corpus luteum taken was frozen 12 minutes or less after death of the animal. Samples of liver were dissected free and snap frozen

after collection of corpora lutea was completed. It was thought that if death and dissection were to cause DNA fragmentation, the liver samples would act as controls for this. After transportation to the laboratory corpora lutea and liver samples were stored at -80°C until required for DNA extraction.

In some cases (see Appendix 1) only one corpus luteum was dissected free and frozen for analysis of oligonucleosome formation. The remaining ovary and corpora lutea were then fixed in paraformaldehyde as described below.

2.2.3.2 Tissue Collected for Histology and Immunocytochemistry

Ovaries were dissected free, weighed, and fixed in 4% (w/v) buffered paraformaldehyde for 24 hours before embedding in paraffin according to standard procedures. Paraffin embedded sections (4μm) were mounted on poly-L-lysine (50μg/L) coated slides. Only ovaries containing corpora lutea were used. One ovary was taken as being representative of the animal. For example, marmoset number 1 had corpora lutea of the current cycle in both ovary A and ovary B. Sections from ovary A may have been used in one study, and sections from ovary B used in another study. In each case, they both fulfilled the purpose of being representative of one animal.

It was assumed that corpora lutea in each ovary were functionally equivalent to each other, in that they were produced in the same cycle. Possible differences in the time of ovulation may have generated corpora lutea of different ages within the same cycle. This possible source of intra-animal variation is discussed in a subsequent section. Fixed ovaries were used for the following studies (see Appendix 1):

- Examination of morphology after haematoxylin and eosin (H&E) staining
- *In situ* 3' end labeling in the apoptosis study
- Immunocytochemistry to identify cells which were
    - steroidogenic,
    - endothelial
    - vascular endothelial growth factor postitive
    - proliferating

In the course of the three years of these studies, the number of animals in each of the nine experimental groups utilised for immunocytochemistry were as follows:

- Early luteal phase, days 2-5, n=7
- Mid luteal phase, day 10, n=8
- Late luteal phase, day 18, n=6
- Follicular phase, luteal day 22-25, n=6
- Late follicular phase, luteal day 25-28, n=4
- 12 hours after administration of PGF2α, n=3
- 24 hours after administration of PGF2α, n=6
- 12 hours after administration of GnRH antagonist, n=3
- 24 hours after administration of GnRH antagonist, n=6

The number of animals indicated in each group were those in which stage or treatment was confirmed by the progesterone concentration of blood sample collected at the time of death. More animals were originally allocated to each of the luteal day 18 and follicular phase groups, but some had elevated progesterone levels suggesting that they were not undergoing luteal regression, and were therefore excluded from these groups. Animals were included in the luteal day 18 group when three progesterone measurements (the third being the terminal bleed) were each lower than the preceding measurement, ie. a consistent decrease in plasma progesterone concentrations indicating functional luteal regression. Follicular phase corpora lutea were included when terminal bleed progesterone levels were less than 31.8 nmol/L.

2.2.3.3 Tissue Collected for Assessment of Proliferation after *In Vivo* Incorporation of Bromo-deoxyuridine

Animals were administered bromodeoxyuridine (BrdU, Boehringer Mannheim, Essex, UK) intravenously by slow infusion at a dose of 20mg in 1ml saline and ovaries were collected one hour later.

Ovaries containing corpora lutea were collected from marmosets in the early luteal phase on luteal days 2-4 (n=3 animals), in the late luteal phase during functional luteal regression on luteal day 18 (n=3 animals) and during structural luteal regression after progesterone levels had fallen to follicular phase values on luteal days 22-25 (n=3). These are included in the numbers indicated above.

2.2.3.4 Tissue Collected for Lipid Study

Ovaries were embedded in OCT (Miles Laboratories, Berks, UK) and transported to the laboratory in liquid nitrogen where 6μm sections were cut using a cryostat (2800 Frigocutt; Reichert-Jung, Cambridge Instruments, Cambs, U.K.) and thaw mounted onto slides coated with poly-L-lysine (50ug/l). Slide-mounted sections were stored at -70°C.

Ovaries were collected on day 10 of the luteal phase (n=4 animals), 24 hours after luteolytic treatment with GnRH antagonist (n=3 animals) and 24 hours after PGF2α (n=3 animals).

2.2.4 Overview of Ovaries Used

The total number of animals used in the course of these studies is detailed in Appendix 1. Collection of ovaries was an ongoing process throughout the three years of these studies. As paraffin blocks were used up, new ovaries were collected to replace them. To illustrate the process of ovary usage, immunocytochemistry with the antibody against von Willebrand Factor VIII antigen (vW), an endothelial cell marker, is described. Immunocytochemistry for vW was carried out on three separate occasions on the following tissues:

mid luteal phase, n=3

PGF2α, 12 hr, n=3

PGF2α, 24 hr, n=4

GnRH antagonist 12 hr, n=3

GnRH antagonist 24 hr, n=4

The first procedure examined PG24 treated ovaries 1-4, procedure 2 examined PG24 treated ovaries 2-5, and procedure 3 included ovaries 3-6. Ideally, all sections would have been included in one assay procedure, however, there were two reasons why this was not done. The first was because only four ovaries were available at the commencement of study, additional immunocytochemistry procedures were conducted as more ovaries became available. The oldest ovaries, however, had been used up by the time the fifth and sixth ovaries were collected. The second reason was one of technical limitations, intra- and inter-assay variation were decreased by keeping the number of sections in each assay constant. The three immunocytochemistry procedures could be compared with each other because at least two sections in each experimental group were included in at least one other procedure. Quantification of different procedures also indicated that there was no significant difference between procedures carried out at different times with different ovaries. This is illustrated by the area of vW positive staining in mid luteal phase control ovaries in the induced regression experiment (4167±1130, n=3), and the mid luteal phase day 10 ovaries in the spontaneous regression experiment (3517±491, n=4). Two ovaries were used in both experiments, the remaining three ovaries were different, but the area of vW-positive staining was not significantly different. Similar results were obtained for all treatment groups and within all immunocytochemistry procedures. In summary, ovaries used in the representative procedure for each study are indicated in Appendix 3, but in the majority of cases, all the ovaries collected during the three years of these studies were examined by each of the techniques described.

2.3 Luteal Morphology

2.3.1 Morphometric Analysis of H&E Stained Sections

Sections were stained with H+E as described then subjected to morphometric analysis using a Highly Optimised Microscope Environment (Brugal *et al.*, 1992), a microscope with an integrated mouse and computer. The orientation and size of the microscope slide were recorded, thereby allowing the establishment of a coordinate

grid system, in which the precise position of each cell in the tissue section was recorded. A computer generated overlay was superimposed over the optical field image. Electronic labels (symbols corresponding to steroidogenic, non-steroidogenic, apoptotic etc.) were attached to cells in the assessed area of luteal tissue by using the mouse to drag an icon from a menu to the identified cell. The location of each cell, and identificatory labels, were saved by the computer. The slide could be replaced by another section, and the procedure repeated. The first slide could be replaced on the stage, its corresponding data file opened, and identification symbols reviewed. Alternatively, the same area minus the identification symbols could be reviewed, allowing two individuals to assess the same area and compare cell identification. This system made it possible to count every cell in a unit area, by marking each counted cell with an identificatory symbol. Cells were not counted twice, and no cells were left uncounted. It also allowed more than one individual to review precisely the same cells. This system was the equivalent of taking a microphotograph of luteal tissue, and marking individual cells on the photograph with a pen.

For this study a 100μm grid was superimposed on the field of view of a x40 objective lens. Each square in the grid had an area of $10000\mu m^2$. Six squares were scored for each animal, these were taken semi-randomly from the luteal tissue visible on the slide. Accessory corpora lutea, and areas of luteal tissue which were smaller than $10000\mu m^2$ were excluded from analysis. At least one square was scored in each of the remaining areas of luteal tissue, therefore all the corpora lutea in each ovary examined were analysed. Selection of the square(s) scored within each corpus luteum was random. In the majority of cases, individual corpora lutea were identifiable in ovarian sections, however it could not be ruled out that a single corpus luteum might be distorted during processing, and that adjacent areas of luteal tissue might therefore originate from the same corpus luteum. Therefore, no attempt was made to count the number of corpora lutea in each ovary.

Every individual cell in each $10000\mu m^2$ square was identified as being either steroidogenic, vacuolated steroidogenic, non-steroidogenic or apoptotic as described

below. In this way, the total number of cells in a 10000μm^2 square area of luteal tissue could be determined, as could the numbers of different cell types. Each cell in the 10000μm^2 square had an identificatory symbol drawn over it within the computer generated overlay. The exact location of the cell and its symbol were stored on the computer. This information was later retrieved and identification confirmed by a pathologist (Dr. David Harrison), who is experienced in assessing apoptosis and oncosis from morphological criteria (Clarke *et al.*, 1993; Howie *et al.*, 1994). Agreement was >99%, disagreement was predominantly over the identification of apoptosis, and in such instances apoptosis was underscored and that score was either added to the non-steroidogenic cell or to the normal steroidogenic cell class.
Cell types for each section were summed and expressed as means±SEM per 60000μm^2 for each experimental group.

2.3.1.1 Identification of Cell Types.

Immunocytochemistry for the steroidogenic enzyme 3ß HSD in these studies (Duncan *et al.*, 1997) and in other studies (Webley *et al.*, 1990; Fehrenbach *et al.*, 1995) identified steroidogenic cells as being >12μm in diameter with regular circular outlines in section, abundant cytoplasm and circular nuclei. Cells with these dimensions in H&E stained serial sections were therefore labelled as 'steroidogenic cells'. It was not possible to identify individual cells in serial sections with accuracy, therefore some cells may not have contained the steroidogenic enzyme 3ß HSD, and may therefore have been functionally inactive. The 'steroidogenic cell' label in this instance meant that the identified cell had the same gross physical and morphological dimensions as cells which were found to be 3ß HSD immunopositive in serial sections.
Some cells had the same dimensions as steroidogenic cells, but contained cytoplasmic vacuoles. Many were 3ß HSD immunopositive in serial sections. These were therefore labeled as 'vacuolated' or 'morphologically abnormal steroidogenic cells'. These varied from essentially intact cells containing small vacuoles (2- 4μm in diameter) to extreme disruption of the cytoplasm leaving a remnant around the nucleus combined with the presence of three to five large vacuoles (6 - 10μm

diameter). It is possible that vacuolation observed in mid luteal day 10 paraformaldehyde fixed corpora lutea was artifactual, since mid luteal phase vacuolated steroidogenic cells were qualitatively different from those observed after both spontaneous and induced luteal regression. Additionally, vacuolation was not observed in cryostat sections of mid luteal phase corpora lutea, whereas the same vacuolated architecture appeared in cryostat sections of regressing corpora lutea. Mid luteal phase vacuolated data was included in the analyses to maintain a consistent definition. Their inclusion also decreased differences between experimental groups, so that errors in identification detracted from, rather than added to, the strength of statistical analyses of data.

Cell types that were not >12μm in diameter with regular circular outlines, abundant cytoplasm and circular nuclei, and were not 3ß HSD immunopositive in serial sections, were labeled 'non-steroidogenic cells'. These were generally elongated with the long axis of 4 - 8 μm, and had large nuclei and little cytoplasm. Since they frequently enclosed lumina containing red blood cells the majority of these cell types were assumed to be endothelial cells. Cells with this morphology were also immunopositive for the endothelial cell marker, von Willebrand Factor VIII related antigen. However, fibroblasts and leukocytes would have also been included in this category.

Apoptosis was characterised both by individual clusters of apoptotic bodies, where each cluster was assumed to have originated from the fragmentation of one cell, and by condensed cells with clearly fragmented nuclei. Apoptotic bodies with the morphological appearance seen in our sections have previously been shown to contain the condensed chromatin and intact organelles characteristic of apoptosis when examined by electron microscopy (Howie *et al.*, 1994).

2.3.1.2 Identification of Corpora Lutea Accessoria

Corpora lutea accessoria are formed when non-ovulated follicles become luteinised (Behrman *et al.*, 1993). In marmosets, large antral follicles undergoing atresia have wide spaces between granulosa cells and disrupted granulosa cell layer architecture. Apoptotic cell death is often observed around the periphery of the antrum. Accessory corpora lutea are formed when the outer theca cell layer and the granulosa cell layer

closest to the basement membrane luteinise (Wehrenberg *et al.*, 1997). Resultant corpora lutea accessoria therefore have a central cavity, and steroidogenic cells which appear to be arranged in layers, reminiscent of the layers of a follicle. They also stain more intensely for lipid (see chapter 3), and are smaller than true corpora lutea of the cycle. Areas of luteal tissue with an obvious central cavity and a arrangement of steroidogenic cells reminiscent of the layers seen in follicles were not included in any analyses of luteal tissue in these studies.

2.3.1.3 Statistical Analysis of Morphological Data

Data were subjected to one-way analysis of variance taking the stage of the cycle as a between-subject variable. Differences between the mean values obtained from the morphological analysis of corpora lutea induced to undergo regression with cloporstenol or antarelix were compared among experimental groups and with untreated corpora lutea from day 10 of the luteal phase in a separate one-way analysis of variance taking the nature of treatment as a between-subject variable. When a significant F value was obtained the data were further analysed by Scheffé's test and significance was assigned at $P<0.05$.

2.3.1.4 Optimisation of Area for Quantification

The number of 10000μm^2 areas that needed to be assessed was counted by scoring a number of squares from different areas of the luteal tissue for four different animals, mid luteal (day 10, n=1), GnRH antagonist (n=1), PGF2α (n=1) and early follicular (day 20-25, n=1). The numbers of each cell type found in successive 10000μm^2 squares were added to the numbers from the previous fields and a series of cumulative mean values was generated. Accumulative means are shown for a GnRH antagonist treated and an untreated animal from day 10 of the luteal phase (Figure 2.4). Mean numbers of each cell type present stabilized after examining four 10000μm^2 fields and scoring further squares did not significantly change the values

observed. Therefore quantification of cell types were based on counts of six $10000\mu m^2$ fields.

Numbers of non-steroidogenic cells in untreated mid-luteal phase and GnRH antagonist treated animals were similar, whereas numbers of vacuolated steroidogenic cells in GnRH antagonist treated corpora lutea were less than the numbers of morphologically normal steroidogenic cells in untreated mid-luteal phase corpora lutea. The difference in accumulative means of morphologically normal and vacuolated steroidogenic cells was two, which corresponded to the accumulated mean of apoptotic cells, which implied that out of every 14 steroidogenic cells, two became apoptotic and 12 became vacuolated.

Figure 2.4: Accumulative Means of Luteal Cell Types.

Twelve randomly selected 10000μm^2 areas of luteal tissue were analysed. Every cell in each unit area was identified, and the numbers of each cell type were determined for each unit area. The mean number of cells for two unit areas was calculated and shown, and the mean was recalculated as successive unit areas were analysed. Untreated mid luteal phase day 10 corpora lutea were comprised of steroidogenic (–*–)and nonsteroidogenic cells (–●–). Corpora lutea collected 24 hours after *in vivo* administration of GnRH antagonist were comprised of vacuolated steroidogenic cells (–Δ–), apoptotic cells or apoptotic bodies (–□–) and nonsteroidogenic cells (–♦–).

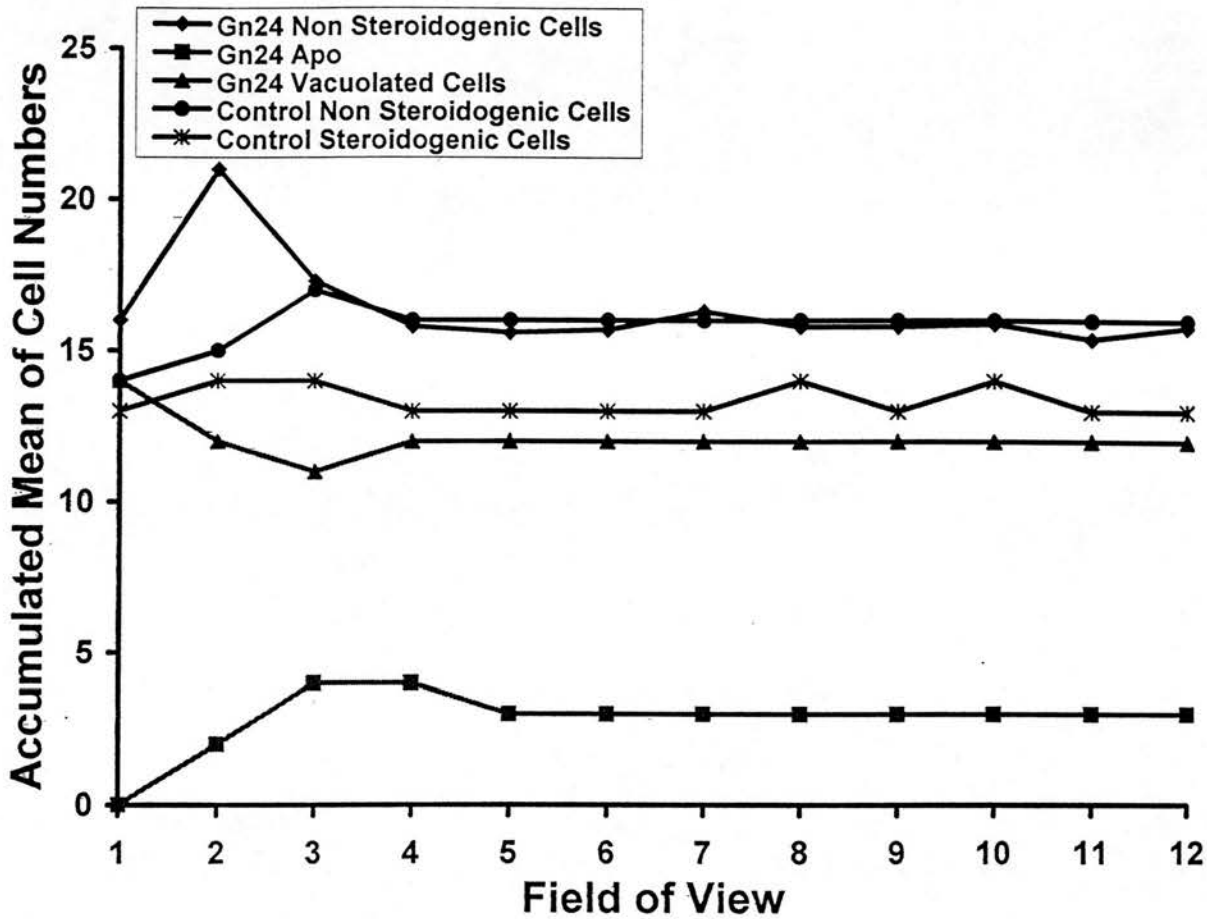
Gn24 Non Steroidogenic Cells
Gn24 Apo
Gn24 Vacuolated Cells
Control Non Steroidogenic Cells
Control Steroidogenic Cells
Accumulated Mean of Cell Numbers
25
20
15
10
5
0
1
2
3
4
5
6
7
8
9
10
11
12
Field of View

2.3.2 The Effect of Location on Morphology Within Corpora Lutea.

Different immunocytochemistry procedures necessarily examined different sectional planes of the corpora lutea. Studies were therefore conducted to determine whether there were differences in morphology according to location in one plane, ie. comparing the centre to the periphery of the corpus luteum. H&E stained sections of one corpus luteum from each of the following experimental groups were examined:

mid luteal phase day 10
PG 24
Gn 24.

Sections were chosen in which one, discrete rounded area of luteal tissue comprised 40 – 70% of the total ovarian area. Smaller corpora lutea were found after the administration of luteolytic agents. Areas of luteal tissue which were less than 40% of the ovarian section after induced regression, or less than 70% during the mid luteal phase, or which were an irregular shape, were assumed to be non-equatorial sections, or parts of corpora lutea which had been distorted during collection and fixation. The numbers of steroidogenic cells were counted in six randomly selected areas from the middle of the area of luteal tissue, and six from the periphery of the tissue as defined by the close juxtaposition of stroma or capsule connective tissue. The mean of each group of six areas was determined, and compared with the mean of the group obtained from the other location within the same corpus luteum. There was no significant difference in the number of steroidogenic cells according to location within the corpus luteum.

2.3.3 Comparison of Morphology between Corpora Lutea from the Same Animal.

Marmosets in these studies had one to four corpora lutea distributed between both ovaries. Ovulations can occur up to 24 hours apart (Tardiff *et al.*, 1993), therefore it was possible that three corpora lutea collected from the same cycle may be of varying ages, and therefore display different characteristics. Four corpora lutea from

one mid luteal phase day 10 animal were dissected free of the ovary and fixed in 4% (w/v) buffered paraformaldehyde as described. Sections were taken from 3 planes of each of the corpora lutea, roughly corresponding to the top, middle and bottom of the luteal sphere. These were stained with H&E and subjected to morphological analysis. These data confirmed that the number of steroidogenic cells per unit area did not vary according to location within each corpus luteum. Data collected from the equatorial plane of each of the four corpora lutea are presented below.

CL #	Mean # steroidogenic cells/unit area±SEM	Mean # nonsteroidogenic cells/unit area±SEM
1	12.33±0.92	14.16±0.71
2	11.33±0.78	15.16±1.17
3	14.3±0.609	15.83±1.17
4	13.66±0.877	21.16±1.86

Six unit areas were scored in each corpus luteum and two one-way analyses of variance were conducted on the steroidogenic and non-steroidogenic cell data respectively, and significance was assigned at $p<0.05$. There was no significant difference between the number of steroidogenic cells in four different corpora lutea. There was also no significant difference between the number of non-steroidogenic cells in three corpora lutea, although the fourth had a significantly higher ($p<0.01$) number of non-steroidogenic cells than the other three. It was concluded that the majority of corpora lutea of the cycle within each animal were morphologically similar to each other.

2.4 Immunocytochemistry and Histology

All fixed sections of ovaries containing corpora lutea were rehydrated by transferring the slides through xylene, 100% ethanol, 95% industrial methylated spirits (IMS), 70% IMS and water. Some procedures then required antigen retrieval by one of the following methods.

- exposure to four 5 minute cycles of microwave irradiation at 700w in 0.01M Na citrate buffer pH 6.0 (Shi *et al.*, 1993). Citrate buffer was replenished to the original volume after each 5 minute cycle of microwaving. Sections were then cooled at room temperature for 20 minutes before washing with TBS.
- a 30 minute incubation at 37^0C in 0.1% trypsin (Sigma, Poole, UK), 0.1% $CaCl_2$, pH 7.4, followed by washing in Tris buffered saline (TBS, 0.05M Tris, NaCl 9g/L).

Procedures utilising diaminobenzidine tetrahydrochloride (DAB) as a visualisation substrate required endogenous peroxidase activity to be blocked by incubating in 3% hydrogen peroxide in methanol for 20 minutes at room temperature.
Sections were then washed three times with Tris buffered saline (TBS, 0.05M Tris, NaCl 9g/L) before application of primary antibody, diluted in TBS. A serial section of each section was included as a negative control. If the primary antibody was a polyclonal, the negative control was treated with pre-immune serum of the same species the primary antibody was raised in. If a monoclonal antibody was used, the negative control sections were treated with the appropriate immunoglobulin (IgG). Negative control serum or IgG's were diluted to the same concentration as the primary antibody. Sections were incubated with antibodies and the appropriate negative controls under various conditions as described in Appendix 2.
After washing with TBS, biotinylated secondary antibodies (anti primary antibody species) in a block (20% serum of the species the secondary antibody was raised in and 5% BSA (w/v) in TBS) were applied to all positive and negative control sections and incubated for 1 hour at room temperature. Visualisation was with avidin biotin complex conjugated to one of:

- alkaline phosphatase (AP, Vector, Peterborough,UK) made up according to manufacturers instructions and applied for 45 minutes at room temperature followed by application of Vector Red (Vector, Peterborough, UK) until pink colouration appeared approximately 2 minutes later.

- horseradish peroxidase (HRP, Vector, Peterborough, UK) made up according to manufacturers instructions and applied for 45 minutes at room temperature followed by application of diaminobenzidine tetrahydrochloride (DAB, 0.04% 3,3'-diaminobenzidine (w/v, Sigma, Dorset, U.K.) in 0.05M TrisCl (Sigma, Dorset, U.K.) pH 8 and 3% H_2O_2 (BDH Laboratory Supplies, Dorset, U.K.) until brown colouration appeared approximately 1 minute later.

Sections exposed to primary antibody were always removed from DAB or Vector Red solution before their corresponding negative controls.
The use of alkaline phosphatase was unaffected by endogenous peroxidase activity, and so allowed omission of the hydrogen peroxide incubation, which shortened the protocol. Since DAB is carcinogenic, the use of Vector Red was considered to be safer, and Vector Red is also fluorescent, which allowed it to be used in studies utilising double labelling.
Comparison of the two visualisation systems: HRP and DAB, or AP and Vector Red, indicated no difference in the amount of immunopositive staining. This was confirmed on three separate occasions when used with von Willebrand Factor VIII related Antigen (vW), Ki67 and Vascular Endothelial Growth Factor (VEGF) antibodies and quantified as described.

Immunocytochemistry procedures were optimised until results were consistent and repeatable, then the procedure was repeated 3 times. Each procedure was assessed semi-quantitatively, and the average procedure quantified rigorously, and presented as the results of that experiment. Specific animals used in the presented, representative procedure are described in Appendix 1. All immunocytochemistry data presented in this thesis were therefore obtained at least three times. All the ovaries available were assessed within the three procedures.

For details of antibodies used, their source, method of antigen retrieval, and the number of animals used in each immunocytochemistry study, please see Appendix 2.

2.4.1 Bromoxydeuridine (BrdU) Protocol I

Ovarian sections were rehydrated as described. BrdU antigen retrieval was by exposure to microwave irradiation as described above. Sections were then cooled at room temperature for 20 minutes and washed with TBS. Detection of BrdU was by using a kit (5-bromo-2'-deoxyuridine Labelling and Detection Kit II, Boehringer Mannheim) according to the manufacturers instructions. Sections were incubated for 10 minutes with Washing Buffer from the kit. Primary antibody (mouse monoclonal antibody to 5-bromo-2'-deoxyuridine-5'-monophosphate containing nucleases in PBS/glycerine) was diluted 1:10 in Incubation Buffer (Tris 66 mmol, $MgCl_2$ 0.66mmol, 2-mercaptoethanol 1 mmol) and negative control sections were treated with mouse immunoglobulin G (Vector Laboratories, California, USA) and this was also diluted 1:10 in incubation buffer before being incubated for 2 hours at 37°C. After washing with TBS, kit secondary antibodies (antimouse immunoglobulin conjugated to alkalline phosphatase in triethanolamine buffer) were diluted 1:10 in TBS and sections incubated for 1 hour at room temperature. Sections were then washed twice with Substrate Buffer (Tris 1M, NaCl 1M pH 9.7, $MgCl_2$ 0.5M). Visualisation was with 300μgml^{-1} nitro blue tetrazolium in buffer (100mmol Tris pH 9.5, 100mmol NaCL and 50mmol $MgCl_2$) with 175μgml^{-1} 5-bromo-4-chloro-3-indolyphosphate and 240μgml^{-1} levamisole. After washing with water sections were counterstained with haematoxylin and Light Green, rinsed in water then quickly rinsed in absolute ethanol, fixed in xylene and mounted in pertex. Sections from each of the nine ovaries (ie. both ovaries from each animal were examined) were subjected to BrdU ICC on at least two separate occasions. This procedure was carried out on four different occasions and gave consistent results.

2.4.2 BrdU Protocol II

The kits used in protocol I were expensive, therefore a cheaper, alternative methodology was developed. Ovarian sections were brought to water and endogenous peroxidase activity blocked as described previously. Sections were washed three times in TBS. BrdU antigen retrieval was by exposure to two 5 minute cycles of microwave irradiation at 700W in glycine-HCl buffer pH 7.4 (0.2M

glycine, 0.2M HCl). Buffer was replenished to the original volume after each 5 minute cycle of microwaving. Sections were then washed three times with TBS before application of primary antibody (mouse monoclonal antibody clone BMC 9318 to 5-bromo-2'-deoxyuridine-5'-monophosphate, Boehringer Mannheim) which was diluted 1:30 in TBS. Negative control sections were treated with mouse immunoglobulin G (Vector Laboratories, California, USA) which was also diluted 1:30 in TBS before all sections were incubated for 18 hours at 4°C. After washing with TBS, rabbit anti mouse IgG (DAKO) was applied at a dilution of 1:60 in block (20% normal rabbit serum, 5% BSA (w/v) in TBS) for 30 minutes at room temperature. This was followed by 3 washes with TBS and incubation with mouse peroxidase anti peroxidase (mouse PAP, DAKO) diluted 1:100 in TBS for 30 minutes at room temperature. Visualisation was by application of DAB as described. Sections from each ovary were subjected to BrdU Protocol II on at least two separate occasions and gave results consistent with Protocol 1.

2.4.2.1 3β Hydroxysteroid Dehydrogenase (3β HSD) colocalised with BrdU

Detection of BrdU was by Protocol 1, but instead of counterstaining and mounting, sections were washed with water. 3βHSD immunocytochemistry proceeded as described above. Sections were counterstained with haematoxylin and Light green before fast dehydration in absolute ETOH, fixation in xylene and mounting in Pertex.

2.4.2.2 Von Willebrand Factor VIII (vW) colocalised with BrdU

VW immunocytochemistry was as described above, followed by application of BrdU Protocol II.

2.4.3 Haematoxylin and Eosin (H&E) Staining

Fixed sections were rehydrated as described for immunocytochemistry, then stained in haematoxylin dye for 5minutes. Sections were placed in running water until the water ran clear, this was found to 'blue' the stain satisfactorily. Sections were counterstained briefly (40 s) in eosin, washed well in running tap water, then dehydrated through increasing concentrations of alcohol and xylene – the reverse

procedure to that followed for rehydration. A drop of mounting medium (Depex) was added to each section, and a coverslip applied. H&E stains nuclei blue and cytoplasm pink.

2.4.4 Light Green Counterstaining

Sections were washed with water before being counterstained with haematoxylin as described. Light Green (0.5% w/v aqueous) was sometimes used as a counterstain instead of eosin, particularly when Vector Red was used.

2.4.5 Oil Red O Staining

Cryostat sections were stained with 0.5% Oil Red O in isopropanol (Sigma, Dorset, U.K.) for 15 minutes at 37^{o}C, differentiated in 60% isopropanol for 5 minutes, washed in water and counterstained with haematoxylin. Unsaturated hydrophobic simple lipids stain red with this system (Bayliss High, 1982).

In summary, each ovary was examined in at least two separate immunocytochemistry procedures, and at least three ovaries (from three different animals) were included in each treatment.

2.5 Quantification and Statistical Analysis of Immunocytochemical Procedures

2.5.1 Quantification of von Willebrand Factor VIII and Proliferating Cell Nuclear Antigen (PCNA)

Sections were examined through a 10x objective lens and a 3.3x phototube, and this field of view measured 31400μm^2 of luteal tissue in our system. These sections were not counterstained, so any colouration was due to either vW or PCNA immunoreactivity, and contrasted markedly with unstained areas of tissue. vW or PCNA positive staining per 31400μm^2 unit area was measured using NIH Image 1.57 software, and this converted the colour image to black and white so that unstained areas were white and stained areas dark greys through to black. It was possible to

determine the optical density which corresponded to the lightest immunoreactivity, and to measure the total area of immunostaining, and also the total number of discrete areas of immunostaining, which had optical densities higher than that threshold. The area of immunostaining was proportional to the number of vW positive endothelial cells, whereas each discrete area of PCNA positive staining corresponded to one proliferating nucleus, so the number of discrete areas indicated the number of proliferating cells in that section. Optical density levels were standardised between slides by viewing a blank part of the slide which did not have any tissue on it, and adjusting the light intensity of the microscope to a predetermined number of optical density units.

Four 31 400μm^2 unit areas of luteal tissue were randomly selected and measured for each section. Accessory corpora lutea were excluded, but at least one area in each of the distinct areas of luteal tissue visible in the ovarian section was included in the analysis. This utilised the assumption that each distinct area of luteal tissue corresponded to one corpus luteum, and therefore a measurement was made from each corpus luteum in that ovary. The mean of all the 31 400μm^2 unit areas of luteal tissue measured was then taken as being representative for that animal. Measuring more than four unit areas did not significantly alter the mean. Negative control sections were measured in the same way, and if an area had an optical density equal to or higher than the lowest threshold for vW or PCNA immunoreactivity, that area was subtracted from the mean value for the corresponding experimental section, so removing the influence of any non-specific staining.

The area of vW immunoreactivity (μm^2) per 31 400μm^2 of luteal tissue was calculated for each animal, and expressed as mean area±SEM for each experimental group. The percentage of luteal area stained was also calculated for each animal, and expressed as mean percentage±SEM for each experimental group.

The number of discrete areas of PCNA immunoreactivity per 31 400μm^2 of luteal tissue was calculated for each animal, and expressed as mean number±SEM for each experimental group.

2.5.2 Statistical Analysis of von Willebrand Factor VIII

Analysis of variance tests the hypothesis that means from two or more samples are equal. If the means are equal, it indicates that the samples are drawn from the same population. In this experiment, if the mean of the samples taken after administration of luteolytic treatments were the same as the mean of the untreated luteal day 10 control, it would indicate that the treatment had had no effect upon the vasculature. Similarly, if there was no difference in means between samples taken at different time points during the luteal phase, it would indicate that the variable 'age of corpus luteum' had no effect on the vasculature. However, when sample means differ, the samples are probably from different populations, and an F-test tests this by analysing the sample variances. A Fishers procedure ensures that the data are normally distributed, and calculates the probability that a given confidence interval will not contain the difference in group means. This procedure is exact when samples of unequal sizes are used.

Corpora lutea from the mid luteal phase were compared with corpora lutea after induction of luteolysis with either PGF2α or GnRH antagonist in a one way analysis of variance which used treatment as a between subject variable. Differences in areas of vW positive staining in early, mid, late and follicular phase corpora lutea were also investigated by one-way analysis of variance using stage of the luteal phase as a between subject variable. When the F-test was significant ($p<0.05$) differences between groups were evaluated by using the Fishers PLSD test.

2.5.3 Identification of PCNA-Positive Cells.

PCNA-positive cell types were identified on the basis that endothelial cell nuclei are elongated and asymmetrical, whereas steroidogenic cell nuclei are spherical and regular. Initial identification of endothelial cells was based on the morphological appearance of cells which were immunopositive for the endothelial cell marker, von Willebrand Factor, and which frequently enclosed lumina containing red blood cells. Initial identification of steroidogenic cells was based on the morphological appearance of cells which were immunopositive for the steroidogenic enzyme, 3β HSD. A typical field of view of luteal tissue was frozen on the NIH 1.57 Image

Analysis visual display unit, and a drawing tool used to delineate endothelial cell nuclei, and steroidogenic cell nuclei. A number of parameters were recorded for each nucleus: the ellipse long axis and the ellipse short axis, the length of the perimeter of the nucleus, the area of the nucleus and the mean optical density of the nucleus. Nuclei were measured in each of a representative corpus luteum collected on day 10 of the luteal phase, in a corpus luteum collected 24 hours after luteolytic treatment with PGF2α, and in a corpus luteum collected 24 hours after treatment with GnRH antagonist. The ellipse axes ratio of steroidogenic cells was consistently less than 1.69, and the ellipse axes ratio of endothelial cells was consistently higher than 1.7 (Figure 2.5). The area of nuclei in section, and the perimeter of PCNA immunopositive areas, were not reliable indicators of different cell types. In addition, the optical density of PCNA immunostaining was the same for both steroidogenic and nonsteroidogenic cells (Figure 2.6); optical density of PCNA immunostaining did not vary according to the size of the nucleus.

Figure 2.5: Nuclear Morphometry of Steroidogenic and Nonsteroidogenic Cells in Marmoset Corpora Lutea.

Ovaries containing corpora lutea were collected on luteal day 10, 24 hours after administration of A. PGF2α analogue, B. GnRH antagonist and C. no treatment. Luteal parenchymal steroidogenic cells and nonsteroidogenic cells were identified using morphological criteria and the length of the major ellipse axis and the minor ellipse axis was determined for each nucleus. The ratio of the ellipse axes is shown plotted against the frequency interval for each ratio. In addition, the cell type of each nucleus measured is identified as being either steroidogenic (black bars) or nonsteroidogenic (white bars).

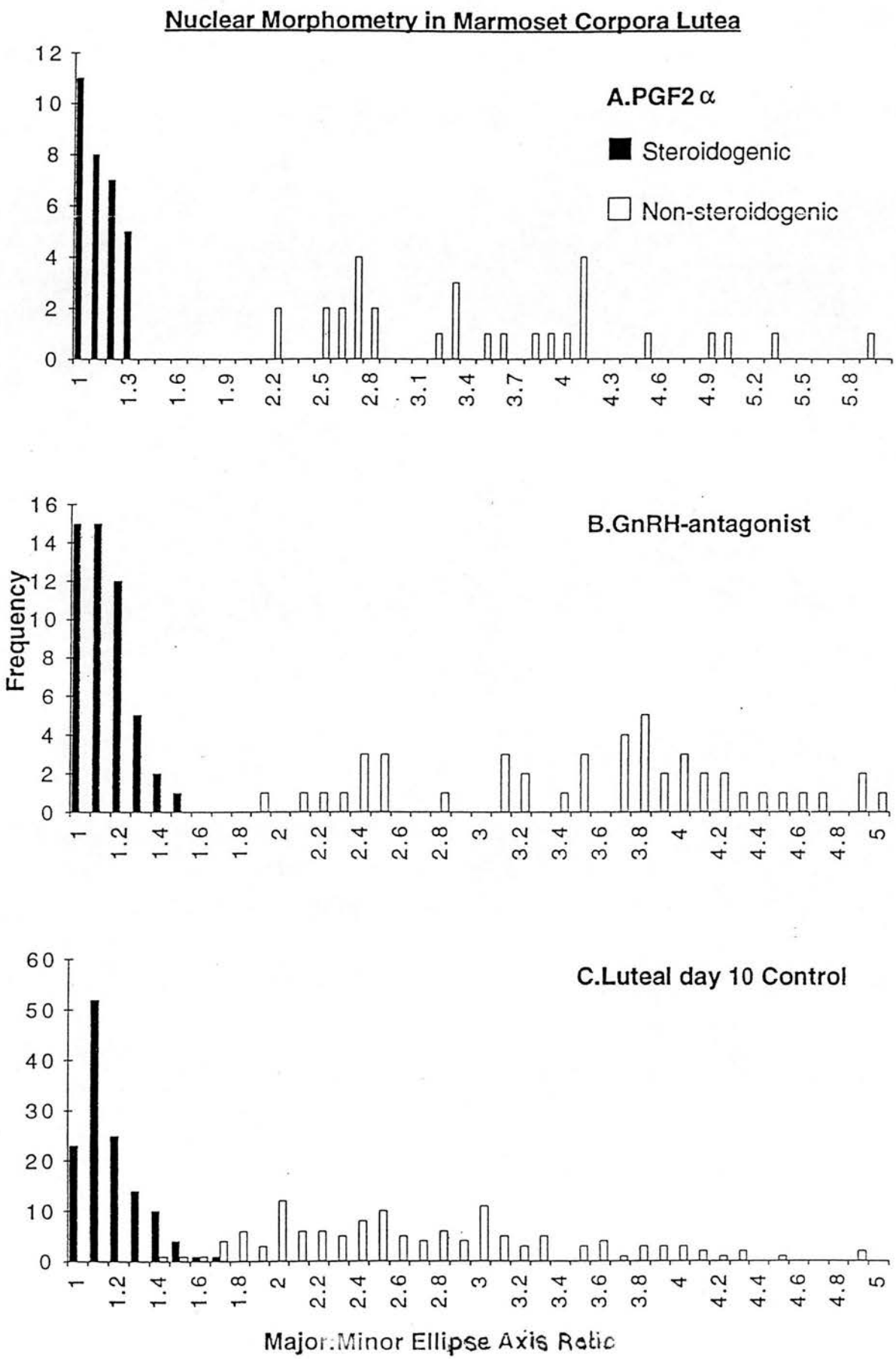
Nuclear Morphometry in Marmoset Corpora Lutea
A.PGF2 α
Steroidogenic
Non-steroidogenic
B.GnRH-antagonist
C.Luteal day 10 Control
Frequency
Major:Minor Ellipse Axis Ratio

Figure 2.6: The Relationship Between Optical Density and Ratio of Elliptical Axes in PCNA Immunostained Luteal Cell Nuclei.

Each data point represents one PCNA immunopositive nucleus. The data set were obtained from one unit area of luteal tissue from a corpus luteum collected on luteal day 10.

Relationship Between Optical Density and Ratio of Elliptical Axis in PCNA Positive Mid Luteal Phase Cell Nuclei

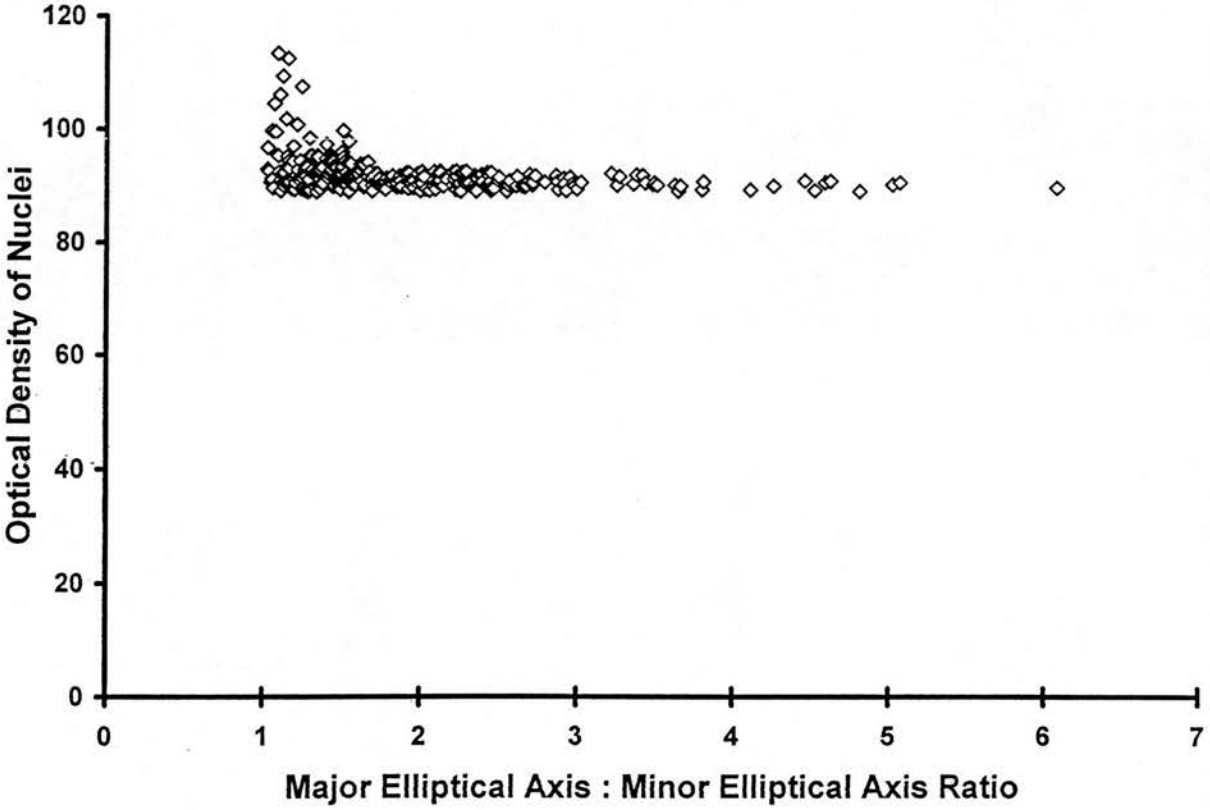

The automatic cell identification method highlighted every area of PCNA immunostaining, then measured the ellipse long and short axes, the optical density, and the area. These data were transferred into Excel spreadsheets, and the ratio of the ellipse long axis to the ellipse short axis determined. The number of areas with ratios less than 1.69 were designated as steroidogenic cell nuclei, and the number of areas with ratios higher than 1.7 were recorded as nonsteroidogenic cell nuclei.

In addition, a comparison was made between the automated method for scoring cells and the standard method of counting and identifying cells by eye. Randomly selected fields of view from representative corpora lutea collected on luteal day 10, 24 hours after PGF2α, and 24 hours after GnRH antagonist were assessed in this comparative study.

The same fields of view were scored using the automated system, and also laser printed in black and white onto standard A4 paper. The number of steroidogenic and nonsteroidogenic cells were assessed by simple observation and by marking cells with a pen to prevent double-counting. The three fields of view were scored by three different individuals, Dr. Hamish Fraser, Dr. Faye Roger and the author. The scorers were unaware of the automatic cell counts until after their assessments were completed.

The automated scoring system overestimated the number of steroidogenic cells and underestimated the number of nonsteroidogenic cells, and these two effects combined to give an overall value for automatic scoring which was 7.7±3.7% (mean±SD, n=4, Figure 2.7) lower than manual scoring. The automatic scoring system did not distinguish between overlapping nuclei, and as nonsteroidogenic cells were usually in closer juxtaposition than steroidogenic cells, the automatic system tended to score two or three overlapping nonsteroidogenic cell nuclei as one. However, the ellipse ratio of overlapping nonsteroidogenic cell nuclei still tended to fall within the range designated as nonsteroidogenic. Automatic steroidogenic cell scoring tended to be higher than manual counts because a subpopulation of nonsteroidogenic cells had rounded nuclei which had a simular nuclear ellipse ratio to steroidogenic cells. These nonsteroidogenic cells with rounded nuclei may have been macrophages or other immune system cells.

Figure 2.7: Comparison of Luteal Cell Nuclei Identification by Manual and Automatic Scoring Methods.

Ovaries containing corpora lutea were collected on luteal day 10, or 24 hours after PGF2α analogue, or 24 hours after GnRH antagonist. Luteal parenchymal steroidogenic cells and nonsteroidogenic cells were either identified using an automated system, or were identified by three independent observers using morphological criteria.

Comparison of Luteal Cell Nuclei Identification by Manual and Automatic Scoring

	Control Luteal day 10		PGF2alpha		GnRH antagonist	
	Manual	Auto	Manual	Auto	Manual	Auto
Steroidogenic	18	20	17	17	12	15
Non-Steroidogenic	33	29	27	22	26	20
Total No. Nuclei Counted	51	49	44	39	38	35

2.5.4 Statistical Analysis of Proliferating Cell Nuclear Antigen

Rationale for using analysis of variance are given in section 2.5.2. Numbers of PCNA immunopositive cells per unit area in mid luteal phase corpora lutea were compared with corpora lutea after induced regression with either PGF2α or GnRH antagonist in a one way analysis of variance using treatment as a between subject variable. Differences in numbers of non-steroidogenic cells in early, mid, late and follicular phase corpora lutea were also investigated by one-way analysis of variance using stage of the luteal phase as a between subject variable. Confidence intervals for the differences between means were evaluated by using Fisher's LSD procedure. This calculates the probability that a given confidence interval will not contain the true difference in group means and is exact when samples of unequal sizes are used.

2.5.5 Quantification and Statistical Analysis of Ubiquitin

Slide identification and treatment were obscured. Independent assessment by two observers (FY and HF) agreed that there were qualitative differences between treatments as described. Quantitative analysis was also conducted blind using a x40 objective lens. Six randomly selected fields of view of luteal tissue were scored for each animal and the mean number of ubiquitin positive cells per x40 field of view was calculated for each animal. Scoring more than five fields of view did not significantly alter the accumulative mean. Localisation of ubiquitin to either nucleus or cytoplasm was also recorded. Mean numbers were calculated for each experimental group and expressed ± SEM. A 2-tailed paired Student's t-test was applied to luteal day 10 controls and each of the two treatment groups. Significance was assigned at $p<0.05$.

2.5.6 Quantification of Ki67

Ovaries collected after induced regression with either GnRH antagonist or PGF2α, and the untreated luteal day 10 corpora lutea they were compared with were quantifed in the same manner as described in the PCNA study above. Briefly, four 31400μm^2 areas of luteal tissue were analysed using NIH 1.57 Image Analysis softwear, and every discrete area of Ki67 immunopositivity was

assumed to be one proliferating nucleus. The mean number of Ki67 positive cells was calculated from the four areas measured, and this was taken as being representative for that animal. Cells were also classified as being either steroidogenic or nonsteroidogenic on the basis of the nuclear ellipse ratio as described above.

Untreated corpora lutea collected through the luteal phase and during regression were analysed using a Highly Optimised Microscope Environment as described previously (Brugal *et al.*, 1992). Six 10 700μm^2 unit areas of luteal tissue per section were randomly selected and the mean of the six unit areas was taken as being representative for that animal. Measuring more than four unit areas did not alter the calculated mean. Cells were scored according to their morphological appearance and classified as being either steroidogenic or non-steroidogenic (see Morphometric Analysis of H&E Stained Sections – Identification of Cell Types), and also whether they were Ki67 positive or negative. The number of Ki67 positive steroidogenic and non-steroidogenic cells per 10 700μm^2 unit area were expressed as a mean±SEM for each experimental group. The number of Ki67 positive steroidogenic cells per 10 700μm^2 unit area for each animal was also expressed as a percentage of the total number of steroidogenic cells per unit area for that animal, and the number of Ki67 positive nonsteroidogenic cells was similarly expressed as a percentage of the total number of nonsteroidogenic cells per 10700μm^2 unit area. The mean percentage±SEM was calculated for each experimental group.

2.5.7 Statistical Analysis of Ki67

Data from mid luteal phase corpora lutea were compared with corpora lutea after induced regression with either PGF2α or GnRH antagonist in a one way analysis of variance using treatment as a between subject variable. Differences in numbers of Ki67 immunopositive cells in early, mid, late and follicular phase corpora lutea were also investigated by one-way analysis of variance using stage of the luteal phase as a between subject variable. Confidence intervals for the

differences between means were evaluated by using the Fishers LSD procedure, and significance was assigned at $p<0.05$.

Percentages and proportions are non-parametric because the distribution curve is only from 0 – 1(00), and therefore does not have the 'tails' of a normal distribution curve. It is possible to conduct a chi square test on percentage data, but this is not rigourous, and it is preferable to transform data to give a normal distribution, and then conduct a rigourous, parametric test upon that data. Percentages of Ki67 positive cells in corpora lutea from the early, mid, late and follicular phases were examined by one way analysis of variance using stage of the luteal phase as a between subject variable. Percentage data were transformed before conducting analysis of variance. Data transformation was by converting the percentage to a ratio <1, then taking the square root and the arc sin of each percentage. Radians were converted into degrees, and one way analysis of variance were conducted on these data. Confidence intervals for the differences between means were evaluated by using Fisher's LSD procedure, and significance was assigned at $p<0.05$.

2.5.8 Quantification of Bromoxydeuridine

BrdU labelled ovarian sections were viewed with an Olympus BH-2 microscope and a 40x objective lens. The field of view was adjusted to contain only luteal tissue. Every BrdU immunopositive cell in that field of view was counted, and further classified as being either steroidogenic or non-steroidogenic. BrdU immunonegative cells were similarly counted and classified as being either steroidogenic or non-steroidogenic. Three fields of view were scored for each ovarian section, and the mean scores of the fields of view were taken as being representative for that animal. Each ovary was examined in at least two separate BrdU runs, and results were consistent between runs as shown in Figure 2.8. Data were expressed as mean±SEM for each experimental group. The number of BrdU immunopositive steroidogenic cells per 40x field of view for each animal was also expressed as a percentage

of the total number of steroidogenic cells per 40x field of view for that animal, and the number of BrdU positive nonsteroidogenic cells was similarly expressed as a percentage of the total number of nonsteroidogenic cells per 40x field of view. The mean percentage±SEM was calculated for each experimental group

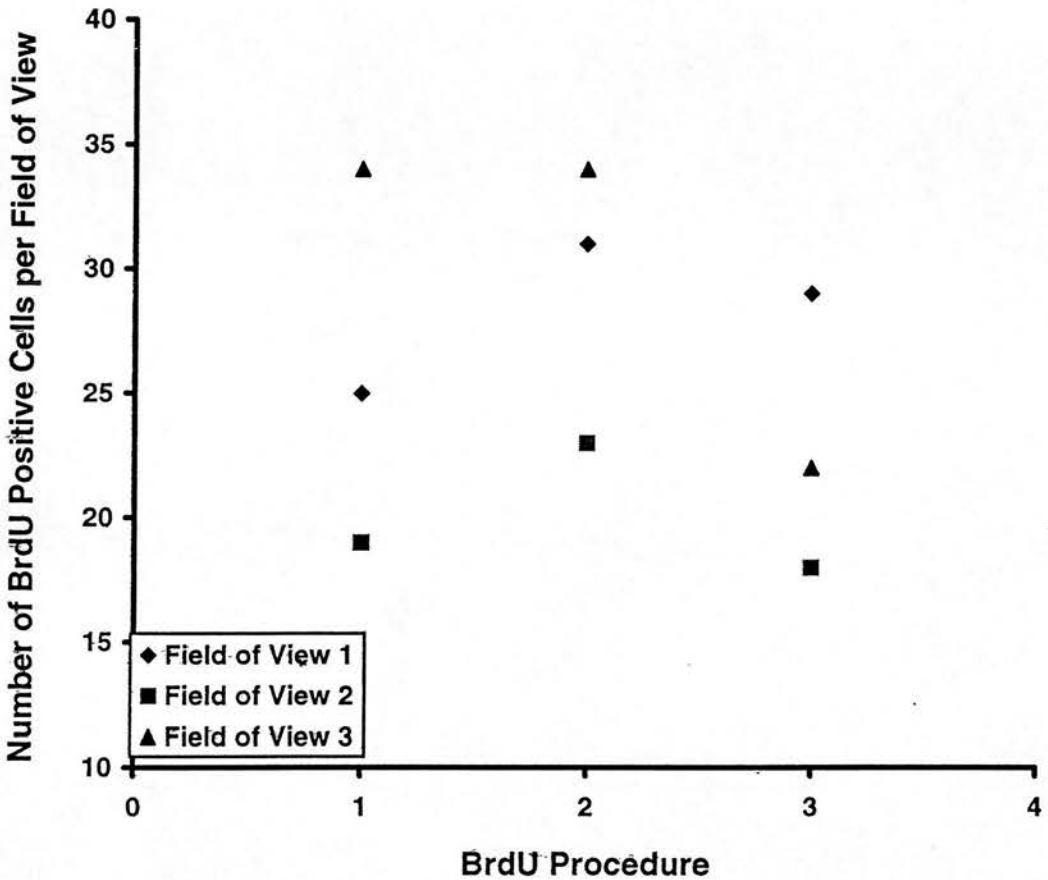

Figure 2.8 : Range of Results in 3 Separate BrdU Procedures in One Marmoset Corpus Luteum Collected During the Early Luteal Phase.

Marmoset ovarian sections were viewed with a 40x objective lens and three fields of view of luteal tissue were randomly selected. Data points represent the total number of BrdU immunopositive cells in each field of view. Serial sections of the same corpus luteum were subjected to BrdU immunocytochemistry on three separate occasions. Fields of view were randomly selected, so the 9 points represented here were all of different areas of luteal tissue.

2.5.9 Statistical Analysis of Bromoxydeuridine

Differences in numbers of BrdU immunopositive cells in early, late and follicular phase corpora lutea were investigated by one-way analysis of variance using stage of the luteal phase as a between subject variable. Confidence intervals for the differences between means were evaluated by using Fisher's LSD procedure, and significance was assigned at $p<0.05$.

Percentages of BrdU positive cells in corpora lutea from the early, late and follicular phases were also examined by one way analysis of variance using stage of the luteal phase as a between subject variable. Percentage data were transformed before conducting analysis of variance. Data transformation was by converting the percentage to a ratio <1, then taking the square root and the arc sin of each percentage. Radians were converted into degrees, and one way analysis of variance were conducted on these data. Confidence intervals for the differences between means were evaluated by using Fisher's LSD procedure, and significance was assigned at $p<0.05$.

2.5.10 Quantification of von Willebrand Factor VIII and BrdU Colocalisation

BrdU and vW colabelled ovarian sections were viewed with an Olympus BH-2 microscope and a 40x objective lens. The field of view was adjusted so that it contained only luteal tissue. Every BrdU immunopositive cell in that field of view was counted, and further classified as being either vW positive or negative. Three fields of view were scored for each corpus luteum, and the mean scores of the fields of view were taken as being representative for that animal.

2.5.11 Statistical Analysis of von Willebrand Factor VIII and BrdU Colocalisation

Bessels Correction for small samples was applied to the data obtained from quantification of von Willebrand Factor VIII and BrdU colocalisation luteal day 2-5 and luteal day 18 corpora lutea. The F-value was assumed to be significant at $p>0.05$.

2.6 Oligonucleosome Formation in Corpora Lutea.

2.6.1 Positive Controls for Oligonucleosome Formation

2.6.1.1 Thymocytes.

Wyllie (1980) demonstrated that thymocytes exposed to glucocorticoid *in vitro* underwent apoptotic cell death during which cell chromatin became cleaved into fragments which were multiples of 185bp and which could be viewed on a 1.8% agarose gel (Wyllie and Morris, 1982; Wyllie *et al.,* 1984). This model served as a positive control in our study of oligonucleosome formation in primate corpora lutea. Three male BalbC mice were killed by cervical dislocation and their thymus glands dissected free into hepes buffered Dulbeccos Modified Eagles Medium (hDMEM). The thymus glands were minced in a petri-dish at room temperature in hDMEM, then passed through a strainer into a centrifuge tube. The cells were washed by adding 5ml of media and centrifuged for 5 minutes at 250G. The resulting supernatant was disposed of and the cell pellet resuspended in media before counting the cells on a haemocytometer. The cell suspension was centrifuged again and the pellet resuspended in DMEM (hepes omitted) at a concentration of 12.5×10^6 cells per ml. One ml of cell suspension was dispensed to each well of a 25 well tissue culture plate. Dexamethasone (9α fluoro-16α-methylprednisolone, Sigma, Poole, England) was dissolved in ethanol to give a 0.01M solution. This was further diluted in DMEM to a concentration of 10^{-4} M. Aliquots (500µl) of this stock solution were stored at ˉ18°C. 10µl of dexamethasone stock solution were added to each of 20 wells to give a final concentration of 10^{-6} M. Cells were incubated for 22 hours at 37°C in 5% CO_2, then centrifuged at 150g for 10 minutes and the cell pellets stored at ˉ70°C until required for DNA extraction.

2.6.1.2 Bovine Corpora Lutea

Juengel *et al.* (1993) were the first to show that 185bp fragments of DNA were formed 12 hours after PGF2α-induced luteolysis in the cow, and that the amount of oligonucleosome formation increased 24 and 48 hours after luteolytic treatment. Zheng *et al.* (1994) also showed oligonucleosome formation in naturally regressing

bovine corpora lutea. We therefore used bovine corpora lutea which were collected 12 hours (n=2) and 24 hours (n=2) after administration of a luteolytic dose of PGF2a (5mg/ml, 25mg/cow Dinaprost given on luteal day 10) as positive controls for oligonucleosome formation. These corpora lutea were kindly donated by Denise Lawler, Royal (Dick) Veterinary School, Edinburgh University.

2.6.2 Negative Controls for Oligonucleosome Formation

A sample of liver was also collected from each marmoset after corpora lutea had been frozen to serve as a negative control tissue.

2.6.3 DNA Extraction and Oligonucleosome Detection

2.6.3.1 DNA Extraction

Cellular DNA was extracted and 3' end labelled by a method modified from Tilly and Hsueh (1993). Ten to 30mg of frozen luteal tissue, or one pellet of cultured thymocytes, were homogenized in 400µl buffer (0.1M NaCl, 0.3M Tris, 0.01M EDTA and 0.2M sucrose, pH 8) with a handheld electric homogeniser (Polytron PT 1200B92, Phillip Harris Co. Ltd, Glasgow). The homogenate was transferred to 1.5ml eppendorfs containing 25µl 10% sodium dodecyl sulphate (SDS), to which was added 12µl 10 mg ml^{-1} proteinase-K (Sigma). Samples were incubated in a 65^0C water bath for 2-3 hours until the homogenated appeared to be digested. Samples were examined briefly and shaken by hand at approximately 30 minute intervals during this incubation. Samples were then centrifuged (5000G for 20 minutes at 4^0C), the supernatant collected, and an equal volume (400µl) of phenol:chloroform:isoamyl alcohol (25:24:1 v:v:v) added. After vortexing and microcentrifugation (13 000rpm for 5 minutes at room temperature), the upper phase was collected and an equal volume (400µl) of chloroform:isoamyl alcohol (24:1 v:v) added. Vortexing and centrifugation were repeated, and the upper phase collected. The supernatant volume was determined, and 5M NaCL was added to 10% of the supernatant volume. Glycogen (20µg/µl, Boehringer Mannheim, Lewes) was added to 1% supernatant volume and 100% ethanol (2.5x supernatant volume) was also added, and inversion mixed before incubation at $^-70^0$C for 12 hours. After

centrifugation (13 000rpm for 30 minutes at 4^0C) the supernatant was discarded and the DNA pellet resuspended in 25µl sterile water, and stored at 4^0C until used.

2.6.3.2 2% Agarose Gel Production

50x concentrated TAE buffer (40mM Tris acetate, 1mM EDTA) stock was made by adding 121g Tris base to 28.55ml glacial acetic acid and 50ml 0.5 M EDTA (pH8), then making up to 500ml with distilled water. To make a 2% agarose gel, 50ml 1xTAE buffer were added to 1g agarose and microwaved until all agarose is dissolved. 2µl of ethidium bromide were added to the agarose before pouring into a mold, inserting a comb and leaving to set at room temperature.

2.6.3.3 DNA Quantification

Lambda DNA (365µg/ml stock, Promega) was used as a DNA standard on a 2% agarose gel. Adjacent lanes contained increasing concentrations of DNA (0.1, 0.2, 0.3, 0.4, 0.5, 1 µg DNA/lane). 2µl of each extracted sample were also examined on the same gel, and the concentration of genomic DNA in each sample calculated from the DNA standards. Extraction from 10-30mg of tissue yielded 0.1-0.5µg/µl DNA per sample. Oligonucleosome 'laddering' was not apparent in these ethidium bromide stained gels.

2.6.3.4 3' End Labeling

15µl of sample DNA and the following reagents: 15µl 5x reaction buffer (1M potassium cacodylate, 0.125M Tris-Cl, 1.25 mg ml^{-1} BSA, pH 6.6), 5µl 25mM CoCl and 1µl of 25 U μl^{-1} terminal transferase (Boehringer Mannheim, Lewes). 2µl (20µCi) of radiolabelled dideoxynucleotide ([α-32P]-dd ATP (3000 Ci $mmol^{-1}$, Amersham) were incubated at 37^0C for 60 minutes. The reaction was terminated by the addition of 20µl 0.25M EDTA., Samples were loaded onto Sephadex G50 Nick Spin Columns (Pharmacia, Uppsala, Sweden) and centrifuged at 500 G for 5 minutes to separate DNA-bound from free radionucleide. 3' end labelled samples were therefore recovered in 50-60µl volumes. 1µg of labelled DNA per sample was electrophoresed on a 2% agarose gel for 2.5 hours at 85V using a 1XTAE (40mM

Tris-acetate, 1mM EDTA) running buffer. Gels were dried and exposed to Kodak X-Omat AR film for 2 hours at $^{-}72^{0}$C initially, followed by a 12hour exposure of the same gel in order to confirm that oligonuclosome formation was absent from negative control samples. Two dried gels were also applied to a PhosphorImager for 5 hours for quantification of oligonucleosomes.
DNA extraction and labeling were conducted at least twice on each sample, and representative gels are shown.

2.6.3.5 Quantification of Oligonucleosomes.

All samples were run on the same gel. The optical density of the lowest three fragments in each sample was determined and their mean calculated. Unequal lane loading was compensated for by adjusting the optical density of the genomic DNA band in each lane to 100%, and then multiplying the mean optical density of oligonucleosome bands by the same correction factor. The mean and SEM of each experimental group was then determined.

2.6.4 *In situ* 3' End Labelling of Marmoset Corpora Lutea.

Paraformaldehyde fixed sections were hydrated by transferring the slides through two troughs of xylene (5 min in each) and 1 minute in each of 100%, 95% and 70% ETOH. Endogenous peroxidase was blocked with a 30 minute incubation in 3% H_2O_2 (BDH Laboratory Supplies, Dorset, U.K.) in methanol. Washing with PBS was followed by a 45 minute incubation in 5ug/ml proteinase K (Sigma, Dorset, U.K.) in PBS at 37^{o}C. Slides were transferred to Sequenza racks (Life Sciences International, Hampshire, U.K.) and rinsed 3 times in PBS. Positive control sections were incubated for 10 minutes at 37^{o}C in 5ug/ml DNase (Bohringer Mannheim, Essex, U.K.) in buffer (30mM TrisCl (Sigma) pH 7.2, 140 mM Na-cacodylate (Agar Scientific Ltd., Essex, England), 4mM $MgCl_2$ (Analar, Poole, England) 0.1mM DTT (Promega, Hampshire, U.K.) then rinsed once in TE buffer (TrisCl 0.1M, EDTA 0.05M) and 3 times in PBS. 3'-OH ends of DNA fragments were labelled with 0.5nM digoxigenin-11-UTP (Bohringer Mannheim, Essex, U.K.) by 50U/ml terminal

deoxynucleotidyl transferase (TdT, Bohringer Mannheim, Essex, U.K.) in buffer (30mM TrisCl (Sigma, Dorset, U.K.) pH 7.2, 140 mM Na-cacodylate (Agar Scientific Ltd., Essex, U.K.), 1.5mM $CoCl_2$ (Bohringer Mannheim, Essex, U.K.) for 1 hour at 37°C. Negative control sections had the TdT replaced by the equivalent amount of buffer. Four rinses with PBS were followed by incubation with horseradish peroxidase-conjugated sheep anti-digoxigenin antibodies (Bohringer Mannheim, Essex, U.K.) 1.5 U/ml in buffer (100mM TrisCl (Sigma, Dorset, U.K.) pH 7.5, 150mM NaCl) for 30 minutes at room temperature. Three PBS washes were followed by visualisation with 0.04% 3,3'-diaminobenzidine (w/v,Sigma, Dorset, U.K.) in 0.05M TrisCl (Sigma, Dorset, U.K.) pH 8 and 3% H_2O_2 (BDH Laboratory Supplies, Dorset, U.K.).

2.6.4.1 Positive and Negative Controls

Positive control serial sections were treated with DNase prior to labeling. The DNase caused DNA fragmentation in every nucleus, therefore this positive control had the potential to yield 100% 3' end labeling. It was found that the amount of labeling in test samples was dependent upon the proteinase K treatment, therefore parameters were adjusted in order that DNase treated sections would have 99% labeling. In this way the amount of apoptosis indicated by 3' end labeling would be a conservative underestimate, rather than a falsely high estimate. The second, internal positive control was based on work demonstrating that follicular atresia occurs through a process of granulosa cell apoptosis (Tilly *et al.*, 1991). Apoptosis occurs in the granulosa cell layer, but not the theca cell layer of primate atretic follicles, and this was demonstrated in 3' end labeled baboon (Tilly 1993) and marmoset (Giebel 1997) ovarian sections. The internal positive control was therefore that granulosa cells would be 3' end labeled in atretic antral follicles in the marmoset ovarian sections used in these studies. The corresponding internal negative controls were that theca cells of atretic follicles, and granulosa cells of morphologically healthy preantral follicles, were not undergoing apoptosis and would not become 3' end labeled. The external negative control was to omit TdT, the enzyme responsible for the tailing

reaction, from the labeling procedure. Even apoptotic cells would not be labeled in these negative controls, and the incidence of 3' end labeling would be 0%.

2.6.4.2 Quantification of 3' End Labeled Sections

Each ovary was 3' end labeled on at least three separate occasions. Results are taken from one representative 3' end labeling run. DNase positive controls and test sections were viewed with a x20 objective lens. 3' end labeled nuclei were counted in three randomly selected fields of view of luteal tissue using an NIH Image Analysis 1.57 programme and the mean calculated to give the number of positive nuclei per x20 field of view. Amount of 3' end labeling in test sections was expressed as a percentage of that seen in DNase positive controls.

2.6.4.3 Statistical Analysis of 3' End Labeled Sections.

Results from the 3' end labelled sections are expressed as means of percentages±SEM of 3' end labelled cells. The data were subjected to a chi square analysis and significance was assigned at $P<0.05$.

Chapter 3: Cell Morphology and Cell Death in the Corpus Luteum of the Marmoset Monkey.

3.0 Introduction

This investigation into the instigation and process of luteal regression starts by examining the cells of the corpus luteum in order to determine the relative proportions of different cell types, and to ascertain whether cell numbers change during luteal regression. Removal of luteal tissue, or structural regression, is most likely to occur through cell death and tissue reorganisation but the nature of luteal cell death, and the temporal relationship between cell death and luteal regression in marmosets, is not clear.

3.0.1 The Cellular Composition of Corpora Lutea.

Corpora lutea are composed primarily of parenchymal steroidogenic cells, fibroblasts and capillary endothelial cells. Immune system cells such as macrophages and eosinophils are also part of the resident population of the corpus luteum. Parenchymal steroidogenic cells are further sub-divided into those which were derived from the granulosa cells of the follicle, granulosa-lutein or large luteal cells, and those derived from the theca cells of the follicle, theca-lutein or small luteal cells (Corner 1956; Behrman *et al.*, 1993; Sawyer et al., 1991; Hild-Petito *et al.*, 1989; Clement 1987; Webley et al., 1990; Sasano et al., 1989). Small and large steroidogenic cells can be identified using a light microscope by determining differences in size and morphological features. In most species small luteal cells form the majority of steroidogenic cells, they have a diameter in the range of 12 to 22 μm, an irregularly shaped nucleus with an infolded nuclear membrane and an irregular stellate shape. Large luteal cells have a diameter in the range of 22 to 35μm, a regular polyhedral shape and regularly shaped spherical nuclei containing prominent nucleoli (O'Shea *et al.*, 1986; O'Shea *et al.*, 1989; Brannian et al., 1993; Deane et al., 1966; Ohara et al., 1987) Electron microscopy reveals the presence of large amounts of smooth endoplasmic reticulum and mitochondria, which is consistent with the steroidogenic function of large and small luteal cells (Ohara *et al.*, 1987; Webley *et al.*, 1990), and in many species large luteal cells also have secretory granules and the organelles required for protein secretion. In ruminants secretory granules in large luteal cells have been shown to contain oxytocin or relaxin

(Gemmell *et al.*, 1974; Paavlova and Christensen, 1981) and in rats and pigs they contain relaxin (Fields 1984; Fields and Fields 1985). Secretory granules are not common in human luteal cells, although they do produce oxytocin and relaxin (Khan-Dawood *et al.,* 1989).

In sheep, small and large luteal cells, and endothelial cells, decrease in number and in size from the mid to late luteal phase, but fibroblast numbers remain constant. There are six times more small than large luteal cells in ovine and bovine corpora lutea (Sawyer *et al.,* 1991; O'Shea *et al.*, 1986; O'Shea *et al.*, 1989). Human corpora lutea, however, have twice as many large as small luteal cells, and this proportion remains constant throughout the luteal phase (Lei *et al.*, 1991). Both bovine and human corpora lutea contain more non-steroidogenic cells than steroidogenic cells, with the majority of these being fibroblasts. In the human corpus luteum there are approximately the same number of macrophages as there are fibroblasts during the mid luteal phase, and three times more macrophages by the late luteal phase (Lei *et al.*, 1991). Macrophages are more numerous in human corpora lutea than they are in ruminant species in which PGF2α from the uterus is the luteolytic signal (Sawyer *et al.*, 1991).

The mid-phase bovine corpus luteum has a dense capillary network made up of fully differentiated endothelial cells with a flattened elongated morphotype and numerous tight junctions (Modlich et al., 1996). Early luteal regression is characterised by the detachment of endothelial cells from capillary basal lamina, and Modlich *et al* (1996) found ultrastructural evidence of steroidogenic cell apoptosis at this time. In rodents luteal regression is characterised by infiltration of the luteal mass by connective tissue and by vacuolisation of steroidogenic cells. The resulting regressing corpus luteum has been described as having 'a honey-comb-like structure in which each space is occupied by a degenerating luteal cell' (Van Blerkom and Motta 1978). Corner (1956) noted that human corpora lutea are in a process of development from days 1-8, with peak steroidogenic activity occurring on luteal days 7 and 8. Thecal cells form an irregular layer several cells thick around the corpus luteum, and also extend into the central cavity along vascular septa, in an arrangement reminiscent of the spokes of a cartwheel. Luteal regression begins on luteal day 9 and is characterised by granulosa-lutein cell shrinkage and vacuolation. Vacuolation

apparently caused by lipid accumulation was either in the form of a number of different sized vacuoles within the cytoplasm, or giant vacuoles which obscured any remaining cytoplasm, or in the formation of "mulberry cells" in which the cytoplasm was packed with uniformly small vacuoles. "Mulberry cells" were only seen on luteal days 13 and 14, and nuclei degenerating into densely-staining irregular masses reminiscent of apoptotic bodies were also seen on luteal day 14. Ongoing fibrosis and shrinkage continued over several months with the eventual formation of a corpus albicans (Clement, 1987). This process has not been described in the marmoset monkey.

3.0.1.1 Characteristics of Marmoset Luteal Cells.

Marmoset corpora lutea do not appear to have two different types of steroidogenic cells based on the criteria of morphology or size. Instead cells positive for 3β HSD, and therefore identified as being steroidogenic using functional criteria, are of uniform size and regular polygonal shape, and have diameters in the range 14-32μm (Webley *et al.*, 1990). Electron micrographs indicate that these cells contain euchromatic and slightly lobed nuclei with one or two nucleoli, smooth endoplasmic reticulum which varies in extent of dilatation between cells, and numerous mitochondria with round to elongate rod shapes and tubular cristae (Fehrenbach *et al.*, 1995; Webley *et al.*, 1990).

3.0.2 Mechanisms of Cell Death

Cell death can be caused by an extra-cellular event, or by an intracellular event (Hockenberry, 1995). In the latter case, extra-cellular conditions appear to stay constant, but an individual cell enters a death pathway. The lack of an extra-cellular impetus for cell death suggests some change in the intracellular environment, and gives rise to the premise that this type of death is 'programmed' – a set of death instructions encoded in the cells' DNA (Majno and Joris, 1995). Apoptosis is one type of programmed cell death, defined by specific morphological and biochemical criteria (Kerr *et al.*, 1972; Schwartzman and Cidlowski, 1993). A common

intracellular signal for apoptosis is DNA damage: if the damage can be repaired the cell continues normal cycling, but if it is irreparable the cell enters an apoptotic pathway (Basu *et al.*, 1998). It is also possible that apoptotic pathways evolved as a defense against viral infection (Haecker and Vaux, 1994).

Cell death caused by changes in the extra-cellular environment may occur through myriad mechanisms (Haecker and Vaux 1994). Conditions that impair cell membrane function commonly result in the loss of osmotic and ionic regulation, but may leave the DNA intact until a later stage of the death process. Other extra-cellular changes may be mediated by receptor binding and transduction pathways, and therefore affect intra-cellular function and DNA integrity relatively early in the death process.

Ubiquitin is a 76-amino acid polypeptide associated with a number of cell death mechanisms, including apoptosis in murine myoblasts (Sandri *et al.*, 1997). Its main role is to mark proteins for degradation (Hershko, 1988) and it is expressed in the nucleus and the cytoplasm (Haas and Bright 1985) of both dying and cycling cells (Lauzon *et al.,* 1993).

3.0.2.1 Apoptosis

During the initial stages of apoptosis the cells shrink, and the chromatin condenses and packs into smooth masses making crescent shapes alongside the nuclear membrane (Kerr *et al.*, 1972). In H&E sections a cell in the initial stages of apoptosis is likely to lack physical contact with neighboring cells, and also might appear slightly smaller than average, with intensely stained nuclei, but in fact would be very difficult to distinguish from non-apoptotic or necrotic cells. In the next phase of apoptosis, endonucleases cleave DNA at 185 base pair (bp) intervals, or at multiples of 185bp's (Wyllie, 1980, Arends *et al.*, 1990). DNA is wound around histones to make nucleosomes which in turn are linked together by 185bp lengths of DNA: the nucleosomes are 'beads' separated by 185bp 'links' (Hsueh *et al.*, 1994). Linker DNA is susceptible to cleavage by endonucleases, and the first fragments to be formed are high multiples of 185bp, and as cleavage proceeds, fragments which are lower multiples of 185bp are generated (Basnakian and James, 1994). If DNA is extracted from apoptotic cells and electrophoresed on an agarose gel, the fragments

of DNA form a characteristic 'ladder' pattern with the 'rungs' of the ladder consisting of fragments of sizes which are multiples of 185bp (Hsueh *et al.*, 1994). If DNA is extracted from a population in which the majority of cells are apoptotic, the 'ladder' can be visualised on ethidium bromide stained gels (Wyllie, 1980, Arends *et al.*, 1990). If only a small percentage of the total population of cells are apoptotic, the quantity of fragmented DNA is too low to be seen on ethidium bromide stained gels (Juengel *et al.*, 1993). A more sensitive visualisation technique employs an enzyme, terminal transferase, to attach a label, either P^{32} or digoxigenin onto the 3' ends of the fragments, which are then subjected to electrophoresis as before (Tilly and Hsueh 1993). DNA fragments generated during apoptosis can also be visualised *in situ*, in tissue sections, using the same method (Gavrieli *et al.*, 1992).

Random DNA fragmentation occurs during cellular necrosis, but generates fragments of different lengths that appear as a smear of DNA after electrophoresis, as opposed to the distinct 185bp 'rungs' of apoptosis (Hsueh *et al.*, 1994). However, *in situ* 3' end labeling does not distinguish between necrotic and apoptotic DNA in tissue sections, therefore 3' end labeled nuclei in tissue sections should be assessed in conjunction with other methods (Phelouzat *et al.*, 1996). Cell death caused by plasma membrane damage and disrupted osmotic regulation is indicated morphologically by the presence of cytoplasmic vacuoles, or ruptured cells, or the presence of leukocytes associated with an inflammatory response. These cells may then progress to necrosis, which is difficult to differentiate from the latter stages of apoptosis. However, there is one major difference between necrosis and apoptosis. Cells in the latter stages of apoptosis undergo nuclear fragmentation or karyorhexis, and the cell buds off apoptotic bodies which contain pyknotic nuclear fragments which may be phagocytosed by macrophages or neighboring cells (Hsueh *et al.*, 1994). Therefore the presence of 3' end labeled fragmented nuclei or apoptotic bodies, either in inter-cellular spaces or in the cytoplasm of otherwise healthy cells, is strongly suggestive of apoptotic DNA fragmentation.

3.0.2.2 Oncosis

Cell death caused by ischemia has been described in detail, and the term 'oncosis' has been suggested for this form of cell death in which cytoplasmic swelling is the most characteristic feature (Majno and Joris 1995). Oncosis is initiated by plasma membrane changes which result in the impaired action of ion pumps and consequent loss of calcium and sodium balance (Bowen 1984). Increased calcium is associated with chromatin aggregation and pyknosis (similar to that seen in apoptosis), followed by karyolysis during which chromatin appears to disappear from the nucleus (dissimilar from the karyorhexis that occurs during apoptosis). Oncosis proceeds with lysosome swelling, dilation and vesiculation of the endoplasmic reticulum and loss of compartmentalisation and cell oedema (Bowen 1984; Trump *et al.*, 1981; Cohen 1991) and would appear as swollen, vacuolated cells in H&E stained tissue sections. Oncosis contrasts with apoptosis in that cells swell, as opposed to the shrinkage that occurs during apoptosis. The nuclei of cells undergoing oncosis remain essentially intact throughout the process, whereas apoptotic nuclei fragment into apoptotic bodies within 34 minutes (Majno and Joris 1995; Bursch *et al.*, 1990). Specific DNA fragmentation characteristic of apoptosis occurs relatively early, but the random, non-specific DNA fragmentation associated with necrosis occurs up to 24 hours after the onset of oncosis (Majno and Joris 1995).

3.0.2.3 Necrosis

Necrosis is a term commonly used to indicate non-apoptotic cell death, however cell death and necrosis are two different things. A process leading to cell death occurs in liver cells as soon as they are exposed to ischemic conditions, but the point of no return, or actual death, occurs approximately 150 minutes after instigation of the ischemic conditions (Majno and Joris 1995). Necrotic changes are only visible after the cell has actually died, and are analogous to the rigor mortis of a cadavar, necrotic changes are similar no matter what the cause of death (Majno and Joris 1995). Necrosis is characterised by random DNA fragmentation and disappearance, and cytoplasmic condensation and cell shrinkage. This resembles the latter stages of apoptosis, with the exception that necrotic cells do not form apoptotic bodies.

3.0.3 Aims of Study.

A morphometric tissue analysis requires that different cell types are identifiable, therefore the first aim of this study is to identify steroidogenic luteal cells by immunocytochemistry for the steroidogenic enzyme 3 beta hydroxysteroid dehydrogenase isomerase, and to derive morphological criteria for identifying steriodogenic cells in H&E stained sections based on this functional definition.

The second aim is to determine the number of steroidogenic and nonsteroidogenic cells in corpora lutea collected during different stages of the luteal phase and after induced luteal regression. Any changes in cell numbers or ratios of cell types will be related to stage of the luteal phase or luteal regression.

The third aim is to examine cell death at different stages of the luteal phase and during regression, with the specific aim of establishing the presence or absence of apoptosis. Three different methods will be used to identify and quantify apoptosis; (i) identification of apoptotic bodies in H&E stained sections, (ii) gel electrophoresis of radioisotope labeled DNA and (iii) *in situ* 3' end labeling. A fourth aim is to examine the expression of ubiquitin in the corpora lutea of the marmoset monkey after induced luteolysis, and to assess ubiquitin as an early indicator of apoptotic cell death.

3.1 Results

3.1.1 Identification of Steroidogenic Cells by Immunocytochemistry for 3β Hydroxysteroid Dehydrogenase Isomerase (3β HSD).

Red 3β HSD immunoreactivity was localised to the cytoplasm of large, circular cells with spherical nuclei (Figure 3.1), and these had the same morphological appearance as the cells which were defined as steroidogenic by Webley *et al.*, (1990) and which were shown in both light and electron micrographs. In addition, Fehrenbach *et al.*

(1995) found cells with this morphological appearance to have 3β HSD activity in mid-luteal phase marmoset corpora lutea.

The majority of parenchymal cells in mid-luteal phase day 10 corpora lutea were 3β HSD immunopositive, but the number of 3β HSD immunopositive cells in early or in late luteal phase corpora lutea was extremely variable, and ranged from less than a third of the cells with the morphological appearance of steroidogenic cells being 3β HSD immunopositive, to nearly 100% of the parenchymal cells being 3β HSD positive. Some 3β HSD immunopositive cells were present in very late corpora lutea collected in the early follicular phase after progesterone concentrations had decreased to follicular phase values. Within each section, 3β HSD immunostaining appeared to be fairly constant, and generally there was not a gradation of immunostaining to indicate that some cells contained more 3β HSD than others. This was not the case after induced luteolysis, however and 24 hours after treatment with either GnRH antagonist or PGF2α (Figure 3.1C and E), some parenchymal cells appeared more intensely immunostained than others. This intense 3β HSD immunopositivity tended to occur in cells which were vacuolated or showing other morphological signs of degeneration, whereas cells which appeared morphologically normal had less intense immunostaining. Cells with the morphological appearence of fibroblasts or endothelial cells were 3β HSD immunonegative. Negative control sections had some non-specific cytoplasmic staining (Figure 3.1B, D and F), but this was of a much lower intensity than that seen in sections which had been exposed to primary antibody.

Figure 3.1: 3β Hydroxysteroid Dehydrogenase (3βHSD) Immunocytochemistry in Marmoset Corpora Lutea After Induced Luteal Regression.

Marmoset ovaries collected after *in vivo* administration of luteolytic agents. Panels A and B; 3βHSD positive and its antibody negative control serial section respectively. Granulosa and theca cells visible in a follicle in top left hand corner, and the remainder is untreated luteal tissue collected during the mid luteal phase on day 10. Panels C and D; 3βHSD positive and its antibody negative control serial section 24 hours after *in vivo* administration of a GnRH antagonist, antarelix. Panels E and F; 3βHSD positive and its antibody negative control serial section 24 hours after treatment with the PGF2α analogue, cloprostenol. All ovaries were collected on luteal day 10. 3βHSD immunopositive cells are pink to dark crimson red, and immunonegative cell nuclei are counterstained blue with haematoxylin. Scale bars represent 20μm.

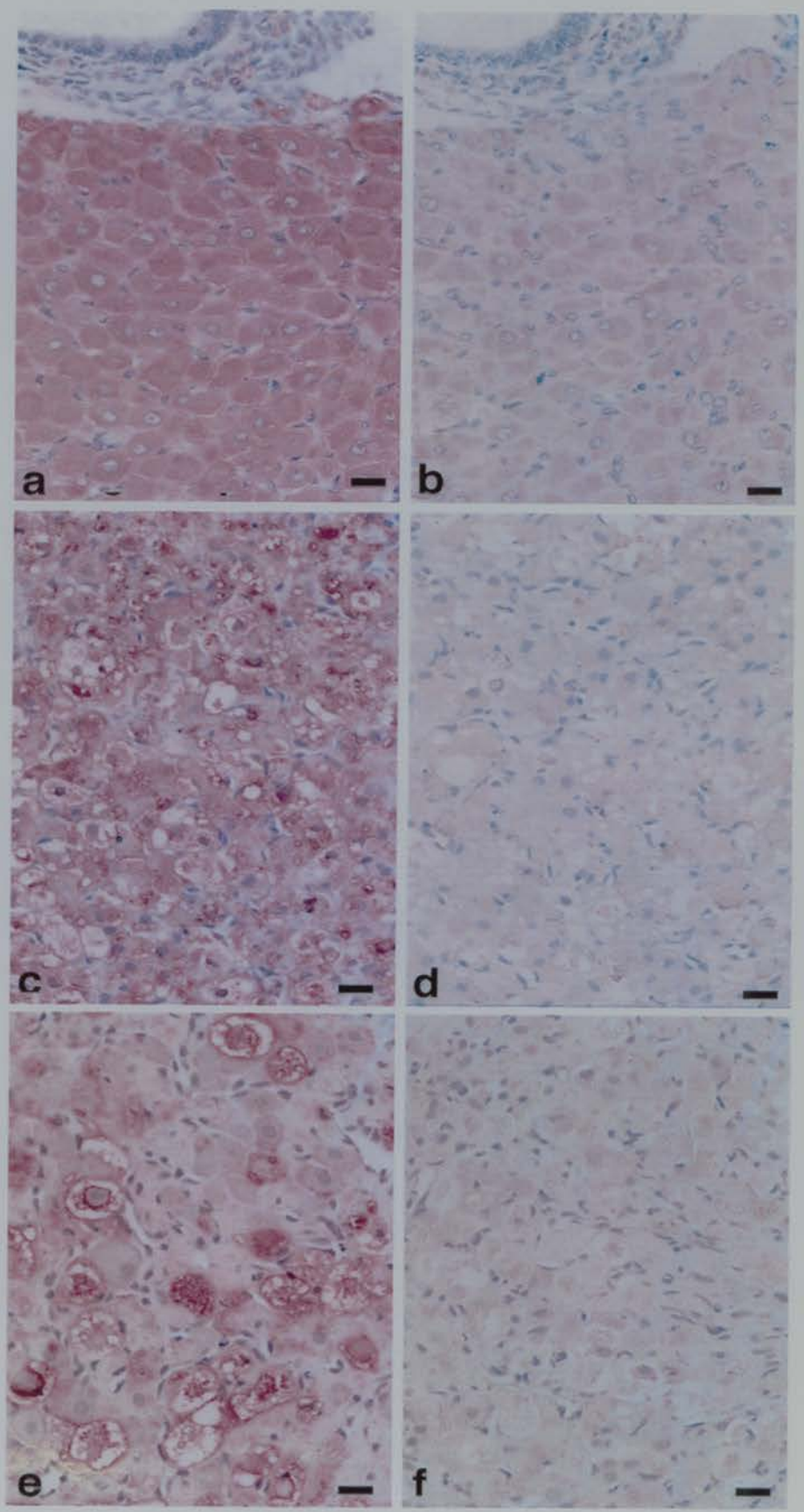
a
b
c
d
e
f

3.1.2 Morphological Analysis Of Haematoxylin and Eosin Stained Sections of Marmoset Corpora Lutea.

Steroidogenic cells in untreated day 10 corpora lutea were commonly in close juxtaposition to non-steroidogenic cells, which appeared to form a network surrounding the steroidogenic cells (Figure 3.2a and Figure 3.3a). Mid luteal phase tissue had a regular close-packed structure which was in marked contrast with the disorganised, irregular structure of tissues undergoing luteal regression (Figure 3.3b and c).

The morphological appearance of non-steroidogenic cells did not appear to change after luteolysis, unlike the parenchymal steroidogenic cells which exhibited a range of cytoplasmic changes apparently bought about by the formation of vacuoles. The vacuoles in naturally regressing corpora lutea from the early follicular phase were small and discrete, and were not present in all steroidogenic cells (Figure 3.4b). The proportion of vacuolated cells, and the size of the vacuoles, had increased by the late follicular phase. Steroidogenic cell vacuolation also occurred after luteolytic treatment (Figure 3.3b, c, d and e), but the vacuoles were larger than those seen in naturally regressing corpora lutea and the steroidogenic cells had an oedematous appearance commonly associated with oncosis (Bowen, 1984). The majority of steroidogenic cells in the corpora lutea from animals treated with GnRH antagonist appeared oedematous (Figure 3.3b and c), whereas in the animals treated with PGF2α, the proportion of vacuolated cells was more variable (Figure 3.3d and c). Some areas contained only a few vacuolated cells while other areas consisted of predominantly vacuolated cells.

Apoptotic bodies were found in all corpora lutea and had the appearance of clusters of small irregular spheres with intense haematoxylin staining (Figure 3.4). Cells in the final stages of apoptosis had condensed cytoplasm and nuclear fragments which exhibited the same intense haematoxylin staining as that seen in apoptotic bodies. There was no obvious separation of apoptotic and vacuolated cells, with the two types commonly found in close juxtaposition (Figure 3.3c and e and Figure 3.4 b,c,d).

Figure 3.2: Haematoxylin and Eosin Stained Marmoset Corpora Lutea During Spontaneous Luteal Regression.

Luteal tissue collected on (a) luteal day 10, (b) luteal day 18 during functional luteal regression, and (c) luteal day 22 during structural luteal regression. Panels (d) and (e) show lower and higher magnifications respectively of the section shown in (c). Steroidogenic and nonsteroidogenic cells are apparent in all panels, vacuolated or apoptotic cells are not visible in (a) or (b), but apoptotic cells are indicated with arrows in (e). (d) although progesterone concentrations are at basal levels and the follicular phase is well under way, the amount of luteal tissue (upper half of the image) is substantial. Scale bars represent 20μm.

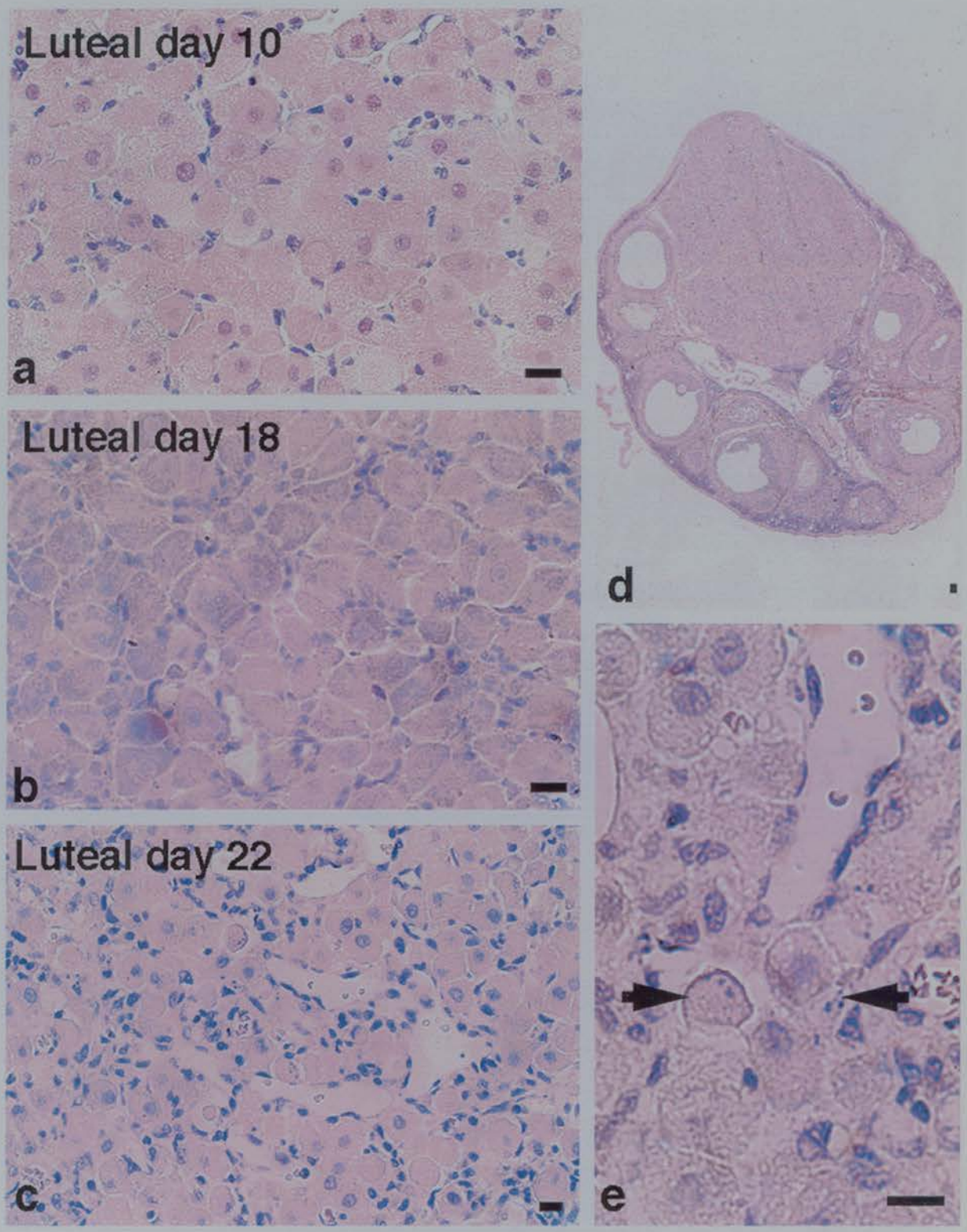
Luteal day 10
a
Luteal day 18
b
Luteal day 22
c
d
e

Figure 3.3: Haematoxylin and Eosin Stained Marmoset Corpora Lutea After Induced Luteal Regression.

Marmoset ovaries collected after *in vivo* administration of luteolytic agents. Panel (a); untreated control corpus luteum collected on day 10 of the luteal phase. Panels (b) and (c); corpora lutea 12 hours and 24 hours respectively after *in vivo* administration of a GnRH antagonist, antarelix. Panels (d) and (e); luteal tissue 12 hours and 24 hours respectively after treatment with the PGF2α analogue, cloprostenol. All ovaries were collected on luteal day 10. Arrows indicate apoptotic bodies or apoptotic cells, and stars mark vacuolated cells. Scale bars represent 20μm.

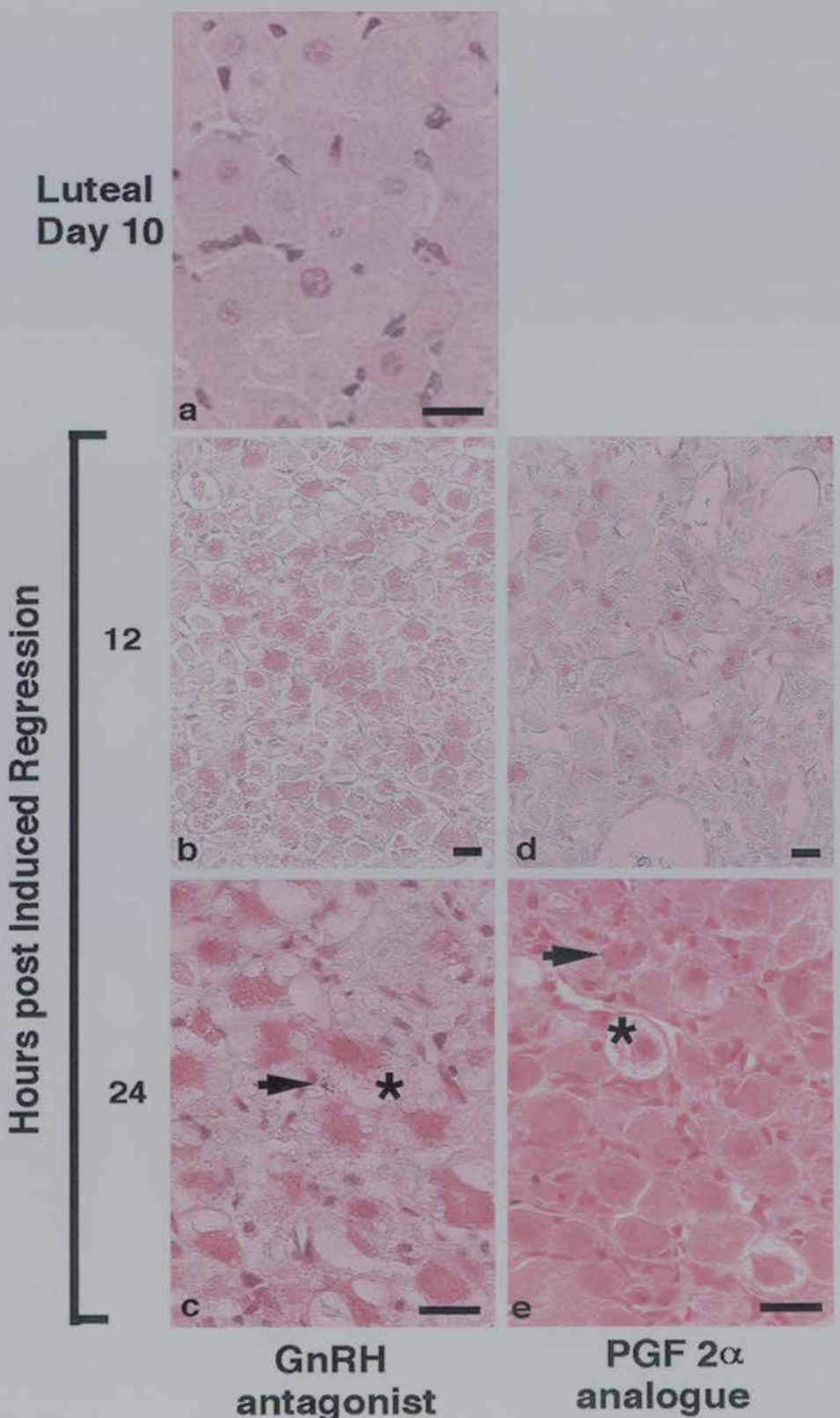
Luteal
Day 10
a
Hours post Induced Regression
12
24
b
d
c
e
GnRH
antagonist
PGF 2α
analogue

Figure 3.4: Haematoxylin and Eosin Stained Sections of Marmoset Corpora Lutea.

Whole ovaries collected on: (a). luteal day 10, arrows indicate nonsteroidogenic cells, 'S' indicates a steroidogenic cell, (b). luteal day 22 during structural luteal regression, (c).24 hours after *in vivo* administration of PGF2α, and (d).24 hours after *in vivo* administration of GnRH antagonist. Arrows indicate apoptotic cells or apoptotic bodies, * indicates a vacuolated cell, 'S' indicates steroidogenic cell in panels b, c and d. Scale bar=20μm.

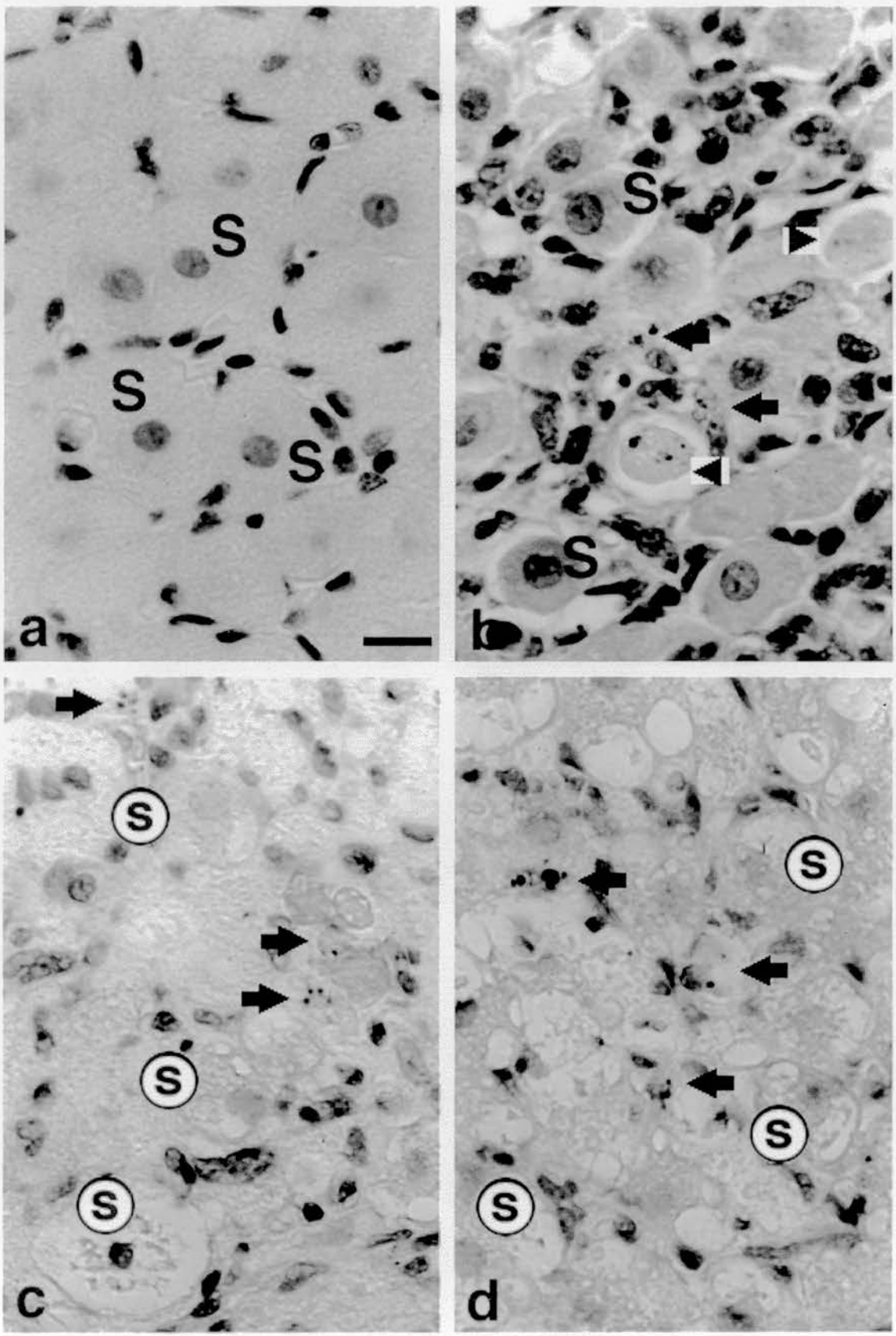
S
S
S
a
S
S
b
S
S
S
c
S
S
d

3.1.2.1 Quantification of Cells in Marmoset Corpora Lutea.

The number of morphologically normal steroidogenic cells per 60 000μm^2 of luteal tissue (Figure 3.5A) was similar in the mid and late luteal phase and in the early follicular phase. The number of morphologically normal steroidogenic cells was significantly decreased in naturally regressing corpora lutea from the late follicular phase (18.3±5.2; $P<0.001$) as well as in corpora lutea in which regression was induced with either PGF2α (12hr, 18.7±14 and 24hr, 34±12.7; $P<0.001$) or GnRH antagonist (12hr, 0 cells and 24hr, 1.25±1.7; $P<0.001$), when compared with the number of normal steroidogenic cells in untreated mid-luteal phase corpora lutea (104±25).

There were 120±30 non-steroidogenic cells in each 60000μm^2 area on luteal day 10 (Figure 3.5B), and numbers remained at this level until luteal day 18 (135±31, n=3), but increased significantly (249±63, n=3, $p<0.05$) after progesterone concentrations had fallen to follicular phase values (Figure 3.6). Non-steroidogenic cell numbers decreased significantly (97±69, n=3, $p<0.05$) late in the follicular phase after luteal day 25.

Non-steroidogenic cells comprised 48±3% of the cells of the corpus luteum during the mid luteal phase Figure 3.7), and this remained the same on luteal day 18. This percentage increased to 68±0.63% on luteal day 22 after progesterone had fallen to follicular phase values, then decreased to 36±18% after luteal day 25.

After induced luteal regression non-steroidogenic cell numbers were slightly reduced 12 hours after luteolytic treatment with PGF2α (98±10, n=3, and GnRH antagonist (69±18, n=3, Figure 3.6), but increased to the same levels as mid luteal phase corpora lutea 24 hours after induction of luteolysis with PGF2α (135±58, n=4) and GnRH antagonist (116±17, n=4, Figure 3.6). Interestingly, the percentage of non-steroidogenic cells was the same before and after induced luteal regression (Figure 3.7), with the exception of corpora lutea collected 12 hours after treatment with GnRH antagonist, in which the percentage of non-steroidogenic cells decreased to 35±6.8% (n=3).

Figure 3.5: Mean Number of Cells per Unit Area in Marmoset Corpora Lutea.

Mean (± SEM) cell numbers per 60 000μm^2 area of luteal tissue. A. Morphologically normal steroidogenic cells, B. Non-steroidogenic cells, C. Apoptotic cells or apoptotic bodies, D. Vacuolated steroidogenic cells in corpora lutea of ovaries collected on days 10 (n=4, Mid. Lut.), 18 (n=3, Late Lut.), 22 (n=3, Early Fol.), and 26 (n=3, Late Fol.) of the luteal phase. Ovaries were also collected 24 hr after administration of prostaglandin 2α analogue (n=4, cloprostenol 1μg i.m.,) or GnRH antagonist (n=4, antarelix 1$mgKg^{-1}$ s.c.) on day luteal day 10. N-values indicate different animals.

Different letters indicate significant differences between untreated corpora lutea from different stages of the cycle with $p<0.01$ in A, C and D, $p<0.05$ in B. PGF2α and GnRH antagonist treated groups are compared only with mid-luteal day 10 and with each other. Different symbols are significantly different with $p<0.01$. No symbol indicates no significant difference between treatments or untreated day 10 controls.

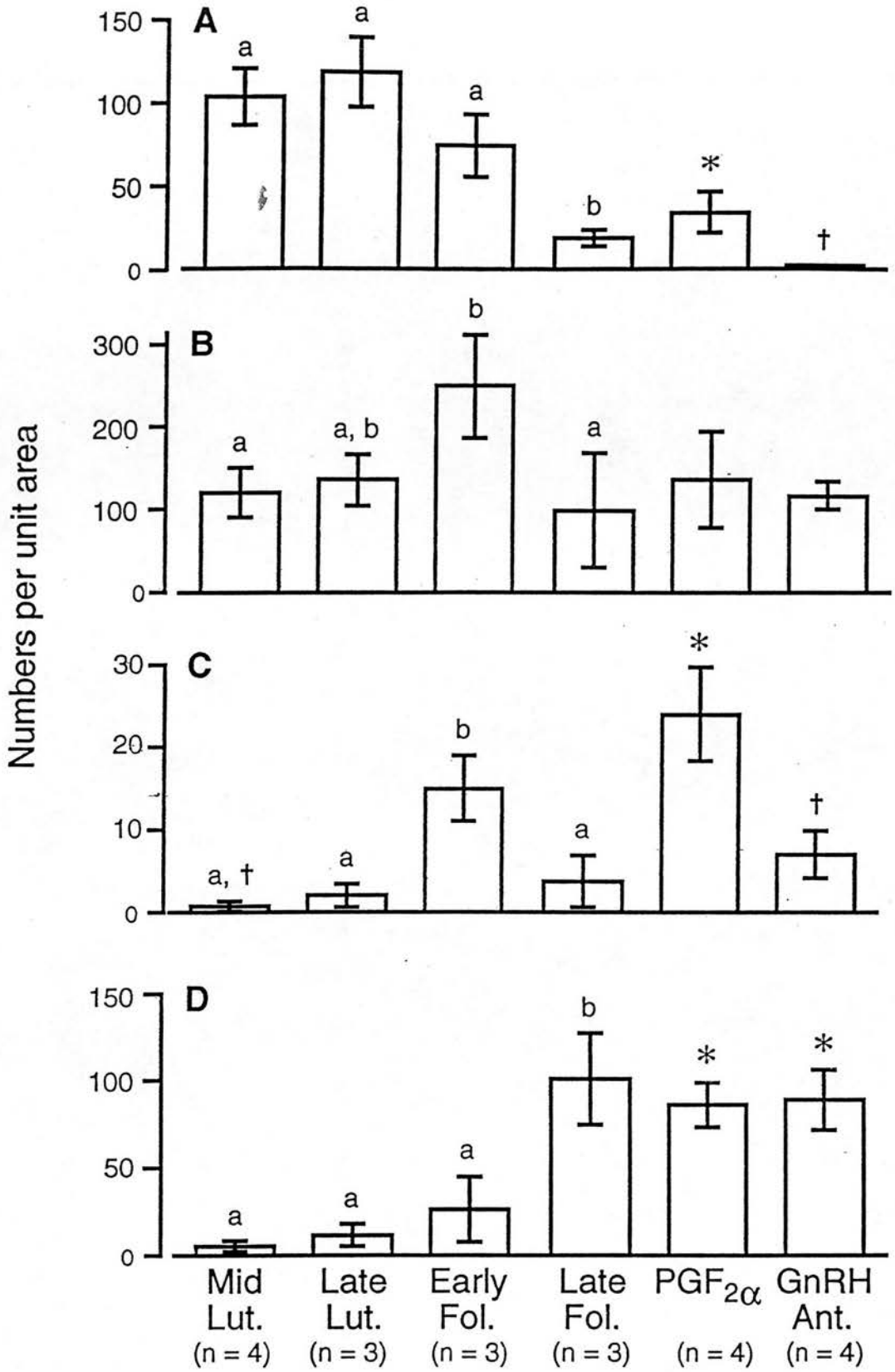
A
B
C
D
Numbers per unit area
150
100
50
0
300
200
100
0
30
20
10
0
a
a
a
b
*
†
a
a, b
b
a
a, †
a
b
a
*
†
a
a
a
b
*
*
Mid Lut. (n = 4)
Late Lut. (n = 3)
Early Fol. (n = 3)
Late Fol. (n = 3)
PGF2α (n = 4)
GnRH Ant. (n = 4)

Figure 3.6: Number of Nonsteroidogenic Cells in Marmoset Corpora Lutea.

Mean (± SEM) nonsteroidogenic cell numbers per 60000μm^2 area of luteal tissue in haematoxylin and eosin stained paraformaldehyde-fixed marmoset ovarian sections. Ovaries containing corpora lutea were obtained on luteal day 10 (n=4), 18 (n=3), 20-24 (n=3) and 25-28 (n=2). Ovaries were also obtained on luteal day 10, 12 and 24 hours after *in vivo* administration of the luteolytic agents PGF2α (PG12, n=3 and PG24, n=4) and GnRH antagonist (Gn12, n=3 and Gn24, n=4). Asterisk indicates significantly different ($p<0.05$) from mid luteal phase day 10. No symbol indicates no significant difference between treatments of untreated day 10 controls.

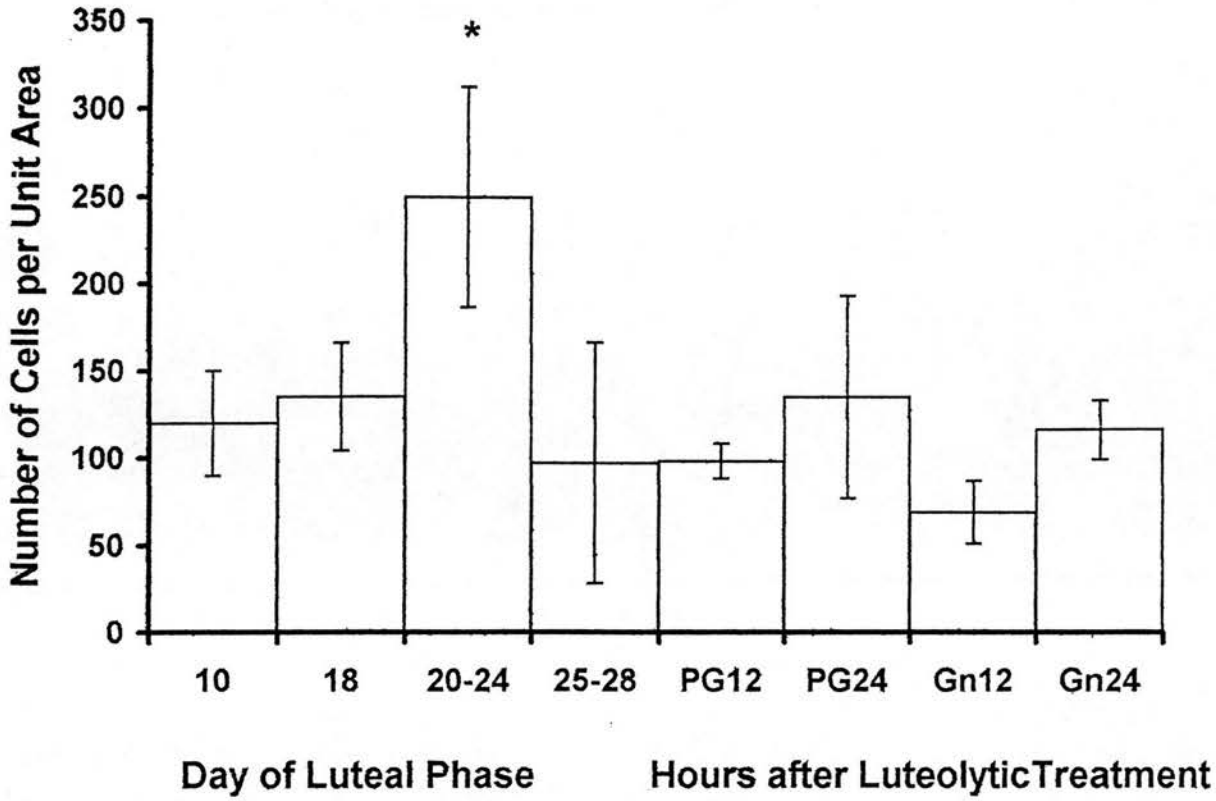

Figure 3.6: Number of Nonsteroidogenic Cells in Marmoset Corpora Lutea

Figure 3.7: Percentage of Nonsteroidogenic Cells in Marmoset Corpora Lutea.

Nonsteroidogenic cell numbers were expressed as a percentage of the total number of cells per 60000μm^2 area of luteal tissue in haematoxylin and eosin stained paraformaldehyde-fixed marmoset ovarian sections. The mean percentage (± SEM) is shown for each experimental group. Ovaries containing corpora lutea were obtained on luteal days 10 (n=4), 18 (n=3), 20-24 (n=3) and 25-28 (n=2). Ovaries were also obtained on luteal day 10, 12 and 24 hours after *in vivo* administration of the luteolytic agents PGF2α (PG12, n=3 and PG24, n=4) respectively, and GnRH antagonist (Gn12, n=3 and Gn24, n=4) respectively.

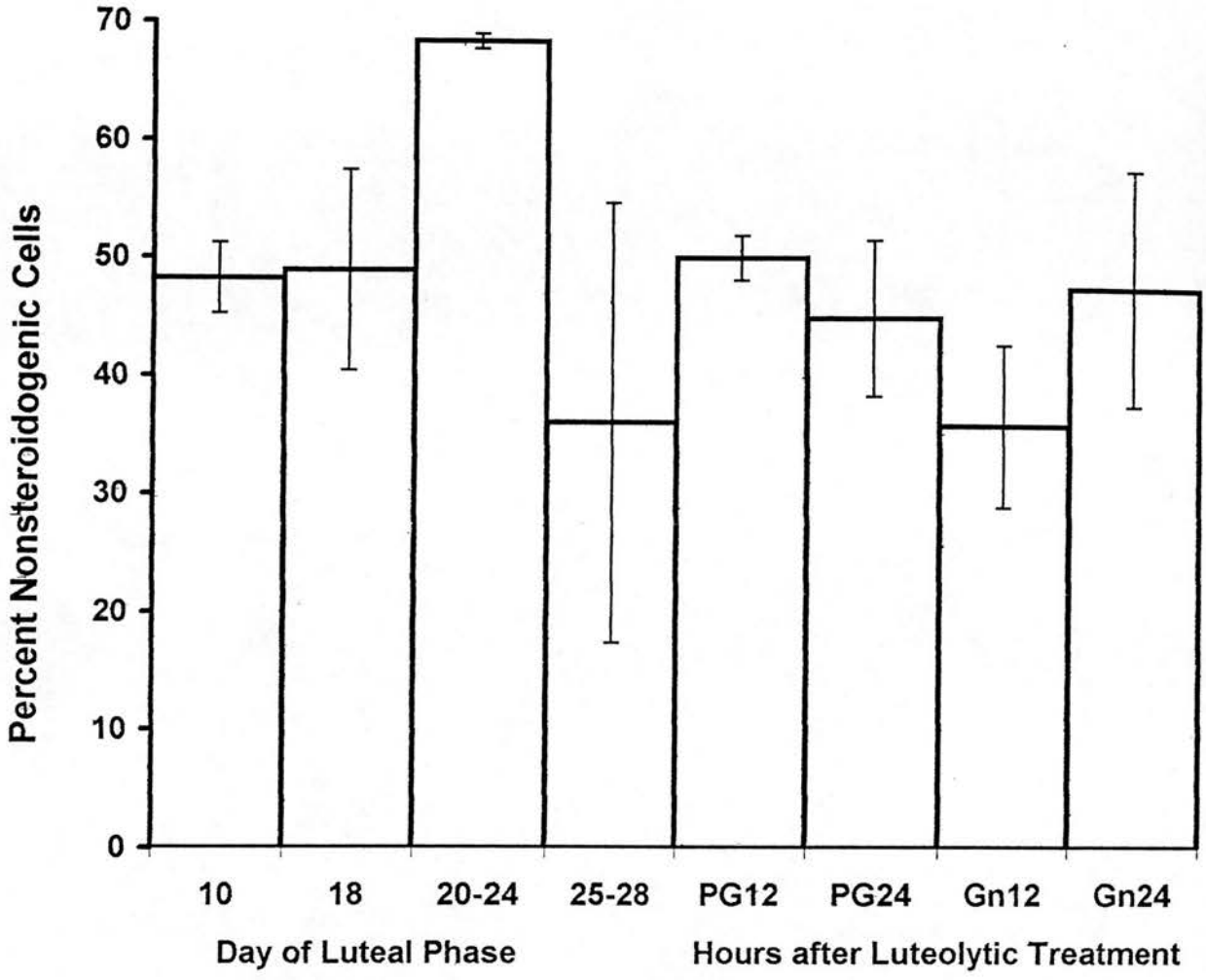

Figure 3-7: Percentage of Nonsteroidogenic Cells in Marmoset Corpora Lutea

Clusters of apoptotic bodies were observed in all corpora lutea studied (Figure 3.4C, Figure 3.8), including those in the mid-luteal phase (0.75±0.6). The incidence of apoptosis was significantly increased to 15±4 ($P<0.001$) in naturally regressing corpora lutea from the early follicular phase, but was similar in corpora lutea from the late luteal (2±0.94) and late follicular (3.66±3.2) phases. Apoptosis was significantly increased 24 hours after PGF2α-induced regression (24±5.6; $P<0.001$) but not 12 hours after administration of PGF2α (1.33±0.8). Apoptosis was also increased 12hr (4±1.2) and 24hr (7±4) after treatment with GnRH antagonist, but the response was variable and not statistically significant (Figure 3.8). Apoptosis was increased significantly from 0.3±0.42% (n=4, Figure 3.9) in the mid luteal phase to 3.46±1.45% (n=3, $p<0.05$, Figure 3.9) in naturally regressing corpora lutea from the early follicular phase, but was similar in corpora lutea from the mid (0.3±0.42%), late luteal (0.85±0.94%) and late follicular (0.63±0.72%) phases. Apoptosis was 2.8±0.28%(n=3) and 8.6±8%(n=3) 12 hours after induced regression with GnRH antagonist and PGF2α respectively. This increased to 6.2±5.2% (Figure 3.9) 24 hours after treatment with GnRH antagonist, but this was not significantly higher than in untreated mid-luteal phase corpora lutea, unlike PGF2α induced regression which resulted in a significant increase 24 hours after treatment to 9.0±3.7% (n=4, $p<0.05$, Figure 3.9) when compared to untreated mid-luteal phase corpora lutea.

The number of vacuolated cells increased gradually with advancing luteal age (Figure 3.5D) and was significantly higher in naturally regressing corpora lutea from the late follicular phase (101±26.9, $p<0.01$) compared with all other naturally regressing corpora lutea. The numbers of vacuolated cells were similarly significantly higher 12 and 24 hours after luteolytic treatment compared with untreated mid-luteal phase corpora lutea ($P<0.001$).

Figure 3.8: Amount of Apoptosis in H&E Stained Sections of Marmoset Corpora Lutea.

Ovaries containing corpora lutea were collected on luteal day 10 (n=4), luteal day 18 (functional luteal regression, n=3), luteal days 22-24 (structural luteal regression, n=3) and luteal days 25-28 (n=3). Ovaries were also obtained 12 hours (PG12, n=3) and 24 hours (PG24, n=4) after *in vivo* administration of the PGF2α analogue, cloprostenol, and 12 hours (Gn12, n=3) and 24 hours (Gn24, n=4) after *in vivo* administration of a GnRH antagonist, anterelix. Luteolytic agents were administered on luteal day 9, 24 hours before collection on luteal day 10. The total number of apoptotic cells or clusters of apoptotic bodies per 60000 μm^2 unit area were determined for each corpus luteum, and shown as the mean±SEM for each stage of the luteal phase.

Data were subjected to one way analysis of variance. The number of apoptotic cells was significantly higher in structurally regressing corpora lutea (luteal days 20-24, $p<0.001$), and 24 hours after induction of luteolysis with PGF2α ($p<0.001$) than in mid luteal day 10 corpora lutea.

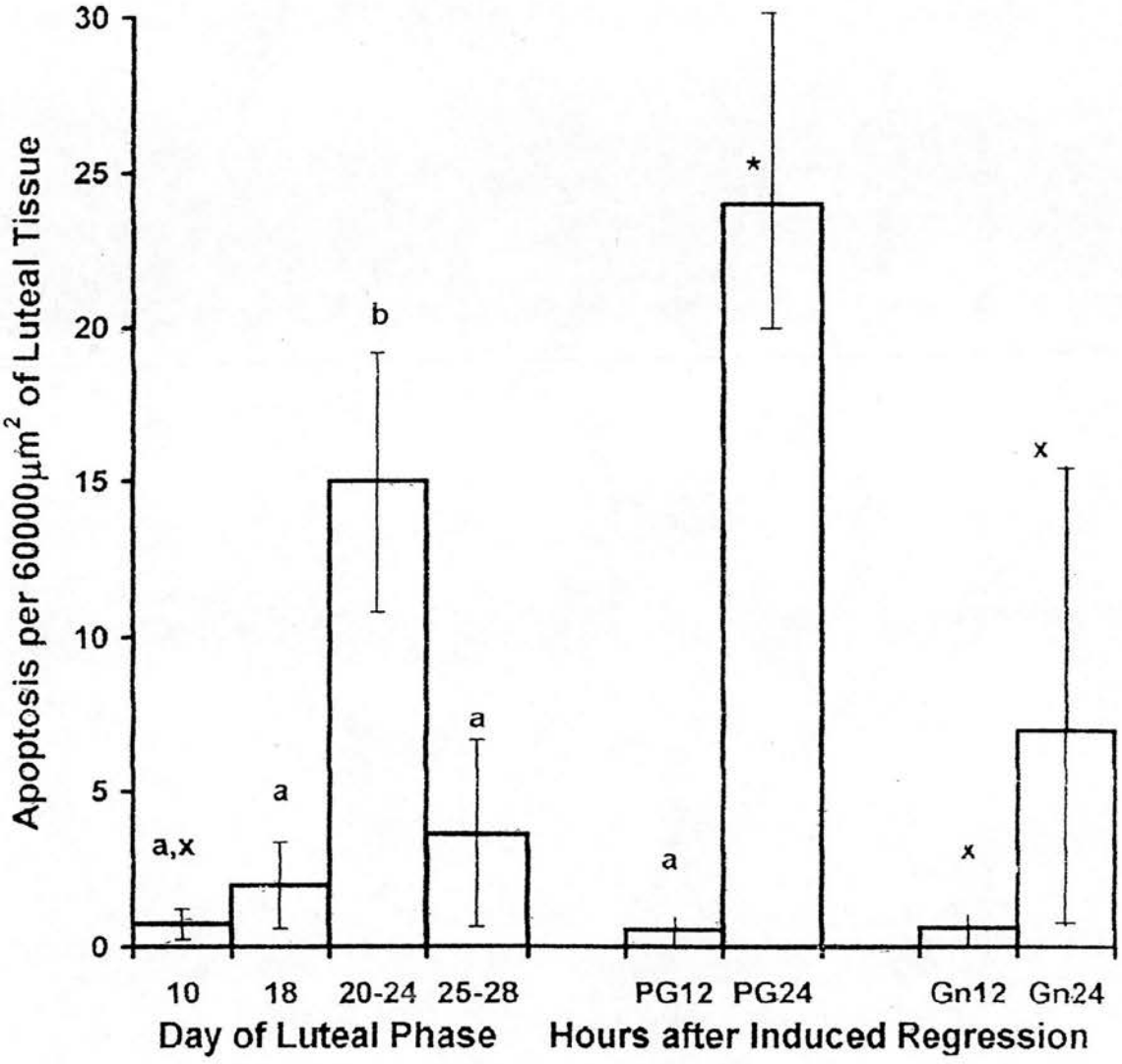

Figure 3.8: **Amount of Apoptosis in H&E Stained Sections of Marmoset Corpora Lutea.**

Figure 3.9: Percent Apoptosis in Marmoset Corpora Lutea.

Mean (± SEM) number of apoptotic cells and apoptotic bodies per 100 cells in marmoset corpora lutea collected during the mid-luteal phase (luteal day 10), early follicular phase (equivalent to structural regression, luteal days 20 - 24), mid-luteal phase 24h after administration of PGF2α, and mid-luteal phase 24h after administration of GnRH antagonist. Open bars apoptotic scores generated by HOME analysis of haematoxylin and eosin stained sections; closed bars apoptotic scores generated by image analysis of *in situ* 3' end labelled ovarian sections. Significant differences are indicated by asterisks (* $P<$ 0.05; ** $P<0.001$).

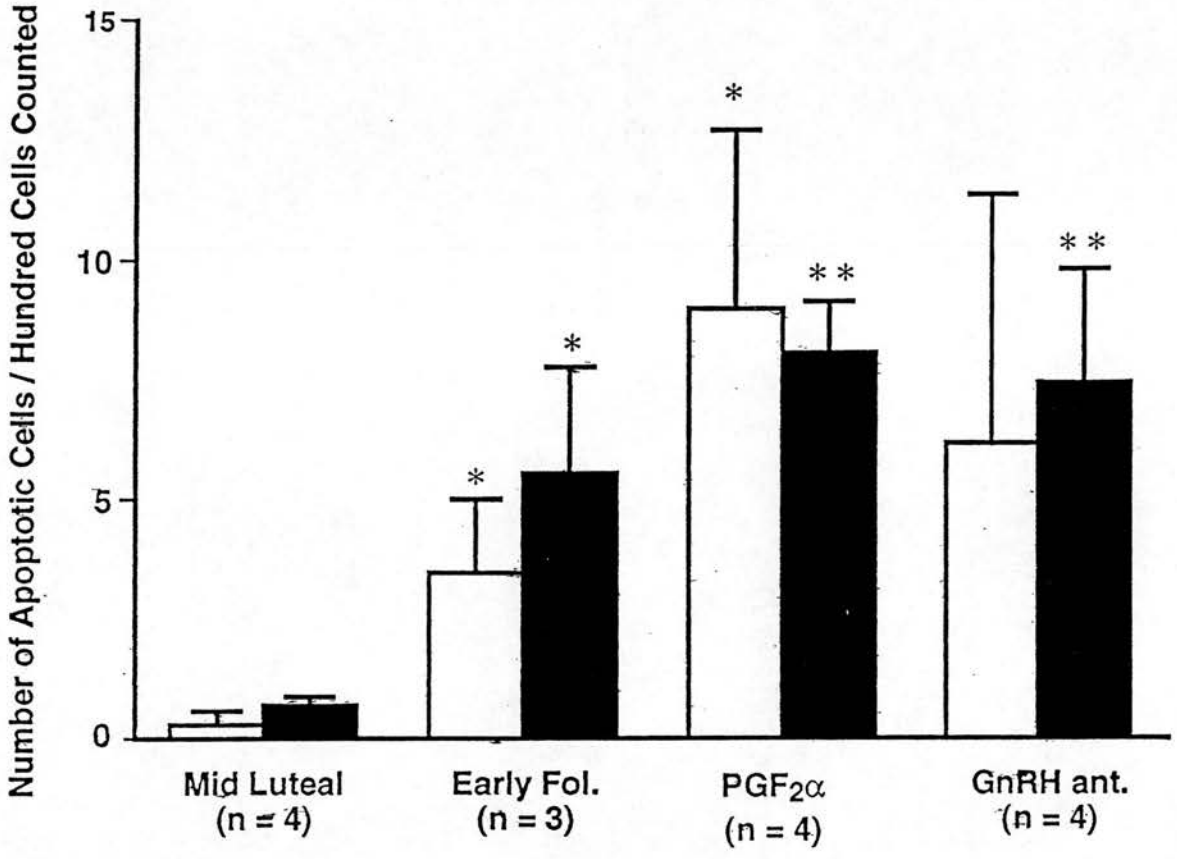
Number of Apoptotic Cells / Hundred Cells Counted
15
10
5
0
*
*
*
**
**
Mid Luteal
(n = 4)
Early Fol.
(n = 3)
PGF2α
(n = 4)
GnRH ant.
(n = 4)

3.1.3 Localisation of Lipids in Marmoset Corpora Lutea.

Examination of H&E stained sections indicated that the number of vacuolated steroidogenic cells in each unit area of luteal tissue increased as the corpus luteum aged, and that the number of vacuolated cells was also higher after induced luteal regression. Vacuolation of the steroidogenic cells was considered to be a morphological change which occurred during spontaneous or induced luteal regression. It was possible that the induction of regression with luteolytic agents caused a rapid decrease in steroidogenesis which resulted in the accumulation of unprocessed lipid substrate in cytoplasmic vacuoles. In this scenario, the vacuoles would retain lipid in cryosections but not in paraformaldehyde fixed sections, and therefore ovarian sections were stained with the lipophillic stain, Oil-Red-O.

In mid luteal phase day 10 control ovaries, the most intense staining for Oil Red O, with variable droplet size, was seen in localized areas of the stroma containing cells having the appearance of steroidogenic cells and which were assumed to represent differentiated interstitial cells (Figure 3.10a and e). In a proportion of antral follicles, intense staining was also seen within the thecal layer while granulosal staining was not recorded in follicles of any size. There was no staining in small antral or preantral follicles. Within luteal tissue, staining was variable and generally more intense in corpora lutea accessoria then in the true corpora lutea. In untreated mid-luteal phase corpora lutea, steroidogenic cell cytoplasm often contained numerous small Oil Red O-stained lipid droplets (3.10a and b). After treatment with either GnRH antagonist (Figure 3.10c and d) or PGF2α (Figure 3.10e and f), the distribution of staining within the non-luteal compartments remained unchanged. In luteal tissue, there was little to suggest lipid accumulation; in particular, lipid droplets were primarily extracellular and the vacuoles did not contain lipid (Figure 3.10d and f).

Figure 3.10: Oil-Red-O Stained Lipid in Marmoset Corpora Lutea After Induced Regression.

Cryosections of marmoset ovaries in which Oil-Red-O stains lipids red, and nuclei are counterstained blue with haematoxylin. The panels show: (a) An untreated control ovary collected on luteal day 10. The corpus luteum of the cycle is in the top right hand corner of the image. Proceeding anticlockwise is intensely staining interstitial tissue which may also be a luteinised follicle, an antral follicle and an accessory corpus luteum in the bottom half of the image. (b) shows the corpus luteum of the cycle depicted in (a) at a higher magnification. Individual steroidogenic cells contain numerous lipid droplets. (c) shows a corpus luteum collected 24 hours after *in vivo* administration of GnRH antagonist, and (d) shows the same corpus luteum at a higher magnification. Faint grey staining indicates the presence of cytoplasm lightly counterstained with haematoxylin, and white areas indicate the location of cytoplasmic vacuoles. Although lipid droplets are present in the corpus luteum, they do not exhibit the same dimensions or localisation as cytoplasmic vacuoles. Panel (e) shows an ovary collected 24 hours after *in vivo* administration of PGF2α, and the corpus luteum of the cycle is in the top right hand corner of the image. Intensely staining interstitial tissue is present at the bottom left hand corner of the image. (f) shows the corpus luteum depicted in (e) at a higher magnification. Cytoplasmic vacuoles do not contain Oil-Red-O stained lipid. All scale bars represent 20μm.

Figure 3.10/3.7 Oil-Red-O Stained Lipid in Marmoset Corpora Lutea After Induced Regression

(photo plate)

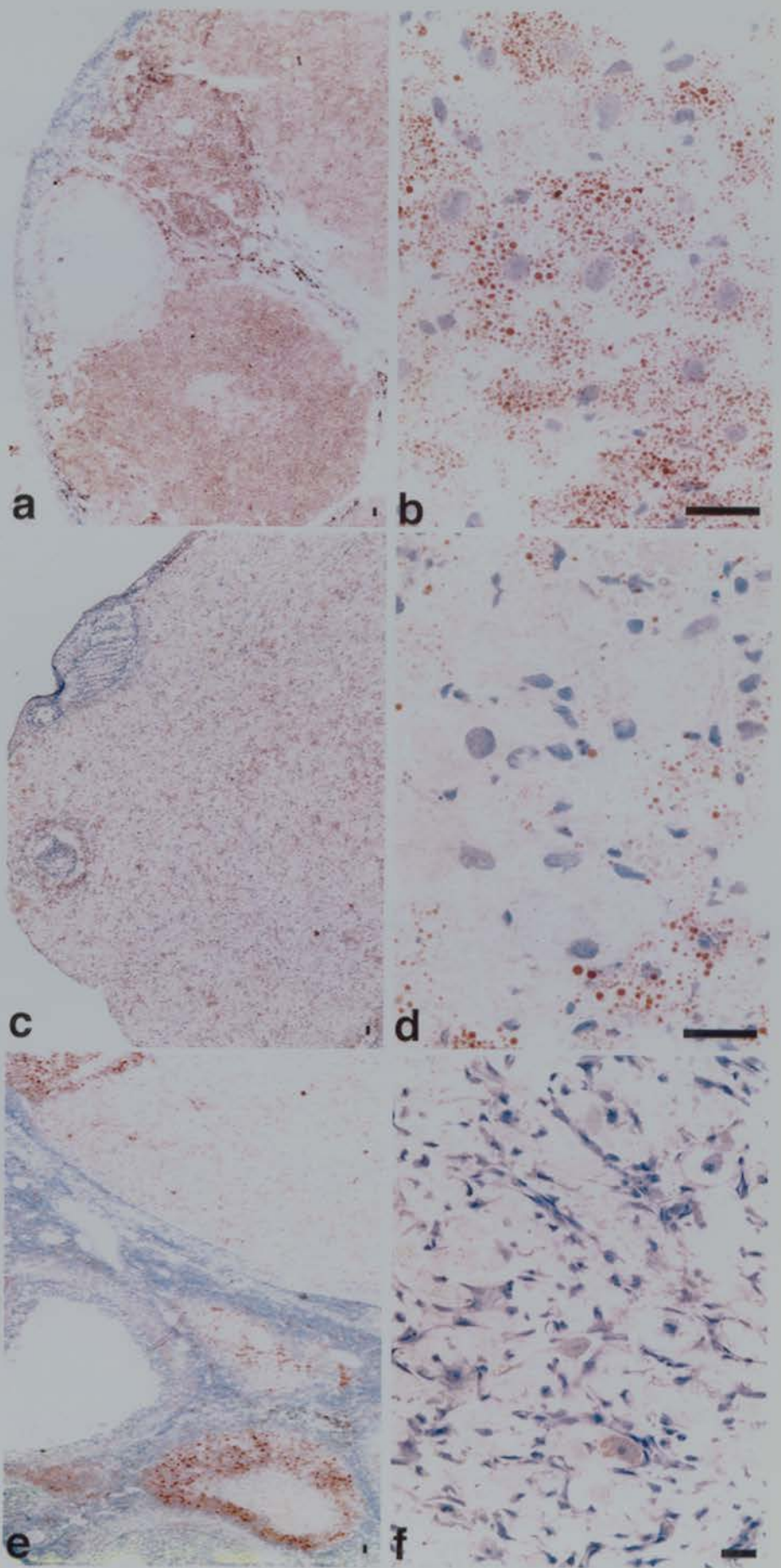
a
b
c
d
e
f

3.1.4 Oligonucleosome Formation in Marmoset Corpora Lutea.

3.1.4.1 Positive Controls for Oligonucleosome Formation

Multiples of 185bp DNA fragments were found in thymocytes induced to undergo apoptosis by treatment with the glucocorticoid analogue, dexamethasone (Figure 3.11, panel A, lane 1). Oligonucleosomes were also found in cow corpora lutea 12 (Figure 3.11, panel A, lane 5), and 24 hours (Figure 3.11, panel A, lanes 3 and 4) after induction of luteolysis with PGF2α, indicating that technical procedures for extraction, labeling and visualisation of apoptotic DNA were in accordance with previous reports (Juengel *et al.*, 1993; Tilly and Hsueh 1993). One PGF2α treated marmoset corpus luteum with oligonucleosome formation (Figure 3.11, panel A, lane 2) confirms that marmoset luteal DNA fragmentation is of the same order as that seen in bovine corpora lutea.

3.1.4.2 Oligonucleosome Formation in Marmoset Corpora Lutea

Low oligonucleosome formation was found in one mid luteal phase day 10 animal (Figure 3.11, panel B, lane 1) but apoptotic DNA fragmentation was absent from three other mid luteal phase animals (Figure 3.11, panel B, lanes 2 and 3 and Figure 3.12, lane 2). The non-specific DNA fragmentation apparent in the mid luteal phase corpus luteum shown in Figure 3.12, lane 2 is a consequence of DNA overloading for that sample, but although there is a high concentration of DNA in that lane, there is no evidence of oligonucleosome formation. Oligonucleosome fragmentation was present in all animals 24 hours (n=3, Figure 3.11B lanes 4 and 5, Figure 3.12 lane 4) and 48 hours (n=1, Figure 3.12, lane 5) after induced regression with GnRH antagonist and also 24 hours (n=6, Figure 3.11B lanes 6 and 7, Figure 3.12 lane 3) after treatment with PGF2α. There was also smearing indicative of non-apoptotic DNA degradation. This was inconsistent in control day 10 samples, but some non-apoptotic DNA fragmentation was always present in the corpora lutea of animals given luteolytic treatments. DNA fragmentation of any type was absent from liver samples (n=8, Figure 3.11B lower lanes, each from the same animal as the corpus luteum shown in the lane above).

Figure 3.11: Oligonucleosome Formation in Bovine, Human and Marmoset Corpora Lutea.

Autoradiogram of 3' end labelled DNA (1μg/lane) electrophoresed on a 2% agarose gel. Panel A, lane 1, thymocytes cultured with dexamethosone; lane 2, marmoset corpus luteum collected 24 hours after *in vivo* administration of PGF2α, lanes 3 and 4, bovine corpora lutea collected from two different animals 24 hours after *in vivo* administration of PGF2α; lane 5, bovine corpus luteum 12 hours after *in vivo* administration of PGF2α; lane 6 human corpus luteum obtained 12 days after the LH surge. Lanes 2-6 from one gel exposed for 12hr, 24hr after the completion of the labeling process. Lane 1 from a separate gel, also exposed for 12hr.

Panel B, lanes 1-3, mid luteal phase day 10 control corpora lutea; lanes 4 and 5, GnRH antagonist administered *in vivo* luteal day 9; lanes 6 and 7, PGF2α administered *in vivo* luteal day 9; all corpora lutea collected on luteal day 10. Lower lanes show negative control liver samples corresponding to the animal in the lane above. Lanes 1-7 from one gel exposed for 12hr, 24hr after the completion of the labeling process 1μg DNA loaded per lane. Molecular Weight markers on right hand side.

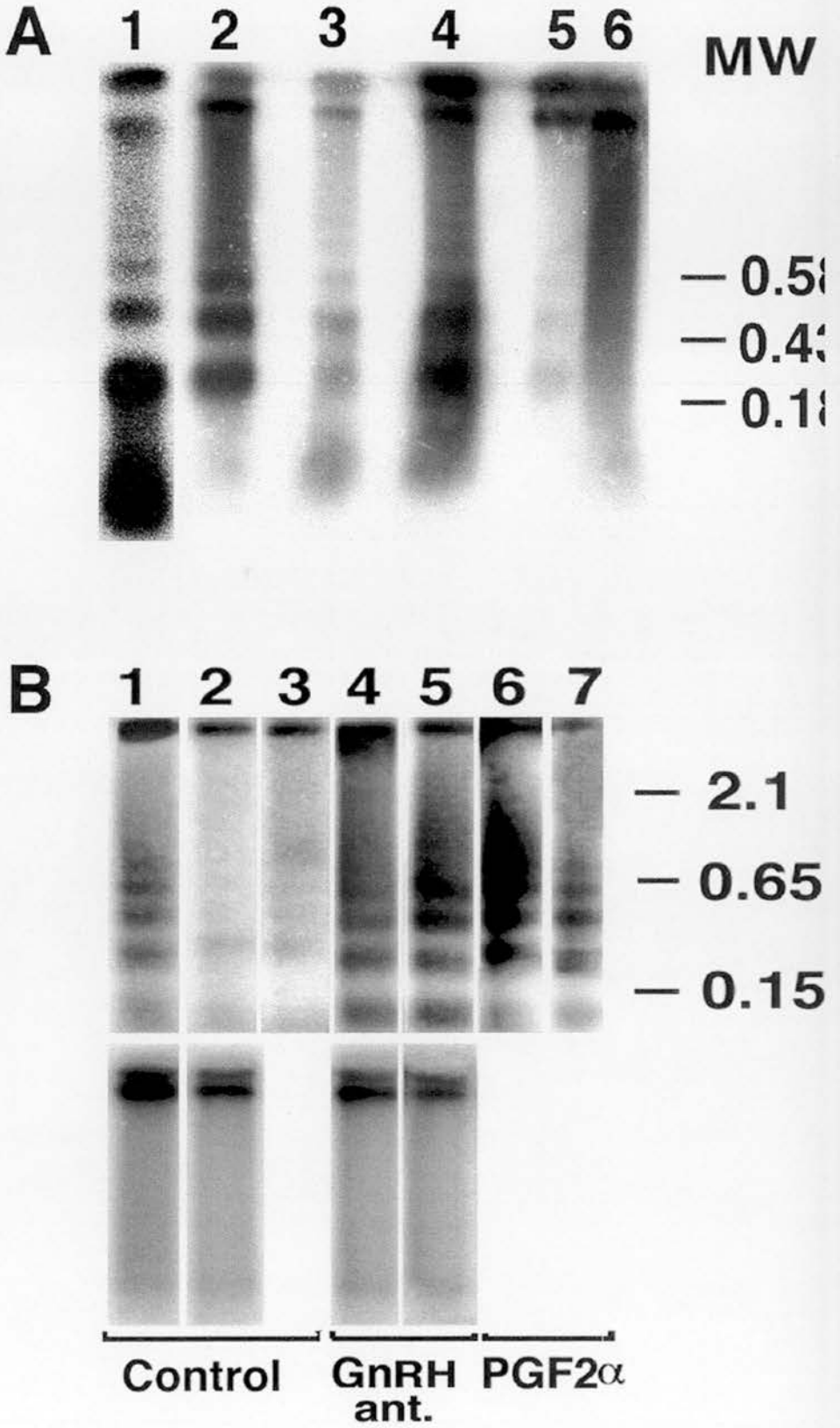
A
1 2 3 4 5 6
MW
— 0.58
— 0.43
— 0.18
B
1 2 3 4 5 6 7
— 2.1
— 0.65
— 0.15
Control
GnRH ant.
PGF2α

Figure 3.12: Oligonucleosome Formation in Marmoset Corpora Lutea.

Autoradiogram of 3' end labelled DNA (1μg/lane) electrophoresed on a 2% agarose gel. Lanes 1 and 2, corpora lutea obtained from animals on luteal day 10; lane 3, 24 hours after *in vivo* administration of PGF2α, lanes 4 and 5, 24 and 48 hours after administration of GnRH antagonist respectively. All samples on same gel exposed for 4 hours immediately following labeling procedure. Molecular weight markers shown on the right hand side.

Oligonucleosome Formation in Marmoset CL

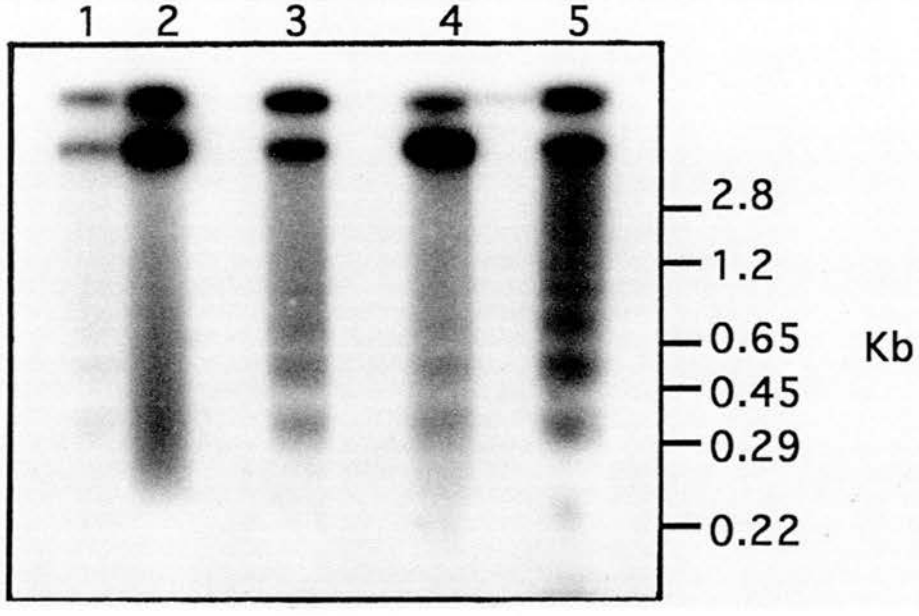

3.1.4.3 Quantification of Oligonucleosome Formation

	# animals	Mean OD ±SEM	P value	Mean Corrected OD±SEM	P value
Control Lut Day 10	4	70 500 ± 24 500	p=0.153	14 ±6.5	p=0.09
			p=0.09		p=0.20
GnRH antag. 24 hr	3	352 600 ± 147 700		110 ± 47	
			p=0.8		p=0.9
PGF2α 24 hr	4	301 400 ± 74 000		103 ± 41	

Oligonucleosome formation in mid luteal phase control corpora lutea is lower (n=4, 14±6) than that seen 24 hours after *in vivo* administration of GnRH antagonist (n=3, 110±47) or PGF2α (n=4, 103±41). Both luteolytic treatments appear to result in the same amount of oligonucleosome formation, although accurate conclusions are confounded by the extremely high inter-animal variability.

3.1.5 In situ 3' End Labeling of Marmoset Corpora Lutea

3.1.5.1 Positive and Negative Controls

Granulosa cells undergoing apoptosis in atretic follicles were 3' end labeled in ovaries from all experimental groups whereas no labeling was seen in theca cell layers, nor in preantral follicles. 90-98% of nuclei were labeled in DNase pretreated

positive control sections, and there was no labeling at all in negative control sections where TdT was omitted from the labeling buffer.

3.1.5.2 3' End Labelled Corpora lutea

Corpora lutea from untreated animals collected on luteal day 10 had 0.675±0.4% labeling (n=4, Figures 4.6 and 4.10). This was significantly increased to 5.54±1.4% (n=3, $p<0.05$, Figures 4. 7 and 4.10) in corpora lutea collected on luteal day 22 in the early follicular phase. Labeled cells had large regular nuclei and abundant cytoplasm, both features characteristic of steroidogenic cells. Cells with elongated nuclei and little cytoplasm were also 3' end labeled; these were identified as being non-steroidogenic and possibly endothelial. In addition to these identifiable cell types, there were also other labeled structures. Some had the morphological appearance of apoptotic bodies whereas others were a condensed, labeled body of cytoplasm which corresponded to the mass of cytoplasm seen in steroidogenic cells. Corpora lutea induced to undergo regression with PGF2α and GnRH antagonist had 8±1% (n=4, Figures 4.9 and 4.10) and 7.4±1.5% (n=4, Figures 4.8 and 4.10) labeling respectively, and these were significantly higher ($p<0.05$) than the labeling seen in untreated corpora lutea from day 10 of the luteal phase. Labeling in GnRH antagonist treated corpora lutea was in apoptotic bodies, and only occasionally seen in bodies of cytoplasm assumed to have originated from steroidogenic cells. Labeling in PGF2α treated corpora lutea was nuclear in cells with abundant cytoplasm which were therefore assumed to be steroidogenic in origin. Apoptotic bodies were also labeled in PGF2α treated corpora lutea. The number of labeled non-steroidogenic cells was lower in GnRH antagonist and PGF2α treated corpora lutea than in spontaneously regressing corpora lutea.

Figure 3.13: *In situ* 3' End Labelling in Mid Luteal Phase Marmoset Corpus Luteum.

Marmoset ovary obtained on luteal day 10. Dark brown DAB staining indicates 3' end labeled cells. (a) apoptotic granulosa cells in an atretic follicle (AF), but very few apoptotic cells in the corpus luteum (CL). (b) DNAse positive control serial section of (a) in which majority of cell nuclei are 3' end labelled. (c) Higher magnification of luteal tissue also shown in (a). Scale bars represent 20μm.

Luteal Day 10 Marmoset Ovary
3' End Labelled in situ.

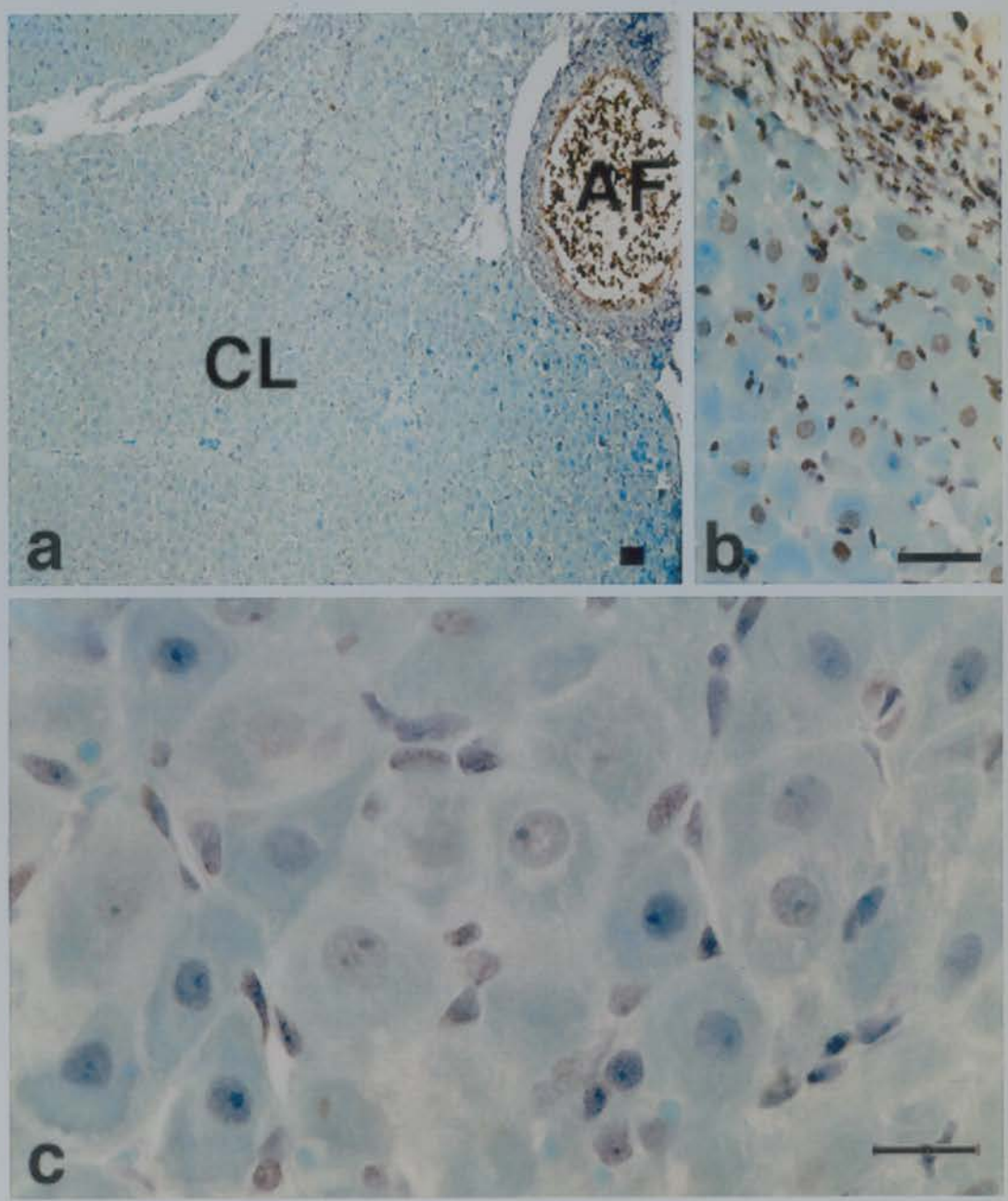

Figure 3.14: *In situ* 3' End Labelling in Regressing Marmoset Corpus Luteum.

Marmoset ovary obtained on luteal day 20 and paraformaldehyde fixed. Dark brown DAB staining indicates 3' end labelled cells. (a) shows brown 3' end labelled cells in an atretic follicle (AF), but very few apoptotic granulosa cells in a non-atretic follicle (F). The corpus luteum (CL) has numerous apoptotic cells (b) Higher magnification of luteal tissue with 3' end labelled steroidogenic cells (large arrows), and 3' end labelled non-steroidogenic cells or apoptotic bodies (small arrows). Scale bars represent 20μm.

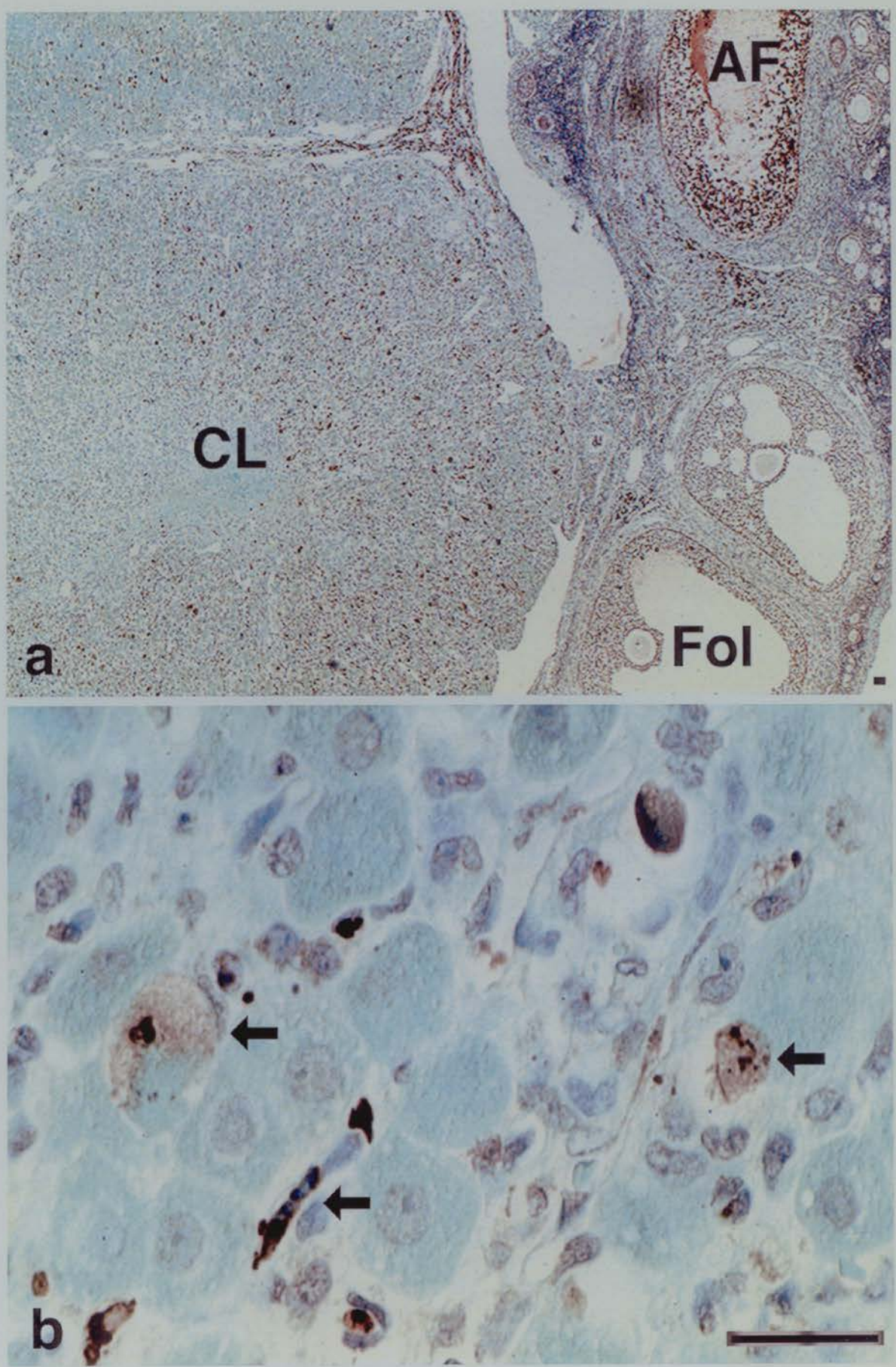
AF
CL
Fol
a
b

Figure 3.15: *In situ* 3' End Labelling Marmoset Corpus Luteum After Induction of Luteolysis With PGF2α.

In vivo administration of cloprostenol on luteal day 9. Ovary obtained 24 hours later on luteal day 10. Dark brown DAB staining indicates 3' end labelled cells. (a) apoptotic granulosa cells in an atretic follicle (AF) and corpus luteum (CL). (b) Higher magnification of luteal tissue with 3' end labelled cells or apoptotic bodies (arrows). Some steroidogenic cells are vacuolated (V). Scale bars represent 20μm.

PGF2α Treated Marmoset Ovary
3' End Labelled in situ.

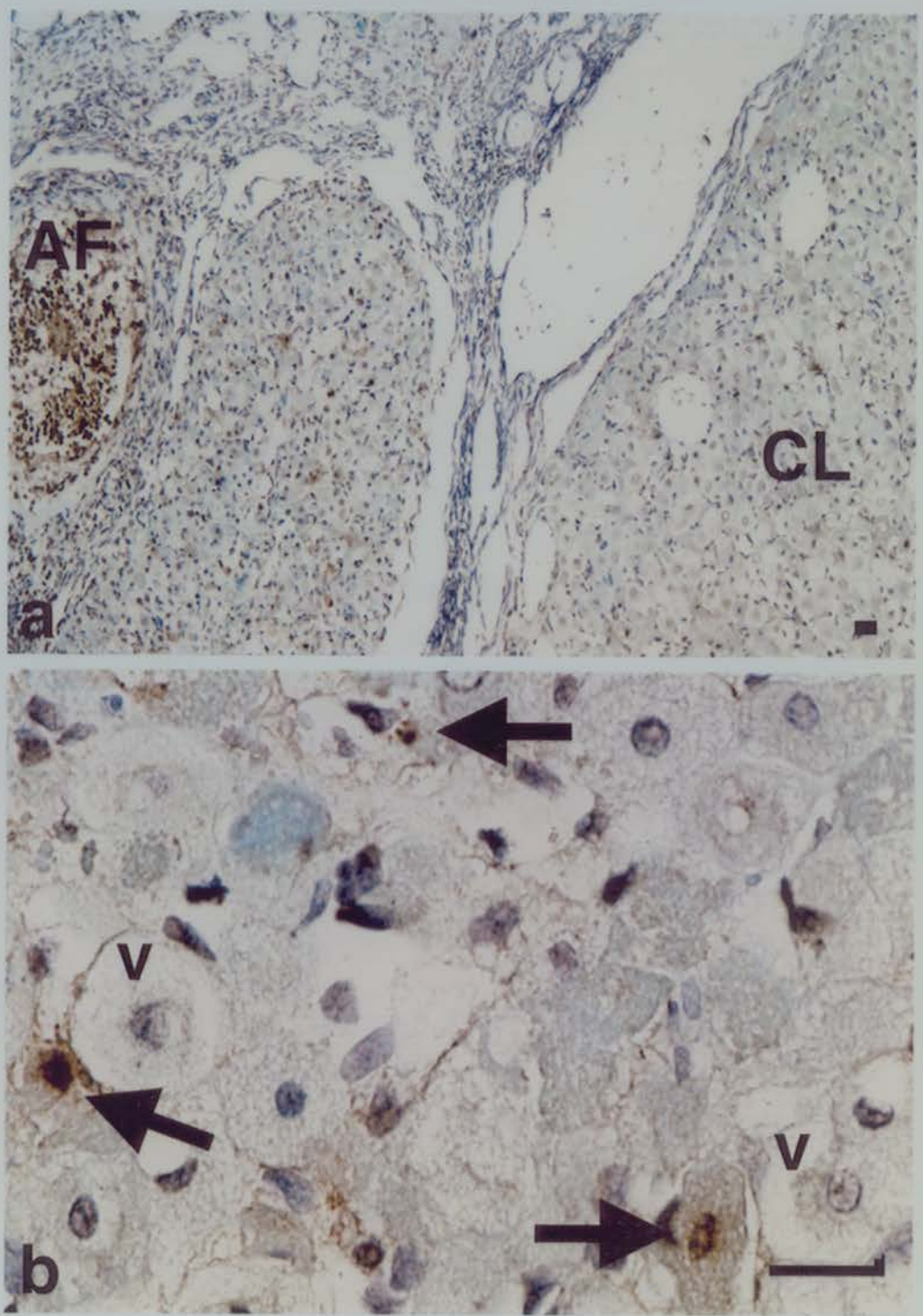

Figure 3.16: *In situ* 3' End Labelling Marmoset Corpus Luteum After Induction of Luteolysis With GnRH antagonist.

In vivo administration of anterelix on luteal day 9. Ovary obtained 24 hours later on luteal day 10. Dark brown DAB staining indicates 3' end labeled cells. (a) apoptotic granulosa cells in an atretic follicle (AF) and apoptotic cells in corpus luteum (CL), (b) DNAse positive control serial section of (a) in which majority of cell nuclei are 3' end labeled. (c) Higher magnification of luteal tissue with 3' end labeled cells or apoptotic bodies (arrows). Some steroidogenic cells are vacuolated (∗). Scale bars represent 20μm.

GnRH Antagonist Treated Marmoset Ovary
3' End Labelled in situ.

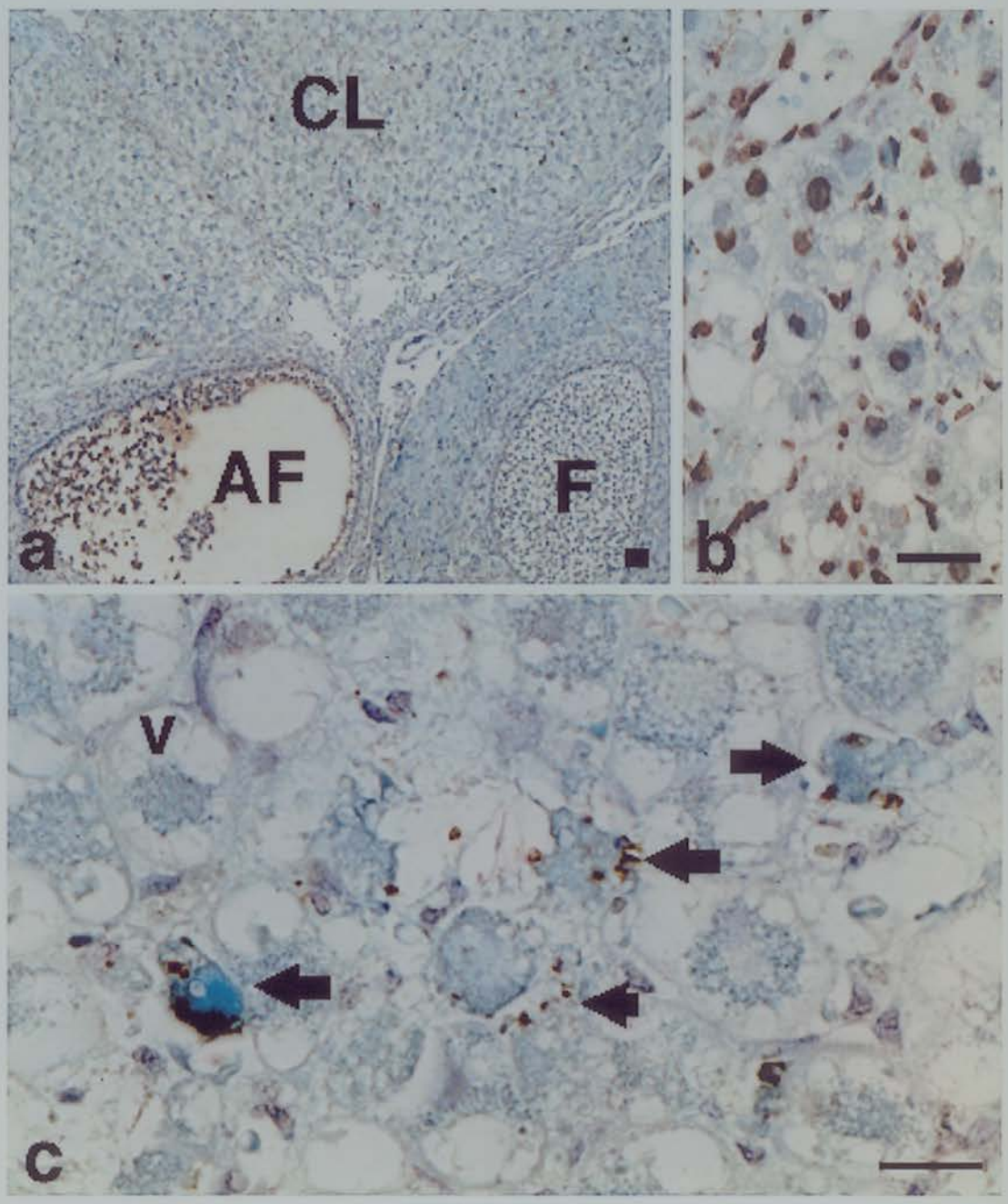

3.1.6 Ubiquitin Expression During Luteal Regression

3.1.6.1 Progesterone Concentrations

On the day of ovary collection progesterone concentrations were at luteal phase values 311±48 nmol L^{-1} (n=3) in all mid luteal phase day 10 control animals but were significantly reduced to 18.33±3.75 nmol L^{-1} ($P<0.01$, n=3) after luteolytic treatment with PGF2α and 36.35±16.32 nmol L^{-1} ($P<0.01$, n=3) after induction of luteolysis with GnRH antagonist.

3.1.6.2 Results of Ubiquitin Immunocytochemisty

Ubiquitin immunostaining (Figure 3.17a) was localised in the nuclei of steroidogenic cells (1.66±0.66 cells per x40 field of view, n=3, Figure 3.18) in mid luteal phase day 10 corpora lutea, but was not found in the nuclei of luteal cells after luteolytic treatment. Cytoplasmic ubiquitin immunoreactivity was apparent in 0.4±0.3 mid luteal phase cells per x40 field of view, and this was significantly increased to 12.24±1.6 cells ($p<0.02$, n=3, Figures 3.17c and 3.18) per field of view in PGF2α treated animals. Ubiquitin immunoreactivity was not found after induction of luteolysis with GnRH antagonist, nor was it found in negative control sections (Figure 3.17e and f).

Figure 3.17: Immunohistological Detection of Ubiquitin in Marmoset Corpora Lutea.

Red-pink staining represents ubiquitin positive immunoreactivity. (A) Ubiquitin-positive nuclei in a mid luteal phase day 10 untreated corpus luteum. (b) Corresponding negative control section for (a), with primary ubiquitin antibody omitted there is no positive immunoreactivity. (c) Ubiquitin-positive cytoplasm in steroidogenic cells in regressed corpus luteum 24 hr after administration of PGF2α analogue. (d) Corresponding negative control section for (b), (e) No ubiquitin immunoreactivity in regressed corpora lutea 24hr after administration of GnRH antagonist. (f) Corresponding negative control section for (e). All scale bars represent 20μm.

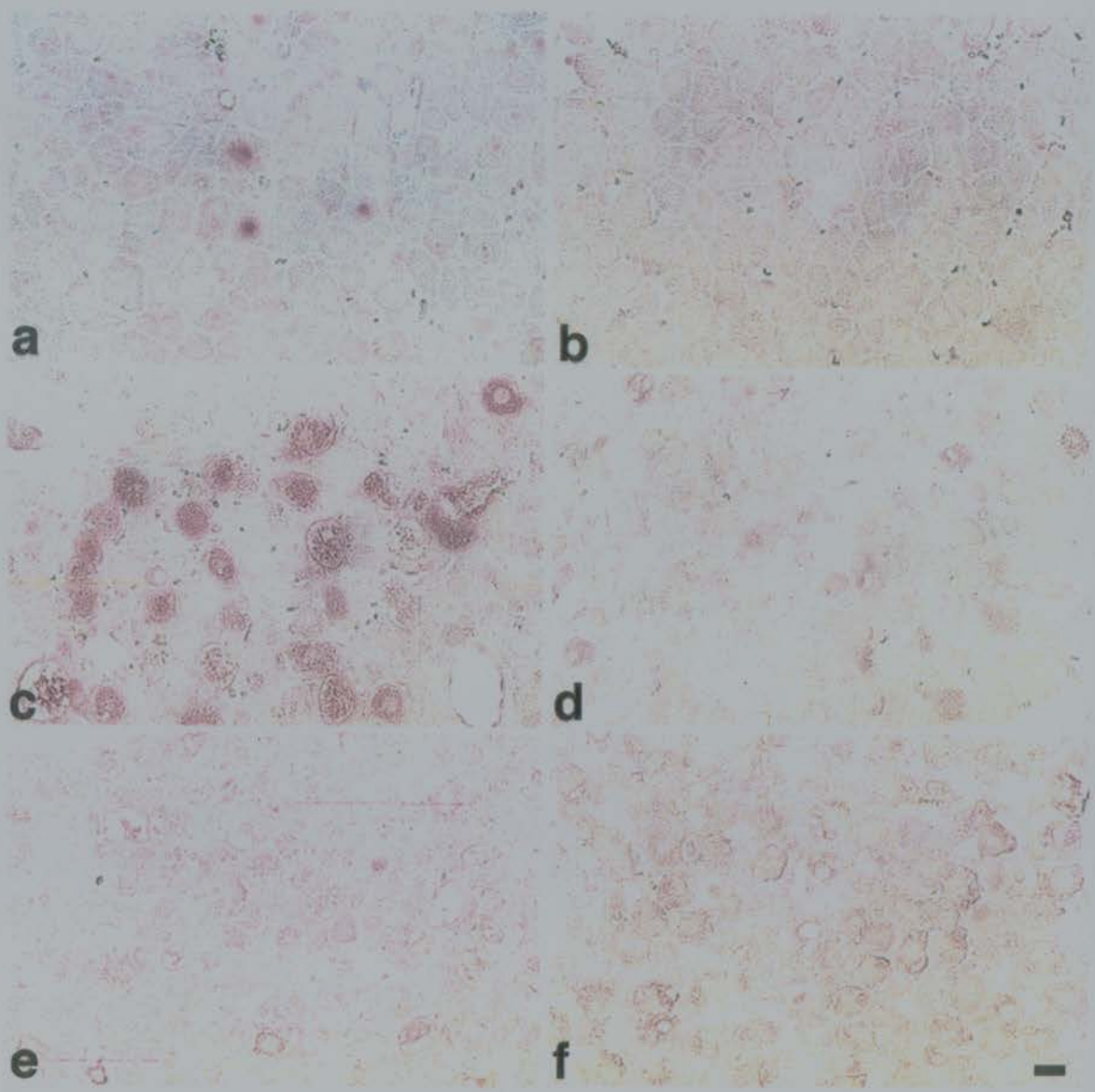
a
b
c
d
e
f

3.2 Discussion

These studies identified steroidogenic cells, and described and quantified morphological changes occurring during natural and induced luteal regression. Observations of steroidogenic cell vacuolation led to an examination of lipid distribution in corpora lutea induced to undergo regression with PGF2α or GnRH antagonist.

Apoptosis was identified and quantified using three different methods: (i) morphological examination of H&E stained marmoset ovarian sections, (ii) gel electrophoresis of DNA extracted from marmoset corpora lutea and (iii) *in situ* 3' end labelling of marmoset ovarian sections. In addition, the localisation of ubiquitin, a protein associated with cell death, was examined during luteal regression.

3.2.1 Identification of Steroidogenic Cells

3β HSD immunocytochemistry confirmed previous reports that large, circular parenchymal luteal cells with regular spherical nuclei and a diameter >12μm are steroidogenic (Webley *et al.*, 1990; Fehrenbach *et al.*, 1995). In macaque corpora lutea, the levels of mRNA for steroidogenic enzymes did not parallel serum progesterone concentrations thoughout the luteal phase (Basset *et al.*, 1991). Levels decreased gradually after the mid-luteal phase, but did not decrease dramatically immediately before luteal regression (Basset *et al.*, 1991; Fairchild-Benyo *et al.*, 1993). In this study in marmosets, the majority of parenchymal cells were 3β HSD-positive in mid-luteal phase corpora lutea, concomitant with peak luteal progesterone production. The number of 3β HSD immunopositive cells decreased in the late luteal phase coincidental with decreasing steroid hormone production and functional luteal regression. Interestingly, some luteal cells remained 3β HSD immunopositive after progesterone concentrations decreased to follicular phase values, both in naturally regressing corpora lutea and after luteolytic treatment with either GnRH antagonist or PGF2α. This may have been artifactual, whereby morphologically abnormal, degenerating cells had a non-specific reaction with 3β HSD antibodies, or it might indicate the presence of cells responsible for basal levels of progesterone production. However the presence of the steroidogenic enzyme 3β HSD does not necessarily

mean that steroidogenic enzymes are being produced, since other components of the steroidogenic pathway may be non-functional (Young *et al.*, 1994). In addition, the 3β HSD protein persists in regressing bovine corpora lutea (Rodgers *et al.*, 1995), supporting the observation that regressing marmoset corpora lutea also retain the protein.

3.2.2 Steroidogenic Cell Morphology During Luteal Regression.

The number of morphologically normal steroidogenic cells decreased with advancing luteal age, and there was a concomitant increase in steroidogenic cell vacuolation. Extensive steroidogenic cell vacuolation was suggested by an earlier study (Fraser *et al.*, 1995). In both this and the earlier study, luteolytic treatment resulted in the development of large vacuoles, or vesicles, within the cytoplasm of the steroidogenic cells. Steroidogenic cells in corpora lutea undergoing structural regression (luteal day 22) contained vacuoles which were smaller and qualitatively different from those seen after induced luteolysis. Both the proportion of vacuolated cells and the size of the vacuoles increased as the corpus luteum regressed spontaneously in the late follicular phase (corresponding to days 24-28 of the preceding luteal phase). Induction of luteolysis may occur through a rapid suppression of steroidogenesis, raising the possibility that the vacuolation observed after induced regression was a result of accumulation of lipid substrates. However, Oil Red O staining of frozen sections indicated that vacuoles were not filled with lipid in pharmacological luteolysis. Unfortunately it was not possible to do the equivalent study in naturally regressing corpora lutea owing to the unavailability of suitable frozen tissue. It is possible that the vacuolation observed in the naturally regressing marmoset corpus luteum may have been a consequence of lipid accumulation. In sheep small luteal cells have cytoplasmic lipid droplets, whereas large luteal cells do not, and it is thought this is because basal progesterone production by large luteal cells is up to 20 times higher than small luteal cells (Sawyer *et al.*, 1991). Lipid droplets accumulate in the cytoplasm of large luteal cells when progesterone production ceases during luteolysis, and this is presumed to be due to an accumulation of substrate. The lipid droplets continued to increase in number and size until at the end of the oestrous

cycle the outlines of the lutein cells were obscured. In the corpus albicans cells contained coarse lipid droplets for another 15 days (Sawyer *et al.*, 1991). Both large and small cells in human corpora lutea contained numerous lipid droplets throughout the luteal phase (Enders, 1973; Ohara *et al.*, 1987). In a classic study of the human corpus luteum (Corner, 1956) cells 'in which the cytoplasm is almost completely obscured by several large vacuoles' were noted to appear by day 12 of the luteal phase, and the number of vacuolated cells was found to increase as the corpus luteum regressed. Vacuolation in steroidogenic cells was also reported in rat corpora lutea after administration of the PGF2α analogue, cloprostenol (Salazar *et al.*, 1976). Steroidogenic cells described as 'vacuolated' had many of the morphological features of cells undergoing death due to ischemia: chromatin aggregation, nuclear pyknosis, loss of compartmentalisation and cell oedema (Trump *et al.*, 1981). Vacuolated cells within regressing corpora lutea had clearly intact nuclei, suggesting they were not undergoing apoptosis. A non-apoptotic form of cell death which is characterised by vacuolation has been reported in neuronal cell cultures (Regan *et al.*, 1995) and in developing tissues (Clarke, 1990) where it has been referred to as 'autophagic degeneration'. In addition, Fehrenbach *et al.* (1995) reported vacuolisation in marmoset corpora lutea after *in vitro* dialysis of culture media. It can therefore be concluded that steroidogenic cells become vacuolated during the process of luteal regression and that the vacuoles are not a consequence of lipid accumulation. However, although it is possible that vacuolated steroidogenic cells were in the initial stages of a type of non-apoptotic death analagous to the autophagic degeneration observed in other systems, further investigations are required to confirm this.

3.2.3 Non-steroidogenic Cell Numbers During Luteal Regression.

Non-steroidogenic cell numbers appeared to increase in structurally regressing corpora lutea, but were unchanged during the remainder of the luteal phase. Interpretation of these data, however, has to take account of shrinkage of luteal tissue during regression and also the type of quantification system used. During regression steroidogenic cell numbers decreased and the tissue shrank, but in the system used for quantification the area of luteal tissue measured was kept constant. The apparent

increase in non-steroidogenic cell numbers was probably a consequence of tissue shrinkage rather than an actual proliferative increase in non-steroidogenic cells. It is likely that in absolute terms, non-steroidogenic cell numbers were similar during functional and structural luteal regression, but that there was a real decrease during very late structural regression. It was not possible to distinguish endothelial cells, fibroblasts or leukocytes in H+E stained sections, and further work is required to determine temporal changes in non-steroidogenic cell sub-populations.

3.2.4 Identification and Quantification of Apoptosis

Apoptosis was found to occur in marmoset corpora lutea after progesterone had fallen to follicular phase values, therefore, functional luteal regression was not initiated by apoptosis. Percent apoptosis calculated from 3' end labeled sections was slightly higher, but not significantly so, than percentages calculated after morphological analysis of H&E stained sections, as would be expected due to 3' end labeling of cells in earlier stages of apoptosis, and also the occurrence of false positives. Both the *in situ* methods of quantification showed remarkably good correspondence with each other, and electrophoresis of extracted DNA concurred with these results. The low oligonucleosome formation observed after electrophoresis in mid luteal day 10 samples was in agreement with the low levels of apoptosis observed in H&E stained sections and in 3' end labeled sections in which only 0.67±0.4% (n=4) of cells were apoptotic. Luteolytic treatment with PGF2α and GnRH antagonist increased apoptotic cell numbers to 8.0±1 and 7.4±1.5 percent respectively in 3' end labeled sections, and there was a corresponding increase in oligonucleosome formation seen after electrophoresis. Increased oligonucleosome formation 24 hours after induction of luteolysis with PGF2α was also demonstrated in bovine (Juengal *et al.*, 1993; 1994; Rueda *et al.*, 1995), ovine (Kennny *et al.*, 1994) and rabbit (Dharmarajan *et al.*, 1984) corpora lutea, but there has been no other demonstration of oligonuclosome formation after a luteolytic dose of GnRH antagonist.

The percentage of 3' end labeled cells was less than 1% in naturally regressing mid-luteal phase CL, and 5.54±1.4% (n=3) of all luteal cells in very late, structurally

regressing CL. In a comparable study of human corpora lutea (Shikone *et al* 1996) found 9±1.1% labeled granulosa-lutein and 12.3±1.2% labeled theca-lutein cells in the mid-luteal phase, and 39.6±2.6% labeled granulosa-lutein and 56.6±5.4% labeled theca-lutein in the late luteal phase, corresponding to functional regression. These figures are extraordinarily high. Apoptosis is a relatively rapid process lasting from several minutes to a few hours in duration. A low incidence of histologically detectable apoptosis, 10% for example, therefore reflects a very substantial rate of cell loss (Kerr *et al.*, 1972; Bursch *et al.*, 1990) whereby the entire tissue might have disappeared in the order of 10 hours. Rates of apoptosis have been found to be 3±0.4% in late structurally regressing bovine corpora lutea (Zheng *et al.*,1994), 5-9% (Sawyer *et al.*, 1990) 24 hours after PGF2α induced regression in sheep and we found 8±1% apoptosis 24 hours after PGF2α induced regression and 5.54±1.4% in structurally regressing corpora lutea in marmosets. A total of 96.2% of luteal steroidogenic cells undergoing apoptosis in regressing human corpora lutea (Shikone *et al.*, 1996) is substantially higher than other reports to date. Corpora lutea in the study of Shikone *et al* (1996) were collected from women who had cervical cancer, but who had regular menstrual cycles. One characteristic of cancer is that apoptosis is inhibited, and it is possible that there may have been a physiological attempt to compensate for the production of apoptosis inhibitors which resulted in increased apoptosis in the corpus luteum. However, increased apoptosis in the presence of cancer has not been observed or reported on, making this seem rather unlikely.

3.2.5 Temporal Expression of Apoptosis During the Luteal Phase.

These results are in agreement with others who have shown an increase in apoptosis when progesterone concentrations have fallen after PGF2α-induced luteolysis in sheep (Rueda *et al.*,1995) and cattle (Juengel *et al.*,1993; Zheng *et al.*,1994).
A number of reports have indicated that apoptosis occurs after progesterone has fallen to follicular phase values. Apoptosis was found in 4 out of 5 bovine corpora lutea after progesterone had fallen from 65.7 to 3.1μg/g of luteal tissue (Zheng *et al.*, 1994), was demonstrated morphologically in regressing ovine corpora lutea in which progesterone content was <10μg/g of luteal tissue (O'Shea *et al.*, 1977), and was

found in pseudopregnant rabbit corpora lutea after *in vitro* progesterone production had fallen significantly ($p<0.05$) (Dharmarajan 1994). Rueda *et al* (1995) found oligonucleosome formation in two out of four ovine corpora lutea collected on luteal day 14 when serum progesterone concentrations were decreasing, and in addition found apoptotic DNA fragmentation 24 hours after administration of PGF2α when progesterone concentrations had fallen. Juengal *et al* (1993) also showed oligonucleosome formation in three bovine corpora lutea collected on day 19 of the luteal phase after serum progesterone concentrations had fallen from >3ng/ml to <1.2ng/ml.

The apoptotic process is fast, and may take only one hour from the apoptotic signal to the formation of oligonucleosomal 'ladders' (Wyllie *et al.*, 1984). Since PGF2α and GnRH antagonist are administered 24 hours before apoptosis occurs, it is unlikely that these are directly responsible for stimulating apoptosis. Apoptosis in regressing corpora lutea appears to be related to the concentration of progesterone, suggesting that progesterone inhibits apoptosis (Peluso and Pappalardo, 1998), and its reduction below a critical threshold concentration removes an inhibitory barrier and allows apoptosis to proceed.

3.2.6 Initiation of Apoptosis in Corpora Lutea

Rat follicles (Chun et al., 1994) and rabbit corpora lutea (Dharmarajan *et al.*, 1994) undergo spontaneous apoptosis *in vitro* which is prevented by the addition of gonadotrophins to the culture media. These data suggest that LH, FSH and CG inhibit apoptosis in corpora lutea. The administration of GnRH antagonist depletes circulating gonadotrophin levels, and the resultant absence of LH and FSH in treated marmosets may therefore result in spontaneous luteal apoptosis.

GnRH has been shown to stimulate apoptosis in follicles, and the amount of apoptosis after GnRH antagonist treatment was the same as in estrogen-replaced, hypophysectomised control rats (Billig *et al.*, 1994), indicating that the binding of antagonist to ovarian GnRH receptors does not cause apoptosis.

PGF2α may also stimulate luteal apoptosis by 'removing' gonadotrophins. PGF2α receptors were present on luteal cells undergoing apoptosis in rat (Orlicky *et al.*, 1992) and mouse (Hasumoto *et al.*, 1997). PGF2α can also disconnect the LH receptor from its secondary messenger pathway by uncoupling the G(s) protein from adenyl cyclase (Abayasekara *et al.*, 1993) and inhibiting the formation of LH-dependent cAMP (Thomas *et al.*, 1978, Dorflinger *et al.*, 1983).

Spontaneous apoptosis *in vivo* might therefore be effected by the endogenous production of PGF2α. Variable steroidogenic cell PGF2α production may result in one cell containing sufficient PGF2α to completely inhibit all LH-stimulated steroidogenesis, and hence be well advanced down an apoptotic pathway, whereas a neighboring cell might have produced only enough PGF2α to have halved LH-stimulated steroidogenesis, and be less likely to undergo apoptosis. This scenario concurs with observed results in which not all steriodogenic cells undergo apoptosis at the same time. The gradual decrease in steroidogenesis over the latter part of the luteal phase may therefore be proportional to gradually increasing intracellular concentrations of PGF2α. Apoptotic pathways were not stimulated until all cells in the corpus luteum had ceased steroidogenesis, suggesting that the local presence of progesterone is sufficient to inhibit apoptosis in a cell which has ceased steroidogenesis. Progesterone may have antioxidant properties (Sugino *et al.*, 1996), and may be able to enter cells by diffusion or by means of a non-classical progesterone receptor (Rae *et al.*, 1998) thereby equalising its antioxidant effects across the whole corpus luteum. When the progesterone concentration of the entire corpus luteum falls below a minimum threshold, oxygen free radicals generated by PGF2α (Riley and Berhman, 1991; Sawada and Carlson, 1991) initiate apoptosis (Tilly and Tilly 1995; Haecker and Vaux, 1994).

3.2.8 Limitations of the Systems Used to Detect Apoptosis

The absolute quantification of apoptosis requires tissue-specific information about the time taken to form apoptotic bodies, and the length of time apoptotic bodies persist in the tissue being examined. Duration of apoptosis as measured from induction to fragmented nuclei is 50 minutes in CD4+ T lymphocytes (Howie *et al.*, 1994) and 10 minutes in liver hepatocytes (Bursch *et al.*, 1990). The duration of luteal cell apoptosis has yet to be elucidated and requires the collection of corpora lutea at consecutive time points after induction of luteolysis.

The length of time apoptotic bodies remain in luteal tissue is dependent upon three factors; the integrity of the vasculature (O'Shea *et al.*, 1977), on blood flow, which decreases after functional regression (Bruce and Hillier, 1974; Niswender *et al.*,1976; Bruce and Moor, 1976; Dharmarajan *et al.*,1994) and on the influx of immune system cells capable of phagocytosing apoptotic bodies (Lei *et al.*,1991). None of these factors have been examined in marmoset corpora lutea.

The assumption that one cluster of apoptotic bodies originated from the fragmentation of one cell may have been another source of error. Clusters of apoptotic bodies were often seen within the vasculature, which raised the possibility that they did not occur *in situ*, but were transported there. A cluster of apoptotic bodies, therefore, may have reflected an obstruction in the vasculature and the build up of apoptotic bodies which originated from a number of different cells.

The three methods used to detect apoptosis were complimentary to each other. The identification of apoptotic bodies and condensed cells with clearly fragmented nuclei in H&E stained sections was relatively simple and certainly inexpensive, but led to possible underestimation because cells in the earlier stages of apoptosis, or cells which were apoptotic but had not undergone nuclear fragmentation, were not counted. *In situ* 3' end labeling probably identified more cells in the earlier stages of apoptosis than were identified in H&E stained sections, but on the other hand may also have given a falsely high score for apoptosis due to the labeling of randomly fragmented necrotic DNA. The vacuolation of steroidogenic cells during luteal regression may have been indicative of a non-apoptotic form of cell death which eventually resulted in random, non-specific DNA fragmentation characteristic of

necrosis. Necrotic cells would be 3' end labeled, and impossible to distinguish from apoptotic cells in which the nucleus had not fragmented. Since electrophoresis of luteal DNA revealed the presence of necrotic DNA, the occurrence of false positives in the 3' end labeled sections was a distinct possibility. However, neither analysis of H&E sections or electrophoresis of luteal DNA falsely identified necrotic cells or DNA as apoptotic.

The number of 3' end labeled cells was also highly dependent upon the concentration and duration of the proteinase K incubation, and on the nature of the tissue being examined. In this study these parameters were optimised to achieve the amount of positive 3' end labeling reported in healthy and atretic follicles (Giebel *et al.*, 1997; Tilly *et al* 1991; Billig *et al,* 1993; Tilly, 1993; Hsueh *et al.*, 1994), and to slightly under-label (90-98%) DNase positive controls. Under-labeling introduced a tendency to underestimate the amount of apoptosis, and it is possible that this counteracted the labeling of false positives, resulting in a final score for apoptosis in 3' end labeled sections which was remarkably close to that obtained by analysis of H&E stained sections. The persistence of apoptotic bodies within luteal tissue may have contributed to an overestimation of apoptosis by all three methods.

Although electrophoresis of extracted DNA differentiated unequivocally between necrotic and apoptotic DNA, quantification of oligonuclesome formation was highly variable. This variability might have been decreased if aspects of the technical procedure had been improved. One source of inaccuracy may have been inaccurate determinations of DNA concentrations by comparison with lambda DNA standards. Accuracy could have been improved by introducing a step to remove RNA from each sample, which would have allowed spectrophometric determination of DNA concentrations. Reprecipitation of labeled DNA would have improved sample quality, and perhaps improved the correlation between amount of radioactivity in genomic DNA and the concentration of genomic DNA. The quantification of electrophoresed oligonucleosomes would also have been improved by counting the radioactivity in each sample, and loading the same amount of radioactivity in each lane. Most of the variation was probably due to inter-animal variation; each sample came from a single corpus luteum from one animal. Corpora lutea can be formed at 20 hour intervals within the same cycle (Torii *et al.*, 1996; Oerke *et al.*, 1996), and

our cycle tracking regime was accurate ±24 hours, therefore there may have been up to 50 hours age difference between corpora lutea when they were subjected to luteolytic treatments. Individual animal variation of age, weight and status would have added to this variation. The variability due to different ages of corpora lutea may have been decreased by analysing oligonucleosome formation in multiple corpora lutea from each animal, and deriving a mean luteal score for each animal, as was done for the *in situ* analyses of apoptosis.

3.2.9 Ubiquitin Expression During Luteal Regression.

Ubiquitin was upregulated in the cytoplasm of steroidogenic cells after PGF2α induced luteolysis in the marmoset. GnRH antagonist induced luteolysis did not cause an increase in ubiquitin expression. Since both *in situ* 3' end labelling and oligonucleosome formation characteristic of apoptotic DNA fragmentation were increased after induced luteal regression with both PGF2α and GnRH antagonist, ubiquitin expression is probably unrelated to apoptosis in marmoset luteal regression. Ubiquitin was found in the nuclei of a small number (how many?!!) of mid luteal phase steroidogenic cells, and 0.67±0.427% steroidogenic cells were 3' end labeled *in situ* at this time, suggesting that nuclear ubiquitin may be related to apoptosis during the mid luteal phase. However it is also possible that it is playing a role in transcription and cell cycle protein regulation (Levinger and Varhavsky, 1982; Huang *et al.*,1986). Ubiquitin was also found in the cytoplasm of parenchymal luteal cells 24 hours after induction of luteolysis with PGF2α. The shift from nucleus to cytoplasm and the increase in number of cells expressing ubiquitin suggests that ubiquitin plays different roles pre and post luteolysis, and may be involved in cytoplasmic proteolysis or protein regulation during PGF2α-induced luteal regression. Murdoch *et al* (1996) reported an increase in luteal ubiquitin mRNA and protein as quickly as two hours after administration of a luteolytic dose of PGF2α to ewes, which implicated ubiquitin in functional luteal regression, since structural regression did not begin until at least 16 hours after administration of PGF2α. This, however, does not preclude ubiquitin from also playing a role in structural regression. Ubiquitin immunoreactivity was not found in any animal subjected to

GnRH antagonist-induced luteolysis. It is possible that ubiquitin expression occurred at an earlier time point and may be involved in functional luteal regression in GnRH antagonist treated animals, but these data suggest that it did not play a role in structural regression. Ubiquitin expression in luteal cells therefore may be a response to PGF2α. Only cells with PGF2α receptors expressed ubiquitin in sheep corpora lutea, and luteal ubiquitin expression may not be specific for luteolysis but be part of a response to cellular stress in which ubiquitin is coexpressed with heat shock protein-70 (Murdoch *et al.*, 1995) which is also upregulated after PGF2α induced regression in rats (Kanna *et al.*, 1995).

Ubiquitin has been shown to be upregulated during apoptosis in a number of systems (Haas *et al.*,1996; Myer and Schwartz, 1996; Lauzon *et al.*, 1993; Sandri *et al.*, 1997; Delic *et al.*,1993) but there does not seem to be a relationship between ubiquitin expression and apoptosis during luteal regression in the marmoset. Cells expressing ubiquitin in PGF2α treated animals did not have the same morphology as 3' end labeled cells in serial sections; ubiquitin positive cells appeared to be dying by a non-apoptotic pathway. In addition to this, oligonucleosome formation indicative of apoptosis occured 24 hours after administration of GnRH antagonist, but this was not coincident with ubiquitin expression in these animals.

3.2.11 Summary.

In summary, 3β HSD immunocytochemistry facilitated the identification of steroidogenic cells, and therefore also allowed all other cells to be defined as nonsteroidogenic cells. It also indicated that luteal regression is not instigated by the loss of 3β HSD enzyme because it was found to be present in functionally regressing corpora lutea, and because it persisted in luteal tissue until after functional regression was completed.

Structural luteal regression was characterised primarily by cell death. Steroidogenic cell death occurred by two different processes; apoptosis, and a process which resulted in vacuole formation in the cell. Vacuolisation may be due to the accumulation of lipids in spontaneously regressing marmoset corpora lutea, but steroidogenic cell vacuoles do not contain lipid in corpora lutea subjected to

induction of regression by the administration of luteolytic agents. It is possible that steroidogenic cell vacuole formation after induced luteal regression may be a consequence of impaired osmotic control, membrane perturbation and subsequent cell oedema.

Nonsteroidogenic cell numbers did not appear to change during functional luteal regression, but did appear to increase during structural luteal regression. However, it is still not known how different populations of nonsteroidogenic cells are affected by luteal regression. This information could be obtained by performing immunocytochemistry with specific markers for endothelial cells, fibroblasts and macrophages. It is also unclear whether increases in nonsteroidogenic cell numbers during structural regression are a result of proliferative increases, or are a consequence of the dynamics of shrinking tissue. This issue could be resolved by determining the number and the type of cells undergoing proliferation in regressing corpora lutea.

apoptosis occurs in regressing marmoset corpora lutea as shown by morphological analysis, by 3' end labeling and by gel electrophoresis of extracted DNA. Apoptosis occurs in both steroidogenic and non-steroidogenic cells after peripheral progesterone concentrations have fallen to follicular phase values in naturally regressing corpora lutea and in corpora lutea induced to undergo regression with PGF2α or GnRH antagonist. Ubiquitin is expressed in the nuclei of a small number of mid luteal phase day 10 steroidogenic cells, and in the cytoplasm of steroidogenic cells after PGF2α induced luteal regression, but is not expressed in luteal cells after a luteolytic dose of GnRH antagonist. Induced luteolysis with both PGF2α and GnRH antagonist is associated with an increase in apoptosis, but ubiquitin expression is not an indicator of apoptosis in the corpus luteum of the marmoset monkey.

3.2.12 Conclusions.

Marmoset luteal cells were identified as being either steroidogenic or nonsteroidogenic. The number of steroidogenic cells decreased as luteal regression proceeded. Steroidogenic cell numbers were depleted by the occurrence of two different processes; apoptosis, and the formation of cytoplasmic vacuoles.

Nonsteroidogenic cell numbers remained constant during the luteal phase and functional luteal regression, but apparently increased during structural luteal regression. It appears that changes in steroidogenic cell numbers precede changes in nonsteroidogenic cell numbers in luteal regression. The decline in progesterone production during functional luteal regression is not bought about by the apoptotic deletion of steroidogenic cells. Apoptosis in primate corpora lutea occurs after functional luteal regression is completed and is characteristic of structural luteal regression.

Chapter 4: The Vasculature of the Corpus Luteum.

4.0 Introduction

Morphological analysis of H&E stained sections of marmoset corpora lutea indicated that the number of nonsteroidogenic cells did not change during the luteal phase or functional luteal regression, but increased during structural luteal regression (see chapter 3). The nonsteroidogenic cells of the corpus luteum are primarily endothelial cells, fibroblasts, and immigrant cells of the immune system. Quantification of nonsteroidogenic cell numbers may not reflect changes in individual sub-populations of nonsteroidogenic cells. Further examination of nonsteroidogenic cells can be facilitated by specific identification of one or more of these types. Approximately 50% of the cells in the corpus luteum are endothelial cells (Lei *et al.*, 1991; Christenson and Stouffer, 1996), and an extensive capillary network penetrates the corpus luteum, so much so that every steroidogenic cell is in contact with at least one capillary (Redmer and Reynolds 1996). The primary function of the corpus luteum is the production of steroid hormones, and steroidogenesis is entirely dependent upon the delivery of cholesterol substrates and regulatory gonadotrophins through the vasculature, and peak progesterone production does not occur until the luteal vasculature is fully developed. Early luteal phase corpora lutea cultured *in vitro* and stimulated with gonadotrophins secrete more progesterone than mid and late luteal phase corpora lutea (Hild-Petito *et al.,* 1989), but maximal secretory activity does not occur *in vivo* until the mid luteal phase, and it is thought that this is due to inadequate development of the luteal vasculature in the early luteal phase (McClellan *et al.*, 1975). It is believed that the vasculature is absolutely vital to normal functioning of the corpus luteum, but it is not clear what role it plays in luteal regression. It is not known whether changes in the vasculature, or changes in blood flow, precede functional luteal regression in the primate, and neither is it clear when or how the vasculature changes during the process of structural regression.

4.0.1 Blood Flow in the Corpus Luteum.

Blood flows through the corpus luteum at the rate of approximately 10 - 15 ml per minute per gram of tissue (Abdul-Karim and Bruce 1973; Bruce and Moor 1976) and this rate of flow is higher than that to any other organ of the body; flows of 0.61,

1.86, and 1.78 ml per minute per gram of heart, brain and kidney respectively have been observed (Bruce and Moor, 1976). Within the ovary rates of blood flow are 2.66 and 6.68 ml per minute per gram of stroma or follicles respectively, showing that blood flow to the follicles is of the same order as that seen to corpora lutea (Bruce and Moor, 1976). It is not known why blood flow through the corpus luteum is so much higher than through other tissues. Blood flow to the ovary bearing the corpus luteum, and also through the corpus luteum, decreases as the luteal phase advances (Niswender *et al.,* 1976; Bruce and Moor, 1976) and studies utilising radioactive microspheres indicate that approximately 90% of the blood flowing to the ovary goes through the corpus luteum during the mid luteal phase (Niswender *et al.,* 1976; Abdul-Karim and Bruce, 1973), but that this decreases to 28% in the late luteal phase (Bruce and Moor, 1976), which indicates that a mechanism for reducing luteal blood flow exists, and an arteriole-venule shunting system which results in reduced blood flow to individual steroidogenic cells has been proposed (Niswender *et al.,* 1976).

4.0.2 Effects of Luteolytic Agents on Luteal Blood Flow.

LH may have effects on luteal blood flow. Administration of anti-LH antibodies to sheep causes a decrease in serum progesterone levels and a concomitant decrease in blood flow to the ovary, and infusion of additional LH causes an increase in serum progesterone levels and an increase in blood flow (Niswender *et al.,* 1976) but the temporal relationships between changes in steroid hormone production and changes in luteal blood flow are unclear. Administration of PGF2α *in vivo* to rabbits does not, however, cause a decreased blood flow to the corpora lutea until 6 hours after a significant decrease in plasma progesterone concentration has occurred (Bruce and Hillier, 1974), so the luteolytic action of PGF2α is unlikely to be mediated by reduced blood flow. It does, however, appear to be mediated by endothelial cells because steroidogenesis was not inhibited by PGF2α in pure cultures of bovine luteal steroidogenic cells, but steroidogenesis was inhibited in mixed cultures of endothelial and steroidogenic cells (Girsh *et al.,*1995). Disruption of the vasculature also prevents the luteolytic effect of PGF2α on dispersed rat or dispersed marmoset

luteal cells *in vitro* (Thomas et al., 1978; Webley *et al.*, 1989). In addition, PGF2α has longer term effects on luteal vasculature; 24 hours after *in vivo* administration of PGF2α to sheep 28% of endothelial cells were morphologically abnormal and capillary lumina were occluded with cellular debris (Sawyer *et al.*, 1990; Stacey *et al.,* 1976). It has also been suggested that vascular occlusion during luteal regression could result in hypoxic conditions, and that ischemia could therefore be a component of structural luteal regression.

4.0.3 The Morphology of Luteal Vasculature.

A number of studies have quantified different cell types of the corpus luteum. In one study, the cellular composition of sheep corpora lutea was determined by a 'hit' technique whereby luteal components were classified as large or small luteal cells, capillaries or connective tissue. The number of 'hits' in endothelial cells or capillary lumina decreased by approximately 50% from the mid to late luteal phase, but the number of 'hits' in leukocytes and in intracapillary debris increased during the same time period, while connective tissue quantification remained constant (Niswender *et al.*, 1976). The decrease in the number of endothelial cell 'hits' occurred before serum progesterone levels decreased, suggesting that changes in luteal vasculature may instigate functional regression. The majority of workers, however, have found that in ruminants structural changes are first seen in the vasculature concomitant with falling serum progesterone values, and that during luteal regression there appears to be a change in the vasculature bought about by the loss of small capillaries and an increase in larger microvessels (Zheng *et al.*, 1993; Redmer and Reynolds 1996). The mid-phase bovine corpus luteum has a dense capillary network made up of fully differentiated endothelial cells with a flattened elongated morphotype and numerous tight junctions (Modlich *et al.,* 1996). Early luteal regression is characterised by the dissociation of endothelial tight junctions, widening capillary basal lamina and disruption of osmotic regulation. Endothelial cell nuclei condense and may fragment in a process which closely resembles the initial stages of apoptosis, and the cells then slough off into the lumen of the blood vessel, so forming localised blockages. This loss of endothelial cells further perturbs

the integrity of capillary basal lamina and accelerates the loss of osmotic equilibrium. Occlusion of the capillaries may also cause ischemia. Parenchymal steroidogenic cells then undergo degenerative changes, either by the formation of vacuoles, or by apoptosis. The loss of steroidogenic cells appears to be accompanied by the loss of small capillaries and their replacement with larger microvessels, and late structural regression is also characterised by α-smooth muscle-actin positive myofibroblast proliferation, which results in the formation of contractile layers around arterioles and small arteries with consequent vasoconstriction and additional detachment of endothelial cells from the basement membrane. This results in further protrusion of endothelial cells into the lumina of small blood vessels, and the eventual occlusion of the vasculature in very late regressing corpora lutea so that the resulting corpus albicans is formed predominantly of fibroblasts and endothelial cells (Deane *et al.*, 1966; O'Shea *et al.*,1977; Modlich *et al.*,1996).

4.0.4 Vascular Endothelial Growth Factor.

The growth and development of blood vessels is controlled by a number of angiogenic factors, one of which, Vascular Endothelial Growth Factor (VEGF), is a secreted heparin-binding endothelial mitogen and is also an important regulator of luteal vascular development (Redmer and Reynolds, 1996). Endothelial cells isolated from macaque corpora lutea respond to VEGF *in vitro* by proliferating (Christenson and Stouffer, 1996) and VEGF has also been found in the corpus luteum of the pig (Ricke *et al.*, 1995), sheep (Doraiswamy *et al.*, 1995a), cynomolgus monkey (Ravindranath *et al.*, 1992), rat (Phillips *et al.*, 1990), mouse (Shweiki *et al.*, 1993) and human (Gordon *et al.*, 1996; Kamat *et al.*, 1995). In bovine corpora lutea, the highest levels of VEGF mRNA are found in the early luteal phase and a gradual reduction then occurs throughout the remainder of the luteal phase (Redmer *et al.*, 1996). VEGF mRNA levels are also reduced by luteolytic treatment with GnRH antagonist, although it took three days for this response to occur (Ravindranath *et al.*, 1992). VEGF has been immunohistochemically located to vascular pericytes in ovine corpora lutea but does not appear to be expressed by endothelial, small or large luteal cells in this species (Redmer and Reynolds, 1996), however VEGF has been

detected by immunocytochemistry in follicular cells and in granulosa-lutein and theca-lutein in the human (Gordon et al., 1996; Kamat *et al.*, 1995). It would appear that while VEGF is likely to be the principal regulator of angiogenesis in the ovary, much has still to be learned about changes in expression and its role during follicular development. In addition, studies on its localisation within the corpus luteum seem to suggest species differences and variation in results between laboratories.
The VEGF receptor, Flt-1, is a tyrosine kinase cell membrane receptor, and it was hypothesised that it might be expressed by endothelial cells in the corpus luteum (Jakeman *et al.,* 1992; Shweiki *et al.,* 1993).

4.0.5 Aims

The aims of this study were to examine luteal vasculature and to characterise relationships between vascular changes and luteolysis. Specific aims were to: (i) quantify non-steroidogenic cell numbers throughout the luteal phase and after spontaneous and induced luteal regression, (ii) to identify endothelial cells and quantify endothelial cell numbers throughout the luteal phase and after spontaneous and induced luteal regression and (iii) to examine the morphological distribution and temporal changes in VEGF in the marmoset corpus luteum.

4.1 Results

4.1.1 Identification of Endothelial Cells using Von Willebrand Factor VIII Antigen (vW).

Ovarian sections subjected to immunocytochemistry with antibodies against von Willebrand Factor VIII antigen (vW) had specific immunoreactivity around lumina containing red blood cells, and there was also vW immunoreactivity which delineated smaller vessels which did not contain erythrocytes (Figure 4.1). There was no vW immunoreactivity in steroidogenic cells, nor in negative control sections (Figure 4.1), although there was some non-specific staining in the cytoplasm of steroidogenic cells when DAB was used in the visualisation procedure. The vW staining was quite diffuse, and masked individual cell nuclei. In addition the trypsin

incubation compromised cellular morphology, and both these factors made it difficult to count individual vW positive endothelial cells, therefore measurement of area of staining was considered to be more accurate than attempting to count individual endothelial cells in these sections. Antigen retrieval techniques utilising microwave irradiation destroyed the vW antigen.

The pattern of vW staining during the early and mid luteal phases was consistent with an extensive capillary network in which every steroidogenic cell was in contact with the vasculature (Figure 4.1a and b). Blood vessels were generally too small in section to be able to see red blood cells. This pattern changed in late regressing corpora lutea, and was characterised by a decrease in capillary staining and an increase in staining of small arterioles and venules in which erythrocytes were frequently identified (Figure 4.1d). The pattern of vW immunoreactivity after induced regression was slightly different from that seen in spontaneously regressing corpora lutea (Figure 4.1f and g). There was a greater range of blood vessel size, with some sections having predominantly small capillaries simular to those seen in untreated mid luteal phase corpora lutea, and others having a combination of small capillaries and dilated blood vessels. Corpora lutea collected 24 hours after treatment with PGF2α or GnRH antagonist did not have the same vascular formation as spontaneously regressing corpora lutea, although the corpora lutea treated with luteolytic agents, and the untreated regressing corpora lutea were equivalent to each other inasmuch as serum progesterone concentrations were at baseline levels.

Figure 4.1: Von Willebrand Factor VIII Antigen (vW) Immunocytochemistry in Marmoset Corpora Lutea. Ovaries collected on (a) luteal days 2-5, (b) luteal day 10, (c) luteal day 18 (functional luteal regression) and (d) luteal days 22-25 (structural luteal regression). Panel (e) is a serial section of (b) and is a representative example of antibody negative control sections. The corpus luteum shown in panel (f) was obtained 24 hours after *in vivo* administration of the luteolytic agent PGF2α analogue, cloprostenol, and (g) shows luteal tissue 24 hours after *in vivo* administration of GnRH antagonist. Specific vW immunostaining is either red-pink or brown-black, and is localised between rounded steroidogenic cells. All pictures are of the same magnification, and the scale bar in (e) represents 20μm.

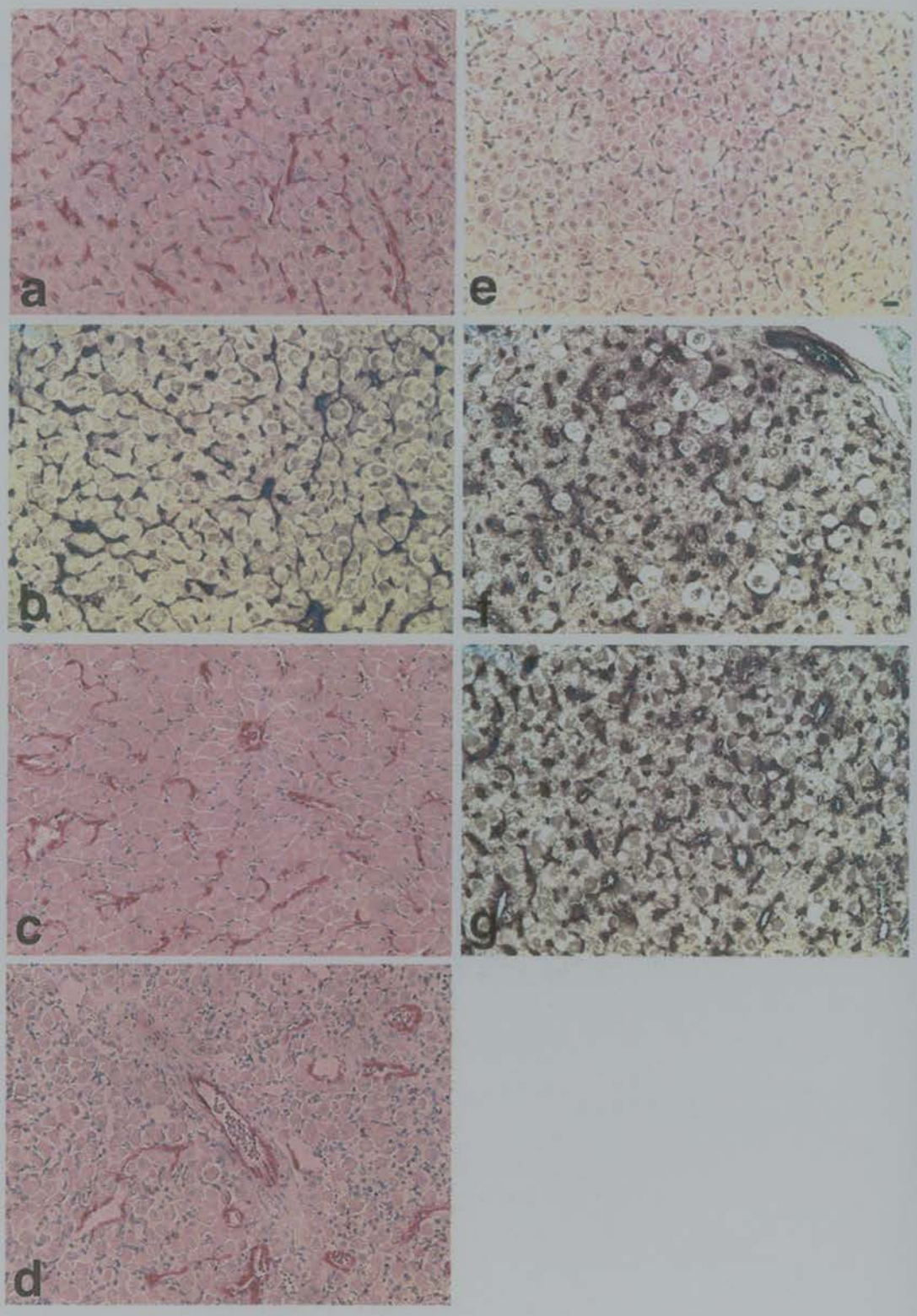
a
e
b
f
c
g
d

4.1.2 Quantification of vW Immunoreactivity After Spontaneous Luteal Regression.

Area of immunoreactive vW staining in the early luteal phase (5215±371μm^2, n=4, Figure 4.2) was significantly higher than at all other stages of the cycle (Luteal days 6-8, 2159±465, $p<0.01$, Luteal day 10, 3517±491, $p<0.01$, Luteal day 18, 3462±420, $p<0.01$, Luteal days 20-24, 4060±191, $p<0.05$) and area of staining decreased gradually until luteal day 18. Area of vW immunoreactivity did not change as progesterone levels fell to follicular phase values (4060±191, n=3). Two animals from which corpora lutea were collected on luteal days 25-28, however, had 2040 and 2101μm^2 of vW immunoreactivity respectively, which suggests that loss of the vasculature may be the last thing to occur in structural luteal regression (Figure 4.2). The pattern of vW staining in the early and mid luteal phases was consistent with an extensive capillary network in which every steroidogenic cell was in contact with the vasculature to a pattern in structurally regressing corpora lutea characterised by a decrease in capillary staining and an increase in staining of small arteries and veins. This was quantified by expressing the area of vW immunoreactivity as a percentage of the total area of luteal tissue in order to derive an approximate measure of the luteal volume occupied by the vasculature. In the early luteal phase the vasculature occupied 7.13±0.5% of the volume of the corpus luteum. By the mid luteal phase this had decreased to 4.81±0.67%, and this was sustained during functional luteal regression (4.73±0.57%, n=3). Structural luteal regression, however, was associated with an increase in vascular volume (5.55±0.26%, n=3).

4.1.3 Quantification of vW Immunoreactivity After Induced Luteal Regression.

Induction of luteolysis resulted in an increase in the area of vW immunoreactivity (Figure 4.3), from 4167±1130μm^2 (n=3) in mid luteal phase corpora lutea to 8835±1218μm^2 (n=3, $p<0.05$) 12 hours and 8403±1607 (n=4, $p<0.05$) 24 hours after administration of GnRH antagonist. Induction of luteolysis with PGF2α did not result in a significant increase in vW immunoreactive staining either 12 (4307±1765, n=3) or 24 (5981±1307, n=4) hours after luteolytic treatment.

Figure 4.2: Area of Endothelial Cell Specific Staining in Marmoset Corpora Lutea.

Histogram showing area of von Willebrand Factor VIII Antigen (vW) specific immunostaining in marmoset corpora lutea. Ovaries containing corpora lutea were collected on luteal days 2-5 (early, n=4), luteal day 10 (mid, n=4), luteal day 18 (functional luteal regression, n=3), luteal days 22-25 (structural luteal regression, n=3) and luteal days 25-28 (late structural regression, n=2). The total area of vW specific immunostaining per 31400μm^2 unit area of luteal tissue was determined for each corpus luteum, and shown as mean±SEM for each stage of the luteal phase. Data were subjected to one way analysis of variance. The area of vW immunostaining per unit area measured during the early luteal phase was significantly higher than at any other time of the luteal phase (**, $p<0.01$).

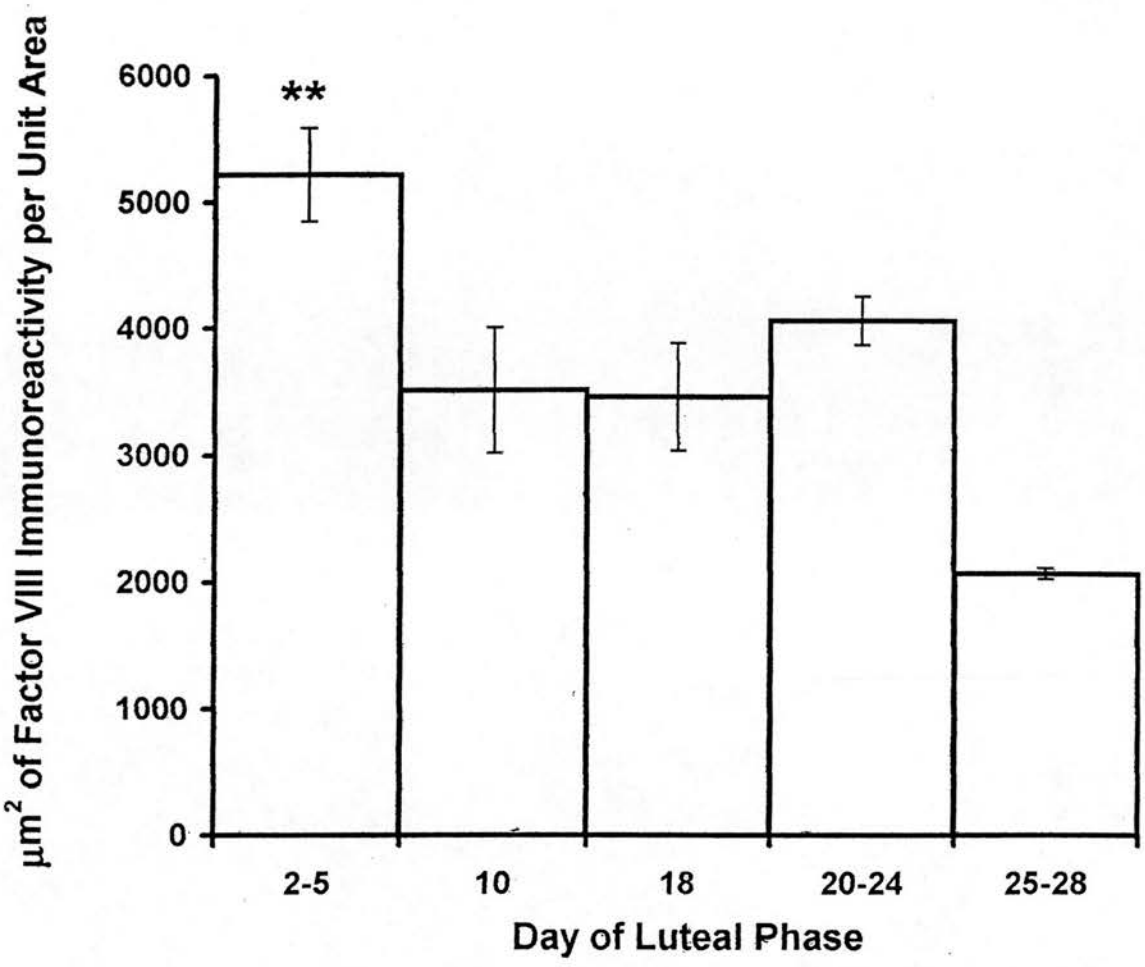

Figure 4.2: Endothelial Cell Specific Staining in Marmoset Corpora Lutea

Figure 4.3: Area of Endothelial Cell Specific Staining in Marmoset Corpora Lutea After Induced Luteal Regression.

Histogram showing area of von Willebrand Factor VIII Antigen (vW) specific immunostaining in marmoset corpora lutea. Ovaries containing corpora lutea were collected on luteal day 10 (control, mid luteal, n=3), 12 hours (PG12, n=3) and 24 hours (PG24, n=4) after *in vivo* administration of the PGF2α analogue, cloprostenol, and 12 hours (Gn12, n=3) and 24 hours (Gn24, n=4) after *in vivo* administration of a GnRH antagonist, anterelix. Luteolytic agents were administered on luteal day 9, 24 hours before collection on luteal day 10. The area of vW immunostaining per 31400μm^2 unit area of luteal tissue was determined for each corpus luteum. The area (mean±SEM) of vW immunostaining 12 and 24 hours after induction of luteolysis with GnRH antagonist was significantly higher than the area of vW immunostaining per unit area of control luteal tissue (*, $p<0.05$).

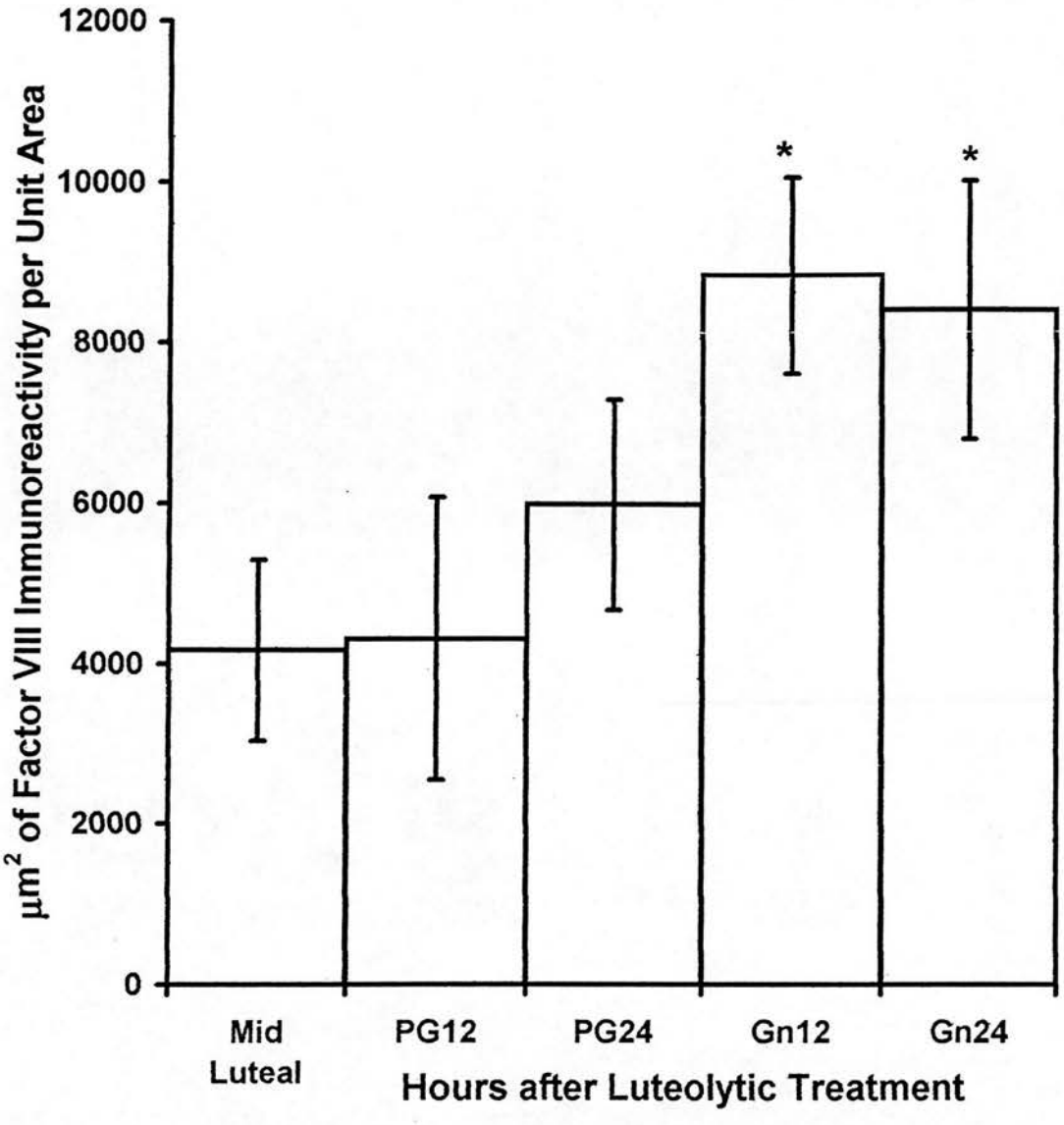

Figure 4.3: Endothelial Cell Specific Staining in Marmoset Corpora Lutea After Induced Luteal Regression.

4.1.4 Vascular Morphology During the Luteal Phase and Spontaneous Luteal Regression.

Luteal vascualture was further examined by determining the number of discrete areas of vW immunostaining at each stage of the luteal phase, and using the assumption that each discrete area of vW immunostaining represented one blood vessel (Figure 4.4). The number of blood vessels per unit area appeared to be highest during the early luteal phase, decreased to a baseline level, then increased gradually during the remainder of the luteal phase. However, the number of individual blood vessels then decreased markedly as structural luteal regression progressed, as would occur if numerous small capillaries were replaced by lower numbers of larger blood vessels.

Figure 4.4: The Relationship Between Luteal Age and the Number of Blood Vessels in Marmoset Corpora Lutea.

Each data point (▲) represents the number of distinct areas of von Willebrand immunostaining per 31400μm^2 unit area of luteal tissue from one animal. Ovaries containing corpora lutea were collected on luteal days 2-5 (early, n=3), luteal day 10 (mid, n=4), luteal day 18 (functional luteal regression, n=4), luteal days 22-25 (structural luteal regression, n=3) and luteal days 25-28 (late structural regression, n=2).

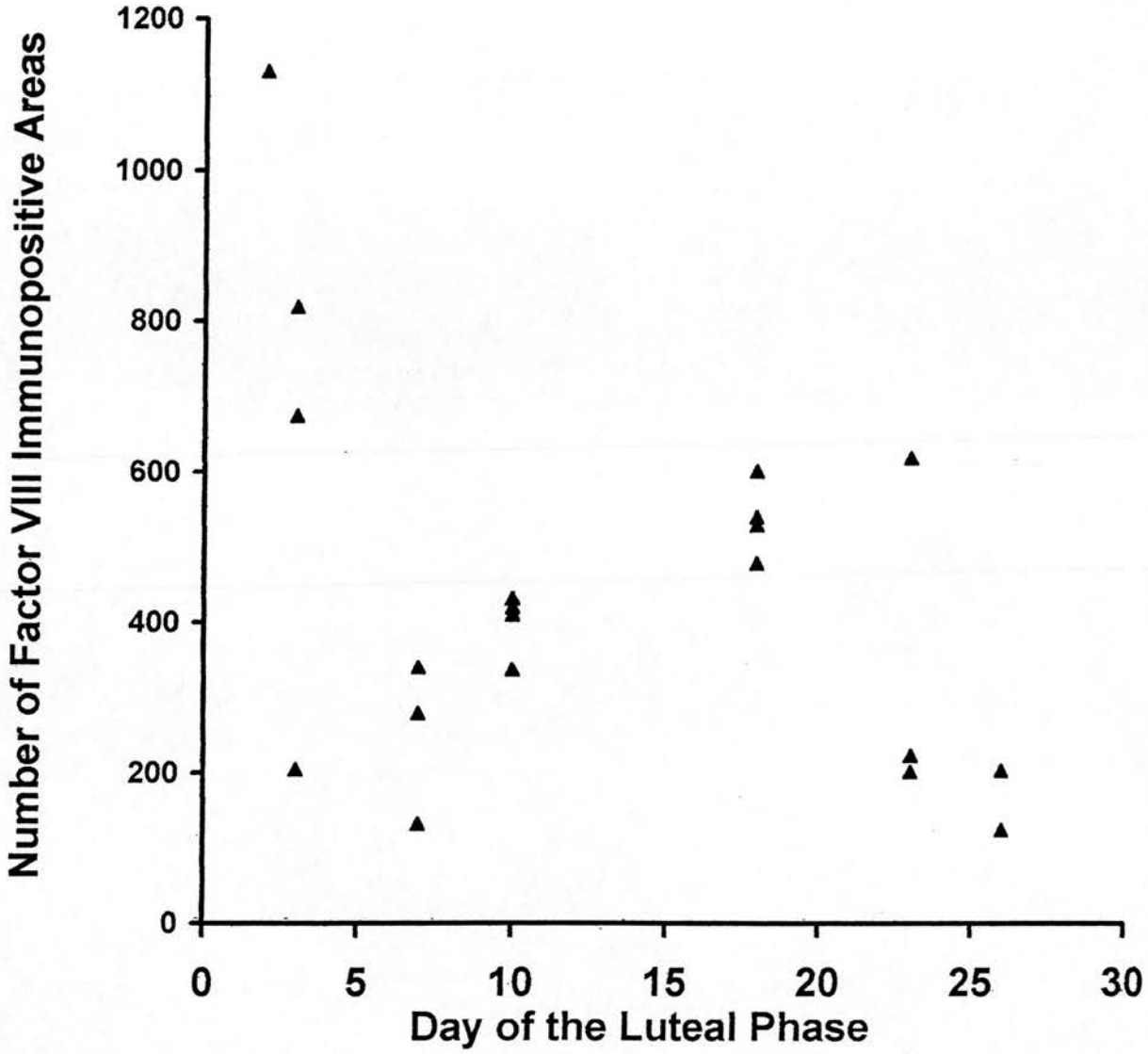

Figure 4.4: **Relationship Between Luteal Age and the Number of Blood Vessels in Marmoset Corpora Lutea.**

4.1.5 Further Techniques for Identification of Endothelial Cells

Since vW ICC obscured endothelial cell morphology, attempts were made to establish an alternative method of endothelial cell identification. Unfortunately these were unsuccessful, and these negative data are reported here briefly.

An antibody against the lectin, Ulex europaeus agglutinin-1 (UEA-1), which binds a sugar found only on primate endothelial cells (Christenson and Stouffer, 1996), was not available for this study, so another lectin, Griffonia (Bandeiraea) simplicifolia lectin I, isolectin B_4 (Vector Laboratories, Peterborough, UK) was used instead. It is a specific endothelial cell marker in mouse, rat and sheep. However, staining in sections of sheep pituitary was inconsistent and not reproducible, and no staining at all occurred in marmoset corpora lutea.

A rat anti mouse monoclonal antibody against CD31/PECAM was kindly donated by Dr Annunciata Vecchi (Istituti di Ricerche Farmacologiche <Mario Negri>, Italy). This antibody was found to identify mouse blood vessel endothelial cells (Vecchi *et al.*, 1994) and we were also informed that it had affinity to endothelial cells in marmoset uterus (Dr Roy Bicknell, Oxford University, pers comm.). The method used was similar to vW ICC with the exception that the hybridoma supernatant was used at a dilution of 1:4 or less, and the secondary antibody was biotinylated goat anti rat (DAKO, High Wycombe, UK). Both human and marmoset cryostat and paraformaldehyde fixed sections were subjected to this ICC protocol, but no immunoreactivity was observed in any of these. Future work could examine (a) the efficacy of different antigen retrieval systems, (b) Apply Dr Vecchi's protocol to her mouse sections in our laboratory, and also determine whether our marmoset sections processed in the laboratory of Dr Vecchi or Dr Bicknell display CD 31 immunoreactivity, since the antibody may have been inactivated during transportation to our laboratory and (c) include mouse positive control sections in our procedure.

Periodic Acid-Schiff procedures stain epithelial mucins (Culling, 1974) and have been used as markers for blood vessels. Accordingly marmoset, macaque and human

paraformaldehyde fixed luteal sections were brought to water, incubated with 1% periodic acid for 5 minutes at room temperature, washed with water for 5 minutes before staining with Schiffs reagent for 15 minutes at room temperature. The sections were then washed and counterstained with haematoxylin before mounting. This procedure was repeated a number of times with minor changes to incubation times and reagents, but the results were always identical. Some blood vessels containing erythocytes did stain brilliant pink in each section, but intra and inter-section staining was very variable, and not all blood vessels stained positive. In addition, the membranes of luteal steroidogenic cells stained pink, and small patches of stroma also had vibrant positive staining, therefore it was concluded that the method was not specific for luteal blood vessels.

Antibodies against the antigen CD34 are commonly used to identify endothelial cells. Although CD34 ICC successfully identifies endothelial cells in human corpora lutea in our laboratory, the same procedure does not immunolocalise endothelial cells in marmoset corpora lutea (Dr. Hamish Fraser, pers. comm.).

4.1.6 Immunolocalisation of Vascular Endothelial Growth Factor (VEGF).

Specific immunoreactivity for VEGF was found in the cytoplasm of luteal steroidogenic cells (Figure 4.5), but not in any other luteal cell type, nor in negative control sections (Figure 4.5 inset, and Figure 4.6b). Oocytes were immunopositive, and theca and granulosa cells in atretic follicles were weakly immunopositive, but theca and granulosa cells in morphologically healthy follicles were VEGF immunonegative (Figure 4.5). The majority of steroidogenic cells in corpora lutea of the early luteal phase had positive VEGF immunoreactivity (Figure 4.6a and c), and intensity of staining was fairly uniform throughout each corpus luteum. Both the number of immunopositive steroidogenic cells and the uniformity of staining decreased as the luteal phase proceeded, so that by luteal day 18 scattered immunopositive cells had weak to intense staining (Figure 4.6d and e). After

progesterone values had fallen to follicular phase values, however, intensity of staining appeared to increase, although the volume of steroidogenic cells also decreases at this time and staining intensity appeared to increase as amount of cytoplasm decreased (Figure 4.6f and g). The number of immunoreactive steroidogenic cells increased 12 hours after luteolysis was induced with either PGF2α or GnRH antagonist (Figure 4.7c and d respectively), but decreased to levels simular to those seen in spontaneously regressing corpora lutea 24 hours after luteolytic treatment (Figure 4.7e and f)

4.1.6.1 A Receptor for VEGF, Flt-1.

Only two sections showed positive staining for Flt-1, the naturally regressing corpus luteum collected on day 18 of the luteal phase, and the corpus luteum collected 12 hours after regression was induced with GnRH antagonist. Flt-1 immunoreactivity was expressed exclusively in large blood vessels within the corpus luteum. Flt-1 immunoreactivity was not found in marmoset corpora lutea at any other stage of the luteal phase, and neither was it found in mid luteal phase human tissue. Flt-1 immunoreactivity was also absent from negative control sections.

Figure 4.5: Vascular Endothelial Growth Factor (VEGF) Immunolocalisation in Mid Luteal Phase Marmoset Corpus Luteum.

Ovary obtained on luteal day 10 and steroidogenic cell cytoplasm shows brown VEGF immmunoreactivity. Cell nuclei counterstained with haematoxylin. Inset is the antibody negative control serial section for the main picture. Scale bar represents 20μm.

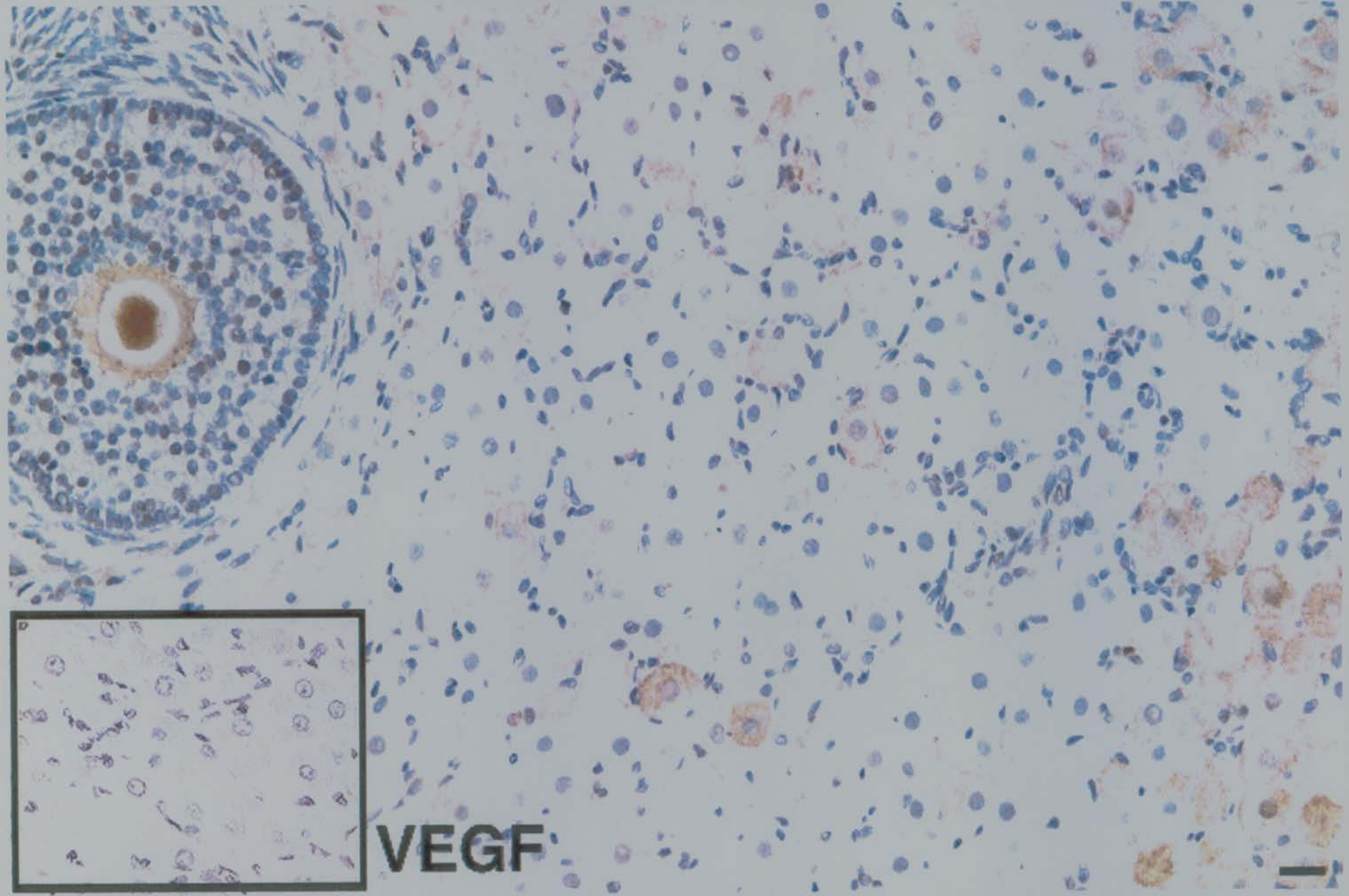
VEGF

Figure 4.6: Vascular Endothelial Growth Factor (VEGF) Immunolocalisation Throughout the Luteal Phase of the Marmoset.

Luteal days 2-5 are shown in (a) and (c), (b) is a serial section of (a) and is a representative example of antibody negative control sections. Luteal day 18 demonstrating functional luteal regression is shown in (d) and (e). (f) and (g) were obtained on luteal days 22-25 and are examples of structural luteal regression. (h) is the antibody negative control serial section of (g) and shows luteal tissue surrounded by developing follicles. Each picture is from a different animal, unless otherwise stated. VEGF immunostaining is pink-red, and scale bars represent 20μm.

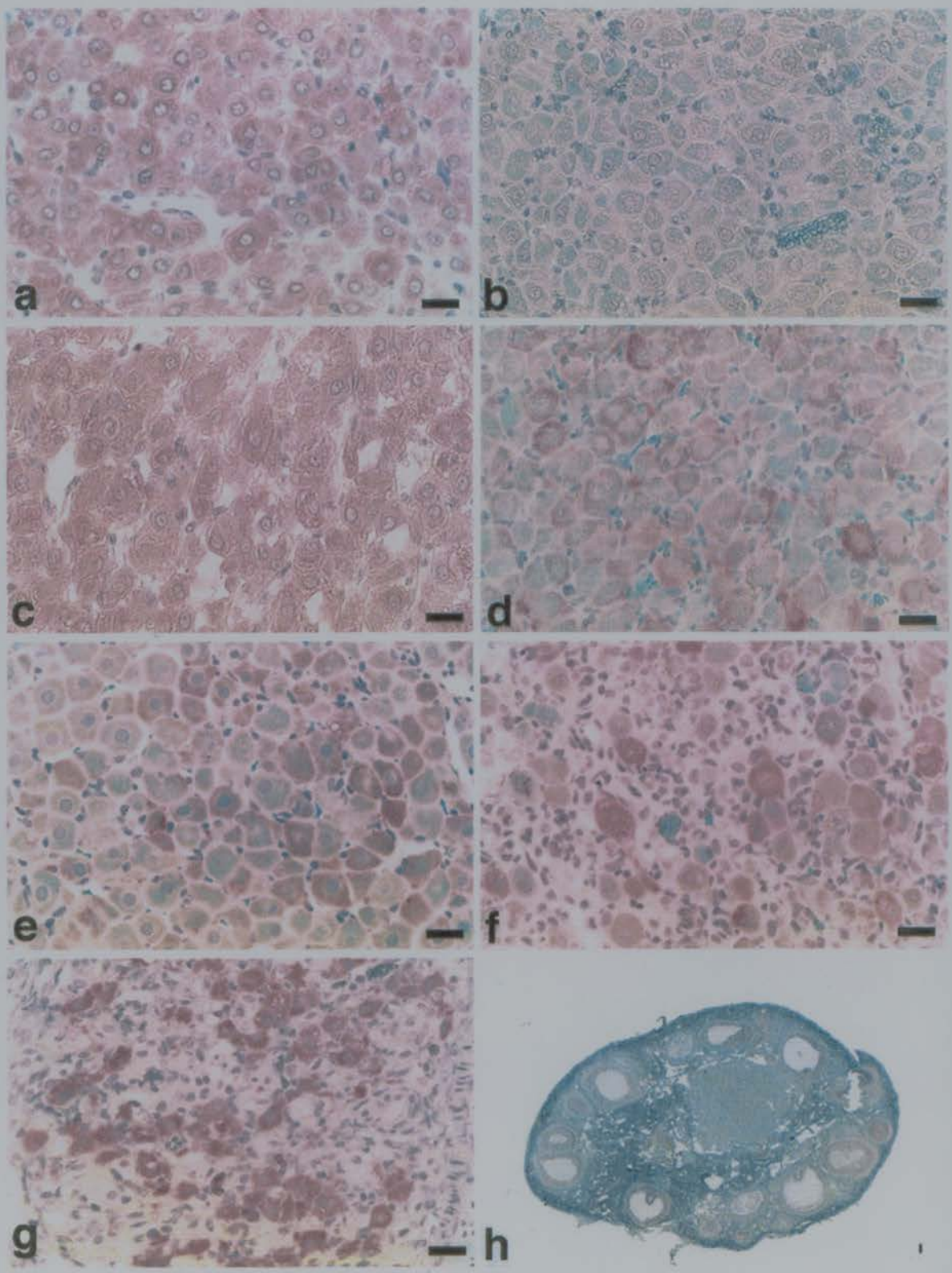
a
b
c
d
e
f
g
h

Figure 4.7: Vascular Endothelial Growth Factor (VEGF) Immunolocalisation During Induced Luteal Regression.

Ovaries collected on (a) luteal day 10, (b) antibody negative control serial section of (d). The corpus luteum shown in panel (c) was obtained 12 hours after PGF2α analogue and (d) shows luteal tissue 12 hours after GnRH antagonist. (e) and (f) are corpora lutea collected 24 hours after in vivo administration of PGF2α and GnRH antagonist respectively. Specific VEGF immunostaining is red-brown and is localised to the cytoplasm of luteal steroidogenic cells, and to oocytes. Scale bars represent 20μm.

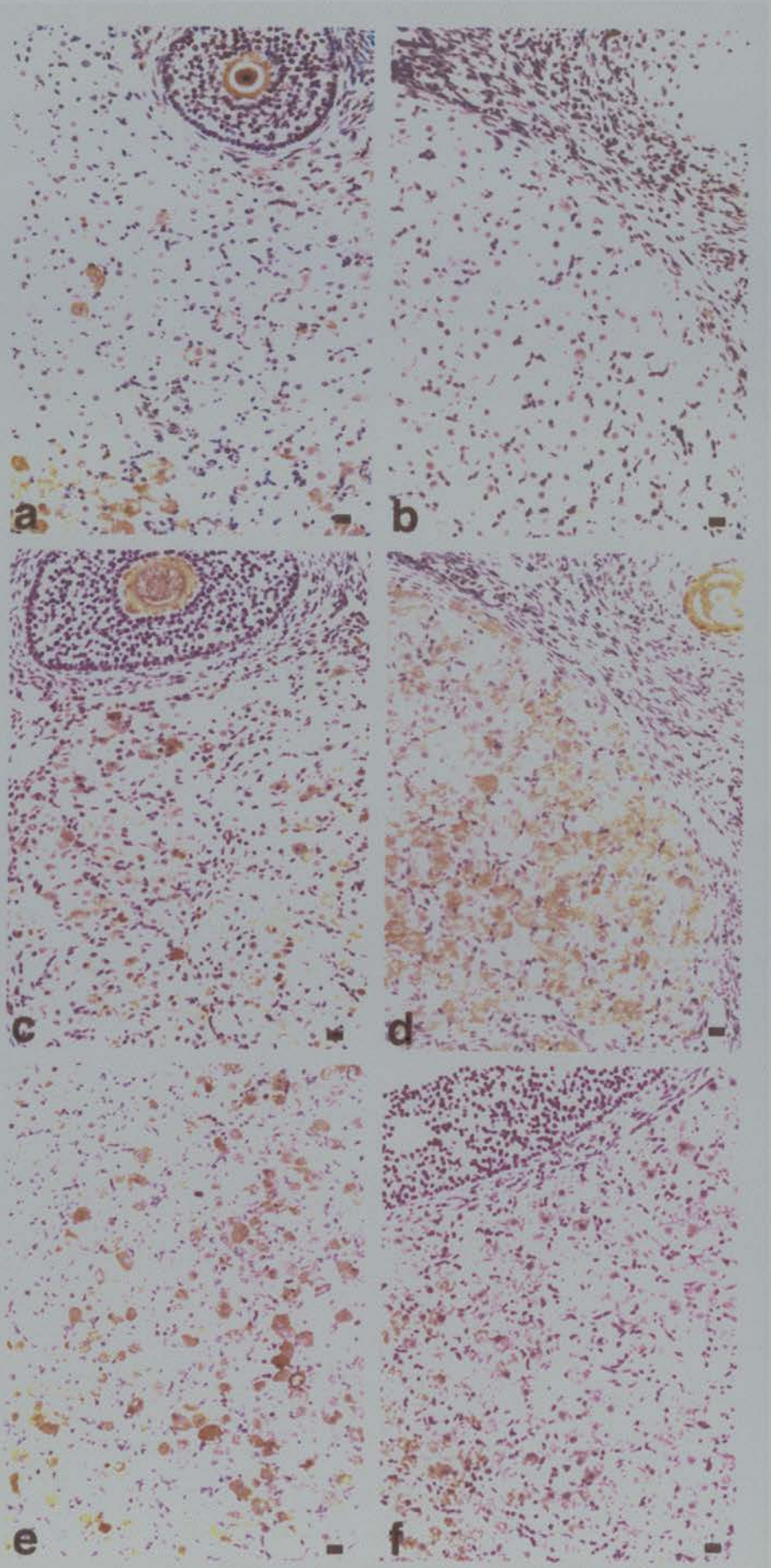
a
b
c
d
e
f

4.2 Discussion

This study has demonstrated for the first time that there are structural changes in the vasculature during the luteal phase of the primate, and has determined the temporal and morphological distribution of proliferating cells in the marmoset corpus luteum, particularly during luteal regression.

4.2.1 Comparison of Nonsteroidogenic and Endothelial Cell Numbers in Corpora Lutea.

The proportion of non-steroidogenic cells in marmoset corpora lutea is lower than in other species. During the mid luteal phase 69±0.7% and 60±0.3% of all luteal cells are non-steroidogenic in human and bovine corpora lutea respectively (Lei *et al.*, 1991), but at the equivalent time in the marmoset luteal phase non-steroidogenic cells comprise 48±3% of the corpus luteum. Lei *et al* (1991) found that the proportion of non-steroidogenic cells increases by approximately 20% as luteal regression proceeds, and we found an increase of the same order during spontaneous luteal regression in the marmoset. Changes in the vasculature after induced luteal regression, however, were different from those observed in naturally regressing corpora lutea. Administration of GnRH antagonist resulted in an initial reduction in nonsteroidogenic cell numbers to 36±7% twelve hours after the treatment followed by an increase to 47±10% 24 hours after the treatment, similar to the proportion of non-steroidogenic cells which is found in untreated luteal day 10 corpora lutea. There was no change in the proportion of non-steroidogenic cells 12 or 24 hours after administration of PGF2α.

The percentage area of luteal section immunopositive for von Willibrand Factor VIII, a specific endothelial cell marker, followed the same pattern as non-steroidogenic cell numbers in naturally regressing corpora lutea, both numbers increased as spontaneous regression proceeded. The area of vW immunopositivity increased significantly, however, both 12 and 24 hours after administration of GnRH antagonist. There are two possible explanations for this situation in which the percentage of non-steroidogenic cells remained constant but the area of endothelial cell-specific staining increased; (1) The percentage of non-steroidogenic, non-

endothelial cells such as macrophages or fibroblasts decreased, so that a greater proportion of the non-steroidogenic cells counted were endothelial cells and (2) the area occupied by individual endothelial cells increased, perhaps owing to decreased numbers of steroidogenic cells.

4.2.2 Effects of Administration of Luteolytic Agents on Luteal Vasculature.

The administration of luteolytic agents did not appear to have major effects on luteal vasculature. The significant increase in the area of vW immunoreactive staining after administration of GnRH antagonist can probably be attributed to the dynamics of shrinking tissue. In this scenario the steroidogenic cells died as a result of GnRH antagonist induced LH-depletion, and blood vessels were therefore able to move closer together thus resulting in increased numbers of blood vessels in each unit area. There was also a slight, non-significant increase in the area of vW immunostaining after administration of PGF2α, and this was of a similar order to that seen during spontaneous regression. Increases in endothelial cell numbers can be attributed partially to the remaining blood vessels moving closer together as the regressing luteal tissue decreases its size, but increases may also be due to proliferation of endothelial cells, so it would be advantageous to study rates of cell proliferation in order to differentiate between these two effects.

PGF2α has no effect on luteal blood flow (Bruce and Hillier, 1974), and the absence of change to non-steroidogenic or endothelial cell numbers after administration of PGF2α supports the hypothesis that the luteolytic effect of PGF2α is not mediated directly by changes to the vasculature, and also leaves open the possiblility that PGF2α acts by stimulating the production of oxygen free radicals. In fact PGF2α may have a number of overlapping luteolytic effects. It may initially instigate functional luteal regression by stimulating the generation of hydrogen peroxide in the corpus luteum (Riley and Behrman, 1991) which may trigger off a cascade of oxygen free radical reactions which inhibit steroidogenesis in a very short period of time. Hydrogen peroxide also induces partial endothelial cell detachment (Bradley *et al.*, 1995), and endothelial cell detachment has been observed during early luteal

regression in ruminants. PGF2α also stimulates luteal endothelial cells to produce endothelin-1, which in turn stimulates vasoconstriction. In addition, PGF2α stimulates bovine luteal steroidogenic cells to produce oxytocin, which further stimulates endothelial cell production of endothelin-1 in a feedback mechanism (Girsh *et al.*, 1996). The combination of vasoconstriction and vascular occlusion afforded by endothelial protrusion into vascular lumina may create hypoxic conditions which contribute to progressive degeneration of the parenchymal steroidogenic cells. In addition to this, Modlich *et al* (1996) found that late luteal regression was effected partially by proliferation of myofibroblastic cells which could cause contraction of the microvasculature. It would therefore be interesting to determine whether proliferation of myofibroblasts occurs during the later stages of luteal regression in the primate.

4.2.3 Morphology of Marmoset Luteal Vasculature.

Immunocytochemistry for vW indicated that during the early and mid luteal phase vascular morphology was consistent with an extensive network of fine capillaries with a high surface area to volume ratio. During luteal regression, however, the area of vW immunostaining decreased while the volume occupied by the vasculature increased, and this apparent contradiction was probably caused by a change in the vasculature from a capilliary network to a lower number of relatively large blood vessels with a low surface area:volume ratio. This was further supported by data indicating that the number of blood vessels per unit area also decreased during structural luteal regression. This data was based on the assumption that each distinct area of vW immunopositive staining represented one blood vessel. Clearly this assumption is inaccurate; the same blood vessel may intersect the histological plane of section any number of times. In addition, it is possible that some endothelial cells may have been vW immunonegative, and this would lead to an underestimation of the amount of vasculature present. However, these inaccuracies would probably have been constant in all the experimental groups, and these data therefore support the hypothesis that there is an initial period of angiogenesis during formation of the corpus luteum, then a period of vascular regression during late functional and early

structural regression, followed by a second period of angiogenesis during structural luteal regression. This appears to result in the formation of larger blood vessels which are suitable for channelling away the cellular debris of structural luteal regression.

Luteal regression in ovine and bovine corpora lutea involves detachment of the endothelial cells from vascular basal lamina, and the occlusion of capillaries with cellular debris. This does not seem to occur to the same extent in marmoset corpora lutea, although it is important to equate the precise time in the luteal phase that capillary occlusion occurs in ruminant corpora lutea with the equivalent time-point in the marmoset luteal phase. The average ovine reproductive cycle is 16.5±0.1 days (Deane *et al.,* 1966). The oestrus, or 'follicular phase' (although in ruminants follicles develop throughout the luteal phase) when progesterone concentrations are at basal levels, begins on Day 0, and ovulation occurs 24 hours later at the beginning of Day 1. Functional luteal regression is therefore completed 16.5 days later. Progesterone values start decreasing on Day 14 (O'Shea *et al.,* 1977), and pronounced morphological changes are also seen at this time; ovine corpora lutea collected on days 14 and 15 of the oestrous cycle had many blood vessels containing cellular debris. Marmoset reproductive cycles are far more variable, both between animals and between the cycles of the same animal, but for the sake of this comparison it can be assumed that it is a 30 day cycle with a 10 day follicular phase and ovulation occurring on the morning of day 11, or day 1 of the luteal phase. Progesterone concentrations begin to decrease from luteal day 14, simular to sheep, but do not fall to follicular phase values until day 19 or 20, therefore functional luteal regression occurs during a period of 2 days in the sheep, and during a period of 4-6 days in the marmoset. Although some structural changes have been observed in human corpora lutea on day 14 of the luteal phase, marmoset corpora lutea have not been subjected to morphological examination at this stage of the luteal phase, however corpora lutea collected on day 18 do show some morphological changes indicative of regression; lower steroidogenic cell volume compared to that seen at luteal day 10 and a slight non-significant increase in the number of apoptotic cells and an increased numbers of steroidogenic cell cytoplasmic lipid droplets. However, vascular changes are not obvious, and there is certainly no widespread distribution of

blood vessels containing large quantities of fragmented cellular debris as there is in ovine corpora lutea. Marmoset corpora lutea collected on luteal days 22-24 after progesterone had fallen to follicular phase values tended to have dilated or relatively large blood vessels which did not contain cellular debris, but again there was no evidence of large numbers of occluded capillaries.

Vascular thrombi were found slightly more frequently after induction of luteolysis with PGF2α or GnRH antagonist, and marmoset corpora lutea collected 24 hours after induction of luteolysis may be considered analogous to ovine corpora lutea collected on day 16, but even these did not display vascular occlusion to the same extent as is seen in ovine corpora lutea. Of course it is not surprising to find that primate corpora lutea are different from ruminant corpora lutea, and these species differences appear to be related to the length of time available to remove luteal tissue. The ovine 'follicular phase' is a mere 24 hours, during which time structural luteal regression has to be essentially complete in order that there be room for a subsequent corpus luteum, whereas the regressing marmoset corpus luteum can complete structural regression during the 10 days of the follicular phase. In sheep, functional and structural luteal regression appear to proceed simultaneously, in cows there is some overlap between functional and structural regression, but not as much as in the sheep, and in the primate the two phases are essentially separated. It is interesting that although functional regression appears to always precede structural regression, it does not seem necessary to complete functional regression before structural regression can proceed, and that the relationship between functional and structural regression within each species can be quite flexible. Functional regression appears to be largely completed before structural regression begins in spontaneously regressing marmoset corpora lutea. Marmoset corpora lutea collected 12 hours after induction of luteolysis, however, had falling progesterone values indicating that functional regression was in progress, and also had regressive morphological changes indicating that structural luteolysis was occurring at the same time.

4.2.4 Vascular Endothelial Growth Factor in the Corpus Luteum.

Blood flow to the corpus luteum is higher than to any other organ in the body, and this high blood flow is related to the steroidogenic capacity of luteal tissue. Therefore it is interesting to find that VEGF is highly expressed in the early marmoset corpus luteum, and also that gonadotrophins upregulate VEGF (Laitinen *et al.*, 1997; Shweiki *et al.*, 1993; Christenson and Stouffer, 1997), suggesting that luteal formation concomitant with upregulated VEGF is one mechanism for ensuring a blood supply sufficient for maintenance of luteal steroidogenesis. Steroidogenic cell VEGF immunoreactivity in marmoset corpora lutea decreases with increasing luteal age, and LH pulsitility also slows with increasing luteal age (Soules *et al.*, 1984), so it would be interesting to determine the effects of LH on VEGF expression in luteal tissue *in vivo*. However the finding that VEGF expression is maintained 12 hours after administration of GnRH antagonist suggests that LH does not regulate VEGF. In addition to this, the lifespan of primate corpora lutea is not prolonged by experimentally maintaining early luteal phase LH pulsitility throughout the late luteal phase, so it is unlikely that reduced luteal blood flow caused by LH downregulation of VEGF expression is a mechanism for instigating functional luteal regression under normal conditions *in vivo*.

VEGF secretion is also increased by hypoxia in human granulosa cells luteinised *in vitro* (Friedman *et al.*, 1997) which suggests that expression of VEGF during functional luteal regression in the marmoset corpus luteum may be due to upregulation by hypoxic conditions, and that VEGF upregulation in the non-steroidogenic corpus luteum of regression may stimulate the formation of large blood vessels which become a means of removing the detritus of structural luteal regression.

The majority of steroidogenic cells in the early luteal phase express VEGF, and it was hypothesised that VEGF-expressing steroidogenic cells contribute to the angiogenic activity which occurs during the early luteal phase and results in extensive capilliarisation of the corpus luteum. In order for VEGF to have an angiogenic effect, it was presumed that luteal endothelial cells would have to express a receptor for VEGF, however a preliminary study of the VEGF receptor, Flt-1, did

not find any expression at all in two early luteal phase corpora lutea, although positive Flt-1 immunoreactivity was found in the large blood vessels of one late luteal phase corpus luteum, and also in another corpus luteum collected 12 hours after administration of GnRH antagonist. Since Flt-1 immunoreactivity was not found in the positive control human luteal section, nor in the two early luteal phase marmoset corpora lutea, it was assumed that technical procedures were inadequate and the study was discontinued. However, retrospectively it was considered that human mid phase corpora lutea might not express Flt-1, and Flt-1 might only be expressed in large blood vessels during functional luteal regression, therefore it is possible that further investigation of the temporal and morphological distribution of Flt-1 would yield interesting results.

Flt-1 is one of three VEGF receptors, so although Flt-1 has not yet been demonstrated in early luteal phase tissue, it is also possible that one of the other receptors, most likely Flk-1/KDR, may mediate the angiogenic effects of VEGF in the early corpus luteum (Lee *et al.,* 1996). Flt-1 is upregulated by hypoxia (Gerber *et al.,* 1997; Sandner *et al.,* 1997), so if it proves to be expressed in the late luteal phase, its presence would support the hypothesis that hypoxic conditions exist in regressing corpora lutea.

4.2.5 Summary

In summary, endothelial cell numbers appear to be highest in the early luteal phase. Since endothelial cell proliferation occurs at a higher rate than cell death from the early to the mid-luteal phase, this result may have been influenced by changes in the volume of individual steroidogenic cells. Steroidogenic cells in newly formed corpora lutea are in the initial stages of hypertrophy, and therefore have lower volumes than mid luteal phase steroidogenic cells. Since the steroidogenic cells utilise less space in the early luteal phase, the number of endothelial cells in each unit area appears to be higher than in mature luteal tissue.

The number of endothelial cells remains constant during the mid luteal phase and during functional luteal regression, but appears to increase during structural luteal regression. Observed increases in endothelial cell numbers may be due to either (a)

the dynamics of shrinking tissue during which parenchymal steroidogenic cells are lost and blood vessels move closer together which results in a higher number of endothelial cells in each unit area, or (b) proliferation of endothelial cells. Examination of cell proliferation during luteal regression is therefore necessary in order to determine the relative importance of these two effects.

The number of individual blood vessels appears to be highest during the luteal phase, but again, this is probably an artifact of the scoring system bought about by the dynamics of expanding tissue. The number of capillaries falls to a baseline by luteal day 7 when the corpus luteum has reached a mature form. There is then a slight, nonsignificant increase in the number of capillaries per unit area as the luteal phase proceeds and also during functional regression. During structural luteal regression, however, there is a marked decrease in the number of individual blood vessels, and this occurs at the same time as the observed increase in individual endothelial cell numbers.

4.2.6 Conclusions.

It is possible to draw two main conclusions about luteal vasculature in the marmoset. (1) Morphological changes in luteal vasculature do not precede functional luteal regression in marmoset corpora lutea and (2) the vasculature changes from an extensive network of fine capillaries during the luteal phase to a vascular system comprised of lower numbers of larger microvessels during structural luteal regression.

Chapter 5: Proliferation in the Corpus Luteum of the Marmoset Monkey.

5.0 Introduction

Luteal regression is essentially a process of cell loss and tissue shrinkage, therefore it appears counter-intuitive to examine cell proliferation in this context, since increasing cell numbers would clearly retard the removal of luteal tissue. However, examination of the vasculature during luteal regression indicated an increase in endothelial cell numbers during structural luteal regression. It was not clear, whether the increase was due to an artefact of the counting system, whereby blood vessels in shrinking tissue moved closer together to gove an artifactual increase in endothelial cell numbers for each unit area, or if the increase was due to endothelial cell proliferation. In addition, the vasculature changed from a network of fine capillaries during the luteal phase to a system of larger arterioles and venules during luteal regression, and this vascular shift could require both cell death to remove capillaries and cell proliferation to form larger vessels. It is therefore important to characterise the rates of proliferation of different cell types within the corpus luteum, and to determine proliferative rates prior to and during luteal regression.

5.0.1 Evaluation of Proliferation

Analysis of proliferation depends on assessment of the number of cells undergoing mitosis in a given population, but mitosis is completed in approximately five minutes, so the likelihood of observing mitotic spreads in histological sections is very low. In electron micrographs of ovine corpora lutea, only one mitotic figure was observed amongst 3548 nuclei examined in a mid luteal phase corpus luteum (O'Shea *et al.,* 1986). However, there are a number of more sensitive methods commonly used for evaluating proliferation, and they all exploit various aspects of the cell cycle.

Figure 5.1: The Cell Cycle

(Adapted from Gerdes *et al.* 1984)

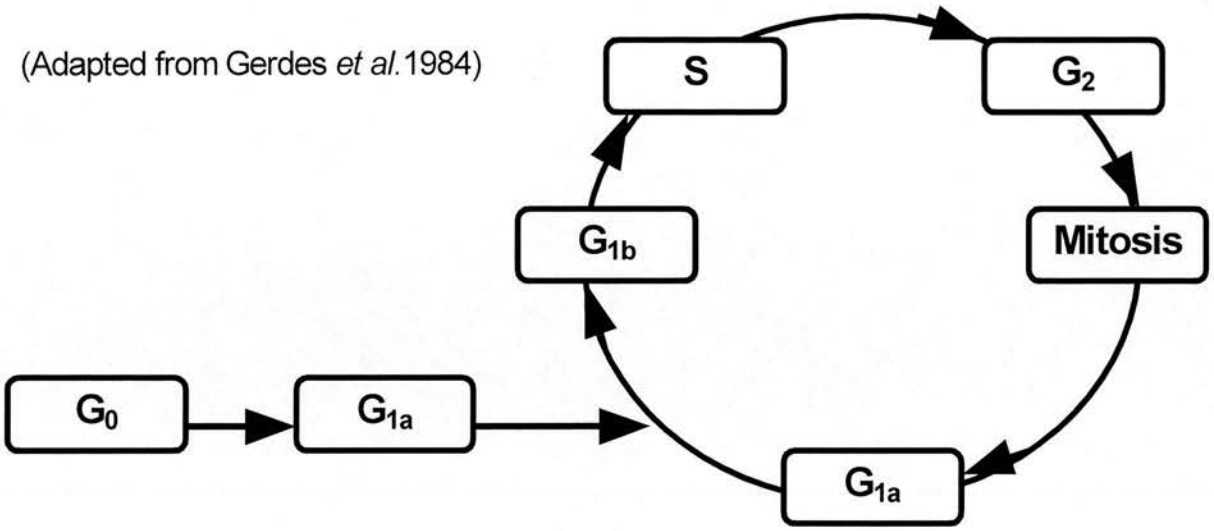

The cell cycle has a period of intense DNA synthesis, the S phase, which can take 7 to 12 hours to complete. This is followed by a post-synthetic gap (G_2) of 1 to 6 hours in length during which the cell undergoes growth and prepares for mitosis. The next phase, mitosis, takes a maximum of two hours to proceed through prophase, metaphase, anaphase and telophase. During the subsequent post-mitotic gap (G_1) cells recover from mitosis and grow to an optimal size. The G_1 phase can be of variable length, and it is also at this stage of the cycle that cells can enter a fifth phase, (G_0), during which they are not actively proliferating. This is considered to be a resting phase in which cell status does not change. Specific proliferative stimuli can cause some cells to re-enter the cell cycle in a state equivalent to the early part of the post-mitotic gap phase (G_{1a}) whereas other cells lose their proliferative competency and never re-enter the cell cycle. Cells permanently in the Go phase are often terminally differentiated (Boulton and Hodgson, 1995).

Quantification of the number of cells in the S or M phase does not give an accurate picture of the overall dynamics of proliferation for a particular tissue, because the duration of these stages may vary between cell types, and with proliferative rate. A complete description quantifies the proportion of the total cell population that is in the S or M-phase, and also quantifies the rate at which cells enter and leave the cell cycle (Boulton and Hodgson, 1995: Sasaki *et al.*, 1988). The higher the proportion of cycling cells in the S-phase, the shorter is the cell cycle for that particular population

of cells. The percentage of the total population of cells that is cycling is known as the growth fraction.

5.0.2 Methods for Assessing Cell Proliferation

DNA synthesis occurs before mitosis, and some methods for assessing proliferation utilise substances which are incorporated into DNA during synthesis *in vivo*, and are then subsequently visualised *ex vivo*. Tritiated thymidine [3H] can be incorporated into newly synthesised DNA in place of thymidine, and can be recognised by autoradiography or by fluorescence-activated cell sorting (FACS) techniques (Boulton and Hodgson, 1995). Bromodeoxyuridine, a modified pyrimidine analogue which is a halogenated derivative of thymidine, can likewise be incorporated into new DNA in place of thymidine. It can then be visualised using standard immunocytochemical techniques which utilise a specific monoclonal antibody raised against bromodeoxyuridine (Boulton and Hodgson, 1995). These two methods have the advantage of labelling proliferating cells *in vivo,* and only the visualisation steps are completed after death or removal of the tissue from the organism being studied. The number of cells labelled using these techniques depends upon the amount of time the DNA nucleotide replacement substance was available to be incorporated into newly synthesised DNA and this in turn is dependent upon the initial concentration and the clearance rate of the substance being used. The number of labelled cells increases as the amount of time between administration of the label and collection of the tissue increases. 'Pulse' labelling occurs when the labelling period is shorter than the duration of the S-phase for the cell population concerned, so that only cells which are in the synthetic phase are labelled (Boulton and Hodgson, 1995). Additional methods for evaluating proliferation detect proteins ostensibly expressed exclusively by proliferating cells, with detection by standard immunocytochemical means. The Proliferating Cell Nuclear Antigen (PCNA) is a 36 kDa acidic nuclear auxiliary protein for DNA polymerase δ which has also been identified as 'cyclin'. The PCNA-DNA polymerase δ complex is required for cell division, hence PCNA is a marker for proliferation. PCNA has a relatively long half life of up to 20 hours (Diebold *et al.*, 1994), and its expression increases during G_1, then peaks during the

S-phase before decreasing during G_2 (Boulton and Hodgson, 1995). PCNA immunoreactivity occurs in the nuclei of proliferating cells but non-specific cytoplasmic staining is also common (Wolf and Dittrich, 1992; Sabattini *et al.*, 1993). The intensity of nuclear staining can be very variable and it has been suggested that nuclei with weak PCNA immunopositivity may have left the cell cycle and be quiescent, but still contain residual amounts of PCNA (Sabattini *et al.*, 1993).

Ki67 antigen is a nuclear non-histone short lived protein which appears in a reticulate structure surrounding the anaphase chromosomes, but which can be detected throughout mitosis (Gerdes *et al.*, 1984). Ki67 has a half life of less than one hour (Bruno and Darzynkiewicz, 1992) and is expressed in all phases of the cell cycle except the early part of G1, and Go. Gerdes *et al* (1984) showed that cells moving from Go to G1 are not Ki67 positive, but in subsequent cycles cells are Ki67 positive during the entire G1 phase. Ki67 antigen also disappears when proliferating cells are induced to differentiate into resting cells (Gerdes *et al.*, 1983) and this suggests that Ki67 is expressed by cycling cells in G1, but not by cells in G1 which are about to enter or which have just left the Go phase of the cell cycle.

5.0.3 Comparison of Ki67, Tritiated Thymidine, Bromodeoxyuridine and PCNA.

The appearance of Ki67 antigen closely paralleled the uptake of tritiated thymidine in peripheral mononuclear blood lymphocytes (PBL) stimulated to proliferate by the addition of phytohemagglutinin A (PHA). In this study (Gerdes *et al.*, 1983) 9.9% of cells were Ki67 positive but negative for tritiated thymidine ([3H]) and 1.3% Ki67 negative but [3H] positive. These data were explained as indicating that 9.9% of the cells were in the G1 or G2 phase of the cell cycle, and that 1.3% of the cells had been labelled during the S phase but had subsequently become quiescent and no longer expressed the Ki67 antigen. The majority of Ki67 positive cells, however, were also [3H] positive.

PCNA immunocytochemistry (ICC) consistently labelled more cells than Ki67 ICC did in the same tissue samples (Sabattini *et al.*, 1993; Jones *et al.*, 1994). It was

suggested this may be due to PCNA having a longer half life than Ki67. Likewise, Ki67 labelled more cells than BrdU in specimens of malignant tumours. In this study (Sasaki *et al.,* 1988), Ki67 immunocytochemistry was carried out on cryostat sections of the tumours, but Brd U incorporation occurred during a 60 minute period of *in vitro* culture of the same tumour specimens, and no control was included to determine the effect of *in vitro* culture on rates of DNA synthesis. However, since Ki67 is expressed during three phases of the cell cycle, and BrdU is only incorporated during the S-phase of the cell cycle, the finding that more cells were Ki67 positive than were BrdU positive was probably correct. In addition, this study found that Ki67 and BrdU values paralleled each other, so that when one specimen had a high Ki67 index, it also had a high BrdU value, indicating that although these two methods gave different absolute proliferative indices, they also yielded the same relative values. Ki67 labels cells at all phases in the cell cycle, so gives a measure of the population of cycling cells, whereas pulsed BrdU only labels cells in the S-phase, so a comparison of Ki67 and BrdU results can give an indication of the proliferative rate of a particular tissue (Sasaki *et al.,* 1988).

5.0.4 Proliferation in Corpora Lutea

In ewes, following administration of 5mg/kg BrdU i.v. 1 hour before obtaining the corpora lutea, the percentage of BrdU labelled cells decreased exponentially as the corpus luteum aged (Jablonka-Shariff *et al.,* 1993). In this study, few BrdU positive cells were also 3βHSD immunopositive, the majority of BrdU positive cells were also Factor VIII positive, but a proportion of BrdU positive cells were neither steroidogenic nor endothelial cells. In bovine corpora lutea the percentage of PCNA positive luteal cells likewise decreased as the luteal phase progressed, and these proliferating cells were thought to be small parenchymal, fibroblast or endothelial cells, but not steroidogenic large luteal cells (Zheng *et al.,* 1994). In macaque ovary, Ki67 immunocytochemistry showed that in corpora lutea cell proliferation was also highest during the early luteal phase and proliferation decreased significantly during the late luteal phase when progesterone levels were falling and functional luteal regression was underway (Christenson and Stouffer, 1996). In these macaque corpora lutea 3βHSD

immunopositive steroidogenic cells were not Ki67 immunopositive at any stage of the luteal phase, but 85-95% of Ki67 immunopositive cells were colabelled with the endothelial cell marker, platelet endothelial cell adhesion molecule 1 (CD31). Another study of proliferation in human corpora lutea used CD34 as a specific endothelial cell marker. In this study the percentage of cells which were both CD34 and PCNA immunopositive decreased as the luteal phase progressed, but this study did not examine non-endothelial cell proliferation (McClure *et al.*, 1994). Rodger *et al* (1997) demonstrated that in human corpora lutea the number of Ki67 immunopositive endothelial cells was highest during the early luteal phase, had decreased to a basal level by the mid luteal phase and remained at this level during the initial stages of functional luteal regression and also during a simulated early pregnancy model. Numbers of Ki67 immunopositive parenchymal cells showed a simular pattern.

5.0.5 Aims

This study aims to quantify and identify cells undergoing proliferation in the marmoset corpus luteum, with particular emphasis on the changes associated with luteal regression. Proliferation will be examined by (i) immunolocalisation of the Proliferating Cell Nuclear Antigen (PCNA) (ii) immunolocalisation of Ki67 Antigen (Ki67) (iii) determining the temporal and morphological distribution of BrdU incorporation in spontaneously regressing corpora lutea and (iv) identifying BrdU positive cells by colabelling with the steroidogenic cell marker 3β hydroxysteroid dehydrogenase (3βHSD), or the endothelial cell marker von Willebrand Factor VIII Antigen (vW).

5.1 Results

5.1.1 PCNA Immunocytochemistry

The nuclei of some granulosa and theca cells in morphologically healthy follicles were PCNA immunopositive (Figure 5.2), whereas the number of PCNA immunopositive cells in atretic follicles was markedly lower, indicating that follicles on the same section as luteal tissue provided good internal positive and negative

controls. Nuclei in negative control sections were not PCNA immunopositive, but non-specific cytoplasmic staining was common, and interfered with quantification. There was only one immunocytochemical run examining spontaneously regressing luteal tissue in which the optical density of non-specific cytoplasmic staining was lower than the optical density of PCNA immunopositive nuclei, and quantitative data are shown for that run. Unfortunately two sections, one from the early luteal phase and one structurally regressing corpus luteum collected in the early follicular phase, were rendered unquantifiable by the procedure, hence resulting in an incomplete data set. The results from other PCNA ICC procedures conducted on spontaneously regressing corpora lutea, however, were consistent with those presented here.
Both steroidogenic and non-steroidogenic cell nuclei were PCNA immunopositive (Figure 5.2). Approximately 4% of the total number of PCNA-positive cells counted per field of view overlapped with another PCNA-positive nucleus.

5.1.1.1 Quantification of PCNA ICC

The number of PCNA immunopositive cells did not change significantly throughout the luteal phase nor during spontaneous luteal regression (Figure 5.3). However the general trend was that the number of proliferating cells was highest during the early luteal phase, lowest during the mid luteal phase, increased again during functional luteal regression and decreased during structural regression after progesterone had fallen to follicular phase values. The total number of PCNA positive cells likewise did not change significantly after administration of the luteolytic agents GnRH antagonist or PGF2α (Figure 5.4), and distinguishing between PCNA immunopositive steroidogenic and nonsteroidogenic cells also failed to reveal any significant changes after induced luteal regression. Interestingly, the number of PCNA immunopositive nonsteroidogenic cells was significantly higher 24 hours after luteolytic treatment with GnRH antagonist (82.5±2.7, n=4) than 24 hours after administration of PGF2α (41±3.16, n=4, $p<0.05$).

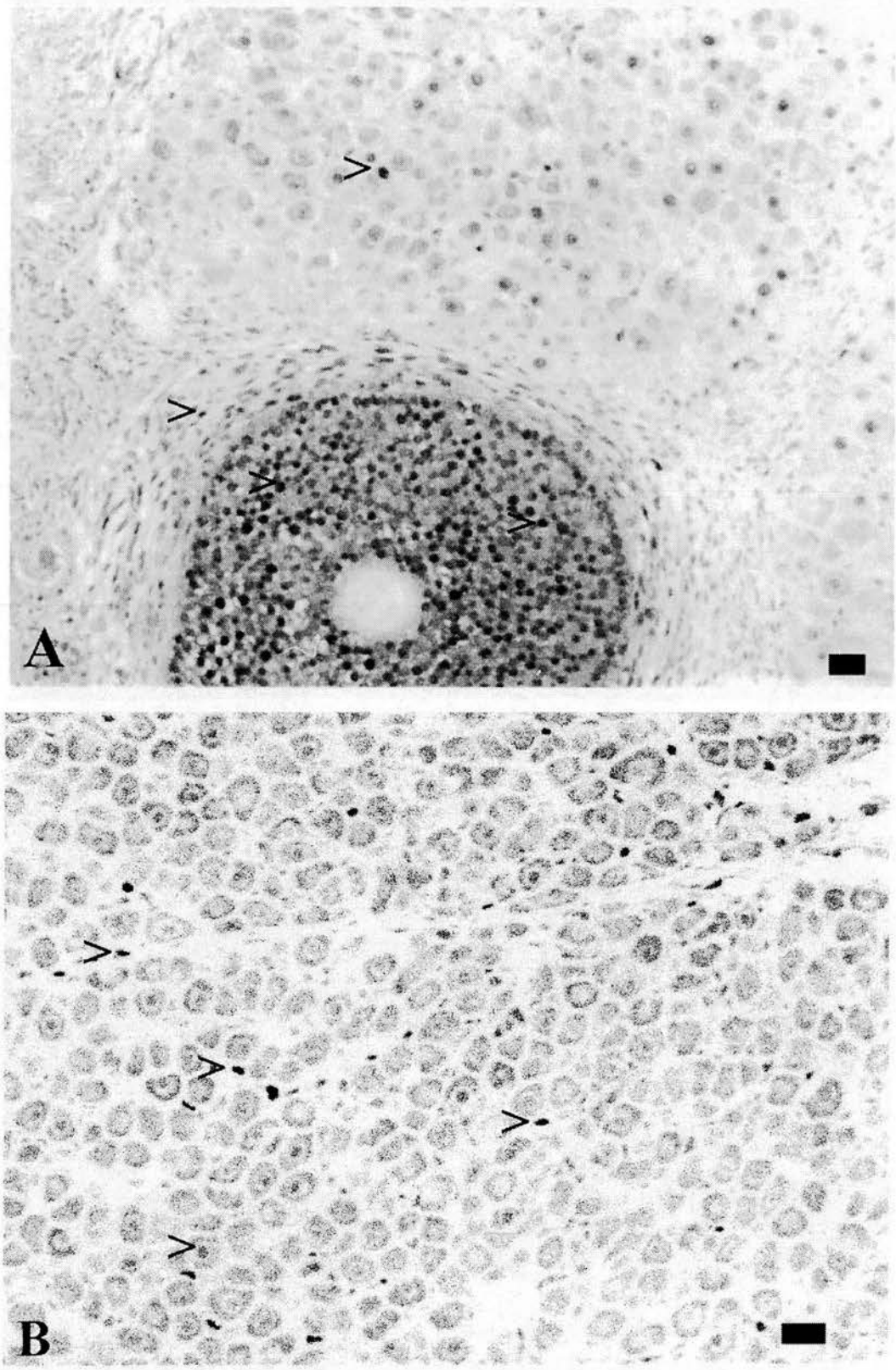

Figure 5.2: Proliferating Cell Nuclear Antigen (PCNA) Immunocytochemistry in a Marmoset Mid Luteal Phase Ovary.

Ovary collected on luteal day 10. A, luteal tissue in upper half, follicle comprising an outer layer of theca and an inner layer of granulosa cells in lower half of picture. B. Luteal tissue. Arrows indicate PCNA positive cells. Scale bars represent 20um.

Figure 5.3: Numbers of Proliferating Cell Nuclear Antigen (PCNA) Immunopositive Cells in Spontaneously Regressing Corpora Lutea.

Ovaries containing corpora lutea were collected on luteal days 2-5 (early, n=3), luteal day 10 (mid, n=4), luteal day 18 (functional regression, n=3) and luteal days 22-25 (structural luteal regression, n=3). The total number of PCNA immunopositive cells per 31400 μm^2 unit area were determined for each corpus luteum, and are shown as mean±SEM for each stage of the luteal phase. One way analysis of variance found no significant differences between means.

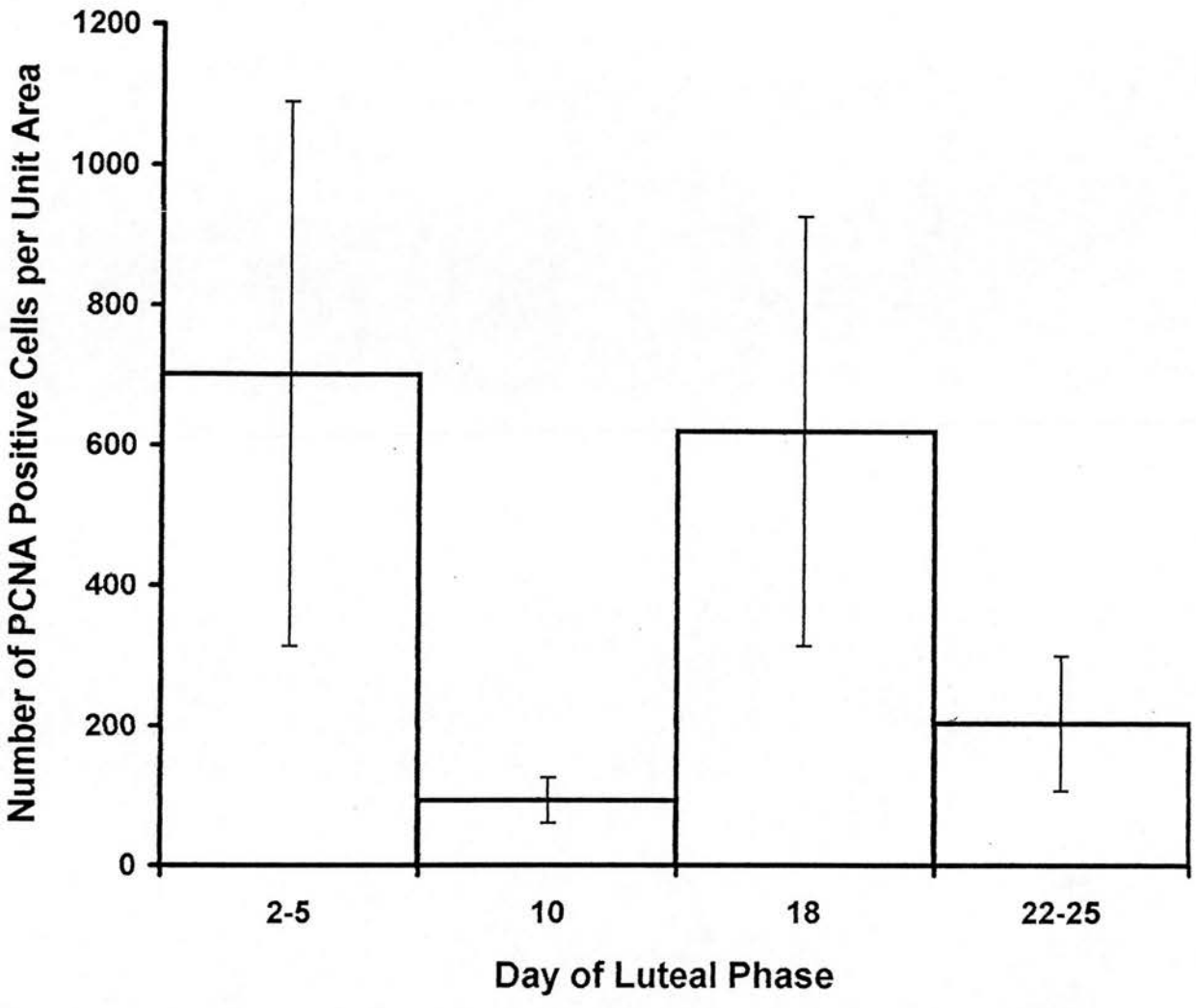
PCNA Positive Cells in Marmoset Corpora Lutea
Number of PCNA Positive Cells per Unit Area
1200
1000
800
600
400
200
0
2-5
10
18
22-25
Day of Luteal Phase

Figure 5.4: Numbers of Proliferating Cell Nuclear Antigen (PCNA) Immunopositive Cells in Corpora Lutea After Induced Luteal Regression.

Ovaries were collected on luteal day 10 (control, n=3), 12 hours (PG12, n=3) and 24 hours (PG24, n=4) after PGF2α analogue, cloprostenol, and 12 hours (Gn12, n=3) and 24 hours (Gn24, n=4) after GnRH antagonist, anterelix. The number of PCNA immunopositive steroidogenic (grey bars) or nonsteroidogenic (white bars) cells per 31400 μm^2 unit area were determined for each corpus luteum, and are shown as mean±SEM for each experimental group. Data were subjected to one way analysis of variance. The number of PCNA-immunopositive nonsteroidogenic cells 24 hours after induction of luteolysis with PGF2α was significantly different from the number of PCNA-immunopositive nonsteroidogenic cells 24 hours after administration of GnRH antagonist ($P<0.05$). There were no significant differences between any other groups

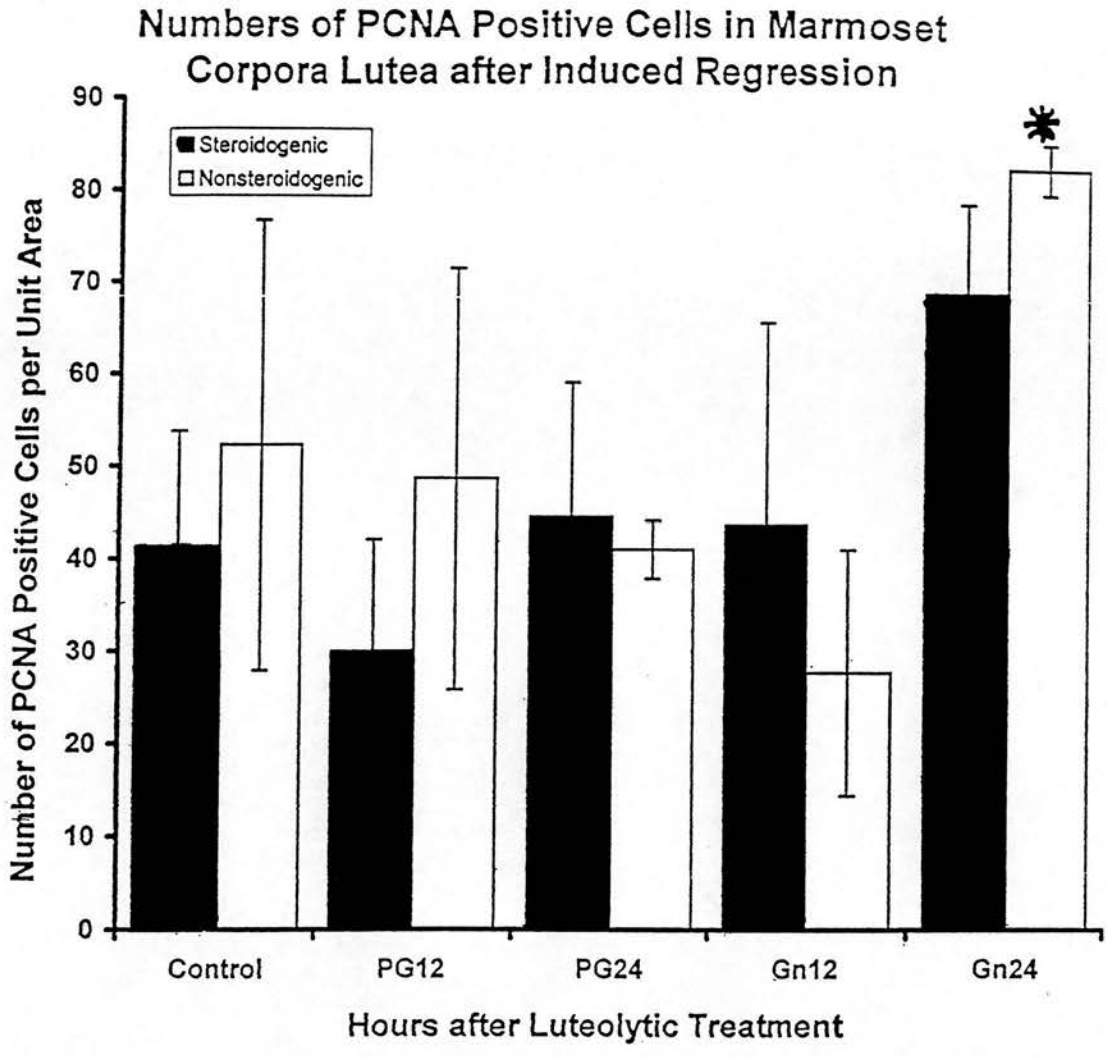
Numbers of PCNA Positive Cells in Marmoset Corpora Lutea after Induced Regression
Steroidogenic
Nonsteroidogenic
Number of PCNA Positive Cells per Unit Area
90
80
70
60
50
40
30
20
10
0
*
Control
PG12
PG24
Gn12
Gn24
Hours after Luteolytic Treatment

5.1.2 Ki67 Immunocytochemistry

The nuclei of some granulosa and theca cells in morphologically healthy follicles were intensely Ki67 immunopositive, whereas the number of Ki67 immunopositive cells in atretic follicles was markedly lower, indicating that follicles on the same section as luteal tissue provided good internal positive and negative controls (Figures 5.5 and 5.6). Nuclei in negative control sections were not Ki67 immunopositive, and cytoplasmic non-specific staining was low or entirely absent (Figure 5.5). Both steroidogenic and non-steroidogenic nuclei were immunopositive in all sections examined. Nonsteroidogenic cell nuclei had intense immunostaining, but the staining in steroidogenic cell nuclei was rarely as intense as in nonsteroidogenic cells and ranged from strong to very faint (Figures 5.5, 5.6 and 5.7). Some endothelial cells were Ki67 immunopositive in mid luteal phase corpora lutea (Figure 5.5), but the identity of Ki67 immunopositive nonsteroidogenic cells after induced regression was not as clear (Figure 5.6). A proportion of Ki67 immunopositive nonsteroidogenic cells in spontaneously regressing corpora lutea were found lining blood vessels, suggesting that they may have been endothelial cells (Figure 5.7C), but the rounded morphology of other Ki67 positive cells combined with non-vascular localisation (Figure 5.7D) suggests a different phenotype.

Figure 5.5: Ki67 Immunocytochemistry in Mid Luteal Phase Day 10 Corpus Luteum.

Marmoset ovarian section shows luteal tissue and a follicle. Ki67 immunopositive cell nuclei are pink to dark crimson red, and negative cell nuclei are counterstained blue with haematoxylin. Inset shows Ki67 antibody negative control, and scale bar represents 20μm.

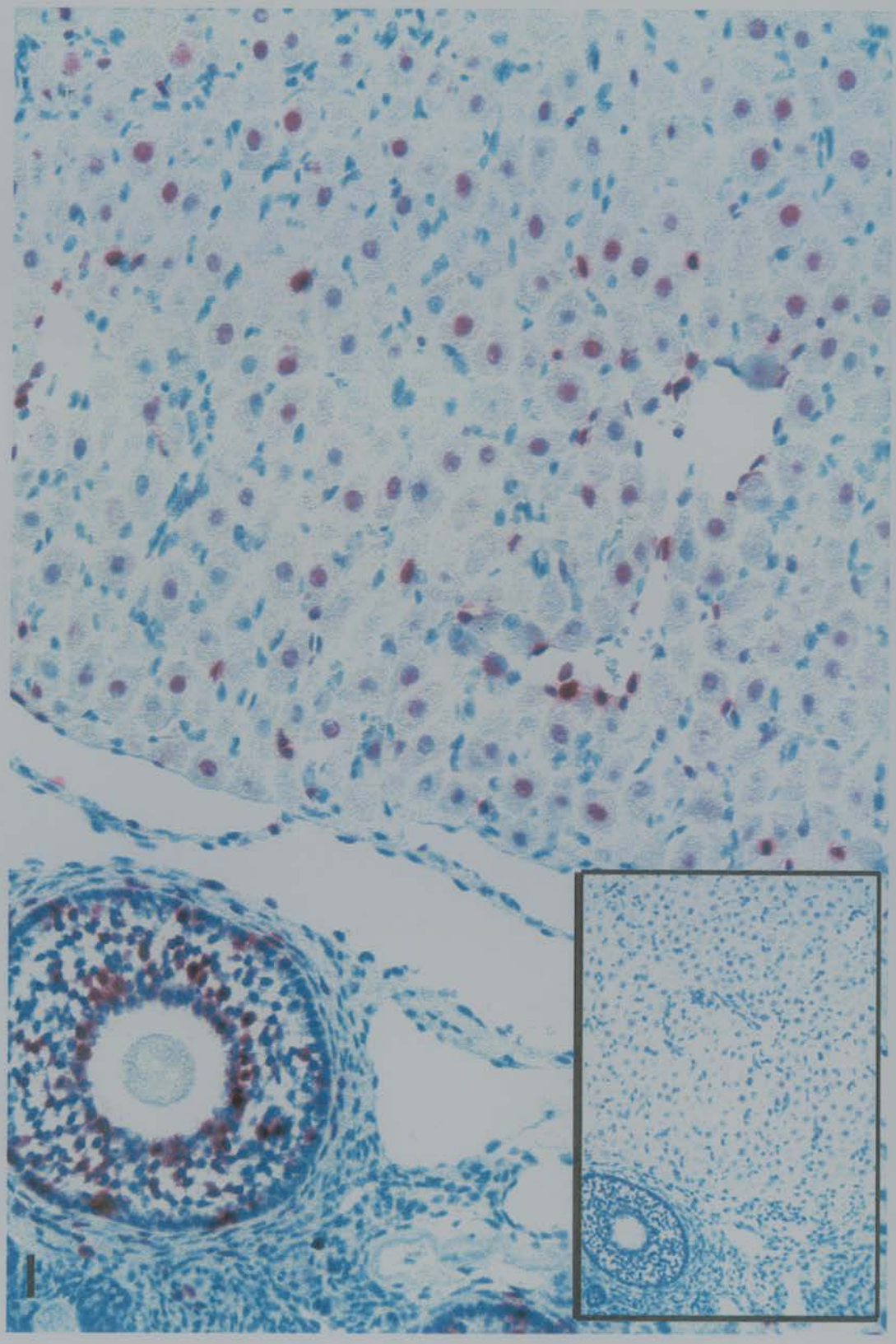

Figure 5.6: Ki67 Immunocytochemistry in Marmoset Corpus Luteum After Induced Luteal Regression.

Panels A and B show corpora lutea 24 hours and 12 hours respectively after *in vivo* administration of GnRH antagonist. Panels C and D show luteal tissue 24 hours and 12 hours respectively after treatment with PGF2α analogue. All ovaries were collected on luteal day 10. Each panel shows luteal tissue and follicular layers of theca and granulosa cells. Ki67 immunopositive cell nuclei are pink to dark crimson red, and immunonegative cell nuclei are counterstained blue with haematoxylin. Scale bars represent 20μm.

a
b
c
d

Figure 5.7: Ki67 Immunocytochemistry in Spontaneously Regressing Marmoset Corpora Lutea. Luteal tissue fixed in 4% paraformaldehyde and collected on A. luteal days 2-5, B. luteal day 10, C. luteal day 18 (functional luteal regression) and D. luteal days 22-25 (structural luteal regression). Insets show the same section at a lower magnification. Ki67 immunopositive cell nuclei are pink to dark crimson red, but immunonegative cell nuclei are not counterstained. Scale bars represent 20μm.

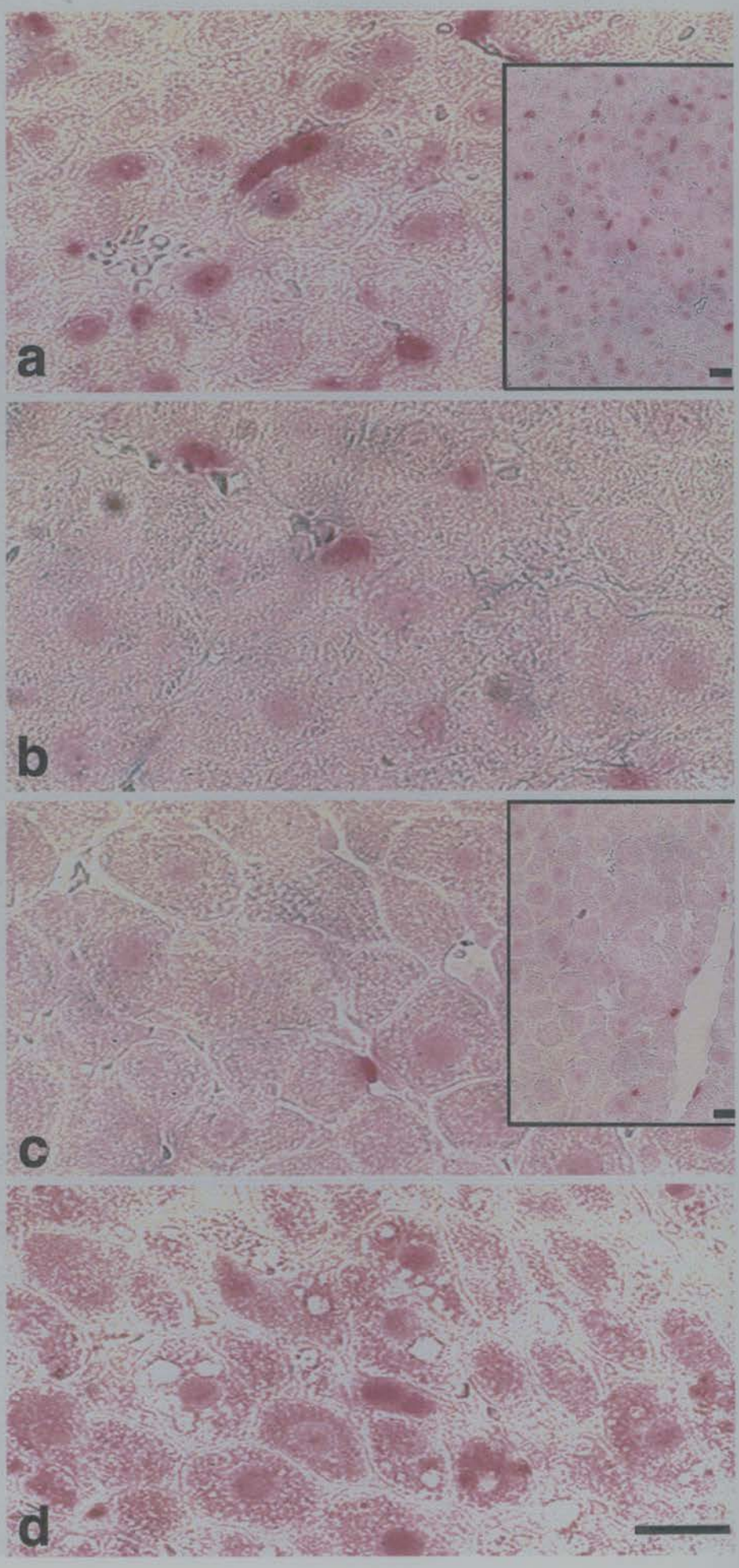
a
b
c
d

5.1.2.1 Quantification of Ki67 ICC.

The numbers of Ki67 immunopositive cells did not change during spontaneous luteal regression (Figure 5.8). The numbers of Ki67 immunopositive steroidogenic cells were constant during the early (10±1.4, mean±sem, n=4) and mid (10.25±3.5, n=4) luteal phases, but decreased markedly by luteal day 18 (4.3±0.7, n=3, Figure 5.8). The numbers of Ki67 immunopositive steroidogenic cells increased to 11.1±4 (mean±sem, n=3) during structural luteal regression. The number of Ki67 immunopositive nonsteroidogenic cells was highest during the early luteal phase (13.9±8.7, n=4, Figure 5.8) and decreased as the luteal phase proceeded to a nadir during functional luteal regression (4±0.4, n=3). This increased significantly to 6±0.6 (n=3, $p<0.05$) immunopositive nonsteroidogenic cells during structural regression. Induction of regression caused the number of Ki67-positive steroidogenic cells to decrease significantly from 18.6±3.2 cells (n=3) in mid luteal phase day 10 corpora lutea to 2.4±1.1 cells (n=3, $p<0.01$) and 2.4±0.7 cells (n=3, $p<0.01$) 24 hours after administration of PGF2α and GnRH antagonist respectively (Figure 5.9). The numbers of Ki67-positive nonsteroidogenic cells, however, were not significantly changed by the administration of luteolytic agents (Figure 5.9).

The percentages of all cells which were Ki67 positive were 8.8±4% (n=3, Figure 5.17) in the early luteal phase, 6.3±2% (n=3) in the mid luteal phase, 4.6±1.9% (n=3) during functional regression, and 5.0±1.8% (n=3) during structural regression. The percentage of Ki67 positive non-steroidogenic cells was 53.5±17% in the early luteal phase, 36±17% in the mid luteal phase, 49±4.7% during functional regression and 39±9% during structural regression (Figure 5.17), indicating that more than half of the Ki67 immunopositive cells were steroidogenic cells. The percentage of Ki67-positive nonsteroidogenic cells decreased significantly from 8.4±0.8% during the early luteal phase, to 0.6±0.3% ($p<0.01$) during functional luteal regression and 2.2±0.5% (n=3, $p<0.01$) during structural luteal regression.

Figure 5.8: Numbers of Ki67 Immunopositive Cells in Spontaneously Regressing Marmoset Corpora Lutea. Ovaries on luteal days 2-5 (early, n=4), luteal day 10 (mid, n=4), luteal day 18 (functional luteal regression, n=3) and luteal days 22-25 (structural luteal regression, n=3). The total number of Ki67 immunopositive steroidogenic (grey bars) and nonsteroidogenic (white bars) cells per 10700 μm^2 unit area were determined for each corpus luteum, and shown as mean±SEM for each stage of the luteal phase. There was no significant differences between means after a one way analysis of variance.

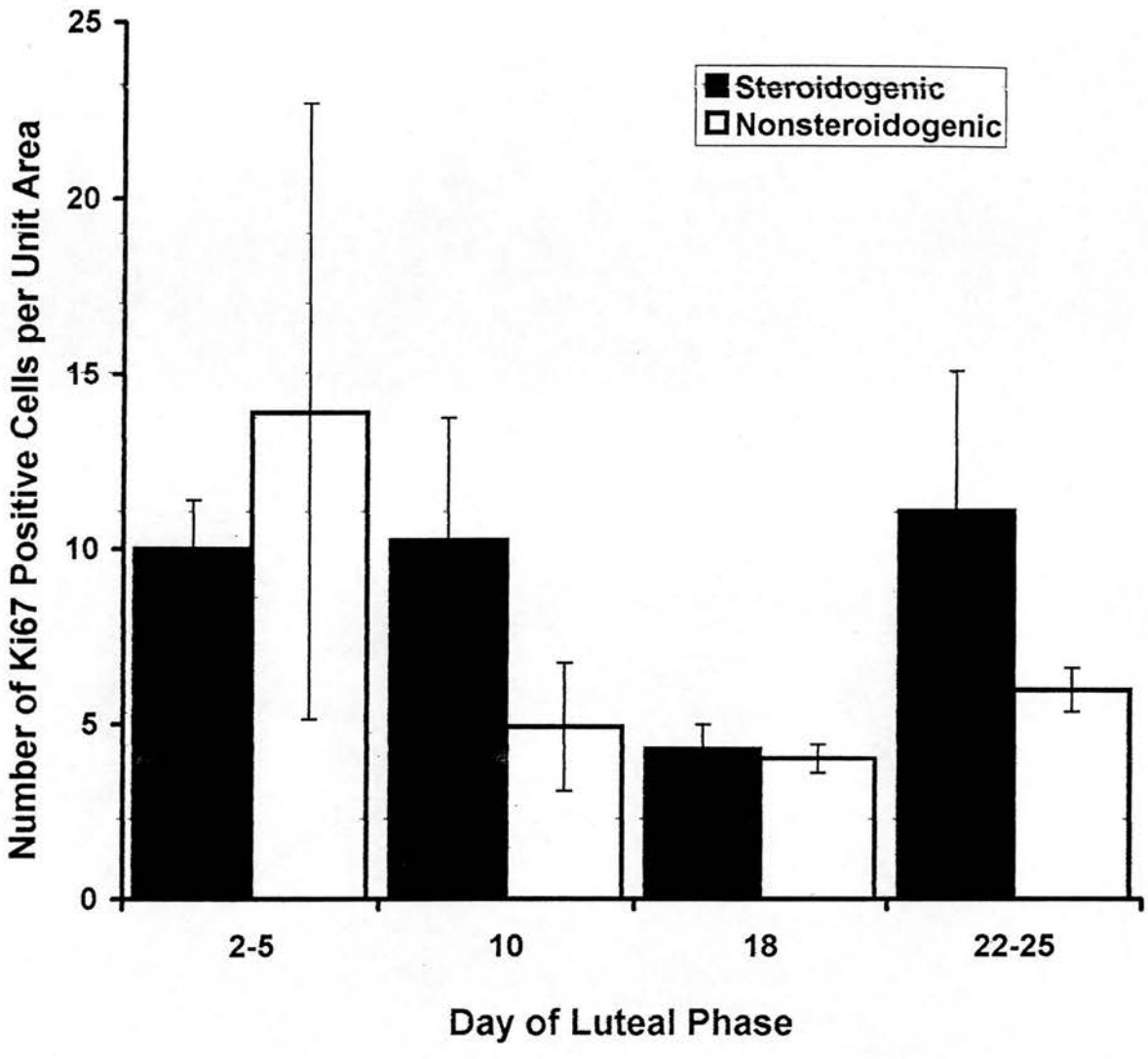
Ki67 Positive Cells in Marmoset Corpora Lutea
Steroidogenic
Nonsteroidogenic
Number of Ki67 Positive Cells per Unit Area
25
20
15
10
5
0
2-5
10
18
22-25
Day of Luteal Phase

Figure 5.9: Numbers of Ki67 Immunopositive Cells in Marmoset Corpora Lutea After Induced Luteal Regression.

Ovaries were collected on luteal day 10 (control, n=3), 12 hours (PG12, n=3) and 24 hours (PG24, n=4) after PGF2α analogue, and 12 hours (Gn12, n=3) and 24 hours (Gn24, n=4) after GnRH antagonist. The number of Ki67 immunopositive steroidogenic (grey bars) or nonsteroidogenic (white bars) cells per 31400μm^2 unit area were determined for each corpus luteum, and are shown as mean±SEM for each experimental group. Data were subjected to one way analysis of variance. The numbers of Ki67-immunopositive steroidogenic cells 12 and 24 hours after induction of luteolysis with either PGF2α or GnRH antagonist were significantly lower than the number of Ki67-immunopositive steroidogenic cells per unit area of control luteal tissue (**, $p<0.01$).

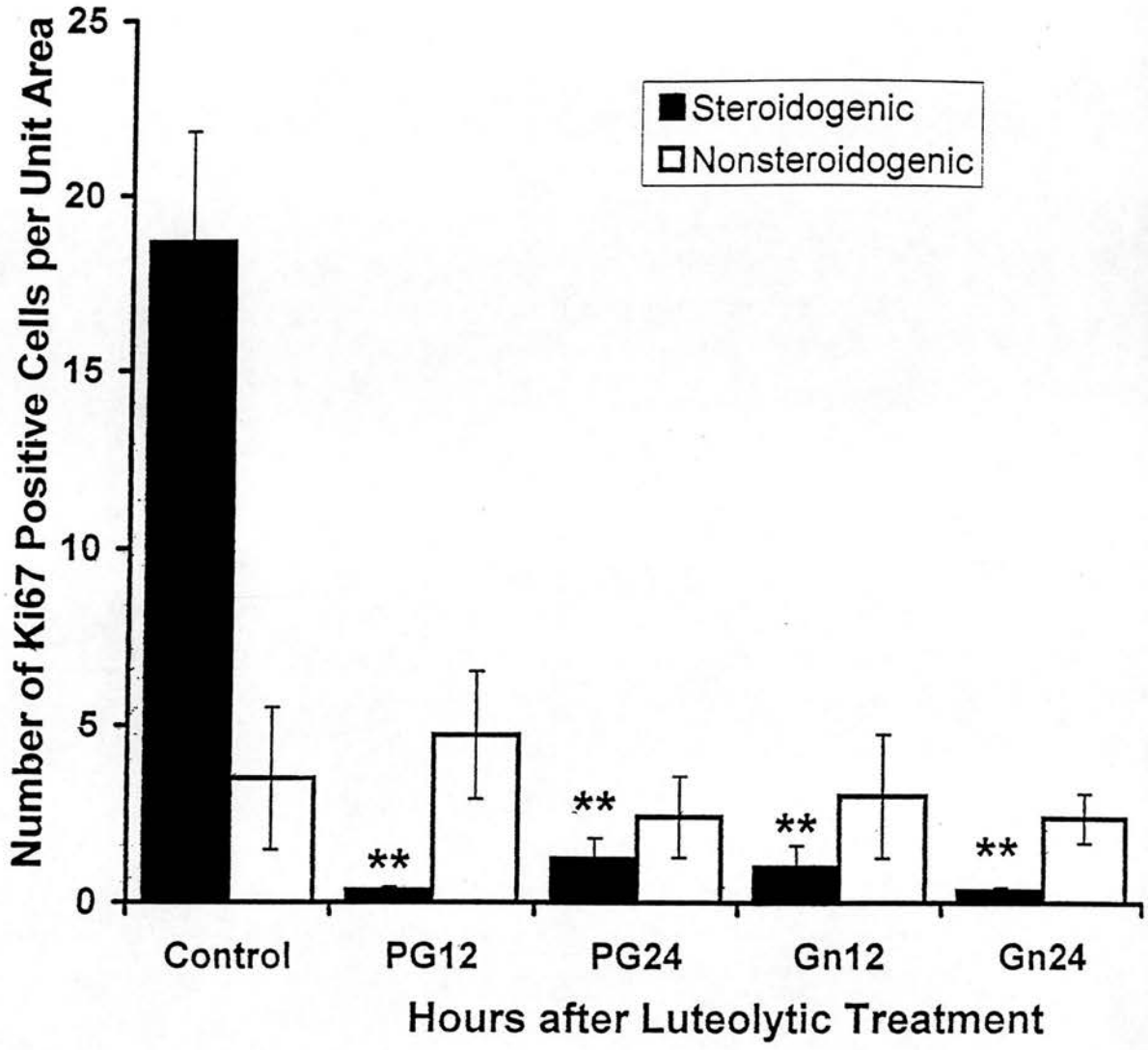
Steroidogenic
Nonsteroidogenic
Number of Ki67 Positive Cells per Unit Area
25
20
15
10
5
0
**
**
**
**
Control
PG12
PG24
Gn12
Gn24
Hours after Luteolytic Treatment

5.1.3 BrdU Immunocytochemistry

The nuclei of some granulosa and theca cells in morphologically healthy follicles were intensely BrdU immunopositive, whereas the number of BrdU immunopositive cells in atretic follicles was markedly lower, indicating that follicles on the same section as luteal tissue provided good internal positive and negative controls (Figure 5.10A). Nuclei in negative control sections were not BrdU immunopositive, and cytoplasmic non-specific staining was entirely absent (Figure 5.10A and B). BrdU immunopositive steroidogenic cells were infrequent, but BrdU immunopositive nonsteroidogenic cells were found in all sections examined. Intensity of staining was also consistent and did not vary according to cell type or luteal stage (Figures 5.10 and 5.11). A proportion of BrdU immunopositive nonsteroidogenic cells in spontaneously regressing corpora lutea were found lining blood vessels, suggesting that they may have been endothelial cells (Figures 5.10C and 5.11A) but the rounded morphology of other BrdU positive nonsteroidogenic cells combined with non-vascular localisation (Figures 5.11A and C) suggests a different phenotype.

5.1.3.1 Quantification of BrdU ICC

BrdU immunopositive steroidogenic cell numbers were low during the early luteal phase (4.3±2.3, mean±SEM, n=3), absent in functionally regressing corpora lutea, and high in some structurally regressing corpora lutea (43±40, n=4, Figure 5.12). The number of BrdU immunopositive nonsteroidogenic cells was 29±5.7 cells per unit area (n=3) in the early luteal phase, but there was a significant decrease (2.7±0.8, n=3, $p<0.01$) in BrdU positive nonsteroidogenic cell numbers during functional luteal regression. This was followed by a significant increase (38±29, n=4, $p<0.01$) in corpora lutea undergoing structural luteal regression after progesterone had fallen to follicular phase values (Figure 5.12).

Figure 5.10: Bromodeoxyuridine (BrdU) Immunocytochemistry in Functionally Regressing Corpus Luteum.

A. Primordial, developing, antral and atretic follicles, B. Primary antibody negative control serial section of (A), and C. Luteal tissue from the same ovary. BrdU positive cell nuclei were immunostained blue-black, immunonegative nuclei were counterstained blue-purple with haematoxylin and cytoplasm was counterstained with Light Green. Scale bars represent 20μm.

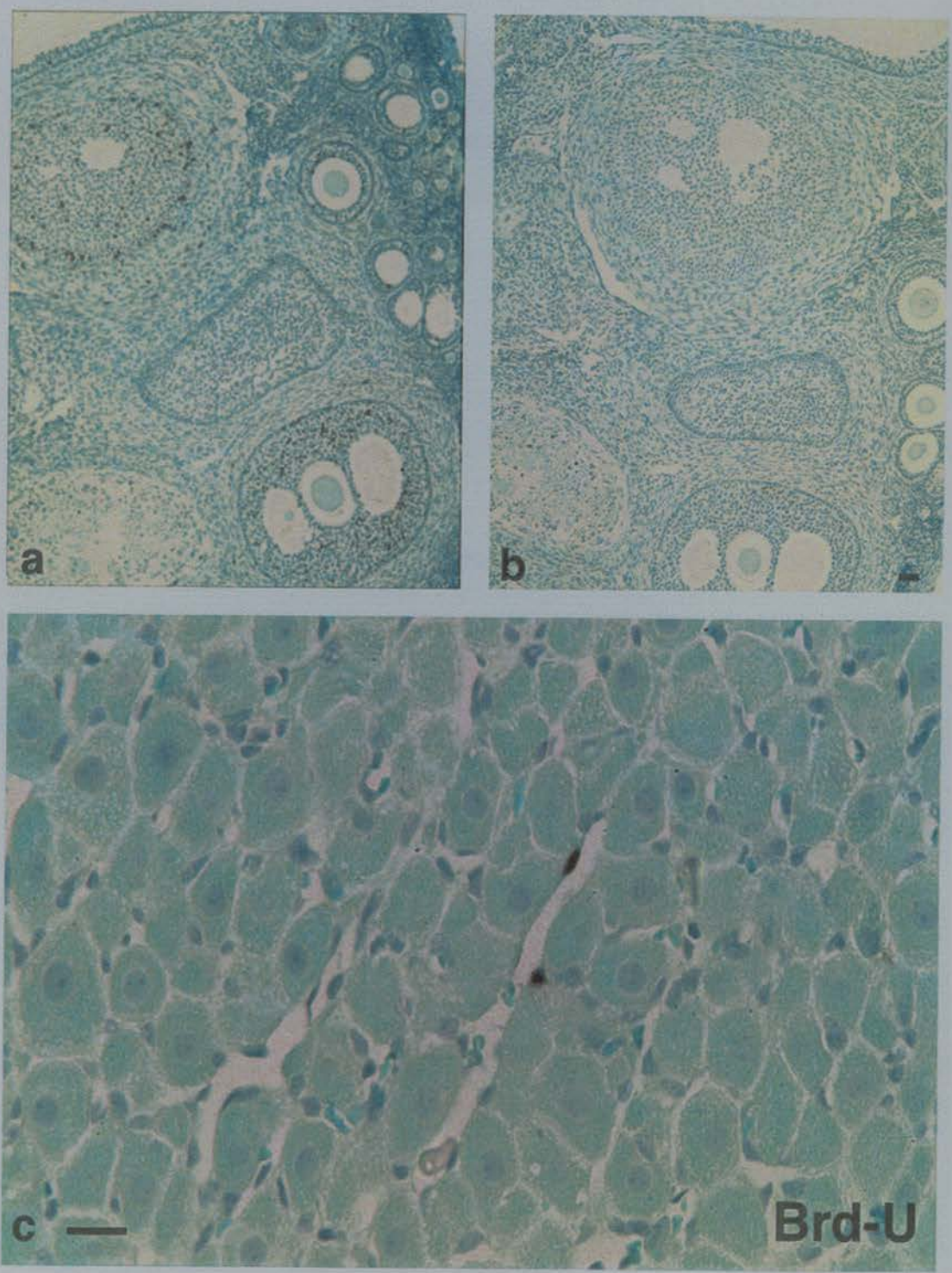
a
b
c
Brd-U

Figure 5.11: Bromodeoxyuridine (BrdU) Immunocytochemistry in Spontaneously Regressing Corpora Lutea.

Ovaries collected on; A. luteal days 2-5, B. luteal day 18 (functional luteal regression) and C. luteal days 22-25 (structural luteal regression). BrdU immunopositive cell nuclei were blue-black, immunonegative nuclei were counterstained blue-purple with haematoxylin and cytoplasm was counterstained with Light Green. Scale bars represent 20μm.

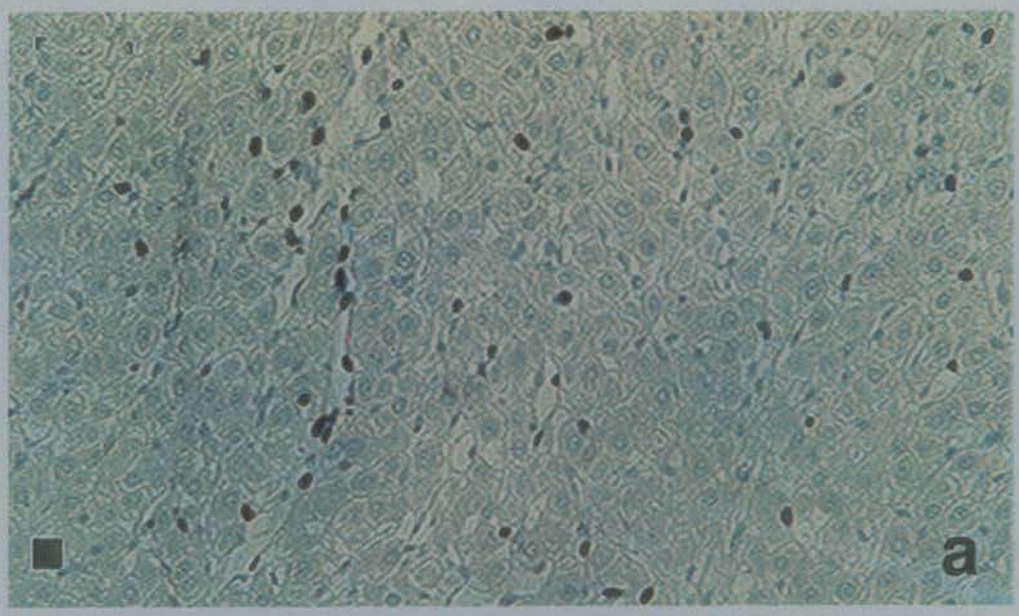
a

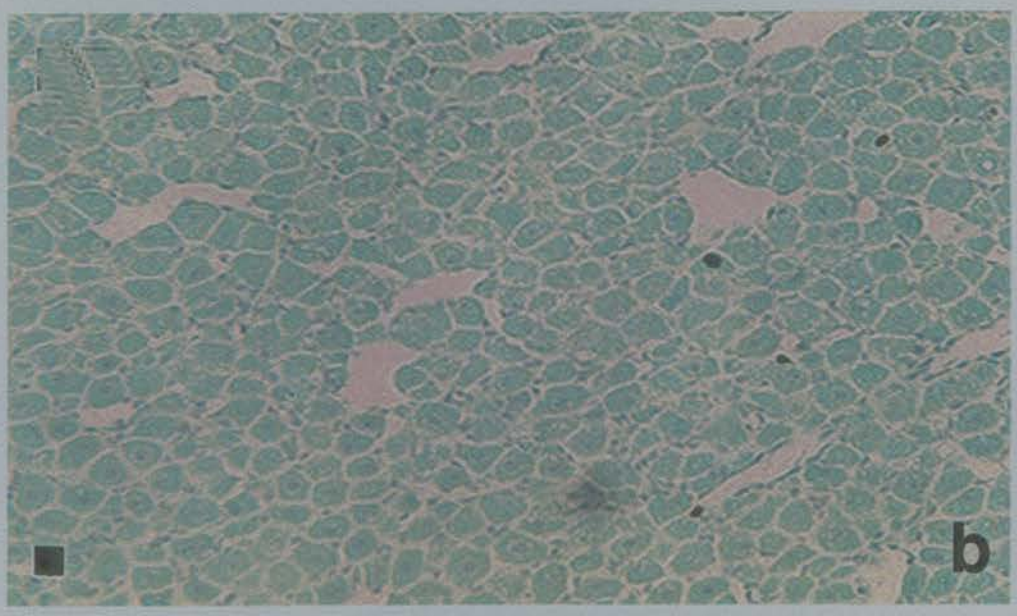
b

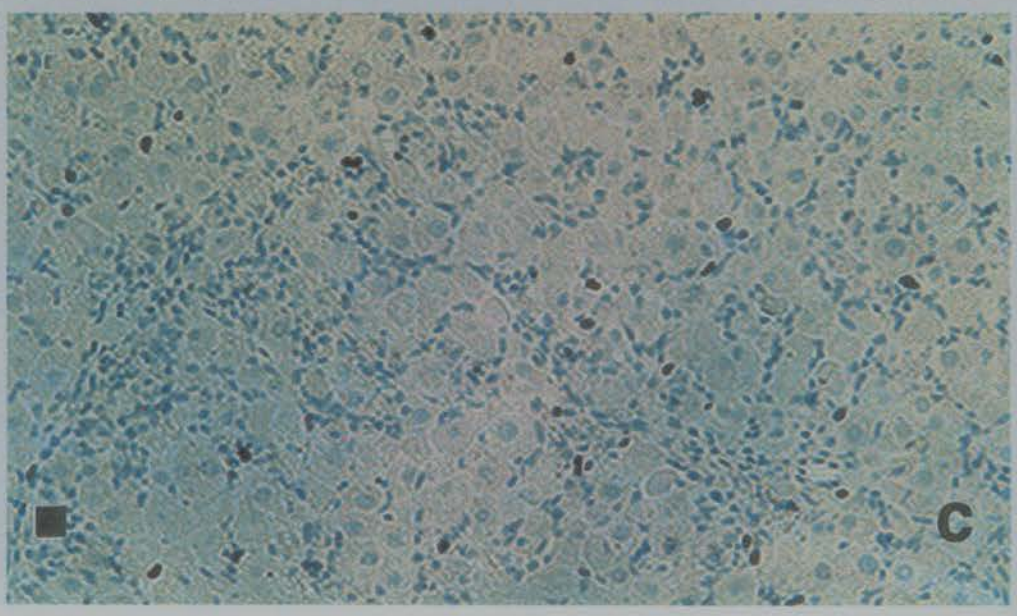
c

Figure 5.12: Numbers of Bromodeoxyuridine (BrdU) Immunopositive Cells in Spontaneously Regressing Marmoset Corpora Lutea.

Ovaries containing corpora lutea were collected on luteal days 2-5 (early, n=3), luteal day 18 (functional luteal regression, n=3) and luteal days 22-25 (structural luteal regression, n=4). The number of BrdU immunopositive steroidogenic (grey bars) and nonsteroidogenic (white bars) cells per 10700 μm^2 unit area were determined for each corpus luteum, and shown as mean±SEM for each stage of the luteal phase. Data were subjected to one way analysis of variance. Mean numbers of BrdU positive steroidogenic cells were not significantly different between groups. The numbers of BrdU-immunopositive nonsteroidogenic cells on luteal day 18 were significantly lower than the number of BrdU-immunopositive nonsteroidogenic cells per unit area of luteal tissue during luteal days 2-5 or 22-25 (**, $p<0.01$).

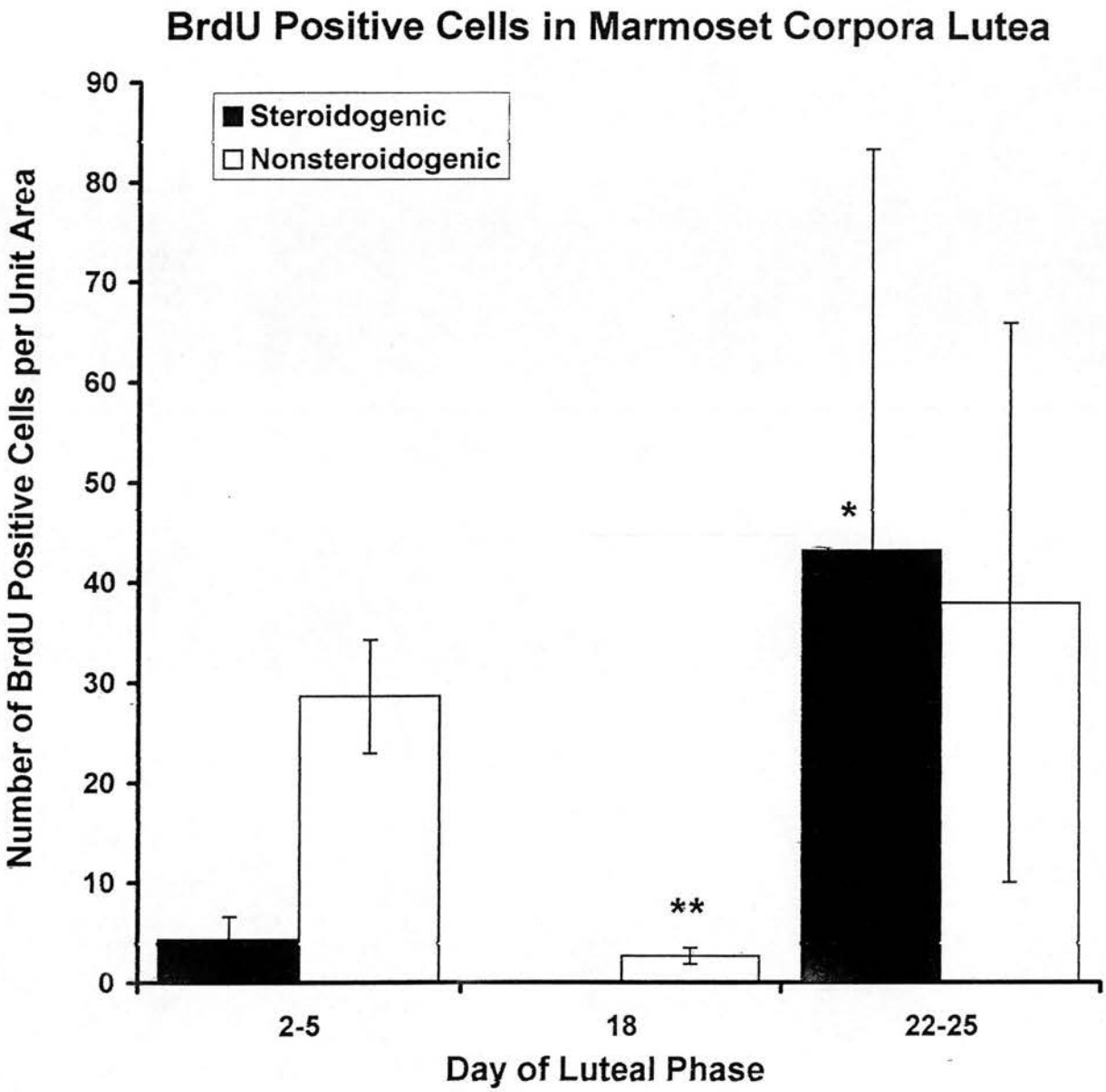
BrdU Positive Cells in Marmoset Corpora Lutea
Steroidogenic
Nonsteroidogenic
Number of BrdU Positive Cells per Unit Area
90
80
70
60
50
40
30
20
10
0
*
**
2-5
18
22-25
Day of Luteal Phase

5.1.4 Identification of BrdU Positive Cells

5.1.4.1 BrdU Colocalisation ICC with 3β Hydroxysteroid Dehydrogenase (3β HSD).

The cytoplasm of cells with the morphological appearance of steroidogenic cells had pink 3β HSD immunostaining (Figure 5.13A). Not all steroidogenic cells were 3β HSD immunopositive, and this was also apparent in 3β HSD ICC (see chapter 3). Brown BrdU immunostaining was localised only to cell nuclei, and BrdU positive cells were not 3β HSD immunopositive. Visualisation substrates can sometimes mask the colour of a second dye used in colocalisation studies. The Vector Red used to visualise 3β HSD immunopositivity was fluorescent, and NBT does not mask fluorescent Vector Red. Figure 5.13B shows that BrdU immunopositive cells are not 3β HSD immunofluorescent, and also that the nuclei of steroidogenic cells are 3β HSD immunonegative as would be expected. Negative control sections were clearly 3β HSD and BrdU immunonegative.

5.1.4.2 BrdU Colocalisation ICC with von Willebrand Factor VIII Antigen (vW).

Pink vW immunopositivity was predominantly cytoplasmic and localised to the edges of lumina which contained red blood cells (Figure5.14A), as well as to cells which had the morphological appearance of nonsteroidogenic cells but which did not clearly enclose a lumen. Positive immunostaining was also apparent in the theca, but not the granulosa layers of follicles (Figure 5.14B). Brown BrdU immunostaining was localised to cell nuclei (Figure 5.14A and B), and was found in granulosa, theca and luteal cells. Figure 5.14C shows that BrdU immunopositive cells are both vW immunofluorescent and vW immunonegative, indicating that only a proportion of the BrdU positive cells are endothelial cells, or that a proportion of endothelial cells are vW negative. Negative control sections were clearly vW and BrdU immunonegative (Figure 5.14D).

Figure 5.13: Immunocytochemistry for Bromodeoxyuridine (BrdU) Colocalised with 3β Hydroxysteroid Dehydrogenase (3βHSD) in Spontaneously Regressing Marmoset Corpora Lutea.

Luteal tissue collected on luteal day 18 during functional luteal regression. Panel A, light field photomicrograph of luteal tissue with BrdU-positive cell nuclei brown-black, and immunonegative nuclei purple. 3βHSD positive cells had red-pink cytoplasmic immunostaining, and 3βHSD immunonegative cells were counterstained with Light Green. The inset is a antibody negative control section for both anti-BrdU and anti-3βHSD antibodies. Panel B is a fluorescent dark field photomicrograph of panel A, in which 3βHSD positive immunostaining fluoresces red, but BrdU positive and immunonegative areas appear black. Scale bars represent 20μm.

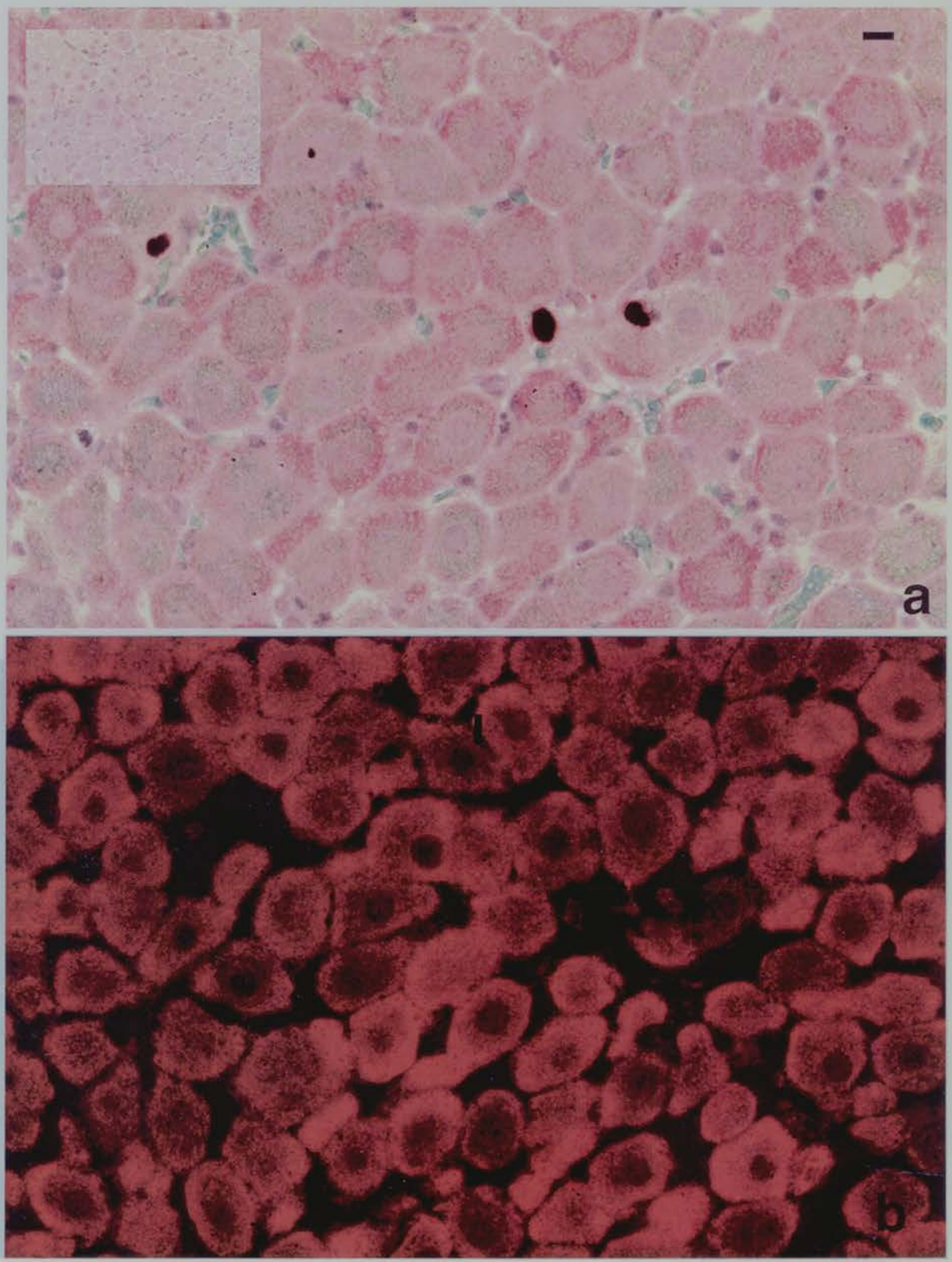

Figure 5.13

Figure 5.14: Immunocytochemistry for Bromodeoxyuridine (BrdU) Colocalised with von Willebrand Factor VIII Antigen (vW) in Spontaneously Regressing Marmoset Corpora Lutea. Luteal tissue collected during the early luteal phase. Panel A; from the left hand side can be seen the granulosa cells and then the theca cells of a follicle, then part of a corpus luteum. BrdU-positive cell nuclei are immunostained brown, and endothelial cells display pink-red vW positive immunostaining. Panel B is a primary antibody negative control section for both anti-BrdU and anti-vW antibodies. Panel C shows a corpus luteum of another animal and Panel D is a fluorescent dark field photomicrograph of panel C, in which vW-positive immunostaining fluoresces red, but BrdU positive and immunonegative areas appear black. Scale bar represents 20μm.

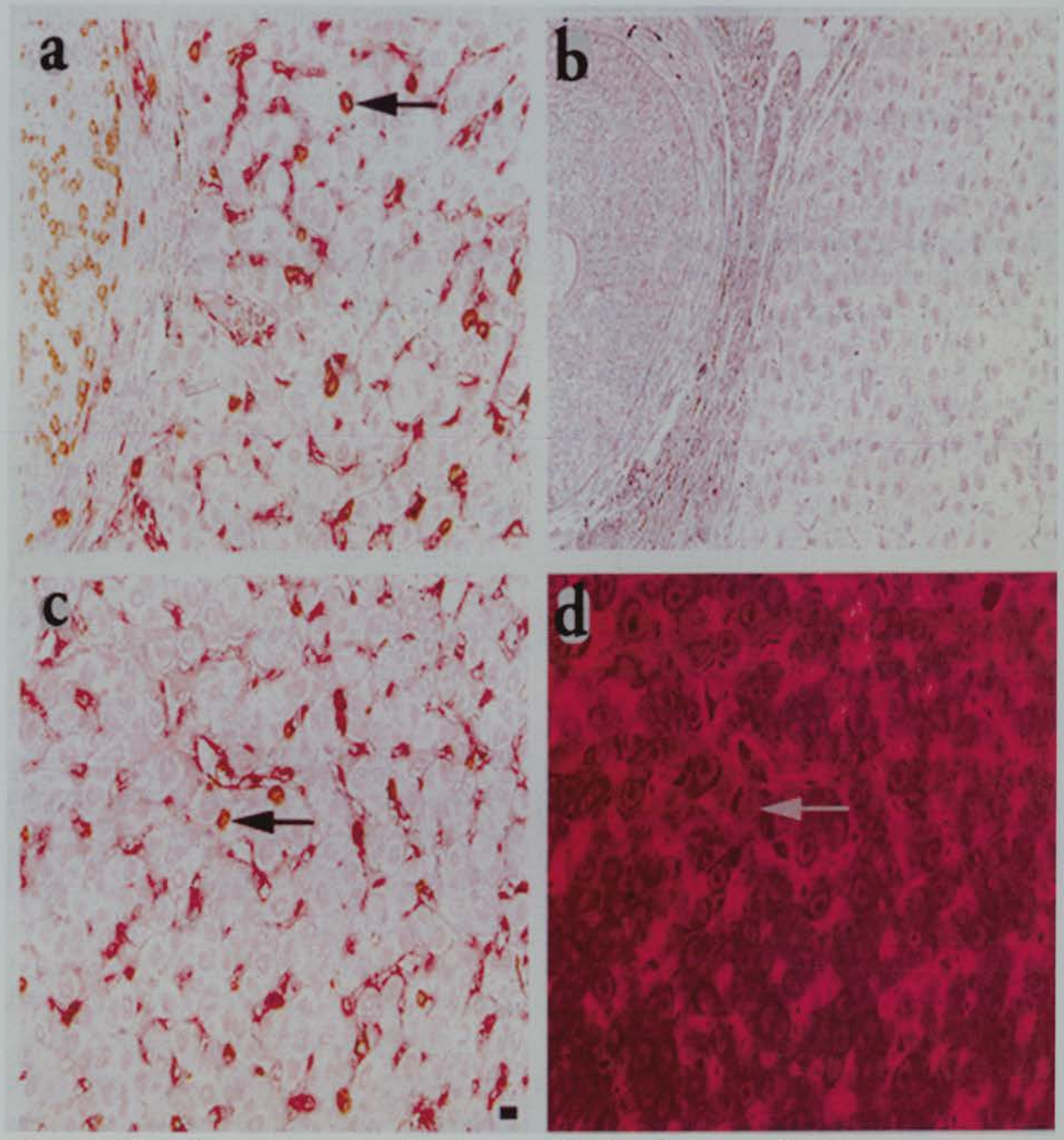

Figure 5.14: Bromodeoxyuridine co-localised with von Willebrand Factor VIII Antigen in marmoset corpora lutea

5.1.4.3Quantification of BrdU Colocalisation ICC with von Willebrand Factor VIII Antigen (vW).

BrdU quantification in corpora lutea collected in the early luteal phase or on luteal day 18 was the same after sections were subjected to BrdU Procedure II, and to the vW/BrdU Colocalisation procedure (Figure 5.15). The numbers of BrdU positive cells were different in structurally regressing corpora lutea. This data was also excluded from statistical analysis because there were only two animals in the group, but is presented here as an indication of relative trends.

In the early luteal phase, 64.6% of BrdU positive cells are vW positive endothelial cells (17±3.5, mean±SEM, n=3, Figure 5.16). The percentage of BrdU positive cells which are endothelial cells increases to 80.76% during functional luteal regression, but the number of proliferating endothelial cells per 40x field of view decreases significantly (0.42±0.2, n=3, $p<0.001$) at this time. There is then an indication that numbers of BrdU positive endothelial cells may return to levels similar to those seen in the early luteal phase (15.7±2.5, n=2, Figure 5.16). The numbers of BrdU positive cells which are not endothelial cells follow a similar pattern and are highest during the early luteal phase (9.3±3.2),they then show a significant decrease during functional luteal regression on luteal day 18 (0.1±0.09, n=3, $p<0.001$) followed by a rebound during structural luteal regression.

Figure 5.15: Numbers of Bromodeoxyuridine (BrdU) Immunopositive Cells in Spontaneously Regressing Marmoset Corpora Lutea After Two Separate Immunocytochemical Procedures.

Ovaries on luteal days 2-5 (early, n=3), luteal day 18 (functional luteal regression, n=3) and luteal days 22-25 (structural luteal regression, n=2). Ovarian sections were subjected to BrdU immunocytochemical Procedure II (white bars) or to a procedure in which BrdU positive cells were colocalised with von Willebrand Factor VIII Antigen (vW, black bars). The number of BrdU immunopositive cells per x40 field of view were determined for each corpus luteum, and shown as mean±SEM for each stage of the luteal phase. Data were subjected to one way analysis of variance and the mean numbers of BrdU positive cells were not significantly different between groups.

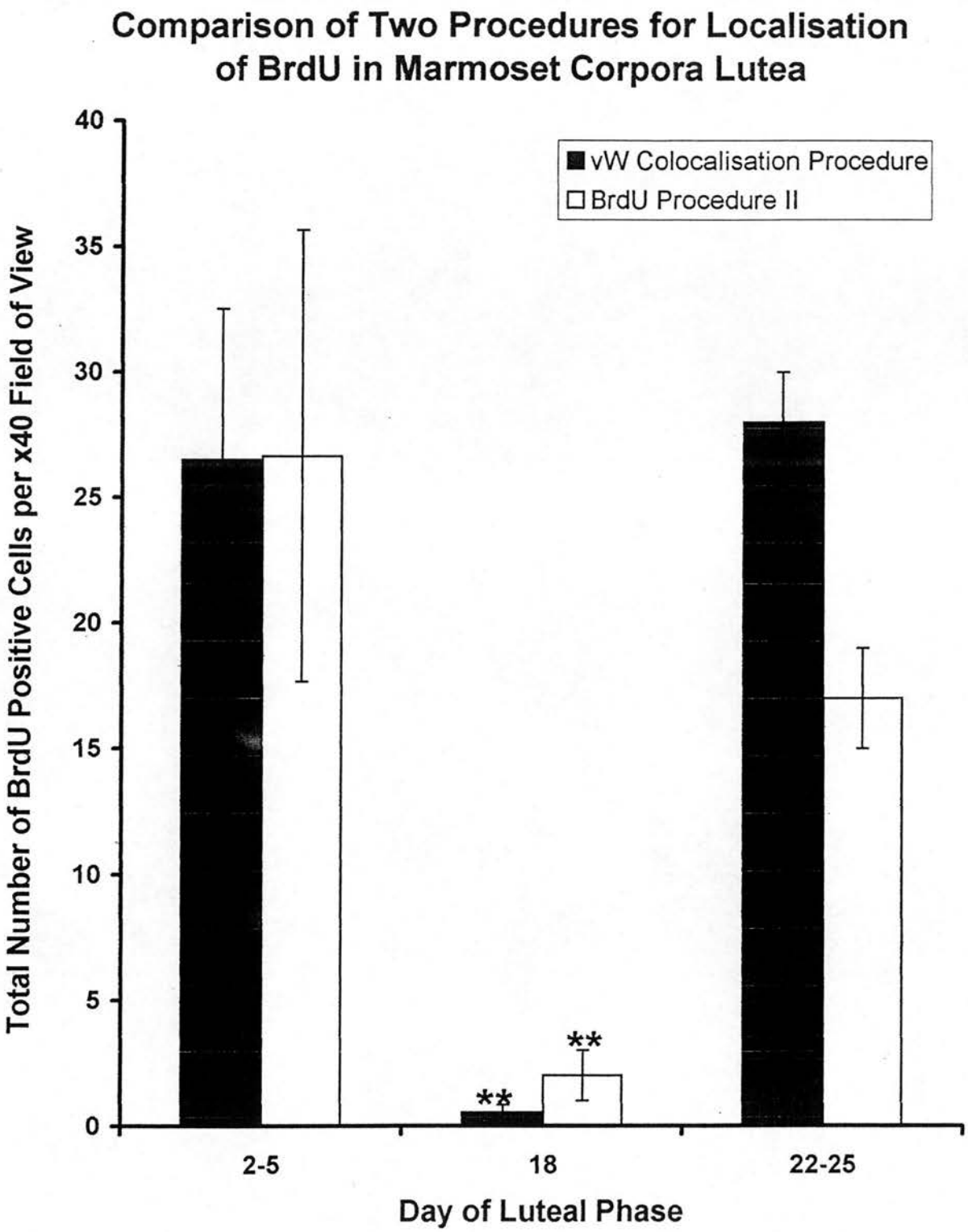
Comparison of Two Procedures for Localisation of BrdU in Marmoset Corpora Lutea
vW Colocalisation Procedure
BrdU Procedure II
Total Number of BrdU Positive Cells per x40 Field of View
40
35
30
25
20
15
10
5
0
**
**
2-5
18
22-25
Day of Luteal Phase

Figure 5.16: Numbers of Proliferating Cells after Colocalisation Immunocytochemistry with Bromodeoxyuridine (BrdU) and von Willebrand Factor VIII Antigen (vW).

Ovaries on luteal days 2-5 (early, n=3), luteal day 18 (functional luteal regression, n=3) and luteal days 22-25 (structural luteal regression, n=2). Cells displayed either dual immunopositivity for both BrdU and vW (black bars) or were immunopositive for BrdU only (white bars). The number of BrdU immunopositive cells per x40 field of view shown as mean±SEM for each stage of the luteal phase. Mean numbers of BrdU-immunopositive cells on luteal day 18 were significantly lower than the number of BrdU-immunopositive cells per x40 field of view during luteal days 2-5 or 22-25 (**, $p<0.01$).

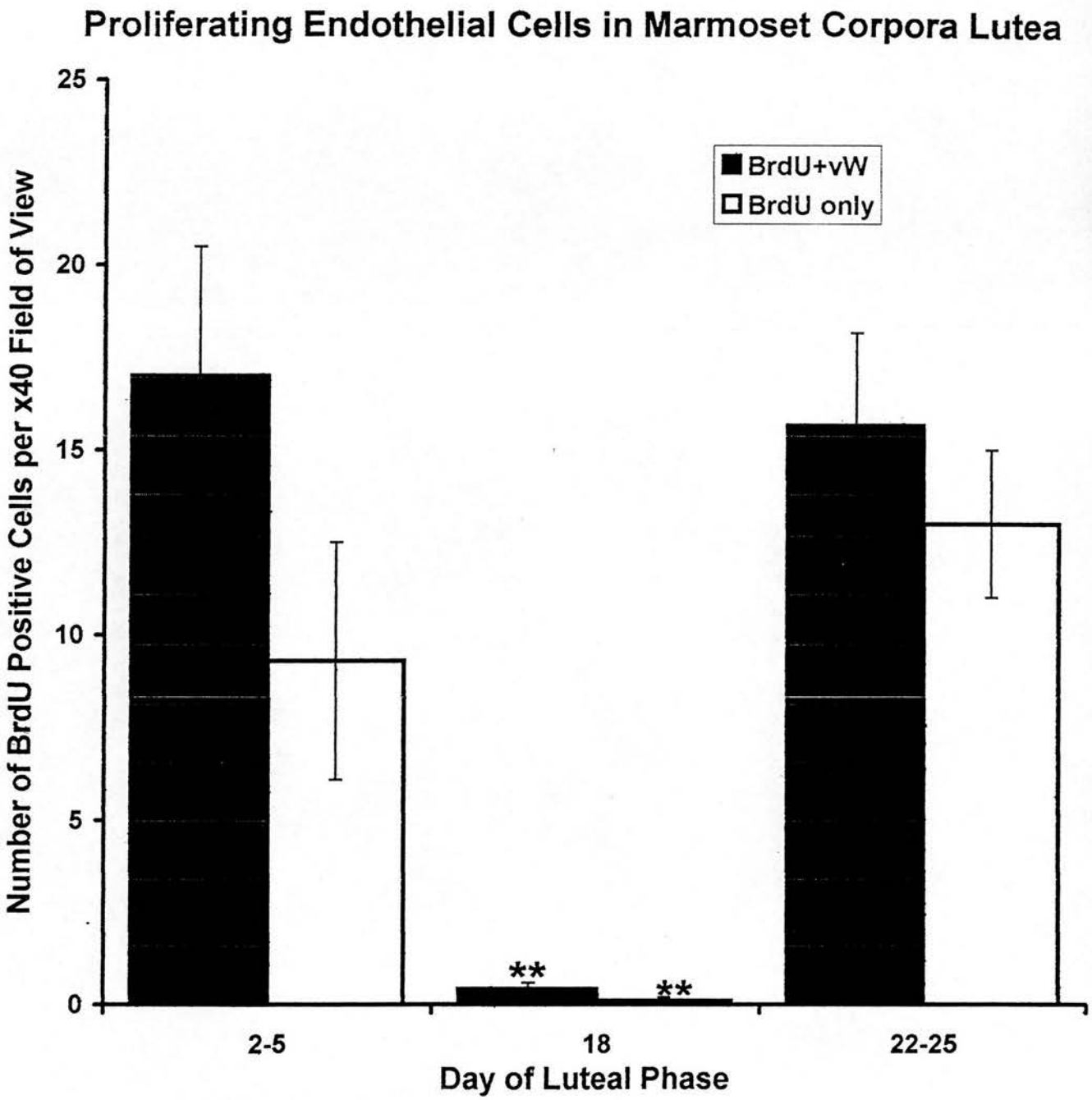
Proliferating Endothelial Cells in Marmoset Corpora Lutea
Number of BrdU Positive Cells per x40 Field of View
25
20
15
10
5
0
BrdU+vW
BrdU only
**
**
2-5
18
22-25
Day of Luteal Phase

5.1.5 Comparison of Ki67 and BrdU ICC

In order to compare assessments of proliferation by Ki67 and BrdU ICC, data were expressed as percentages (Figure 5.17). The percentage of BrdU positive cells was always lower than the percentage of Ki67 positive cells, except in structurally regressing corpora lutea in which the mean percentage of BrdU positive nonsteroidogenic cells was higher than the mean percentage of Ki67 nonsteroidogenic cells. In this case the median number of BrdU positive cells was 2.16 and the median of the equivalent Ki67 positive cells was 5.45, so if the variation was compensated for, BrdU measurement in this case was also lower than Ki67, as would be expected. Ki67 and BrdU measurements of nonsteroidogenic cells paralleled each other reasonably well, but percentages of Ki67 positive steroidogenic cells tended to be significantly higher than percentages of BrdU positive steroidogenic cells. The percentage of proliferating nonsteroidogenic cells was high during the early luteal phase (BrdU, 8.36±0.8, n=3; Ki67, 9.9±5.6, n=3, Figure 5.17) but decreased significantly by luteal day 18 when functional luteal regression was occurring (BrdU, 0.55±0.3, n=3, $p<0.001$ and Ki67, 4.3±2, n=3, $p<0.01$). Percent proliferation did not change significantly (Ki67, 4±0.4, n=3 and BrdU, 2.2±0.5, n=3, Figure 5.17) as luteal regression proceeded, and remained low during stuctural luteal regression.

Figure 5.17: Percentages of Ki67 and BrdU Immunopositive Cells in Spontaneously Regressing Marmoset Corpora Lutea.

Ovaries collected on luteal days 2-5 (early, n=3), luteal day 18 (functional luteal regression, n=3) and luteal days 22-25 (structural luteal regression, n=3). The total number of Ki67 immunopositive nonsteroidogenic (dark grey bars), BrdU nonsteroidogenic (white bars), Ki67 steroidogenic (light grey bars) and BrdU steroidogenic (hatched bars) cells per 10700 μm^2 unit area expressed as a percentage of the total number of nonsteroidogenic or steroidogenic cells for that unit area. Data are shown as the mean percentage±SEM for each stage of the luteal phase. The mean percentages of nonsteroidogenic cells on luteal day 18 and on luteal days 22-25 were significantly lower than the mean percentages of nonsteroidogenic cells per x40 field of view during luteal days 2-5 (BrdU **, $p<0.001$; Ki67 *, $p<0.05$).

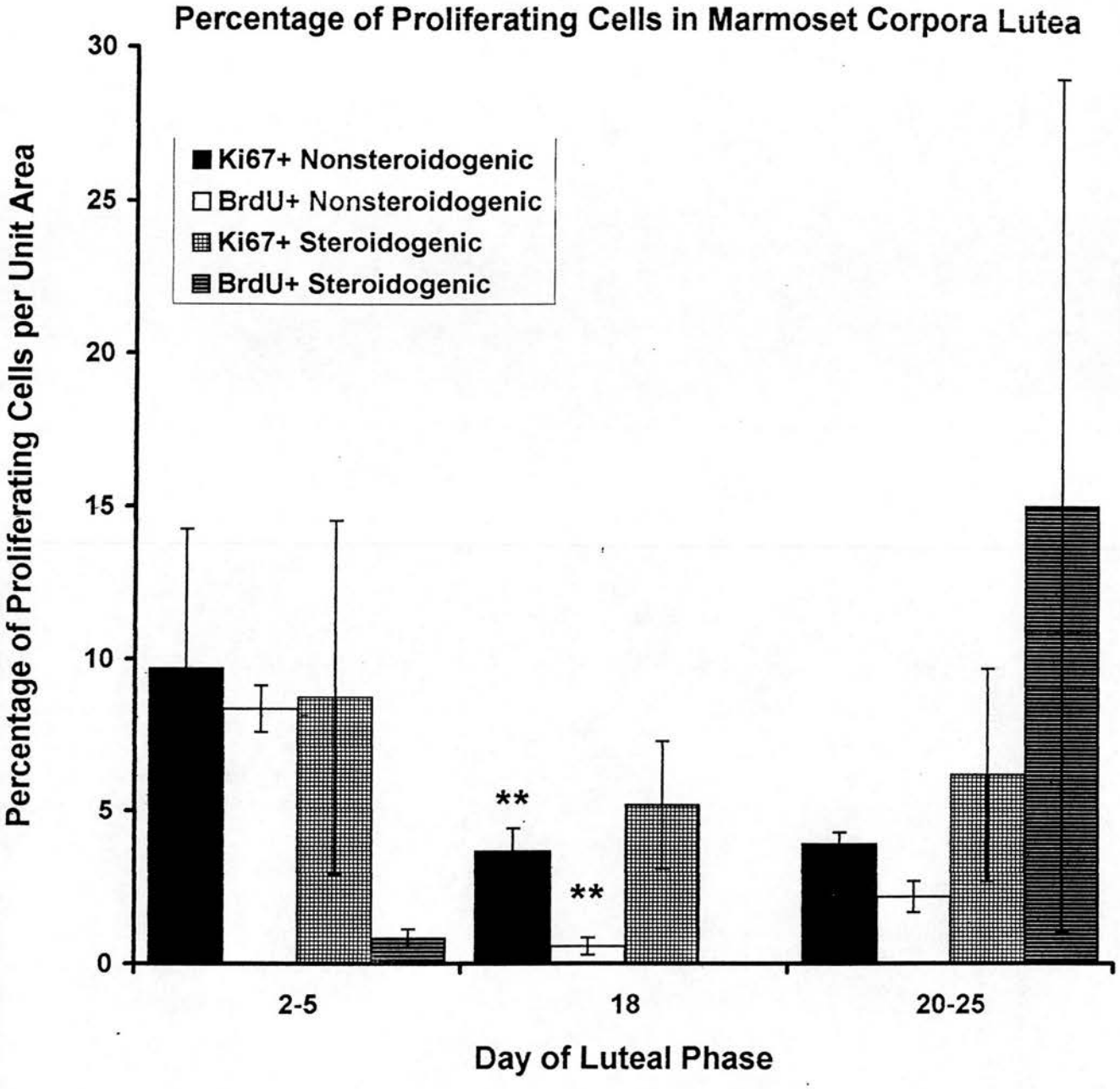
Percentage of Proliferating Cells in Marmoset Corpora Lutea
Ki67+ Nonsteroidogenic
BrdU+ Nonsteroidogenic
Ki67+ Steroidogenic
BrdU+ Steroidogenic
Percentage of Proliferating Cells per Unit Area
30
25
20
15
10
5
0
**
**
2-5
18
20-25
Day of Luteal Phase

5.2 DISCUSSION

5.2.1 The Automated Quantification System.

The use of an automated cell counting system allowed relatively large areas of luteal tissue to be assessed in a short period of time, and it also incorporated rigorous objectivity: nuclei were deemed to be immunopositive on the basis of an optical density threshold which was consistent throughout the entire assessment. Humans had to make decisions about whether to include a cell in the count, and in addition the criteria for making those decisions could change as the analysis proceeded. The automated system could not distinguish overlapping cells, but these errors were compensated for by counting large numbers of cells, and by only using the system to analyse tissue sections in which the number of overlapping cells was less than 5% of the total cell number.

Determination of the ratio between the ellipse long axis and the ellipse short axis of each nucleus was an acceptable means of immunopositive cell identification, as long as the frequency of overlapping immunopositive nuclei remained low and therefore this method became increasingly inaccurate as the number of immunopositive nuclei increased. The area of nuclear immunopositivity and the length of the perimeter of PCNA immunopositivity were not good indicators of cell type because they varied according to the plane of sectioning for that particular cell. A steroidogenic nucleus sectioned at its tip could have a similar area and perimeter to an endothelial cell nucleus cut in perfect cross-section. The ratio of nuclear axis, however, was a measure of shape in which a perfect circle would have a ratio of 1. Of 203 steroidogenic cell nuclei measured in three different corpora lutea, none had a ratio higher than 1.8, indicating that since steroidogenic cell nuclei are regularly shaped spheres, sectioning in different planes did not greatly alter the basic circular ratio. Variation was greatest in the untreated mid luteal phase day 10 sample (Figure 6.2), and this was probably because steroidogenic cells were easily identifiable by the mass of cytoplasm, and every steroidogenic cell in measured fields of view was scored. Luteolytic treatment with either GnRH antagonist or PGF2α, however, made some cells unidentifiable on morphological grounds alone, and these cells were not included in the analysis, so introducing a bias towards clearly identifiable cell types

which more closely approached morphological norms in these samples. Nonsteroidogenic cell ellipse ratios showed greater variation than steroidogenic cell nuclear ratios, and this reflected the greater number of shapes which can be obtained by sectioning an elongated oval. Misidentification was possible if endothelial cell nuclei were sectioned in transverse cross section which would give a circular shape with a similar ratio to steroidogenic cell nuclei. However nuclei with ratios < 1.7 and with an area corresponding to endothelial cell nuclei area were very rare, and did not adversely affect results, so this was not a significant problem. There was subpopulation of nonsteroidogenic cells which had ratios <1.7, but which also had areas in the same range as steroidogenic cells. These had the morphological appearance of immune system cells, and macrophage numbers increase in luteal tissue as regression proceeds (Lei *et al.,* 1991), therefore this misidentification may have significantly affected results, and requires further characterisation. Overall, variation within experimental groups was 27.7±15% (mean±SD, n=8, PCNA, Fig. 5) and 32.88±15% (mean±SD, n=8, Ki67, Fig. 10), and inaccuracy due to the automated counting system was 7.7±3.72% (Fig. 3). Reducing the variation by 7.7% might have made a statistical difference in the PCNA study when comparing the results obtained 24 hours after administration of GnRH antagonist with mid luteal phase controls, but compensating for variation due to the automated counting system does not change results obtained from any other examination of the effects of induced regression upon cell proliferation.

5.2.2 Suitability of Experimental Design.

High variability within experimental groups may be attributable to the lack of differentiation between younger (ovulated more recently) and older corpora lutea. In marmosets, ovulations can occur as much as 24 hours apart in the same cycle, therefore the figure derived from one ovary encompassed variability in luteal age. The cycle tracking regime was accurate ± 24hours, therefore an ovary collected on day 4 of the luteal phase may in fact have been 3 or 5 days post-LH/ovulation. The Ki67 figure derived from each experimental group therefore encompassed variability attributable to cycle tracking. In addition, the large SEM in the early luteal phase

group probably reflected the degree of differentiation/luteinisation in individual cells, and variable maturation of the corpora lutea. The large SEM in 20-25 day old CL probably reflected variability in the length of the luteal phase. Marmosets had a luteal phase of 20±10 days (mean ± S.D, n=87, range 6 - 63 days). Median length of luteal phase was 18 days, but functional regression could start from day 12 onwards, and progression of functional and structural regression was highly variable. Ovaries collected on luteal day 22 might be starting structural regression in one animal, whilst another animal might have completed structural regression by luteal day 22. Therefore, the interpretation of these results is confounded by large inter-animal variation as well difficulty in determining the exact stage of the luteal phase. These two sources of variation were sufficient to obscure significant changes in rates of proliferation in the experimental design used. These studies attempted to relate changes in rate of proliferation with stage of luteal regression, but it would have been more accurate to determine relative changes in proliferation within the cycles of individual animals, however considerations of animal welfare precluded this. Alternatively, different quantification systems may have yielded results which were more sensitive to changes in proliferative rates.

5.2.3 Interpretation of Data from PCNA Study.

The 18 hour long half-life of PCNA rendered this method of analysing proliferation too insensitive for use in the corpus luteum, where noticeable changes occur within six to twelve hours during luteal regression. The long half -life of PCNA may also be the reason why so many more cells were identified as being proliferative than were identified using Ki67 or BrdU.

5.2.4 Steroidogenic Cell Proliferation in Marmoset Corpora Lutea.

Steroidogenic cells were immunopositive with three different markers for proliferation, PCNA, Ki67 and BrdU. This was unexpected, since a number of studies have demonstrated that steroidogenic cell numbers do not increase as the luteal phase progresses in ovine (O'Shea *et al.*, 1986), bovine (O'Shea *et al.*, 1989) human (Lei *et al.,* 1991) or marmoset (see chapter 3) corpora lutea. If the number of

steroidogenic cells labelled by the above techniques were actually proliferating, then equal or slightly higher rates of cell death would be required to maintain constant steroidogenic cell numbers, but there is no evidence for such high levels of cell death during the early or mid luteal phases (Corner, 1956; Zheng *et al.,* 1994, and see chapter 3). This suggests that luteal steroidogenic cells may be in the cell cycle, and thus expressing the cell cycle antigens PCNA and Ki67, but that they may be arrested in one part of the cell cycle and do not proceed to synthesis or mitosis. It is noticeable that extremely low numbers of steroidogenic cells label with BrdU in the early luteal phase, when granulosa or theca-lutein might conceivably be proliferating during the process of transformation from follicle to corpus luteum, but that there were no BrdU labelled steroidogenic cells in late luteal phase corpora lutea, indicating that steroidogenic cells were not synthesising DNA at this time. The number of BrdU labelled steroidogenic and nonsteroidogenic cells increased during structural luteal regression, but numbers of Ki67 immunopositive steroidogenic cells remained constant. One of the first stages of apoptosis can be activation of endogenous endonucleases and fragmentation of DNA, and it is possible that the very early stages of DNA fragmentation might also be accompanied by futile DNA repair processes. It has been shown that apoptotic glandular prostate cells incorporate BrdU during futile DNA repair when the cells are in the G0 phase (Berges *et al.,* 1993), therefore high numbers of BrdU labelled non-proliferating cells might be observed in tissues in which there are also high rates of apoptosis. It is possible that the high numbers of BrdU labelled steroidogenic and nonsteroidogenic cells observed in structurally regressing corpora lutea are not actually proliferating, but are in the initial stages of cell death. This could be determined by measuring the amount of DNA in these subpopulations of BrdU-labelled cells, and differentiating between normal, non-proliferating diploid DNA content and the increased DNA content normally found in proliferating cells.

It was considered that the immunostaining of steroidogenic cells with Ki67 and PCNA might be an artefact of the antigen retrieval system, since some workers have not specifically reported immunopositive steroidogenic cells using these antibodies (McClure *et al.*, 1994) however others have reported that parenchymal luteal cells are immunopositive in the bovine (Zheng *et al.*, 1994), ovine (Jablonka-Shariff *et al.*,

1993), macaque (Christenson and Stouffer, 1996) and human (Rodger *et al.*, 1997) corpora lutea, but that these proliferation-labelled parenchymal cells did not colabel with the steroidogenic cell marker 3βHSD, indicating that one of the conditions under which cells with the morphological appearance of steroidogenic luteal cells may express cell cycle antigens is that they are not actually steroidogenic and they do not produce steroid hormones and express cell cycle antigens simultaneously. Our data support this hypothesis; BrdU immunopositive parenchymal cells in regressing corpora lutea were all 3βHSD immunonegative. Additionally, the same antigen retrieval system was used by Rodger *et al* (1997) to examine proliferation in human corpora lutea. The majority of parenchymal luteal cells which were Ki67 immunopositive and which had the morphological appearance of steroidogenic cells did not colabel with 3βHSD.

In addition to this, the number of Ki67 immunopositive steroidogenic cells was significantly decreased after induction of luteolysis with either GnRH antagonist or PGF2α, whereas numbers of Ki67 immunopositive nonsteroidogenic cells remained unchanged. This differential regulation of cell types by luteolytic agents requires further investigation.

5.2.5 Nonsteroidogenic Cell Proliferation in Marmoset Corpora Lutea.

The number of Ki67 immunopositive nonsteroidogenic cells was highest during the early luteal phase, but decreased to a lower level by the mid luteal phase, then stayed at this level during structural and functional luteal regression. Numbers of Ki67 immunopositive nonsteroidogenic cells were also the same after induction of luteolysis with either GnRH antagonist or PGF2α, so the numbers of Ki67 immunopositive nonsteroidogenic cells remain at mid luteal phase levels throughout both induced and spontaneous luteal regression. However, it is possible than the two sources of variation mentioned, inter-animal variation and inaccuracy in determining the exact stage of the luteal phase, may be responsible for obscuring a significant decrease in nonsteroidogenic cell proliferation during functional luteal regression. Figure 5.18 details the data concerned, and shows that only one of four mid luteal

phase corpora lutea had lower numbers of proliferating cells than luteal day 18 corpora lutea. It could be speculated that this particular animal might have had a proliferation rate approaching zero had it been possible to sample the same corpus luteum at a later time in the same cycle. Ki67 nonsteroidogenic cell data does not contradict the hypothesis that a significant decrease in the number of nonsteroidogenic cells undergoing proliferation occurs during functional luteal regression. This was followed by a slight, nonsignificant increase in Ki67 positive nonsteroidogenic cell numbers during structural regression, coincident with a slight, nonsignificant increase in area of vW immunostaining at the same time. Nonsteroidogenic cell numbers doubled between functional and structural regression (see chapter 3), but numbers of proliferating nonsteroidogenic cells barely changed, indicating that the increase in nonsteroidogenic cell numbers observed during structural luteal regression is primarily due to the dynamics of shrinking tissue in which remaining cells move closer together and therefore increase the number of cells observed in each unit area.

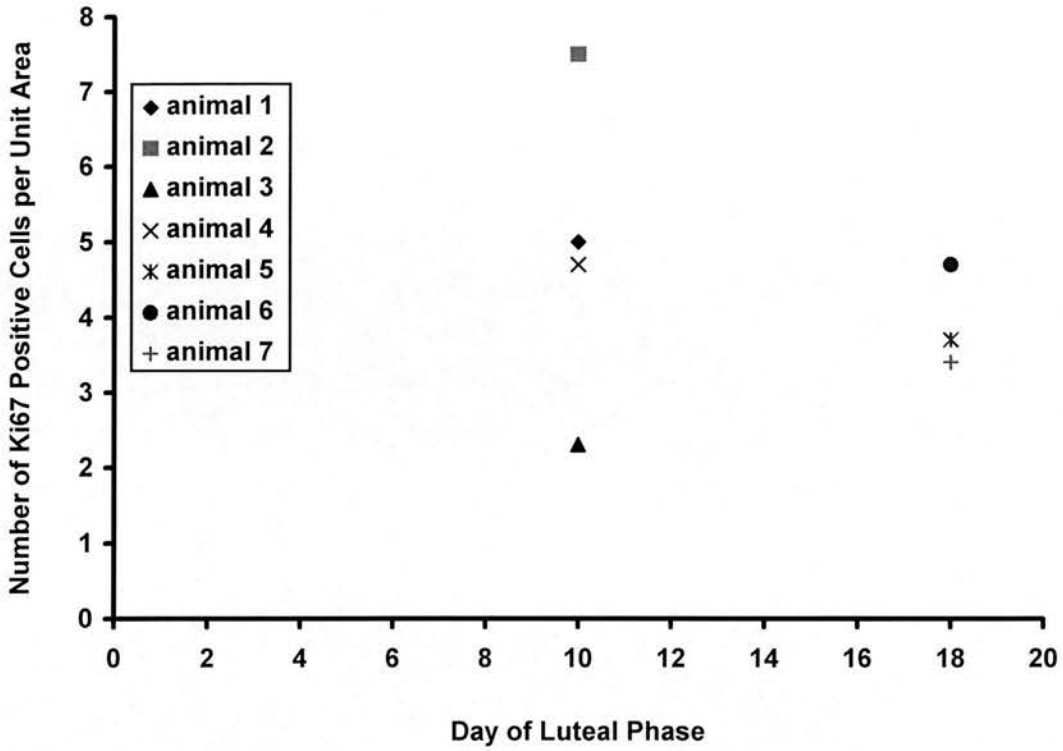

Figure 5.18: Interanimal Variation in Ki67 Immunocytochemistry Quantification.

The total number of Ki67 immunopositive cells in each unit area was determined for one corpus luteum per animal. Data points also indicate which day of the luteal phase individual corpora lutea were collected.

The number of BrdU immunopositive nonsteroidogenic cells was highest during the early luteal phase, lowest during functional luteal regression and increased during structural luteal regression. As previously stated, the increase during structural luteal regression can probably be attributed to BrdU incorporation by dying cells rather than being a true indication of proliferation. With this modification, BrdU and Ki67 data show good agreement with each other.

A proportion of BrdU positive cells were neither steroidogenic nor vW positive endothelial cells. There are two possible explanations for this, that some endothelial

cells are not positive for the vW antigen, or that the proliferating cells were another cell type, such as macrophages, or fibroblasts.

5.2.6 Summary

High levels of nonsteroidogenic cell proliferation during the early luteal phase are commensurate with the initial formation of the luteal vasculature (Rodger *et al.*, 1997), and decreased nonsteroidogenic cell proliferation during the mid luteal phase is consistent with a moderate turnover rate during which normal wear and tear of the vasculature is counteracted by low levels of proliferation which maintain constant cell numbers. Labelling with BrdU indicates that there is then a significant decrease in nonsteroidogenic cell proliferation at the end of the luteal phase when progesterone levels are falling and functional luteal regression is underway. The percentage of nonsteroidogenic cells which were proliferating at this time was 0.5±0.3% (mean±SEM, n=3), and the percentage of all cell types undergoing apoptosis at this time was 0.85±0.94% (mean±SEM, n=3, see chapter 4). These figures are not significantly different, but since luteal regression is probably characterised by a combination of decreasing rates of proliferation and increasing rates of apoptosis, these data may indicate that functional luteal regression is the period of time during which these factors first become apparent. Certainly the rate of apoptosis is significantly higher (3.46±1.45%, mean±SEM, n=3, see chapter 4) than the rate of proliferation (2.19±0.5%, mean±SEM, n=3, Fig. 20) after progesterone has fallen to follicular phase values and structural luteal regression is underway.
In short, the number of proliferating endothelial cells is highest during the early luteal phase, then when the corpus luteum is fully formed, endothelial cell proliferation falls to a basal level sufficient for maintenance of the luteal vasculature. Endothelial cell proliferation then decreases markedly during functional luteal regression, and stays low during structural regression.

5.2.7 Conclusions

It is therefore possible to draw two main conclusions: 1. One component of functional luteal regression is a dramatic reduction in luteal cell rates of proliferation

and 2. the observed increase in nonsteroidogenic cell numbers during structural luteal regression is primarily due to the dynamics of shrinking tissue in which remaining cells move closer together and increase the number of cells observed in each unit area.

Chapter 6: Discussion

6.0 Discussion

This project examined luteal regression in the marmoset monkey (*Callithrix jacchus*). Endocrinological and cellular changes that occurred during luteal regression were described, and three candidate mechanisms for the initiation and regulation of luteal regression were examined: apoptotic cell death, vascular changes, and the effects of PGF2α.

6.1 Cell Death and Luteal Regression

Apoptosis is a form of programmed cell death displaying specific biochemical and morphological criteria (Kerr *et al.*, 1972; Arends *et al.*, 1990). Macrophage numbers in human corpora lutea increase as the luteal phase advances (Lei *et al.*, 1991), coincident with decreasing progesterone production and functional luteal regression. Macrophages secrete TNFα (Zhao *et al.*, 1998), which has been shown to induce apoptosis (Witty *et al.*, 1996; Jo *et al.*, 1995). It was hypothesised, therefore, that luteal cell apoptosis was stimulated by TNFα secreted by macrophages. The resulting reduction in the number of steroidogenic cells would result in a decrease in the amount of progesterone produced by the corpus luteum as a whole, and therefore initiate functional luteal regression.

Results described in this thesis have shown that apoptosis does indeed occur in primate corpora lutea, and that there is a low basal rate of approximately 0.3% of all cells undergoing apoptosis throughout the luteal phase. However there is not a significant increase in the number of cells undergoing apoptosis until after functional luteal regression is completed. Recent work has demonstrated that progesterone inhibits apoptosis in rat granulosa cells (Peluso and Pappalardo, 1998) and this supports our finding that luteal apoptosis did not occur until after serum progesterone concentrations had fallen to follicular phase values. Therefore, apoptotic cell death does not instigate functional luteal regression in primates.

Apoptotic cell death is, however, a component of structural luteal regression in primates, and there may be an association between PGF2α concentration and the occurrence of apoptosis. It is possible that the endogenous production of PGF2α

stimulates the production of oxygen free radicals (Sawada *et al.* 1991) which may stimulate apoptotic pathways (Haeker and Vaux, 1994, Murdoch 1998). Expression of the PGF2α receptor corresponds with apoptosis in rat (Orlicky *et al.*, 1992) and mouse (Hasumoto *et al.*, 1997) corpora lutea.

A second possibility is that steroid hormones inhibit apoptosis (Peluso and Pappalardo, 1998), and the cessation of steroidogenesis therefore removes that inhibition and apoptosis occurs. Since progesterone (Sugino *et al.*, 1996) and estogen (Murdoch 1998) have antioxidant properties, the production of highly reactive oxygen species might be delayed until steroidogenic hormone levels decrease below a threshold concentration.

The combination of these two possibilities suggests that the exogenous administration of PGF2α would first cause a decrease in progesterone levels by production of the mildly reactive H_2O_2 (Behrman and Aten, 1991; Behrman and Preston, 1989). The lowering of progesterone below a particular threshold would result in loss of antioxidant protection and the consequent generation of highly reactive oxygen free radicals with the ability to stimulate apoptotic pathways. The administration of GnRH antagonist removes the trophic support for steroidogenesis, similarly resulting in decreased progesterone levels and increased apoptosis. If apoptosis is associated with decreased progesterone concentrations, the exogenous administration of both PGF2α and GnRH antagonist would result in similar levels of apoptosis. This was supported by observed results; there was no significant difference in the incidence of apoptosis in H&E stained sections or i*n situ* 3' end labeled sections or in P^{32} labeled oligonucleosomes.

The endogenous production of PGF2α might begin on luteal day 12-14 in marmosets, and gradually inhibit LH-stimulated progesterone production (Michael *et al.*, 1994). Apoptosis would be delayed until the total luteal production of progesterone fell below a specific threshold – these studies suggest that threshold would be approximately 32nmol/L – at which point apoptosis could occur.

During non-apoptotic cell death damaged proteins may be hydrolysed by ubiquitin (Majno and Joris, 1995). Ubiquitin expression was only found in PGF2α, but not in

GnRH antagonist treated luteal tissue. The ubiquitin-mediated degradation of proteins is an energy-dependent system that requires ATP, and therefore ubiquitin expression can only occur in live cells (Majno and Joris, 1995). The finding that GnRH antagonist treated cells did not express ubiquitin could be interpreted to mean that all the cells were already dead, or that the cells were not in a cell death pathway, or that cell death was occurring via different mechanisms in PGF2α and GnRH antagonist treated animals.

The initial observations of steroidogenic cell vacuolation in H&E stained sections were interpreted as being indicative of cell death because of the morphological similarity to cells undergoing oncosis after an ischemic event. This was further supported by observing randomly fragmented DNA characteristic of necrosis (in the oligonucleosome study), and so the assumption was made that the fragmented DNA originated from the vacuolated cells. However, vacuolated cells were not 3' end labeled, which suggested that random DNA fragmentation did not occur in vacuolated cells, and that the DNA was intact. It is possible that the randomly fragmented DNA originated from only a small proportion of the vacuolated cells, and that a higher proportion of vacuolated cells were either in the very early stages of a death pathway, or were not undergoing cell death at all. The presence of ubiquitin suggested that the early stages of a non-apoptotic cell death pathway occurred 24 hours after PGF2α administration, but that the later stages of DNA fragmentation had not taken place. In contrast, the lack of ubiquitin, combined with the lack of 3' end labeled vacuolated cells, 24 hours after administration of GnRH antagonist, suggested that these cells had not progressed as far down a death pathway as had PGF2α treated cells. Therefore the lack of ubiquitin expression in vacuolated cells in GnRH antagonist treated animals and the presence of ubiquitin in PGF2α treated animals, suggested that GnRH antagonist treatment did not stimulate non-apoptotic cell death pathways, whereas PGF2α administration did.

Progesterone levels were significantly decreased 4 hours after the administration of GnRH antagonist to marmosets (Webley *et al.*, 1991), and macaques (Fraser *et al.*, 1986). The administration of hCG to marmosets 24 hours after administration of GnRH antagonist did not restore steroidogenesis (Webley *et al.*, 1991), and

macaques also failed to resume progesterone production after the administration of GnRH antagonist in the mid to late luteal phase (Fraser *et al.*, 1986). A recent study however, found that administration of the GnRH antagonist antide on luteal day 6 did not ablate progesterone production, which recovered to control levels 48 hours later (Duffy *et al.*, 1999). Administration of daily GnRH antagonist on luteal days 6, 7 and 8 caused steroidogenic cells to be vacuolated (Duffy *et al.*, 1999). Cell vacuolation, but not apoptosis was increased 12 hours after the administration of either PGF2α or GnRH antagonist to marmosets in these studies. This suggests that the primate corpus luteum can be subjected to decreased progesterone concentrations for 8-12 hours before apoptotic pathways are activated, but it is not known when vacuolation occurs in relation to decreased progesterone levels, nor the cause of vacuolation. Oil–Red-O staining, however, indicated that vacuolation was not due to an accumulation of intracellular lipid.

In summary, marmoset functional regression is not caused by apoptosis, but apoptotic cell death does occur during structural luteal regression. Another, non-apoptotic form of cell death in which ubiquitin plays a role appears to be stimulated by PGF2α, but not by GnRH antagonist. Lastly, decreased steroidogenesis may cause cytoplasmic vacuolation in luteal steroidogenic cells.

6.2 Vascular Changes and Luteal Regression

The induction of regression with luteolytic agents did not cause a decrease in endothelial cell numbers, indicating that the inhibition of steroidogenesis could occur independently of changes to the vasculature. This was supported by the examination of corpora lutea undergoing spontaneous functional regression *in vivo*, vascular changes were not observed. Therefore, functional luteal regression is not initiated by structural changes in the vasculature in primates.

The number of endothelial cells per unit area increased after the administration of luteolytic agents, but the number of Ki67 positive proliferating endothelial cells per unit area remained constant, indicating that the number of endothelial cells in each corpus luteum did not increase. Therefore the increase in the number of endothelial

cells per unit area was probably an artifact attributable to the dynamics of shrinking tissue. In this scenario steroidogenic cells died and the remaining non-steroidogenic cells occupied spaces left by deleted steroidogenic cells. Since the same unit area was scored before and after administration of luteolytic agents, there would appear to be increased numbers of endothelial cells per unit area.

The number of endothelial cells per unit area was significantly increased after administration of GnRH antagonist, but not after administration of PGF2α. Conversely, the incidence of apoptosis was slightly higher in PGF2α treated animals. It is likely that more endothelial cells underwent apoptosis after administration of PGF2α than after GnRH antagonist, resulting in fewer endothelial cells in PGF2α than in GnRH antagonist treated corpora lutea.

Endothelial cells do not express PGF2α receptors (Orlicky *et al.*, 1992) therefore endothelial cell apoptosis was probably mediated by PGF2α action on steroidogenic cells. The steroidogenic cell response to PGF2α which resulted in endothelial cell apoptosis was probably not a consequence of inhibition of LH-stimulated steroidogenesis, since the same effect was not observed after GnRH antagonist treatment. Endothelin 1 (ET-1) has been demonstrated in porcine (Flores *et al.*, 1995) and human (Apa *et al.,* 1998) corpora lutea and levels in bovine corpora lutea were highest during regression (Girsh *et al.*, 1996). ET-1 inhibited steroidogenic enzymes and progesterone production in rat granulosa cells (Tedeschi *et al.*, 1992) and inhibited progesterone production by human luteal cells *in vitro* (Apa *et al.*, 1998). ET-1 expression in bovine corpora lutea was significantly elevated 2 hours after administration of PGF2α but before a significant decrease in progesterone levels (Girsh *et al.*, 1996). Vasopressin and oxytocin also stimulated endothelial cell production of ET-1 (Girsh *et al.*, 1996), and PGF2α stimulated steroidogenic cell oxytocin production (Heath *et al.*, 1983).

Oxytocin and oxytocin receptors have been demonstrated in primate corpora lutea (Einspanier *et al.*, 1994; Dawood and Khan-Dawood 1986; Khan-Dawood and Dawood 1998), and receptor numbers peak during the mid luteal phase in baboons (Khan-Dawood *et al.,* 1993). Therefore it is possible that in primates, the endogenous production of PGF2α stimulates steroidogenic cell secretion of oxytocin, which

stimulates endothelial cell ET-1 production during the mid-luteal phase. Mid luteal phase endothelial cell production of ET-1 might inhibit steroidogenic cell progesterone production, and augment the direct inhibitory effects of PGF2α upon steroidogenesis. It is possible that a period of oxytocin stimulation is required to prime endothelial cells for apoptosis during structural luteal regression, and hence PGF2α, but not GnRH antagonist treatment would result in endothelial cell apoptosis at the end of functional luteal regression.

Endothelial cell numbers did not change during spontaneous functional or structural regression, although endothelial cell proliferation decreased significantly during functional regression, then increased during structural regression. Endothelial cells did not undergo apoptosis during functional regression, but probably did die by apoptosis during structural regression, suggesting that the increase in endothelial cell proliferation during structural regression served to maintain endothelial cell numbers. There was, however, a change from a pervasive network of capillaries during the mid luteal phase to a less extensive vascular bed comprised of larger arterioles and venules during structural luteal regression. It is possible that the combination of endothelial cell apoptosis and proliferation were required to effect this change. The extensive network of small blood vessels observed during the mid-luteal phase and functional regression was associated with steroidogenesis. The replacement of this vascular bed with a lower number of larger blood vessels during structural regression may have reflected a functional requirement to transport the debris of luteal regression away from the ovary.

6.3 The Role of PGF2α in Luteal Regression

Although primate luteal regression is not caused by PGF2α from the uterus (Beling *et al.*, 1970), primate corpora lutea produce prostaglandins (Challis *et al.*, 1976; Swanston *et al.*, 1977; Valenzuela *et al.*, 1983; Kauma *et al.*, 1990), and ovarian vein prostaglandin metabolite concentrations increase as luteolysis proceeds (Auletta *et al.*, 1984), therefore it is possible that endogenous PGF2α might be luteolytic in

primates. Administration of exogenous PGF2α to corpora lutea might mimic a spontaneous, *in vivo* mechanism.

Steroidogenic cells express PGF2α receptors, and PGF2α has been shown to inhibit LH receptor secondary messenger transduction (Behrman and Preston, 1989; Behrman and Aten, 1991), prior to and distal from LH-stimulated cAMP accumulation (Michael and Webley 1993), therefore PGF2α could inhibit LH-stimulated progesterone production and bring about functional luteal regression. The *in vivo* administration of PGF2α did not inhibit hCG stimulated steroidogenesis in pregnant marmosets (Hearn and Webley 1987), but it is possible that receptor transduction might be modulated by ligand binding, and LH might elicit a different response than hCG. The *in vivo* administration of PGF2α to marmosets in the mid luteal phase halved serum progesterone concentrations within an hour, and coadministration of hCG did not prevent inhibition of steroidogenesis (Webley *et al.*, 1991) supporting the premise that PGF2α inhibits LH receptor secondary messenger pathways.

The insertion of implants containing PGF2α into pig corpora lutea in the mid luteal phase resulted in significantly increased macrophage numbers 6 hours later, and significantly decreased progesterone levels 12 hours later (Hehnke *et al.,* 1994). Implants containing vehicle resulted in an increase in macrophage numbers but no change in progesterone concentration, indicating that the presence of macrophages alone did not induce luteolysis, but that the combination of macrophages and PGF2α was necessary for induction of functional luteolysis (Hehnke *et al.,* 1994). This supports the idea that the changing responsiveness of the corpus luteum to PGF2α might be related to the immigration of leukocytes, or accumulation of specific cytokines or growth factors, with increasing luteal age.

A number of leukocytes secrete factors which either inhibit gonadotrophin-stimulated steroidogenesis, or stimulate the production of oxygen free radicals, or stimulate steroidogenic cell production of PGF2α, and these interactions are summarised in Figure 6.1.

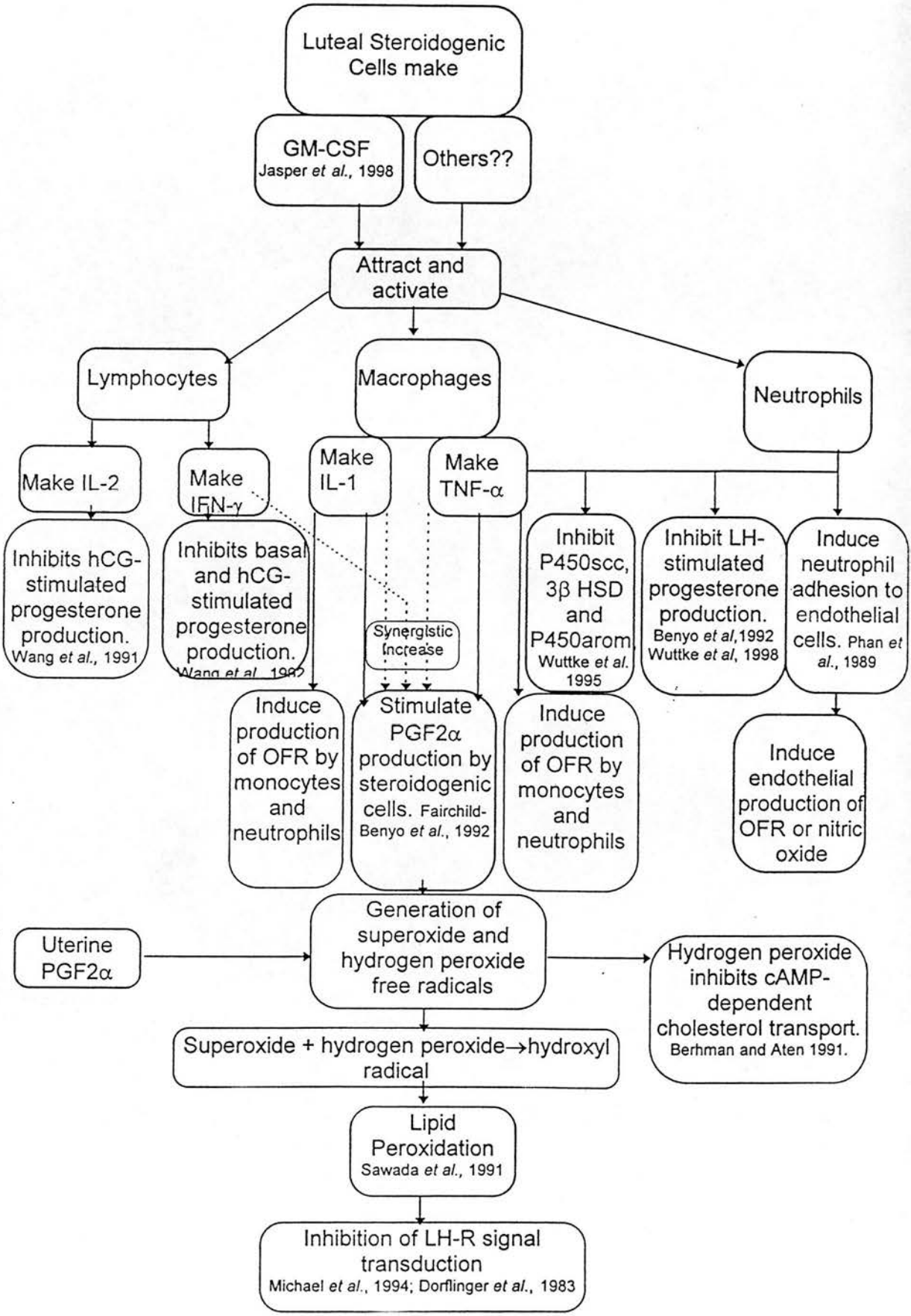

Figure 6.1: Mechanisms of Functional Luteal Regression

Data in this thesis support the hypothesis that endogenous steroidogenic cell production of PGF2α causes functional luteal regression by:

1. Stimulating steroidogenic cell hydrogen peroxide production with a consequent inhibition of cAMP-stimulated cholesterol transport and decreased steroidogenesis. Formation of LH-dependent cAMP was inhibited 15 minutes after administration of PGF2α in rats (Thomas *et al.*, 1978, Dorflinger *et al.*, 1983) and this was due to uncoupling of the G(s) protein from adenyl cyclase (Abayasekara *et al.*, 1993).
2. Inhibition of LH-R secondary messenger pathways, with a subsequent reduction in steroidogenic cell ability to respond to LH.
3. Stimulation of steroidogenic cell oxytocin production, which stimulates endothelial cell endothelin-1 production, which inhibits basal steroidogenic cell progesterone production.
4. Decreased steroidogenesis results in the generation of highly reactive oxygen free radicals. The combination of superoxide and hydrogen peroxide radicals produces the highly reactive hydroxyl ion, which causes lipid peroxidation, disruption of osmotic control and possible cytoplasmic vacuolation. May also disrupt receptor transduction pathways, by preventing the binding or dissociation of G-proteins.
5. Reduction of steroid hormone levels below a specific threshold results in the further generation of reactive oxygen free radicals which cause both random and apoptotic DNA fragmentation, with consequent apoptotic and non-apoptotic cell death.

6.4 The Relationship Between Functional and Structural Luteal Regression.

The original question about the initiating mechanism of luteal regression remains unanswered, although the temporal relationship between functional and structural regression has been clarified. In the marmoset monkey plasma progesterone concentrations were greatly reduced before the first signs of structural regression

were observed. These morphological changes were subtle; a slight decrease in parenchymal steroidogenic cell volume and a slight, nonsignificant increase in the number of vacuolated and apoptotic cells, but there was no change in the number of endothelial cells. The only major change was that the number of 3βHSD immunopositive cells decreased at this time. Major morphological changes only occurred after progesterone had fallen to follicular phase values and functional luteal regression was completed. The main morphological change during structural luteal regression was steroidogenic cells apoptosis or vacuolation.

It is therefore proposed that functional luteal regression largely precedes structural luteal regression in primates. This is clearly not the case in ruminants, in which functional and structural regression seem to occur simultaneously. These species differences appear to be related to the length of time available to remove luteal tissue. The ovine 'follicular phase' is a mere 24 hours, during which time structural luteal regression has to be essentially completed in order that there be room for a subsequent corpus luteum, whereas the regressing marmoset corpus luteum can complete structural regression during the 10 days of the follicular phase. In sheep, functional and structural luteal regression appear to proceed simultaneously. In cows there is some overlap between functional and structural regression, but not as much as in the sheep, and in the primate the two phases are essentially separated.

The use of luteolytic agents in marmosets suggested that the two components of luteolysis are partially independent of each other. Marmoset corpora lutea collected 12 hours after induction of luteolysis had falling progesterone values indicating that functional regression was in progress, and regressive morphological changes indicating that structural luteolysis was occurring at the same time. In spontaneously regressing corpora lutea functional and structural luteal regression occured one after the other, but after the administration of luteolytic agents functional and structural regression overlapped, suggesting that the temporal relationship between the two is flexible and structural regression can begin at any time after the initiation of functional luteal regression.

6.5 Future Directions

This thesis seems to have raised more questions than it has answered. The key questions, and some experiments to determine the answers, are summarised here.

1. Does hysterectomy fail to prevent luteolysis in marmosets as it does in other primates?

2. Does PGF2α production by the corpus luteum occur from luteal day 12 until regression is completed?
   Measure PGF2α and PGE luteal content and luteal secretion by corpora lutea collected on luteal days 10, 12, 15, 16, 18 and 20.

3. Do progesterone and/or estrogen protect against apoptosis?
   Induce luteal regression with either GnRH antagonist or PGF2α, but administer exogenous steroid hormones to maintain serum concentrations. Collect corpora lutea 24 hours after the administration of luteolytic agents and determine apoptotic index.

4. Which free radical species are generated *in vivo* during functional and luteal regression? Is apoptosis during luteolysis caused by oxygen free radicals?

5. Does exogenous PGF2α stimulate luteal ET-1 and/or oxytocin production in marmosets? Does the administration of GnRH antagonist fail to stimulate luteal ET-1 and or oxytocin production?
   Do ET-1 levels correlate with progesterone concentrations for individual animals?
   Immunocytochemistry for ET-1 and oxytocin on existing ovarian sections.

6.6 Summary

There were six key findings in this thesis: (1) Induction of luteal regression with either PGF2α or GnRH antagonist resulted in two morphological changes to

steroidogenic cells. One change had the morphological and biochemical features of apoptosis, and the other change resulted in the formation of cytoplasmic vacuoles which were not filled with lipid. (2) Steroidogenic cells in naturally regressing corpora lutea also developed cytoplasmic vacuoles, but these were qualitatively different from those formed after induced luteal regression. (3) Apoptosis in naturally regressing corpora lutea did not occur until after progesterone had decreased to follicular phase values, therefore apoptosis is unlikely to be an instigating mechanism in functional luteal regression. (4) Endothelial cell numbers remained constant after administration of luteolytic agents, indicating that induced luteal regression was not effected by vascular changes. (5) Similarly, the vascualture did not change during functional regression in untreated animals, but vascular remodelling occured during structural luteal regression. The vasculature changed from an extensive network of small capillaries to a system comprised of a lower number of larger blood vessels. (6) Luteal cell proliferation decreased during functional luteal regression.

6.7 Conclusion

Luteal regression in primates can be divided into two separate processes, functional luteal regression and structural luteal regression. Functional luteal regression is characterised by decreased steroidogenesis, and its completion can be delineated by the presence of follicular phase concentrations of serum progesterone. Decreased rates of cellular proliferation are concomitant with functional luteal regression, but the relationship between decreased proliferation and decreased steroidogenesis is unclear and requires further work. Functional regression is not caused by the apoptotic deletion of steroidogenic cells, nor by a decrease in endothelial cell numbers, nor by structural changes to the vasculature. It is suggested that the endogenous production of PGF2α commences on luteal day 12, and this inhibits LH-stimulated progesterone production. In addition, PGF2α may stimulate an oxytocin-ET-1 feedback loop that inhibits basal progesterone production. Decreased progesterone production may cause cytoplasmic vacuolation. Reduction in steroid hormone levels below a specific threshold results in the generation of highly reactive

oxygen free radicals that cause apoptotic cell death. Structural luteal regression is therefore characterised by decreased numbers of luteal cells, and by vascular remodelling to replace the extensive network of small blood vessels with a lower number of larger blood vessels suitable for transporting the debris of structural regression away from the ovary.

Bibliography

Abaysekara DRE, Michael AE, Webley GE, and Flint APF (1993) Mode of action of prostaglandin F2 alpha in human luteinised granulosa cells: role of portein kinase C. *Molecular and Cellular Endocrinology* **97** 81-91.
Abbott DH and Hearn JP (1978) Physical, hormonal and behavioural aspects of sexual development in the marmoset monkey, *Callithrix jacchus. Reproduction and Fertility* **53** 155-166.
Abbott DH, Hodges JK and George LM (1988) Social status controls LH secretion and ovulation in female marmoset monkeys (*Callithrix jacchus*). *Journal of Endocrinology* **117** 329-339.
Abbott DH (1992) Reproduction in female marmoset monkeys, *Callithrix jacchus* In: *Reproductive Biology of South American Vertebrates*. Editor WC Hamlett. Publ. Springer-Verlag, New York pp 245-261
Abbott DH, Saltzman W, Schultz-Darken and Smith TE (1997) Specific neuroendocrine mechanisms not involving generalized stress mediate social regulation of female reproduction in cooperatively breeding marmoset monkeys. *Annals of the New York Academy of Sciences* **807** 219-237
Abdul-Karim RW and Bruce NW (1973) Blood flow to the ovary and corpus luteum at different stages of gestation in the rabbit. *Fertility and Sterility* **24** 44-47.
Antczak M, Van Blerkom J and Clark A (1997) A novel method of vascular endotheial growth factor; leptin and transforming growth factor-β2 sequestration in a subpopulation of human ovarian follicle cells. *Human Reproduction* **12** 2226-2234
Arends MJ, Morris RG and Wyllie AH (1990) The role of the endonuclease, *American Journal of Pathology* **136** 593-608
Aten R, Duarte K and Berhman H (1992) Regulation of ovarian antioxidant vitamins, reduced glutathione and lipid peroxidation by luteinising hormone and prostaglandin F2a. *Biology of Reproduction* **46** 401-407.
Auletta FJ, Caldwell BV and Speroff L (1976) Estrogen-induced luteolysis in the rhesus monkey: reversal with indomethacin. *Prostaglandins* **11** 745-749.
Auletta FJ, Kamps DL, Pories S, Bisset J and Gibson M, (1984) An intracorpus luteum site for the luteolytic action of prostaglandin F2a in the rhesus monkey. *Prostaglandins* **27** 285-290.
Auletta FJ, Paradis DK, Wesley M and Duby RT (1984) Oxytocin is luteolytic in the rhesus monkey. *Journal of Reproduction and Fertility* 72 401-406.
Auletta FJ, Kamps DL, Wesley M and Gibson M (1984) Luteolysis in the rhesus monkey: ovarian venous estrogen, progesterone and prostaglandin F alpha-metabolite. *Prostaglandins* **27** 299-310.
Auletta FJ and Kelm LB (1994) Mechanisms controlling corpus luteum function in the rhesus monkey (Mucaca mulatta): inhibitory action of hCG on luteolysis induced by PGF2α. *Journal of Reproduction and Fertility* **102** 215-220.
Bacich DJ, Rohan RM, Norman RJ, and Rodgers RJ (1994) Characterization and relative abundance of alternatively spliced luteinizing hormone receptor messenger ribonucleic acid in the ovine ovary. *Endocrinology* **135** 735-744.
Backstrom CT, McNeilly AS, Leask RM and Baird DT (1982) Pulsatile secretion of LH, FSH, prolactin, oestradiol and progesterone during the human menstrual cycle. *Clinical Endocrinology* **17** 29-42.

Bagavandoss P, Kunkel S, Wiggins R and Keyes P (1988) Tumour necrosis factor-α production and localisation of mactophages and T lymphocytes in the rabbit corpus luteum. *Endocrinology* **122** 1185-1187.
Baird DT, Baker TG, McNatty KP and Neal P (1975) Relationship between the secretion of the corpus luteum and the length of the follicular phase of the ovarian cycle. *Journal of Reproduction and Fertility* **45** 611-619
Baird DT (1991) The ovarian cycle In, SG Hillier (ed) *Ovarian Endocrinology* Blackwell Scientific Publications, Oxford, England, pp 1-24
Basnakian AG and James SJ (1994) A rapid and sensitive assay for detection of DNA fragmentation during early phases of apoptotis. *Nucleic Acids Research* **22** 13 2714-2715
Basset SG, Little-Ihrig L, Mason JI and Zeleznik AJ (1991) Expression of messenger ribonucleic acids that encode for 3β-hydroxysteroid dehydrogenase and cholesterol side-chain cleavage enzyme throughout the luteal phase of the macaque menstrual cycle. *Journal of Clinical Endocrinology and Metabolism* **72** 362-366.
Basu A and Haldar S., (1998) The relationship between Bcl2, Bax and p53: consequences for cell cycle progression and cell death. *Molecular Human Reproduction* **4** 1099-1109.
Bayliss High OB (1982) Lipids. In *Theory and Practice of Histological Techniques* pp218-241, Ed. JD Bancroft & A Stevens.Churchill Livingstone, London.
Barret J, Abbott DH and George LM (1990) Extension of reproductive suppression by pheromonal cues in subordinate female marmoset monkeys, *Callithrix jacchus*. *Journal of Reproduction and Fertility* **2** 411-418.
Bellamy OC, Malcomson R, Harrison DJ and Wyllie AH (1995) Cell death in health and disease: the biology and regulation of apoptosis. *Cancer Biology* **6** 3-16.
Beling CG, Marcus SL and Markham SM (1970) Functional activity of the corpus luteum following hysterectomy. *Journal of Clinical Endocrinology* **30** 30-39.
Behrman HR, Aten RF and Pepperell JR (1991) Cell-to-cell interactions in luteinization and luteolysis In *Ovarian Endocrinology*, Ed. Hillier SG, Blackwell Scientific Publications
Behrman H and Aten R (1991) Evidence that hydrogen peroxide blocks hormone-sensitive cholesterol transport into mitochondria of rat luteal cells. *Endocrinology* **128** 6 2958-2966.
Behrman HR, Endo T, Aten RF, Musicki B (1993) Corpus luteum function and regression. *Reproductive Medicine Review* **2** 153-180.
Behrman H and Preston S (1989) Luteolytic actions of peroxide in rat ovarian cells *Endocrinology* **124** 2895-2900.
Bennegard B, Dennefors B and Hamberger L (1984) Interaction between catecholamines and prostaglandin F2 alpha in human luteolysis. *Acta Endocrinol Copenh.* **106** 532-537.
Bennegard B, Hahlin M and Hamberger L (1990) Luteotrophic effects of prostaglandins I2 and D2 on isolated human corpora luteum *Fertility and Sterility* **54** 459-464.
Bennegard B, Hahlin M, Wennberg E and Noren H, (1991) Local luteolytic effect of prostaglandin F2a in the human corpus luteum. *Fertility and Sterility* **56** 1070-1076.

Benyo DF and Pate JL (1992) Tumor necrosis factor-a alters bovine luteal cell synthetic capacity and viablility *Endocrinology* **130** 854-860.
Berges RR, Furuya Y, Remington L, English HF, Jacks T and Isaacs JT (1993) Cell proliferation, DNA repair, and P53 function are not required for programmed death of prostatic glandular cells induced by androgen ablation. *Proceedings of the National Academy of Sciences of the USA (Medical Sciences)* **90** 8910-8914.
Billig H, Furutta I and Hsueh AJ (1993) Estrogens inhibit and androgens enhance ovarian granulosa cell apoptosis *Endocrinology* **133** 5 2204-2211.
Billig H, Furuta Itsuko and Hsueh AJ (1994) Gonadotrophin-releasing hormone directly induces apoptotic cell death in the rat ovary: biochemical and in situ detection of deoxribonucleic acid fragmentation in granulosa cells. *Endocrinology* **134** 245-252
Boulton RA and Hodgson HJF (1995) Assessing cell proliferation: a methodological review. *Clinical Science* **88** 119-130.
Bowen ID (1984) Laboratory techniques for demonstrating cell death. In *Cell Ageing and Cell Death*, pp 5-40, Ed I Davies & D.C. Sigee. Cambridge University Press, Cambridge.
Bradley JR, Thiru S and Pober JS (1995) Hydrogen peroxide-induced endothelial cell retraction is accompanied by a loss of the normal spatial organisation of endothelial cell adhesion molecules. *American Journal of Pathology* **147** 627-641.
Brannian JD, Shiigi SM and Stouffer RL (1991) Differential uptake of fluorescent-tagged low density lipoprotein by cells from the primate corpus luteum: isolation and characterisation of subtypes of small and large luteal cells. *Endocrinology* **129** 3247-3252
Brannian JD, Stouffer RL, Shiigi SM and Hoyer PB (1993) Isolation of ovine luteal cell subpopulations by flow cytometry *Biology of Reproduction* **48** 495-502.
Brannstrom M and Janson PO (1991) The biochemistry of ovulation. In, SG Hillier (ed) *Ovarian Endocrinology* Blackwell Scientific Publications, Oxford, England, pp 132-166
Brannstrom M and Norman RJ (1993) Involvement of leukocytes and cytokines in the ovulatory process and corpus luteum function. *Human Reproduction* **8** 1762-1775
Bredt DS and Snyder SH (1994) Nitric oxide: a physiologic messenger molecule. *Annual Review of Biochemistry* **63** 175-195.
Bruce NW and Hillier K (1974) The effect of prostaglandin F2a on ovarian blood flow and corpora lutea regression in the rabbit. *Nature* **249** 176-177.
Bruce NW and Moor RM (1976) Capillary blood flow to ovarian follicles, stroma and corpora lutea of anesthetized sheep. *Journal of Reproduction and Fertility* **46** 299-304.
Brugal G, Dye R, Krief B, Chassery J-M, Tanke H and Tucker JH (1992) HOME: The Highly Optimized Microscope Environment. *Cytometry* **13** 109-116.
Bruno and Darzynkiewicz, (1992) Cell cycle dependent expression and stability of the nuclear protein detected by Ki67 antibody in HL-60 cells *Cell Proliferation* **25** 31-40
Bursch W, Paffe S, Putz B, Barthel G and Schulte-Hermann R (1990) Determination of the length of the histological stages of apoptosis in normal liver and in altered hepatic foci of rats. *Carcinogenesis* **11**, 5, 847-853.

Cameron JL and Stouffer RL, (1982) Gonadotropin receptors of the primate corpus luteum. II. Changes in available luteinizing hormone and chorionic gonadotropin-binding sites in macaque corpus luteal membranes during the nonfertile menstrual cycle. *Endocrinology* **110** 2068-2073.
'Cell cycle and replication' 1993 In: *Wheater's Functional Histology* Editors: PR Wheater, HG Burkitt, VG Daniels 3rd Edition pp 31-40
Challis JRG, Calder AA, Dilley S, Forster CS, Hillier K, Hunter DJS, MacKenzie IZ and Thorburn GD (1976) Production of prostaglandins E and F by corpora lutea, corpora albicantes and stroma of the human ovary *Journal of Endocrinology* **68** 401-408.
Chandrasekher YA, Brenner RM, Molskness TA, Yu Q and Stouffer RL (1991) Titrating luteinizing hormone surge requirements for ovulatory changes in primate follicles. II. Progesterone receptor expression in luteinizing granulosa cells. *Journal of Clinical Endocrinology and Metabolism* **73** 584-589
Chegnini N and Flanders KC (1992) Presence of transforming growth factor-β and their selective cellular localisation in human ovarian tissue of various reproductive stages *Endocrinology* **130** 1707-1715.
Christenson LK and Stouffer RL (1996) Isolation and culture of microvascular endothelial cells from the primate corpus luteum. *Biology of Reproduction* **55** 1397-1404.
Christenson LK and Stouffer RL (1997) Follicle-stimulating hormone and luteinizing hormone/chorionic gonadotrophin stimulation of vascular endothelial growth factor production by macaque granulosa cells from pre- and periovulatory follicles. *Journal of Clinical Endocrinolgy and Metabolism* **82** 2135-2142.
Chun SY, Billig H, Tilly J, Furura I, Tsafriri A, Hsueh AJ (1994) Gonadotrophin suppression of apoptosis in cultured preovulatory follicles: mediatory role of endogenous insulin-like growth factor-I. *Endocrinology* **135** 1845-1853
Clarke AR, Purdie CA, Harrison DJ, Morris RG, Bird CC, Hooper ML and Wyllie AH (1993) Thymocyte apoptosis induced by p53-dependent and independent pathways. *Nature* **362** 849-852.
Clarke PGH (1990) Developmental cell death: morphological diversity and multiple mechanisms. *Anatomical Embryology* **181** 195-213.
Clement PB (1987) Histology of the ovary. *American Journal of Surgical Pathology* **11** 277-303.
Cohen JJ (1991) Programmed cell death in the immune system. *Advances in Immunology* **50** 55-85.
Cole MD. (1986) The myc oncogene: its role in transformation and differentiation. *Annual Review of Genetics* **20** 361-384.
Corner GW. Sr. (1945) Development, organisation and breakdown of the corpus luteum in the rhesus monkey. *Contributions To Embryology*, **31** 117-146.
Corner GW Jr. (1956) The histological dating of the human corpus luteum of menstruation. *American Journal of Anatomy* **98** 377-401.
Cui K-H and Mathews CD (1994) Anatomy of the adult female common marmoset (Callithrix jacchus) reproductive system. *Journal of Anatomy* **185** 481-486
Culling, CFA (1974) Carbohydrates. In *Handbook of Histopathological and Histochemical Techniques (including museum techniques).* Third Edition Butterworths Chapter 14 pp259-269.

Dawood MY and Khan-Dawood F (1986) Human ovarian oxytocin. Its source and relationship to steroid hormones. *American Journal of Obstetrics and Gynaecology* **154** 756-763.
Deane HW, Hay MF, Moor RM, Rowson LE and Short RV (1966) The corpus luteum of the sheep: relationships between morphology and function during the oestrous cycle *Acta Endocrinologica* **51** 245-263.
Deghenghi R, Boutignon F, Wuthrich P and Lenaerts V (1993) Anterelix (EP 24332) a novel weter solubel LHRH antagonist. *Biomed and Pharmacother* **47** 107-110.
Delic J, Morange M and Magdelenat H (1993) Ubiquitin pathway involvement in human lymphocyte gamma irradiation induced apoptosis. *Molecular Cell Biology* **13**(8) 4875-83.
Dennefors BL, Sjogren A, Hamberger L (1982) Progesterone and adenoine 3',5'-monophosphate formation by isolated human corpora lutea of different ages: influences of human chorionic gonadotropin and prostaglandins. *Journal of Clinical Endocrinology and Metabolism* **55** 102-107.
Deveraux QL, Takahashi R., Salvesen GS and Reed JC (1997) X-linked IAP is a direct inhibitor of cell-death proteases. *Nature* **388** 300-304.
Dharmarajan AM, Goodman SB, Tilly KI and Tilly JL (1994) Apoptosis during functional corpus luteum regression: evidence of a role for chorionic gonadotropin in promoting luteal cell survival. *Endocrine Journal* **2** 295-303.
Diebold J, Dopfer K, Lai M and Lohrs U (1994) Comparison of different monoclonal antibodies for the immunohistochemical assessment of cell proliferation in routine colorectal biopsy specimens. *Scandinavian Journal of Gastroenterology* **29** 47-53.
Djahanbakhch O, McNeilly AS, Hobson BM and Templeton AA (1981) A rapid luteinising hormone radioimmunoassay for the prediction of ovulation *British Journal of Obstetrics and Gynaecology* **88** 1016-1020
D'Mello SR and Galli C (1993) SGP2, ubiquitin, 14K lectin and RP8 mRNAs are not induced in neuronal apoptosis. *Neuroreport* **4**(4) 355-8.
Doraiswamy V, Grazul-Bilska AT, Redmer DA and Reynolds LP (1995a) Immunoneutralisation of angiogenic activity from ovine corpora lutea (CL) with antibodies against fibroblast growth factor (FGF)-2 and vascular endothelial growth factor (VEGF.) *Biology of Reproduction* **52** (Supplement 1) 112.
Dorflinger L, Luborsky J, Gore S and Berhman H (1983) Inhibitory characteristics of prostaglandin F2α in the rat luteal cell. *Molecular and Cellular Endocrinology* **33** 225-241.
Duffy DM, Stewart DR and Stouffer RL (1999) Titrating luteinising hormone replacement to sustain the structure and function of the corpus luteum after gonadotrophin-releasing hormone antagonist treatment in rhesus monkeys. *Journal of Clinical Endocrinology and Metabolism* **84** 342-249.
Duncan WC, McNeilly AS, Fraser HM, and Illingworth PJ (1996) Luteinizing hormone receptor in the human corpus luteum: lack of down-regulation during maternal recognition of pregnancy. *Human Reproduction* **11** 2291-2297.
Duncan WC, Illingworth PJ and Fraser HM (1996) Expression of the tissue metalloproteinases-1 in the primate ovary during induced luteal regresssion. *Journal of Endocrinology* **151** 203-213.

Duncan WC, McNeilly AS and Illingworth PJ (1996) Expression of tissue inhibito or metalloproteinases-1 in the human corpus luteum after luteal rescue. *Journa of Endocrinology* **148** 59-67.
Duncan WC, Illingworth PJ, Young FM and Fraser HM (1997), Induced luteolysis in the primate: rapid loss of luteinising hormone (LH) receptors. *Human Reproduction* **13**, 9, 203-213
Eley RM, Summers PM and Hearn JP (1987) Failure of the prostaglandin F2 alpha analogue, cloprostenol, to induce functional luteolysis in the olive baboon (*Papio cynocephalus anubis*) *Journal of Medical Primatology* **16** 1-11.
Einspanier A, Jarry H, Pitzel L, Holtz W and Wuttke W (1991) Determination of the secretion rates of estradiol, progesterone, oxytocin, and angiotensin II from teriary follicles and freshly fromed corpora lutea in freely moving sows. *Endocrinology* **129** 3404-3409.
Einspanier A, Ivell R, Rune G and Hodges JK (1994) Oxytocin gene expression and oxytocin immunoactivity in the ovary of the common marmoset monkey (*Callithrix jacchus*). *Biology of Reproduction* **50** 1216-1222.
Einspanier A, Jurdzinski A and Hodges JK (1997) A local oxytocin system is part of the luteinization process in the preovulatory folicle of the marmoset monkey (Callithrix jacchus). *Biology of Reproduction* **57** 16-26
Enders AC (1973) Cytology of the corpus luteum. *Biology of Reproduction* **8** 158-182.
Enright H, Hebbel RP and Nath KA (1994) Internucleosomal cleavage of DNA as the sole criterion for apoptosis may be artifactual. *Journal of Laboratory Clinical Medicine* **124** 63-68
Evan GI, Wyllie AH, Gilbert GS, Littlewood TD, Land H, Brooks M, Waters CM, Penn LZ and Hancock DC (1992) Induction of apoptosis in fibroblasts by c-myc protein. *Cell* **69** 119-128.
Eppig JJ (1991) Mammalian oocyte development In, Stephen G Hillier (ed.), *Ovarian Endocrinology* Publ Blackwell Scientific Publications, Oxford, England, pp 107-131
Fairchild-Benyo D, Little-Ihrig L and Zeleznik AJ (1993) Noncoordinated expression of luteal cell messenger ribonucleic acids during human chorionic gonadotropin stimulation of the primate corpus luteum. *Endocrinology* **133** 699-704.
Fairchild-Benyo D, Ravindranath N, Basset S, Hutchieson J and Zeleznik AJ (1993) Cellular aspects of corpus luteum function in the primate. *Human Reproduction* **8** 102-106
Fehrenbach A, Einspanier A, Nicksch E and Hodges JK (1995) Assessment of tissue integrity, ultrastructure and steroidogenic activity of corpora lutea of the marmoset monkey, *Callithrix jacchus*, following *in vitro* microdialysis. *Tissue and Cell* **27** 4 467-481.
Fields PA (1984) Intracellular localisation of relaxin in membrane-bound granules in the pregnant rat luteal cell *Biology of Reproduction* **30** 753-762.
Fields PA and Fields MJ (1985) Ultrastructural localisation of relaxin in the corpus luteum of the nonpregnant, psuedopregnant and pregnant pig *Biology of Reproduction* **18** 94-98.
Fitz TA, Mayan MH, Sawyer HR and Niswender GD (1982) Characterisation of two steroidogenic cell types in the ovine corpus luteum. *Biology of Reproduction* **27** 703-711.

Flores JA, Winters TA, Knight JW and Veldhuis JD (1995) Nature of endothelin binding in the porcine ovary. *Endocrinology* **136** 5014-5019.
Fraser HM, Abott M, Laird NC, McNeilly AS, Nestor JJ and Vickery BH (1986) Effects of an LH-releasing hormone antagonist on the secretion of LH, FSH, prolactin and ovarian steroids at different stages of the luteal phase in the stumptailed macaque (*Macaca arctoides*). *Journal of Endocrinology* **111** 83-90.
Fraser HM, Nestor Jr JJ and Vickery BH (1987) Suppression of luteal function by a luteinizing hormone-releasing hormone antagonist during the early luteal phase in the stumptailed macaque monkey and the effects of subsequent administration of human chorionic gonadotropin. *Endocrinology* **121** 612-618.
Fraser HM, Robertson DM and de Kretser DM (1989) Immunoreactive inhibin concentrations in serum throughout the menstrual cycle of the macaque: suppression of inhibin during the luteal phase after treatment with an LHRH antagonist. *Journal of Endocrinology* **121** R9-R12.
Fraser HM, Lunn SF, Whitelaw PF and Hillier SG (1995a) Induced luteal regression: differential effects on follicular and luteal inhibin/activin subunit mRNAs in the marmoset monkey. *Journal of Endocrinology* **144** 201-208.
Fraser H, Lunn S, Cowen G and Illingworth P (1995b) Induced luteal regression in the primate: evidence for apoptosis and changes in c-myc protein. *Journal of Endocrinology* **147** 131-137.
Fraser HM, Lunn SF, Morris KD, Deghenghi R. (1997) Initiation of high dose GnRH antagonist treatment during the late follicular phase in the macaque abolishes luteal function irrespective of effects upon the LH surge. *Human Reproduction* **12**, 101-106.
Friedman CI, Danforth DR, Herbosa-Encarnacion C, Arbogast L, Alak BM and Seifer DB (1997) Follicular fluid vascular endothelial growth factor concentrations are elevated in women of advanced reproductive age undergoing ovulation induction. *Fertility and Sterility* **68** 607-512.
Fridovich I (1986) Biological effects of the superoxide radical. *Archives of Biochemistry and Biophysics* **247** 1-11.
Fulghesus AM, Lanzone A, Di Simone N, Nicoletti MC, Caruso A and Mancuso S (1993) Indomethacin *in vivo* inhibits the enhancement of the progesterone secretion in reponse to gondotrophin-releasing hormone by human corpus luteum. *Human Reproduction* **8** 35-39.
Fuller GB and Hansel W (1970) Regression of sheep corpora lutea after treatment with antibovine luteinising hormone. *Journal of Animal Science* **31** 99-103.
Gatzuli E, Aten R and Berhman HR (1991) Inhibition of gonadotrophin action and progesterone synthesis by xanthine oxidase in rat luteal cells. *Endocrinology* **128** 2253-2258.
Gavrieli Y, Sherman Y and Ben-Sasson SA (1992) Identification of programmed cell death in situ via specific labeling of nuclear DNA fragmentation *Journal of Cell Biology* **119** 493-501.
Gerber HP, Condorelli F, Park J and Ferrera N (1997) Differential transcriptional regulation of the two vascular endothelial growth factor receptor genes. Flt-1, but not Flk-1/KDR is upregulated by hypoxia. *Journal of Biological Chemistry* **272** 23659 - 23667.

Gerdes J, Schwab U, Lemke H and Stein H, (1983) Production of a mouse monoclonal antibody reactive with a human nuclear antigen associated with cell proliferation. *International Journal of Cancer* **31** 13-21
Gerdes J, Lemke H, Baisch H, Wacker H.H, Schwab U and Stein H (1984) Cell cycle analysis of a cell proliferation-associated human nuclear antigen defined by the monoclonal antibody Ki67. *The Journal of Immunology* **133** 1710-1715.
Gemmell RT, Stacy BD and Thorburn GD (1974) Ultrastructural study of secretory granules in the corpus luteum of the sheep during the estrous cycle *Biology of Reproduction* **11** 447-462.
Gibson M and Auletta FJ (1986) Effect of prostaglandin synthesis inhibition on human corpus luteum function. *Prostaglandins* **31** 1023-1028.
Giebel J, Hegele-Hartung C and Rune GM (1997) Proliferation and apoptosis in follicles of the marmoset monkey (Callithrix jacchus) ovary. *Anat Anz* **179** 413-419
Gilchrist RB, Wicherek M, Nayudu PL, Norman RJ, Armstrong DT and Hodges JK (1999) Changes in ovarian follicle distribution in the marmoset monkey: relation to cycle stage and age. Proceedings of the 11th World Congress on IVF and Human Reproductive Genetics, Sydney
Girsh E, Greber Y and Meidan R (1995) Luteotrophic and luteolytic interactions between bovine small and large luteal-like cells and endothelial cells. *Biology of Reproduction* **52** 954-962.
Girsh E, Wang W, Mamluk R, Arditi F, Friedman A, Milvae RA and Meidan R (1996) Regulation of endothelin-1 expression in the bovine corpus luteum: elevation by prostaglandin F2 alpha. *Endocrinology* **137** 5189-5190.
Gillim SW, Christensen AK. and McLennan CE (1969) Fine structure of the human menstrual corpus luteum at its stage of maximum secretory activity. *American Journal of Anatomy* **126** 409-428.
Goding JR (1974) The demonstration that PGF2a is the uterine luteolysin in the ewe. *Journal of Reproduction and Fertility* **38** 261-271.
Gore BZ, Caldwell BV and Speroff L (1973) Estrogen-induced human luteolysis. *Journal of Clinical Endocrinology and Metabolism* **36** 615-619.
Gordon JD, Mesiano S, Zaloudek CJ and Jaffe RB (1996) Vascular endothelial growth factor localisation in human ovary and fallopian tubes: possible role in reproductive function and ovarian cyst formation. *Journal of Clinical Endocrinology and Metabolism* **81** 353-359.
Gougeon A (1982) Rate of follicular growth in the human ovary. In *Follicular Maturation and Ovulation*, Ed. Rolland R, pp 155-163. Excerpta Medica, Amsterdam.
Gougeon A (1998) Ovarian follicular growth in humans: ovarian aging and population of growing follicles. *Maturitas* **30** 137-142
Grinwich DL, Hichens M and Behrman HR, (1976) Control of the LH receptor by prolactin and prostaglandin F2α in rat corpora lutea. *Biology of Reproduction* **14** 212-218.
Groome NP, Illingworth PJ, O'Brien M, Pai R, Rodger FE, Mather JP and McNeilly AS (1996) Measurement of dimeric inhibin B throughout the human menstrual cycle. *Journal of Clinical Endocrinology and Metabolism* **81** 1401-1405
Guedes MLC and Miraglia T (1977) The rete ovarii and follicle formation in marmosets (Callithrix jacchus and Callithrix pencillata) *Acta hisotchem* **60** 247-252

Guo K, Wolf V, Dharmarajan AM., Feng Z., Bielke W, Saurer S and Friis R (1998) Apoptosis-associated gene expression in the corpus luteum of the rat. *Biology of Reproduction* **58** 739-746.
Haas AL, Baboshina O, Williams B and Schwartz LM (1996) Coordinated induction of the ubiquitin conjugation pathway accompanies the developmentally programmed death of insect skeletal muscle. *Journal of Biological Chemistry* **270** (16) 9407-12.
Haas AL and Bright PM (1985) The immunochemical detection and quantification of intracellular ubiquitin-protein conjugates. *The Journal of Biological Chemistry* **260** 23 12464-12473.
Haecker G and Vaux D (1994) Viral, worm and radical implications for apoptosis. *TIBS* **19** 99-100
Halliwell B and Gutteridge J (1989) Oxygen is poisonous - an introduction to oxygen toxicity and free radicals. In *Free Radicals in Biology and Medicine*, Clarendon Press, Oxford pp 10-15.
Hamburger V and Levi-Montalcini (1949) Proliferation, differentiation and degeneration in the spinal ganglion of the chick under normal and experimental conditions. *Journal of Experimental Zoology* **111** 457-462.
Harding RD, Hulme MJ, Lunn SF, Henderson S and Aitken RJ (1982) Plasma progesterone levels throughout the ovarian cycle of the common marmoset (*Callithrix jacchus*) *Journal of Medical Primatology* 11 43-51.
Harlow CR., Hearn JP and Hodges JK (1984) Ovulation in the marmoset monkey: endocrinology, prediction and detection. *Journal of Endocrinology* **103** 17-24.
Harter L and Erkert HG (1993) Alteration of circadian period length does not influence the ovarian cycle length in common marmosets, Callithrix jacchus (Primates). *Chronobiology International* **10** 3 165-175
Harrison LM, Kenny N and Niswender GD (1987) Progesterone production, LH receptors and oxytocin secretion by ovine luteal cell types on days 6, 10 and 15 of the oestrous cycle and day 25 of pregnancy. *Journal of Reproduction and Fertility* **79** 539-548.
Hasumoto K, Sugimoto Y, Yamasaki A, Morimoto K, Kakizuka A, Negishi M and Ichikawa A (1997) Association of expression of mRNA encoding the PGF2α receptor with luteal cell apoptosis in ovaries of psuedopregnant mice. *Journal of Reproduction and Fertility* **109** 45-51.
Hearn JP (1983)The common marmoset (Calithrix jacchus) from Reproduction in *New World Primates, New Models in Medical Science* Editor JP Hearn pp183-215
Hearn JP (1987) Marmosets and tamerins, In *The Care and Mangement of Laboratory Animals* 6th Edition Publ Longman Scientific and Technical Editor T. Poole PP 568-579
Hearn JP and Webley GE (1987) Regulation of the corpus luteum of early pregnancy in the marmoset monkey: local interactions of luteotrophic and luteolytic hormones *in vivo* and their effects on the secretion of progesterone. *Journal of Endocrinology* **114** 231-239.
Heath E, Weinstein P, Merritt B, Shanks R, Hixon J (1983) Effects of prostaglandins on the bovine corpus luteum: granules, lipid inclusions and progesterone secretion. *Biology of Reproduction* **29** 977-985.

Heger W, Hoyer GA and Neubert D (1988) Identification of the main gestagen metabolite in marmoset (*Callithrix jacchus*) urine by NMR HPLC and MS spectroscopy. *Journal of Medical Primatology* **17** 19-29.
Heger W and Neubert D (1987) Determination of ovulation and pregnancy in the marmoset (*Callithrix jacchus*) by monitoring of urinary hydroxypregnanolone excretion. Journal of Medical Primatology **16** 151-164.
Hehnke KE, Christenson LJ, Ford SP and Taylor M (1994) Macrophage infiltration into the procine corpus luteum during prostaglandin F2α-induced luteolysis. *Biology of Reproduction* **50** 10-15.
Hehnke-Vagnoni KE, Clark CE, Taylor MJ and Ford SP (1995) Presence and localisation of tumor necrosis factor alpha in the corpus luteum of nonpregnant and pregnant pigs. *Biology of Reproduction* **53** 1339-1344.
Hershko A (1988) Ubiquitin-mediated protein degradation. *The Journal of Biological Chemistry* **263** 30 15237-15241.
Hild-Petito SA, Shiigi SM and Stouffer RL (1989) Isolation and characterization of cell subpopulations from the monkey corpus luteum of the menstrual cycle. *Biology of Reproduction* **40** 1075-1085.
Hillier SG, Harlow CR, Shaw HJ, Wickings EJ, Dixson AF and Hodges JK (1987) Granulosa cell differentiation in primate ovaries: the marmoset monkey (*Callithrix jacchus*) as a laboratory model. In Stouffer, R.L. (ed.), *The Primate Ovary*. Plenum Press, New York, NY, USA, pp 61-73
Hillier SG (1991) Cellular basis of follicular endocrine function In, SG Hillier (ed) *Ovarian Endocrinology* Blackwell Scientific Publications, Oxford, England, pp 73-106
Hillier SG., Harlow CR., Shaw HJ., Wickings EJ., Dixson AF and Hodges JK (1988) Cellular aspects of pre-ovulatory folliculogenesis in primate ovaries. *Human Reproduction* **3** 501-511
Hillier SG, Tetsuka M and Fraser HF (1997) Location and developmental regulation of androgen receptor in primate ovary. *Human Reproduction* **12** 107-111
Hockenbery DM, Zutter M, Hickey W, Nahm M and Korsmeyer SJ (1991) BCL2 protein is topographically restricted in tissues characterized by apoptotic cell death. ***Proceedings of the National Academy of Sciences***, USA, **88** 6961-6965
Hockenberry D (1995) Defining apoptosis ***American Journal of Pathology*** **146** 16-19
Hodges JK, Cottingham PG, Summers PM and Yingnan L (1987) Controlled ovulation in the marmoset monkey (Callithrix jacchus with human chorionic gonadotropin following prostaglandin-induced regression. *Fertility and Sterility* **48** 299-305.
Hodges JK., Green DI., Cottingham PG., Sauer MJ., Edwards C and Lightman SL (1988) Induction of luteal regression in the marmoset monkey (*Callithrix jacchus*) by a gonadotrophin-releasing hormone antagonist and the effects on subsequent follicular development. *Journal of Reproduction and Fertility* **82** 743-752.
Horten EW and Poyser NL (1976) Uterine luteolytic hormone: a physiological role for prostaglandin F2 alpha. *Physiological Reviews* **56** 595-651.

Houmard BS and Ottobre JS (1989) Progesterone and prostaglandin production by primate luteal cells collected at variouys stages of the luteal phase: modulation by calcium ionophore. *Biology of Reproduction* **41**(3) 401-408.
Howie S, Sommerfield A, Gray E and Harrison DJ (1994) Peripheral T lymphocyte deletion by apoptosis after CD4 ligation in vivo: selective loss of CD 44 and "activating" memory T cells. *Clinical and Experimental Immunology* **95** 195-200.
Hsueh AJ and Jones PB (1981) Extrapituitary actions of gonadotrophin releasing hormone. *Endocrine Review* **2** 437-461
Hsueh JW, Billig H and Tsafriri A (1994) Ovarian follicle atresia: a hormonally controlled apoptotic process. *Endocrine Reviews* **15** 6 707-724
Huang SI, Barnard MB, Xu M, Matsui SI, Rose SE and Garrard WT (1986) The active immunoglobulin κ chain gene is packaged by non-ubiquitin-conjugated nucleosomes. *Proceedings of the National Academy of Sciences, USA*. **83**, 3738-3742
Hutchison JS and Zeleznik AJ (1985) The corpus luteum of the primate menstrual cycle is capable of recovering from a transient withdrawal of pituitary gonadotrophin support. *Endocrinology* **117** 1043-1049.
Hutchison JS, Nelson PB and Zeleznik AJ (1986) Effects of different gonadotropin pulse frequencies on corpus luteum function during the menstrual cycle of rhesus monkeys *Endocrinology* **119** 1964-1967.
Hutchison JS, Kubrik CJ, Nelson PB and Zeleznik AJ (1987) Estrogen induces premature luteal regression in rhesus monkeys during spontaneous menstrual cycles, but not in cycles driven by exogenous gonadotrophin-releasing hormone. *Endocrinology* **121** 466-474.
Illingworth PJ, Fraser HM, Young FM, Lunn SF and Cowen GM (1994) Localisation of C-myc in the human corpus luteum. Abstr 969 Endocrine Society, 76th Annual Meeting.
Irmler M, Thomas M, Hahne M, Schneider P, Hofman K, Steiner V, Bodmer J, Schroter M, Burns K, Mattman C, Rimoldi D, French L and Tschopp J (1997) Inhibition of death receptor signals by cellular FLIP. *Nature* **388** 190-195.
Jablonka-Shariff A and Olson LM, (1997) Hormonal regulation of nitric oxide synthases and their cell-specific expression during follicular development in the rat ovary *Endocrinology* **138** 460-468.
Jablonka-Shariff A, Grazul-Biska AT, Redmer DA and Reynolds LP (1993) Growth and cellular proliferation of ovine corpora lutea throughout the estrous cycle. *Endocrinology* **138** 1871-1879.
Jakeman LB, Winer J, Bennett GL, Altar CA and Ferrara N (1992) Binding sites for vascular endothelial growth factor are localised on endothelial cells in adult rat tissues. *Journal of Clinical Investigations* **89** 244-253.
Jasper MJ, Brannstom M, Olofsson JD, Petrucco OM, Mason H, Robertson SA and Norman RJ (1996) Granulocyte-macrophage colony-stimulating factor: presence in human follicular fluid, protein secretion and mRNA expression by ovaria cells. *Molecular Human Reproduction* **2** 555-562.
Ji I, Slaughter R, Ellis J, Ji T and Murdoch W (1991) Analyses of ovine corpora lutea for tumor necrosis factor mRNA and bioactivity during prostaglandin-induced luteoysis. *Molecular and Cellular Endocrinology* **81** 77-80.

Jo T, Tomiyama T, Ohashi K, Saji F, Tanizawa O, Ozaki M, Yamamoto R, Yamamoto T, Nishizawa Y and Terada N (1995) Apoptosis of cultured mouse luteal cells induced by tumor necrosis factor-alpha and interferon-gamma. *Anatomical Records* **241** 70-76.
Jones S, Roland NJ, Caslin AW, Cooke TG, Cooke LD and Forster G (1994) A comparison of cellular proliferation markers in squamous cell carcinoma of the head and neck. *Journal of Laryngology and Otology* **108** 859-864.
Juengel JL, Garverick HA, Johnson Al, Youngquist RS and Smith MF (1993) Apoptosis during luteal regression in cattle. *Endocrinology* **132** 250-254.
Kaltenbach C, Graber J, Niswender G and Nalbandov A (1968) Luteotrophic properties of some pituitary hormones in nonpregnant or pregnant hypophysectomised ewes *Endocrinology* **82** 818-824.
Kamat KR, Brown LF, Manseau EJ, Senger DR and Dvorak HF (1995) Expression of vascular permeability factor/vascular endothelial growth factor by human granulosa and theca lutein cells. Role in corpus luteum development. *American Journal of Pathology* **146** 157-165.
Karim SMM and Hillier SK (1979) Prostaglandins in the control of animal and human reproduction. *British Medical Bulletin* **35** 173-180
Kauma SW, Curry TE, Powell DE, Clark MR (1990) Localisation of prostaglandin endoperoxide synthase in the human corpus luteum *Human Reproduction* **5**(7) 800-804
Kenny N, Williams RE and Kelm LB (1994) Spontaneous apoptosis of cells prepared from the nonregressing corpus luteum. *Biochemistry and Cell Biology* **72** 531-536.
Kerr JFR (1971) Shrinkage necrosis: a distinctive mode of cellular death. *Journal of Pathology* **105**, 13-20.
Kerr JFR, Wylie AH and Currie AR (1972) Apoptosis: A basic biological phenomenon with wide-ranging implications in tissue kinetics. *British Journal of Cancer* **26** 239, 18-27.
Khan-Dawood FS (1987) Immunocytochemical localisation of oxytocin and neurophysin in human corpora lutea. *American Journal of Anatomy* **179** 18-24
Khan-Dawood FS, Goldsmith LT, Weiss G and Dawood MY (1989) Human corpus luteum secretion of relaxin, oxytocin and progesterone *Journal of Clinical Endocrinology and Metabolism* **68** 627-631.
Khan-Dawood FS, Kanu EJ and Dawood MY (1993) Baboon corpus luteum: Presence of oxytocin receptors. *Biology of Reproduction* **49** 262-266.
Khan-Dawood FS and Dawood MY (1998) Comparitive aspects of oxytocin in baboon (Papio hamadryus anubis) and human corpora lutea. *Human Reproduction* Update **4** 371-382.
Khanna A, Aten R and Behrman H (1995) Heat shock protein-70 induction mediates luteal regression in the rat. *Molecular Endocrinology* **9** 11 1431-1440.
Kholkute SD and Nandedkar T (1983) Follicular growth and induction of ovulation by gonadotrophins in the comon marmoset, Callithrix jacchus. *Indian Journal of Experimental Biology* **21** 536-538
Knickerbocker JJ, Wiltbank MC and Niswender GD (1988) Mechanisms of luteolysis in domestic livestock. *Domestic Animal Endocrinology* **5** 91-107

Kondo H, Maruo T and Mochizuki M (1995) Immunohistochemical evidence for the presence of tumor necrosis factor-alpha in the infant and adult human ovary *Endocrine Journal* **42** 771-780.
Kyprianou N, English HF and Isaacs JT (1988) Activation of a Ca2+-Mg2+-dependent endonuclease as an early event in castration-induced prostatic cell death. *Prostate* **13** 103-107.
Lahav M, West LA, and Davies JS (1988) Effects of prostaglandin F2 alpha and a gonadotropin releasing agonist on inositol phospholipid metabolism in isolated rat corpora lutea of various ages. *Endocrinology* **123** 1044-1052.
Laitinen M, Ristimaki A, Honkasalo M, Narko K, Paavonen K and Ritvos O (1997) Differential hormonal regulation of vascular endothelial growth factors VEGF, VEGF-B, and VEGF-C messenger ribonucleic acid levels in cultured human granulosa-luteal cells. *Endocrinology* **138** 4748-4756.
Lauzon RJ, Patton CW and Weissman IL (1993) A morphological and immunohistochemical study of programmed cell death in *Botryllus schlosseri* (Tunicata, Ascidiacea). *Cell Tissue Research* **272** 115-127.
Lee C, Coulam C, Jiang N and Ryan R (1973) Receptors for human luteinizing hormone in human corpora lutea tissue *Journal of Clinical Endocrinology and Metabolism* **36** 148-152.
Lei ZM, Chegini N and Rao ChV (1991) Quantitative cell composition of human and bovine corpora lutea from various reproductive states. *Biology of Reproduction* **44** 1148-1156.
Levinger L and Varhavsky A (1982) Selective arrangement of ubiquitinated and D1 protein-containing nucleosomes within the *Drosophila* genome. *Cell* **28** 375-385
Li TC, Rogers AW and Dockery P (1988) A new method of histologic dating of human endometrium in the luteal phase*Fertility and Sterility* **50** 52-60.
Liu JH and Yen SSC (1983) Induction of midcycle gonadotopin surge by ovarian steroids in women: a critical evaluation. *Journal of Clinical Endocrinology and Metabolism* **57** 797-802.
Lopez-Ruiz MP, Choi MSK, Rose MP, West AP and Cooke BA (1992) Direct effect of arachadonic acid on protein kinase C and LH-stimulated steroidogenensis in rat leydig cells; evidence for tonic inhibitory control of steroidogenesis by protein kinase C. *Endocrinology* **130** 1122-1130.
Macklon NS and Fauser BCJM (1998) Follicle development during the normal menstrual cycle. *Maturitas* **30** 181-188
Majno G and Joris I (1995) Apoptosis, oncosis and necrosis; an overview of cell death. *American Journal of Pathology* **146** 3-15.
March CM., Goebelsmann U., Nakamura RM and Mishell DR (1979) Roles of oestradiol and progesterone in eliciting the midcycle luteinizing hormone and follicle-stimulating hormone surges. *Journal of Clinical Endocrinology and Metabolism* **49** 507-513.
Mais V, Kazer RR, Cetel NS, Rivier J, Vale W and Yen SSC (1986) The dependency of folliculogenesis and corpus luteum function on pulsatile gonadotropin secretion in cycling women using a gonadotropin-releasing hormone antagonist as a probe. *Journal of Clinical Endocrinology and Metabolism* **62** 1250-1255.
Marsh J (1970) The stimulatory effect of luteinizing hormone on adenyl cyclase in the bovine corpus luteum. *Journal of Biological Chemistry* **245** 1596-1603.

McClure N, Macpherson AM, Healy DL, Wreford and Rogers PAW (1994) An immunohistochemical study of the vascularisation of the human graafian follicle. *Human Reproduction* **9** 1401-1405.
McCracken JA, Glew ME and Scaramuzzi R (1970) Corpus luteum regression induced by prostaglandin F2a. *Journal of Clinical Endocrinology and Metabolism* **30** 544-546.
McClellan MC, Diekman MA, Abel JH and Niswender GD (1975) Interrelationships between luteinising hormone, progesterone and the morphological development of normal and superovulated corpora lutea in sheep. *Cell and Tissue Research*
McNatty KP, Makris A, deGrazia C, Osathanondh R and Ryan KS, (1979) The production of progesterone, androgens and oestrogens by human granulosa cells, thecal tissue and stromal tissue from human ovaries in vitro. *Journal of Clinical Endocrinology and Metabolism* **49**: 687-690.
McNeilly AS, Kerin J, Swanston I, Bramley T and Baird D (1980) Changes in the binding of human chorionic gonadotropin/luteinizing hormone, follicle stimulating hormone and prolactin to human corpora lutea during the menstrual cycle and pregnancy *Journal of Endocrinology* **87** 315-325.
Michael AE, Abayasekara DRE, and Webley GE, (1994) Cellular mechanisms of luteolysis *Molecular and Cellular Endocrinology* **99** R1-R9.
Michael AE and Webley GE (1991) Prostaglandin F2 alpha stimulates cAMP phosphodiesterase via protein kinase C in cultured human granulosa cells. *Molecular and Cellular Endocrinology* **82** 207-214
Michael A and Webley GE (1993) Roles of cyclic AMP and inositol phosphates in the luteolytic action of cloprostenol, a prostaglandin F2a analogue, in marmoset monkeys (*Callithrix jacchus*). *Journal of Reproduction and Fertility* **97** 424-431.
Modlich U, Kaup F-P, Augustin H (1996) Cyclic angiogenesis and blood vessel regression in the ovary: blood vessel regression during luteolysis involves endothelial cell detachment and vessel occlusion. *Laboratory Investigation* **74** 771-780.
Monroe AK, Atkinson LE and Knobil E (1970) Patterns of circulating luteinizing hormone and their relation to plasma progesterone levels during the menstrual cycle of the rhesus monkey. *Endocrinology* **87** 453-456.
Morris RG, Hargreave AD, Duvall E and Wyllie AH (1984) Hormone induced cell death: Surface changes in thymocytes undergoing apoptosis. *American Journal of Pathology* **115** 426-436.
Murdoch WJ (1995) Temporal relationships between stress protein induction, progesterone withdrawal and apoptosis in corpora lutea of ewes treated with prostaglandin F 2 alpha. *Journal of Animal Science* **73** 1789-1792.
Murdoch WJ, Austin KA and Hansen TR (1996) Polyubiquitin upregulation in corpora lutea of prostaglandin treated ewes. *Endocrinology* **137** 10 4526-29.
Murdoch WJ (1998) Inhibition by oestradiol of oxidative stress-induced apoptosis in pig ovarian tissues. *Journal of Reproduction and Fertility* **114** 127-130.
Musicki B, Aten RF and Behrman HR (1994) Inhibition of protein synthesis and hormone-sensitive steroidogenesis in response to hydrogen peroxide in rat luteal cells *Endocrinology* **134** 588-595

Myer A & Schwartz LM (1996) Allelic variation of the polyubiquitin gene in the tobacco hawkmoth, *Manduca sexta*, and its regulation by heat shock and programmed cell death. *Insect Biochemistry and Molecular Biology* **26** 1037-1046.
Neill JD, Johansson EDB and Knobil E (1969) Failure of hysterectomy to influence the normal pattern of cyclic progesterone secretion in the rhesus monkey. *Endocrinology* **84** 464-465
Nishimori K, Dunkel L, and Hsueh AJW (1995) Expression of luteinising hormone and chorionic gonadotropin receptor messenger ribonucleic acid in human corora lutea during menstrual cycle and pregnancy. *Journal of Clinical Endocrinology and Metabolism* **80** 1444-1448
Niswender GD, Reimers TJ, Dickman MA and Nett TM (1976) Blood flow: a mediator of ovarian function. *Biology of Reproduction* **14** 64-81.
Niswender GD, Juengel JL, McGuire WJ, Belfiore CJ and Wiltbank MC (1994) Luteal function: the estrous cycle and early pregnancy. *Biology of Reproduction* **50** 239-247
Nubbemeyer R, Heistermann M, Oerke AK and Hodges JK (1997) Reproductive efficiency in the common marmoset (Callithrix jacchus): A longitudinal study from ovulation to birth monitored by ultrasonography. *Journal of Medical Primatology* **26** 139-146
Oerke AK, Einspanier A and Hodges JK (1996) Noninvasive monitoring of follicle development, ovulation and corpus luteum formation in the marmoset monkey (Callithix jacchus) by ultrasonography. *American Journal of Primatology* **39** 99-113
Ohara A, Mori T, Taii S, Ban C and Narimoto K (1987) Functional differentiation in steroidogenesis of two types of luteal cells isolated from mature human corpora lutea of menstrual cycle *Journal of Clinical Endocrinology and Metabolism* **65** 1192-1200.
Olson LM, Jones-Burton CM and Jablonka-Shariff A (1996) Nitric oxide decreases estradiol synthesis in rat luteinised ovarian cells: possible role for nitric oxide in functional luteal regression. *Endocrinology* **137** 3531-3539.
Orlicky DJ, Fisher L, Dunscombe N and Miller GJ (1992) Immunohistochemical localisation of PGF2α receptor in the rat ovary. *Prostaglandins, Leukotrienes and Essential Fatty Acids* **46** 223-229.
O'Shea JD, Nightingale MG and Chamley WA (1977) Changes in small blood vessels during cyclical luteal regression in sheep. *Biology of Reproduction* **17** 162-177.
O'Shea JD, Rodgers RJ and Wright PJ (1986) Cellular composition of the sheep corpus luteum in the mid- and late luteal phases of the oestrous cycle. *Journal of Reproduction and Fertility* **76** 685-691.
O'Shea JD, Rodgers RJ and D'Occhio MJD (1989) Cellular composition of the cyclic corpus luteum of the cow. *Journal of Reproduction and Fertility* **85** 483-487.
Owen S, Thomas C, West P, Wolfensohn S and Wood M (1997) Report on primate supply for biomedical scientific work in the UK. *Laboratory Animals* **31** 289-297
Paavlova LG and Christensen AK (1981) Characterization of granule types in luteal cells of the sheep at the time of maximum progesterone secretion *Biology of Reproduction* **25** 203-215.

Patwardhan VV and Lanthier A (1985) Luteal phase variations in endogenous concentrations of prostaglandins PGE and PGF and in the capacity for their in vitro formation in the human corpus luteum. *Prostaglandins* **30** 91-98
Petroff MG., Petroff BK and Pate JL (1999) Expression of cytokine messenger ribonucleic acids in the bovine corpus luteum. *Endocrinology* **140** 1018-1021.
Phan SH, Gannon DE, Varani J, Ryan US and Ward PA (1989) Xanthine oxidase activity in rat pulmonary artery endothelial cells and its alteration by activated neutrophils. *American Journal of Pathology* **134** 1201-1211.
Phelouzat M, Laforge T, Quadri RA, Arbogast A and Proust JJ (1996) Chemiluminescent detection of apoptotic DNA: A qualitative and quantitative method. *BioTechniques* **21** 214-216
Phillips HS, Hains J, Leung DW and Ferrara N (1990) Vascular endothelial growth factor is expressed in the rat corpus luteum. *Endocrinology* **127** 965-967.
Peluso JJ and Pappalardo A (1998) Progesterone mediates its anti-mitogenic and anti-apoptotic actions in rat granulosa cells though a progesterone-binding protein with gamma aminobutyric acidA receptor-like features. *Biology of Reproduction* **58** 1131-1137.
Penny LA., Armstrong DG., Baxter G., Hogg C., Kindahl H., Bramley T., Watson ED., and Webb R 1998 Expression of monocyte chemoattractant protein-1 in the bovine corpus luteum around the time of natural luteolysis. 1998 Biology of Reproduction 59 1464-1469.
Powell WS, Hammerstrom S, Sammuelsson B and Sjoberg B (1974) PGF2α receptor in human corpora lutea. *Lancet* **1** 1120.
Poyser NL (1981) *Prostaglandins in Reproduction.* Research Studies Press, New York.
Punta K, Charreau E and Pignataro O (1996) Nitric oxide inhibits Leydig cell steroidogenesis. *Endocrinology* **137** 5337-5343.
Puri CP, Patil RK, Kholkute SD, Elgar WA and Swamy XR (1989) Progesterone antagonist lilopristone: a potent abortifacient in the common marmoset. *American Journal of Obstetrics and Gynaecology* **161** 248-253
Rao CV, Griffen LP and Carmen Jr FR (1977) PGF2α binding sites in the human corpora. *Journal of Clinical Endocrinology and Metabolism* 44 1032-1036.
Ravindranath N, Little-Ihrig LL, and Zelznik AJ (1992) Characterisation of the levels of messenger ribonucleic acid that encode for luteinising hormone receptor during the luteal phase of the primate menstrual cycle. *Journal of Clinical Endocrinology and Metabolism* **74** 779-785.
Redmer DA, Dai Y, li J, Charnock-Jones DS, Smith SK, Reynolds LP and Moor RM (1996) Characterisation and expression of vascular endothelial growth factor (VEGF) in the ovine corpus luteum. *Journal of Reproduction and Fertility*
Redmer DA and Reynolds LP (1996) Angiogenesis in the ovary. *Reviews of Reproduction* **1** 182-192.
Regan RF, Panter SS, Witz A, Tilly JL and Giffard RG (1995) Ultrastructure of excitotoxic neuronal cell death in murine cortical culture. *Brain Research* **705** 188-198.
Ricke WA, Redmer DA and Reynolds LP (1995) Initial characterization of mitogenic factors produced by porcine corpora lutea throughout the estrous cycle. *Biology of Reproduction* **52** (Supplement 1) 112.

Riley JC and Berhman HR (1991) Oxygen radicals and reactive oxygen species in reproduction. *Proceedings of the Society for Experimental Biology and Medicine* **198** 781-791.
Riley JC and Behrman H (1991b) *In vivo* generation of hydrogen peroxide in the rat corpus luteum during luteolysis *Endocrinology* **128** 1749-1753.
Riley JCM and Carlson JC (1987) Involvement of phospholipase A activity in the plasma membrane of the rat corpus luteum during luteolysis *Endocrinology* **121** 776-781.
Roberts JS and McCracken JA (1976) Does prostaglandin F2α released from the uterus by oxytocin mediate the oxytocic action of oxytocin? *Biology of Reproduction* **15** 457-461.
Robker RL and Richards JS (1998) Hormonal control of the cell cycle in ovarian cells: Proliferation versus differentiation. *Biology of Reproduction* **59** 476-482
Rodger FE, Fraser HM, Duncan WC and Illingworth PJ (1995) Immunolocalisation of bcl-2 in the human corpus luteum *Molecular Human Reproduction* vol 1, *Human Reproduction* **10** 1566-1570
Rodger FE, Young FM, Fraser HM and Illingworth PJ (1997) Endothelial cell proliferation follows the mid-cycle luteinizing surge, but not human chorionic gonadotrophin rescue, in the human corpus luteum. *Human Reproduction* **12** 1723-1729.
Rodgers RJ, Vella CA, Young FM, Tian XC, Fortune JE (1995), Levels of cytochrome P450 cholesterol side-chain cleavage enzyme and 3b-hydroxysteroid dehydrogenase during prostaglandin F2a-induced luteal regression in cattle. *Reproduction, Fertility and Development*. **7**, 1213-1216.
Rodriguez MC and Segaloff DL, (1990) Extracellular domain of lutotropin/choriogonadotropin receptor in rat luteal cells as revealed by site-specific antibodies. *Endocrinology* **127** 674-681.
Rueda BR, Wegner JA, Marion SL, Wahlen DD and Hoyer PA (1995) Internucleosomal DNA fragmentation in ovine luteal tissue associated with *in vivo* and *in vitro* analysis. *Biology of Reproduction* **52** 305-312.
Sabattini E, Gerdes J, Gherlinzoni F, Poggi S, Zucchini L, Melilli G, Grigioni F, Del Vecchio M, Leoncini L, Falini B and Piler S (1993) Comparison between the monoclonal antibodies Ki67 and PC10 in 124 malignant lymphomas *Journal of Pathology* **169** 397-403.
Salamonsen L, Jonas H, Burger H, Buckmaster J, Chamley W, Cumming I, Findlay J and Goding J (1973) A heterologous radioimmuoassay for follicle-stimulating hormone: application to measurement of FSH in the ovine estrous cycle and in several other species including man *Endocrinology* **93** 610-618.
Salazar H, Furr BA, Smith GK, Bentley M and Gonzalez-Angulo A (1976) Luteolytic effects of a prostaglandin analogue, cloprostenol (ICI 80,996) in rats: ultrastructural and biochemical observations. *Biology of Reproduction* **14** 458-472.
Saltzman W, Schultz-Darken NJ and Abbott DH (1997) Familial influences on ovulatory function in common marmosets (Callithrix jacchus) *American Journal of Primatology* **41** 159-177
Sandner P, Wolf K, Bergmaier U, Gess B and Kurtz A (1997) Induction of VEGF and VEGF receptor gene expression by hypoxia: divergent regulation in vivo and in vitro. *Kidney International* **51** 448-453.

Sandri M, Podhorska-Okolow M, Geromel V, Rizzi C, Arslan P, Franceschi C, and Carraro U (1997) Exercise induces myonuclear ubiquitination and apoptosis in dystrophin-deficient muscle of mice. *Journal of Experimental Neuropathology and Neurology* **56**45-57.
Sasaki K, Matsumura K, Tsuji T, Shinozaki F and Takahashi M (1988) Relationship between labelling indices of Ki-67 and BrdUrd in human malignant tumours. *Cancer* **62** 989-993.
Sargent EL, Baughman WL, Novy MJ and Stouffer RL (1988) Intraluteal infusion of a prostaglandin synthesis inhibitor, sodium meclofenamate, causes premature luteolysis in rhesus monkeys *Endocrinology* **123** 2261- 2269.
Sasano H, Okanoto M, Mason JI, Simpson ER, Mendelson CR, Sasano N and Silverberg SG (1989) Immunolocalisation of aromatase, 17α-hydroxylase and side-chain-cleavage cytochromes P-450 in the human ovary. *Journal of Reproduction and Fertility* **85** 163-169.
Saunders JW (1966) Death in embryonic systems. *Science* **154** 604-607.
Savard K, (1973) The biochemistry of the corpus luteum *Biology of Reproduction* **8** 183-202.
Sawada M and Carlson J (1991) Rapid plasma membrane changes in superoxide radical formation, fluidity and phospholipase A2 activity in the corpus luteum of the rat during induction of luteolysis. *Endocrinology* **128** 2992-2998
Sawyer HR, Niswender KD, Braden TD and Niswender GD (1990) Nuclear changes in ovine luteal cells in response to PGF2a. *Domestic Animal Endocrinology* **7** 229-238.
Sawyer HR, Wiepz GJ, Wiltbank MC and Niswender GD (1991) Structure and function of steroidogenic cells in the corpus luteum. In *Local Regulation of Ovarian Function, The Proceedings of the Second Organon Round Table Conference*, Eds. Sjoberg N, Hamberger L, Janson P, Owman C and Coelingh Bennink H. Parthenon, pp243-261.
Schwartzman RA and Cidlowski JA (1993) Apoptosis: the biochemistry and molecular biology of programmed cell death. *Endocrine Review* **14** 133-151.
Shi S, Chaiwun B & Young L (1993) Antigen retrieval technique utilizing citrate buffer or urea solution for immunohistochemical demonstration of androgen receptor in formalin-fixed paraffin sections. *Journal of Histochemical Cytochemistry* **41** 1599-1604.
Shikone T, Yamoto M, Kokawa K, Yamashita K, Nishimori K and Nakano R (1996) Apoptosis of human corpora lutea during cyclic luteal regression and early pregnancy. *Journal of Clinical Endocrinology and Metabolism* **81** 6 2376-2380.
Shutt DA, Shearman RP, Lyneham RC, Clarke AH, McMahon GR and Goh P (1975) Radioimmunoassay of progesteron, 17-hydroxyprogesterone, estradiol-17beta and prostaglandin F in human corpus luteum. *Steroids* **26**(3) 299-310.
Shweiki D, Itin A, Neufeld G, Gitay-Goren H and Keshet E (1993) Patterns of expression of vascular endothelial growth factor (VEGF) and VEGF receptors in mice suggest a role in hormonally regulated angiogenesis. *Journal of Clinical Investigations* **91** 2235 -2243.
Simula AP, Amato F, Faast R, Lopata A, Berka J and Norman RJ (1995) Luteinising hormone/chorionic gonadotrophin bioactivity in the common marmoset (Callithrix jacchus) is due to a chorionic gonadotrophin molecule with a structure

intermediate between human chorionic gonadotrophin and human luteinising hormone. *Biology of Reproduction* **53** 380-389

Silvia WJ, Fitz TA, Mayan MH and Niswender GD (1984) Cellular and molecular mechanisms involved in luteolysis and maternal recognition of pregnancy in the ewe. *Animal Reproductive Science* **7** 57-74.

Singh J, Pierson RA and Adams GP (1997) Ultrasound image attributes of the bovine corpus luteum: structural and functional correlates. *Journal of Reproduction and Fertility* **109** 35-44.

Somers JP, Benyo D, Little-Ihrig L and Zeleznik A (1995) Luteinization in primates is accompanied by loss of a 43-kilodalton adenosine 3',5'-monophosphate response element-binding protein isoform. *Endocrinology* **136** 4762-4768

Soules MR, Steiner RA, Clifton, DK, Cohen NL, Aksel S and Bremner W (1984) Progesterone modulation of pulsatile luteinizing hormone secretion in normal women. *Journal of Clinical Endocrinology and Metabolism* **58** 378-383

Steinetz BG, Randolph C and Mahoney CJ (1995) Patterns of relaxin and steroids in the reproductive cycle of the common marmoset (Callithrix jacchus): effects of prostaglandin F2α on relaxin and progesterone secretion during pregnancy. *Biology of Reproduction* **53** 834-839

Stacey BD, Gemmell RT and Thorburn GD (1976) Morphology of the corpus luteum in the sheep during regression induced by prostaglandin F2α. *Biology of Reproduction* **14** 280-291.

Stevens VC, Sparks SJ and Powell JE (1970) Levels of oestrogens, progestogens and luteinizing hormone during the menstrual cycle of the baboon. *Endocrinology* **87** 658-666.

Smith P (1930) Hypophysectomy and a replacement therapy in the rat. *American Journal of Anatomy* **45** 205-273.

Smith KB, Lunn SF and Fraser HM (1990) Inhibin secretion during the ovulatory cycle and pregnancy in the common marmoset monkey. *Journal of Endocrinology* **126** 489-495.

Sotrel G, Helvacioglu A, Dowers S, Scommegna A and Auletta FJ (1981) Mechanism of luteolysis: effect of estradiol and prostaglandin 2 alpha on corpus luteum luteinizing hormone/human chorionic gonadotrophin receptors and cyclic nucleotides in the rhesus monkey. *American Journal of Obstetrics and Gynaecology* **139** 134-140.

Soules MR, Steiner RA, Clifton DK, Cohen NL, Aksel S, and Bremner WJ (1984) Progesterone modulation of pulsatile LH secretion in normal women *Journal of Clinical Endocrinology and Metabolism* **58** 378-383.

Stouffer RL, Chandrasekher Y, Slayden O and Zelinski-Wooten M (1993) Gonadotrophic and local control of the developing corpus luteum in rhesus monkeys. *Human Reproduction* **8** 107-108

Strauss JF and Miller WL (1991) Molecular basis of ovarian steroid synthesis In, SG Hillier (ed) *Ovarian Endocrinology* Blackwell Scientific Publications, Oxford, England pp167-189

Sugino N, Shimamura K, Tamura H, Ono M, Nakamura Y, Ogino K and Kato H (1996) Progesterone inhibits superoxide radical production by mononuclear phagocytes in psuedopregnant rats. *Endocrinology* 12 749-754.

Summers PM, Wennink CJ and Hodges JK (1985) Cloprostenol-induced luteolysis in the marmoset monkey (*Callithrix jacchus). Journal of Reproduction and Fertility* **73** 133-138.
Suzuki T, Sasano H, Takaya R, Fukaya T, Yajima A, Date F and Nagura H (1998) Leukocytes in normal-cycling ovaries: immunohistochemical distribution and characterisation. *Human Reproduction* **13** 2186-2191.
Swanston IA, McNatty KP and Baird DT (1977) Concentration of prostaglandin $F_{2\alpha}$ and steroids in the human corpus luteum. *Journal of Endocrinology* **73** 115-122.
Tardif SD, Lacker HM and Feuer M (1993) Follicular development and ovulation in the marmoset monkey as determined by repeated laparoscopic examination. *Biology of Reproduction* **48** 1113-1119
Tagliaro CH., Schneider MP., Scheider H., Sampaio IC., Stanhope MJ (1997) Marmoset phylogenetics, conservation perspectives, and evolution of the mtDNA control region. *Molecular Biology of Evolution* **14** 674-684.
Tedischi C, Hazum E, Kokia E, Ricciarelli E, Adashi E and Payne D (1992) Endothelin-1 as a luteinisation inhibitor: inhibition of rat granulosa cell progesterone accumulation via selective modulation of key steroidogenic steps affecting both progesterone formation and degredation. *Endocrinology* **131** 2476-2478.
The Biology, Rearing and Care of Young Primates, Eds., JK Kinwood and K Strathatos, Chapt. 6, Oxford University Press
Thomas J, Dorflinger L and Berhman H, (1978) Mechanism of the rapid antigonadotropic action of prostaglandins in cultured luteal cells. *Proceedings of the National Academy of Sciences* (USA) **75** 1344-1348.
Tilly JL, Kowalski KI,, Johnson AL & Hsueh AJ (1991) Involvement of apoptosis in ovarian follicular atresia and postovulatory regression. *Endocrinology* **129** 5 2799-2801.
Tilly JL, Kowalski KI, Johnson AL and Hsueh JW (1991) Involvement of apoptosis in ovarian follicular atresia and postovulatory regession. *Endocrinology* **129** 2799-2801
Tilly JL, Kowalski K, Schomberg DW and Hsueh AJ (1992) Apoptosis in atretic ovarian follicles is associated with selective decreases in messenger ribonucleic acid transcriptes for gonadotropin receptors and cytochrome P450 aromatase. Endocrinology **131** 502-510
Tilly JL, Billig H, Kowalski K and Hseuh AJ (1992) Epidermal growth factor and basic fibroblast growth factor suppress the spontaneous onset of apoptosis in cultured rat ovarian granulosa cells and follicles by a tyrosine kinase-dependent mechanism. *Molecular Endocrinology* **6** 1942-1950
Tilly JL (1993) Ovarian follicular atresia: a model to study the mechanisms of physiological cell death. *Endocrine Journal* **1** 67-72.
Tilly JL and Hsueh A (1993) Microscale autoradiographic method for the qualitative and quantitative analysis of apoptosis. *Journal of Cellular Physiology* **154** 519-526.
Tilly JL and Tilly K (1995) Inhibitors of oxidative stress mimic the ability of follicle stimulating hormone to suppress apoptosis in cultured rat ovarian follicles *Endocrinology* **136** 242-252

Torii R, Abbott DH and Nigi H (1996) Morphological changes of the ovary and hormonal changes through the ovarian cycle of the common marmoset (Callithrix jacchus) *Primates* **37**(1) 49-56

Trump BF, Berezesky IK and Osornio-vargas AR (1981) Cell death and the disease process - the role of calcium. In *Cell Death in Biology and Pathology*, pp. 209-242, Ed. ID Bowen & RA Lockshin. London: Chapman & Hall.

Ueda N and Shah SV (1994) Apoptosis *Journal of Laboratory and Clinical Medicine* **124** 169-177

Valenzuela G, Balmaceda J, Harper MJK and Asch R (1983) Platelets bind to rhesus monkey corpora lutea and stimulate its prostaglandin synthesis *Fertility and Sterility* **39** 370-373.

Van Blerkom J and Motta P (1978) A scanning electron microscope study of the luteo-follicular complex. *Cell Tissue Research* **189** 131-153.

Van Vooris B, Dunn M, Synder G and Weiner C (1994) Nitric oxide: an autocrine regulator of human granulosa-luteal cell steroidogenesis. *Endocrinology* **135** 1799-1806.

Vaux DL and Hacker G (1995) Hypothesis: apoptosis caused by cytotoxins represents a defensive response that evolved to combat intracellular pathogens. *Clinical and Experimental Pharmacology and Physiology* **22** 861-863

Vecchi A, Garlanda C, Lampugnani MG, Resnati M, Matteucci C, Stoppacciaro A, Schnurch H, Risau W, Ruco L, Mantovani A and Dejana E (1994) Monoclonal antivodies specific for endothelial cells of mouse blood vessels. Their application in the identification of adult and embryonic endothelium. *European Journal of Cell Biology* **63** 247-254.

Vendola KA, Zhou J, Adesanya OO, Weil SJ and Bondy CA (1998) Androgens stimulate early stages of follicular growth in the primate ovary. *Journal of Clinical Investigations* **101** 2622-2629

Vijayakumar R and Walters WA (1983) Human luteal tissue prostaglandins, 17β-estradiol and progesterone in relation to the growth and sequence of the corpus luteum *Fertility and Sterility* **39** 298-303.

Walker PR, Kokileva L. LeBlanc J and Sikorska M (1993) High molecular weight oligonucleosome formation. *BioTechniques* **15** 1032-1040

Wandjii SA, Srsen V, Nathanielsz PW, Eppig JJ and Fortune JE (1997) Initiation of growth of baboon follicles in vitro. *Human Reproduction* **12** (9) 1993-2000

Wang F, Riley JCM and Behrman HR, (1993) Immunosuppressive glucocorticoid blocks extrauterine luteolysins in the rat. *Biology of Reproduction* **49** 66-75.

Wang LJ, Robertson SA, Seamark RF and Norman RJ (1991) Lymphokines, including interleukin-2, alter gonadotrophin-stimulated progesterone production and proliferation of human granulosa-lutein cells in vitro. *Journal of Cellular Endocrinology and Metabolism* **72** 824-831.

Wang LJ, Pascoe V, Petrucco OM and Norman RJ (1992) Distribution of leukocyte subpopulations in the human corpus luteum. *Human Reproduction* **7** 197-202.

Wang HZ, Lu SH, Han XJ, Zhan W, Sheng WX, Sun ZD and Gong YT (1992) Inhibitory effect of interferon and tumor necrosis factor on human luteal function *in vitro. Fertility and Sterility* **58** 941-945.

Webley GE and Hearn JP (1987) Local production of progesterone by the corpus luteum of the marmoset monkey in response to perfusion with chorionic gonadotrphin and melatonin *in vivo*. *Journal of Endocrinology* **112** 449-457.
Webley GE, Luck M and Hearn JP (1988) Stimulation of progesterone secretion by cultured human granulosa cells with melatonin and catecholamines *Journal of Reproduction and Fertility* **84** 669-677
Webley GE, Richardson M, Summers P, Given A and Hearn J, (1989) Changing responsiveness of luteal cells of the marmoset monkey *(Callithrix jacchus)* to luteotrophic and luteolytic agents during normal and conception cycles. *Journal of Reproduction and Fertility* **87** 301-310.
Webley GE, Hodges JK, Given A and Hearn JP (1991) Comparison of the luteolytic action of gonadotrophin-releasing hormone antagonist and cloprostenol, and the ability of human chorionic gonadotrophin and melatonin to override their luteolytic effects in the marmoset monkey. *Journal of Endocrinology* **128** 121-129.
Webley GE, Richardson MC, Smith CA, Masson GM and Hearn JP (1990) Size distribution of luteal cells from pregnant and non-pregnant marmoset monkeys and a comparison of the morphology of marmoset luteal cells with those from the human corpus luteum.*Journal of Reproduction and Fertility* **90** 427-437.
Wehrenberg U, Giebel J and Rune GM (1998) Possible involvement of transforming growth factor-beta 1 and transforming growth factor-beta receptor type II during luteinization in the marmoset ovary. *Tissue Cell* **30** 360-367
Wehrenberg U, Wulff C, Husen B, Morohashi K and Rune GM (1997) The expression of sf-1/Ad4BP is related to the process of luteinization in the marmoset (*Callithrix jacchus*) ovary. *Histochemistry and Cell Biology* **107** 345-350.
Wildt L., Hausler A., Marshall G., Hutchinson JS., Plant TM., Belchetz P., Knobil E (1981) Frequency and amplitude of gonadotrophin-releasing hormone secretion in the rhesus monkey. *Endocrinology* **109** 376-384.
Wiltbank MC, Gallagher KP, Dysko RC and Keyes PL (1989) Regulation of blood flow to the rabbit corpus luteum: effects of estradiol and chorionic gonadotrophin. *Endocrinology* **124** 605-611.
Wiltbank MC, Diskin MG, Flores JA and Niswender GD (1990) Regulation of the corpus luteum by protein kinase C II. Inhibition of lipoprotein-stimulated steroidogenesis by prostaglandin F 2 alpha. *Biology of Reproduction* **42** 239-245.
Wiltbank MC, Gallagher KP, Christensen AK, Brabec RK and Keyes PL (1990) Physiological and immunocytochemical evidence for a new concept of blood flow regulation in the corpus luteum. *Biology of Reproduction* **42** 139-151.
Witty JP, Bridgham JT and Johnson AL (1996) Induction of apoptotic cell death in hen granulosa cells by ceramide. *Endocrinology* **137** 5269-5277
Wolf H and Dittrich K (1992) Detection of proliferating cell nuclear antigen in diagnostic histopathology. *The Journal of Histochemistry and Cytochemistry* **40** 1269-1273.
Wulff C, Soldan C, Straube W and Rune GM (1996) Functional hererogeneity of luteal cells in the common marmoset (Callithrix jacchus). *Proceedings of the 54th Meeting of the Society for the Study of Reproduction* **Abst 244** p117
Wuttke W, Jarry H, Pitzel l, Knoke I, Cieslar S and Dietrich E (1992) Luteotrophic and luteolytic effects of peptides in the porcine and human corpus luteum Proc IX Ovarian Workshop, Chapel Hill, NC, USA p16.

Wuttke W, Jarry H, Knoke I, Pitzel L and Spiess S (1995) Luteotrophic and luteolytic effects of oxytocin in the porcine corpus luteum. *Advances in Experimental and Medical Biology*. **395** 495-506.
Wuttke W, Pitzel L, Knoke I and Jarry H (1995) Interactions between PGF2α and TNF to induce luteolysis in porcine corpora lutea. *Biology of Reproduction* **52** suppl. 1. Abs. 31.
Wuttke W, Spiess S, Knoke I, Pitzel L, Leonhardt S and Jarry H (1998) Synergistic effects of prostaglandin F2α and tumor necrosis factor to induce luteolysis in the pig. *Biology of Reproduction* **58** 1310-1315.
Wyllie AH (1980) Glucocorticoid-induced thymocyte apoptosis is associated with endogenous endonuclease activation. *Nature* **284** 555-556.
Wyllie AH and Morris RG (1982) Hormone induced cell death: Purification and properties of thymocytes undergoing apoptosis after glucocorticoid treatment. *American Journal of Pathology* **109** 78-87.
Wyllie AH, Morris RG, Smith AL and Dunlop D (1984) Chromatin cleavage in apoptosis: association with condensed chromatin morphology and dependence on macromolecular synthesis. *Journal of Pathology* **142** 67-77.
Yen SSC, (1972) Variation of pituitary responsiveness to synthetic LRF during different phases of the menstrual cycle *Journal of Clinical Endocrinology and Metabolism* **35** 931-934.
Young FM, Luderer W and Rodgers RJ (1994) The antioxidant β-carotene prevents covalent crosslinking between cholesterol side-chain cleavage cytochrome P450 and its electron donor in bovine luteal cells. *Molecular and Cellular Endocrinology*. **109,** 113-118.
Young FM, Illingworth PJ, Lunn SF, Harrison DJ and Fraser H (1997) Cell death during luteal regression in the marmoset monkey. *Journal of Reproduction and Fertility* **111** 109-119.
Zackrisson U, Mikuni M, Wallin A, Delbro D, Hedin L and Branstrom M (1996) Cell-specific localisation of nitric oxide synthases (NOS) in the rat ovary during follicular development, ovulation and luteal formation. *Biology of Reproduction* **11** 2667-2673.
Zeleznik AJ (1991) Control of luteal endocrine function. In *Ovarian Endocrinology*, Ed. Hillier SG, Blackwell Scientific Publications. pp 167-189.
Zelenski-Wooten MB and Stouffer RI (1990a) Intraluteal infusions of prostaglandins of the EDI and A series prevent PGF2α-induced, but not spontaneous luteal regression in rhesus monkeys *Biology of Reproduction* **43** 507-516.
Zelenski-Wooten MB, Sargent EL, Molskness TA and Stouffer RL (1990b) Disparate effects of the prostaglandin synthesis inhibitors, meclofenamate and flurbiprofen on monkey luteal tissue *in vitro*. *Endocrinology* **126** 1380-1387.
Zhao Y., Burbach JA, Roby KF, Terranova and Brannian JD (1998) Macrophages are the major source of tumor necrosisfactor α in the porcine corpus luteum. *Biology of Reproduction* **59** 1385-1391.
Zheng J, Fricke PM, Reynolds LP and Redmer DA (1994) Evaluation of the growth, cell proliferation and cell death in bovine corpora lutea throughout the estrous cycle. *Biology of Reproduction* **51** 623-632.

Zheng J, Redmer DA and Reynolds LP (1993) Vascular development and heparin-binding growth factors in the bovine corpus luteum at several stages of the estrous cycle *Biology of Reproduction* **49** 1177-1189.

Appendix 1: Marmoset Details and Ovary Usage

Animal	Age (days)	Weight (g)	Left Ovary (mg)	# CL	Right Ovary (mg)	# CL	Luteal Day	Fate (Key at foot of table)
Early Luteal Phase								
543	1218	406	183	1	78	0	3	vW, flt-1, PCNA
581	1293		75	1	102	2	3	PCNA
619	905	410	163		171		4	PCNA
622	722	399	90		146		4	PCNA
679	1271	466	88	0	168	3	3	BrdU, Ki67, vW, VEGF
728	745	390	152	1	46	0	2	BrdU, Ki67, vW, VEGF
730	700	383	120	1	148	2	3	BrdU, Ki67, vW
Mid Luteal Phase								
447	2308	422	136	1	200	2	10	DNA, vW, VEGF, PCNA
480	1306			1		1	8	vW, flt-1
530				1		1	8	H&E, Apo, vW
533	1637	505	221	1	200	2	10	H&E, Apo, vW, DNA, Flt-1, PCNA, Ki67
546		401	246	2	134	2	8	H&E, DNA, vW, PCNA
552	1531	400		1		1	10	DNA
644	1018	512	118	1	273	3	10	H&E, Ki67, vW, PCNA, Apo, VEGF, 3b, Ub
683	1004		98	1	93	1	10	Ki67, Ub, VEGF, Apo, 3b, vW, PCNA
705	1585		123		61		10	Ki67, Ub, VEGF, vW, 3b, PCNA
Functional Luteal Regression								
473		370	90	1	118	1	18	H&E, vW, PCNA
539	1698	410	121	1	56	0	18	H&E, PCNA
579	1415	391	60	0	99	2	18	H&E, vW, PCNA, Ki67, Apo
701	938	419	107	1	135	2	18	BrdU, Ki67, vW, VEGF, 3b, Flt-1
712	832		157	2	58	0	18	BrdU, vW, VEGF, 3b
719	860	395	95	1	172	1	18	BrdU, Ki67, VEGF, 3b
Structural Luteal Regression								
655	1857		84		84		22	BrdU, Flt-1
662	1307		82		65		23	H&E, Ki67, vW, VEGF, PCNA, 3b, Apo
641	553		233		181		22	H&E, PCNA, 3b, Apo
700	1032	387	103	1	107	0	23	BrdU, Ki67, vW, VEGF
716	772		79		147		23	BrdU, VEGF, Ki67, vW
545			116	1	115	2	24	H&E, PCNA, 3b, Apo
554	1600			2			26	H&E, vW
567			204		235		27	H&E
640	687		76		113		26	vW
675	686		120		126		26	H&E

Animal	Age (days)	Weight (g)	Left Ovary (mg)	# CL	Right Ovary (mg)	# CL	Luteal Day	Fate
Prostaglandin Induced Luteal Regression								
681	762	394	120	1	121	2	12hr	H&E, vW, VEGF, PCNA, Ki67
693	1673		109	2	96	2	12hr	H&E, vW, VEGF, PCNA, Ki67
708	1517	307	161	1	127	1	12hr	H&E, vW, VEGF, PCNA, Ki67
532		378	67	0	133	1	24hr	DNA
542	1738	464	135	2	133	2	24hr	H&E, DNA, Apo, PCNA
549			117	1	147	2	24hr	DNA
569	1201		186	2	100	2	24hr	DNA
572	1263		38	0	120	3	24hr	DNA
573	1438	475	64	0	106	1	24hr	H&E, vW, apo
582	1254	445	44	0	138	3	24hr	H&E, Ub, vW, PCNA, Ki67
611	1175	518	186	1	143	1	24hr	H&E, DNA, Ki67, Apo, PCNA, VEGF, 3b, Ub
676	1135		50	0	144	2	24hr	Ki67, vW, VEGF, 3b, Ub
690	971		161		45		24hr	Ki67, vW, VEGF, 3b, Apo, PCNA
576	1208		68		80		48hr	H&E
GnRH Antagonist Induced Luteal Regression								
665	858	340	64	0	153	2	12hr	H&E, vW, VEGF, PCNA, Ki67
689	716	390	88	0	143	2	12hr	H&E, vW, VEGF, PCNA, Ki67
709	1517	331	74	0	158	2	12hr	H&E, vW, VEGF, PCNA, Ki67
507	1700	400	86	1	127	2	24hr	DNA
528	1697	440	133	1	120	1	24hr	H&E, Ub, vW, VEGF, PCNA, Ki67
612	1336		108	2	44	0	24hr	H&E, Ki67, vW, Apo, PCNA, VEGF, 3b.
624	916	442	36		155	3	24hr	DNA
627	1141	330	105	2	29	0	24hr	H&E, Ub, Apo
686	742	393	69	0	162	3	24hr	DNA, H&E, vW, Apo, PCNA, VEGF, 3b.
704	1582		110	2	64	0	24hr	Ki67, vW, Apo, PCNA, VEGF, 3b.
714	1642		122		141		24hr	DNA, Ub, Flt-1, Ki67
525	1648	401	94	1	80	1	48hr	DNA
478	?	323	77	1	72	1	48hr	H&E
505							48hr	DNA
580	1448	562	112		169		48hr	H&E

Key	
DNA	DNA extracted and examined for oligonucleosome formation
H&E	Morphological examination of H&E stained sections
Apo	*In situ 3' End Labelling*
vW	von Willebrand Factor VIII Antigen
PCNA	Proliferating Cell Nuclear Antigen
3b	3b Hydroxysteroid Dehydrogenase Isomerase
VEGF	Vascular Endothelial Growth Factor
Ki67	Ki67
Flt-1	Flt-1
BrdU	Bromoxydeuridine
Ub	Ubiquitin

Appendix 2: Immunocytochemistry Procedures

Antibody	Source	Antigen Retrieval	Dilution	Incubat - ion	Number of Animals Used (Day of Luteal Phase)								
					2-5	10	18	22-24	25-28	PGF2α 12hr	PGF2α 24hr	GnRH ant 12hr	GnRH ant 24hr
3-beta hydroxysteroid dehydrogenase isomerase polyclonal rabbit anti human	Prof Van Luu-The, The CHUL Research Centre, Quebec, Canada	Microwave	1:300	4°C, 18hr		3	3	3			3		3
Ubiquitin polyclonal rabbit anti human	DAKO, High Wycombe, UK	Microwave	1:50	4°C, 36hr		3					3		3
* Von Willebrand Factor VIII polyclonal rabbit anti human	DAKO, High Wycombe, UK	Trypsin	1:250	4°C, 18hr	4	3 4	4	3	2	3	4	3	4
Vascular Endothelial Growth Factor polyclonal rabbit anti cow	Santa Cruz Biotechnology, California, USA	Microwave	1:250	37°C 1hr	2	4 4	3	3		3	3	3	4
Flt-1 (c-17) polyclonal rabbit anti human	Santa Cruz Biotechnology, California, USA	Microwave	1:50	37°C 1hr	2	2	1	1				1	1
Proliferating Cell Nuclear Antigen monoclonal mouse anti human	DAKO, High Wycombe, UK	Microwave	1:100	4°C, 18hr	4	4 4	3	3		3	4	3	4
Ki67 Antigen monoclonal mouse anti recombinant Ki67 protein fragment	Novocastra Laboratories Ltd. Newcastle, UK	Microwave	1:50	4°C, 18hr	3	4 4	3	3		3	4	3	4

* ovaries collected from 3 animals on days 6 – 8 were also included in this study.